THE INFLUENCE OF COMPOSITION ON THE OPTICAL PROPERTIES OF ELECTRODEPOSITED GOLD

BY

GERALDINE BROWN

A thesis submitted to the University of Aston in Birmingham for the degree of Doctor of Philosophy

April 1980

THE INFLUENCE OF COMPOSITION ON THE OPTICAL PROPERTIES OF ELECTRODEPOSITED GOLD

by

Geraldine Brown

SUMMARY

In industry the colour of a gold alloy electrodeposit is checked by visual comparison with standard panels. The aims of the present work have been to assess the application of spectrophotmetric techniques to the measurement of the colour of gold alloy electrodeposits and to examine the factors that influence the colour of thin deposits. The minimum thickness of deposit required to produce its final colour and completely hide the underlying substrate was measured and found to depend on the nature of the substrate, the plating solution and the operating conditions. Bright and matt electrodeposits were studied.

The influence of alloying gold by adding copper, silver and indium to the plating solution were investigated. CIE chromaticity coordinates were calculated from spectrophotometric data using a computer programme written for the purpose. The addition of silver to a simple gold bath caused the colour of the deposit to change from yellow through green to near white in a smooth progression as the amount of silver in solid solution steadily increased. The colour of deposits formed when additions of copper were made was complicated by the formation of intermediate phases. A colour in the blue region of the spectrum was obtained in a few experiments investigating the influence of indium additions to the gold bath.

Key words: gold, electrodeposit, colour, chromaticity

ACKNOWLEDGEMENTS

The author wishes to thank the City of Birmingham Polytechnic for support during this project. Thanks are due to Mr R R Whitworth and colleagues in the Department of Mechanical and Production Engineering for their advice and help, in particular Mr C Stewart for colour photography, Dr G A Atkinson and Mr J Cherrington for help with computer programmes, and Mr T Beard for help with Talysurf measurements.

The author is also very grateful to Mr R Howells and his staff at the University of Aston for their patient instruction and help with the electron microscope work.

The author's thanks are also due to the following firms: Marston Excelsior for platinised titanium, Precious Metal Depositors for gold electroplating solutions, and Brown and Alderson for interim duplication facilities.

Lastly, but certainly not least, the author wishes to thank her supervisor Dr D J Arrowsmith for his kind and painstaking help and advice.

INDEX

page

LIST OF ILLUSTRATIONS

The illustrations are placed in the text immediately after their first mention

LIST OF TABLES

The Tables are placed in the text immediately after their first mention

INTRODUCTION

Pure gold is a noble metal of fine yellow colour, and it is one of the few metals which may be found in nature uncombined.[1] This is because it is an extremely unreactive metal, as its standard electrode potential of +1·7 volts shows.[2] Most metals are basically white or grey in colour but gold shares with copper the distinction of having a definite colour.[3]

It has been known for many years that the addition of alloying elements to gold changes the colour depending upon the particular element or elements added. Increase in hardness and strength also occurs.[4] It has also been the practice to electrodeposit alloy golds from specially formulated solutions. It is possible to obtain wide variations in deposit colour by variations of bath composition and electroplating conditions. Fig. 1 gives a selection of some of the electrodeposits produced in the present work.

Fig. 1

A selection of coloured golds

Fischer and Weimer[5] give a table indicating these changes and this

is reproduced in Appendix 1. Much work has already been done on formulations and conditions and comprehensive surveys have been published.[6-9] Thus it was decided that this aspect should not be repeated in the present work, but that the main emphasis should be directed towards the effect of substrate on the final colour, and the feasibility of using colour measurement for control of colour.

It is the practice to control the colours of electrodeposits obtained by reference to standard panels compared by the naked eye.[10] Although it is recognised that the human eye is very sensitive, this method must be subjective. Thus we require a method which does not depend on the human element and which yields a "colour value", which can be quoted without reference to opinion. In this way a numerical value defined in, for example, Great Britain, may be compared to one produced in Japan without reference to actual weather conditions (as it affects incident light) or to individual idiosyncrasies.

We may ask, "why is it necessary to define colour?" The answer is that, in for example the jewellery trade, it is very important. Components may be produced in different departments or even different firms, but when they are assembled it is vital that they shall match. When we buy a gold watch, and select a bracelet for it, it is necessary that they match because slight differences are easily apparent to the sensitive human eye.

When a metallic deposit is electroplated on to a substrate the original colour of the substrate is gradually covered and then transformed to the colour proper to the deposit itself. Thus we

require to know at what thickness a stable colour is obtained and whether or not this stability lasts indefinitely with increasing thickness. It is known that even in components of relatively simple shape there is wide variation of current density over the surface[11] and therefore by implication thickness. Hence, unless we obtain the minimum thickness for "colour stability" on the low current density areas, and less than any possible maximum on the high current density areas, colour variations will be apparent. In the alloy baths it is considered important that the variation of colour with deposit composition should be established.

In order to establish a numerical definition of colour, absorbancy measurements were made on nickel discs surface finished by various different processes, and on electroplated nickel discs. A small number of experiments were carried out on a variety of metals during the establishment of the experimental procedures. Reflectivity curves were derived from the absorbance measurements and from these chromaticity coordinates, which enabled the colour to be categorised.

Chapter 1 is devoted to a survey of the literature and a general discussion of the relevant theory. The experimental apparatus and procedure is described in Chapter 2. In Chapters 3 to 9 the experimental results are given, and are discussed, where necessary for continuity, in interjections designated "comment". Chapter 10 is the main discussion of the present work in which the various strands are gathered together, and in which suggestions for further work are given. The conclusions section completes the text of the report and Appendices 1-16 are included.

CHAPTER 1

THEORY AND LITERATURE SURVEY

1·1 INTRODUCTION

The intention of this chapter is to discuss the underlying theory of colour in general, the theory of the techniques used in its measurement, and the relationship of these concepts to gold and gold alloys. Additionally the theory of the scanning electron microscope will be briefly considered. Previous work in the field of colour measurement will be surveyed. Accordingly the work will be arranged in the following order:

(i) The nature of colour

(ii) The measurement and assessment of colour

(iii) The effect of internal structure on the resulting colour of metals and alloys

(iv) The growth of electrodeposits

(v) The electrodeposition of alloys

(vi) The electrodeposition of gold and gold based alloys

(vii) Previous work on the measurement of the colours of metals and alloys

(viii) The scanning electron microscope

1·2 COLOUR AND LIGHT

Except where indicated by other references much of the information used in the following discussion has been obtained from works by Clulow[12] and Wright.[13]

1·2·1 The Nature of Colour

Clulow states that colour and light are inseparable, and that in order to understand colour we must first understand the nature of light. Light is a form of electro-magnetic energy, and it travels or is transmitted through space and transparent materials in a wave like manner. White light consists of light of various wavelengths from 400 to 700 nm. The diagram given in Fig. 1·1 shows what is meant by the term wavelength

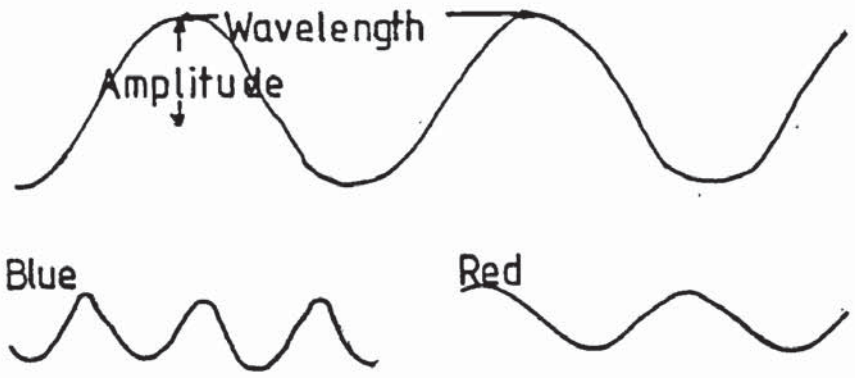

Fig. 1·1

Diagrammatic representation of the wavelengths of light, illustrating the terms wavelength and amplitude

Light has the property of stimulating the nerves of the eye and producing the sensations of sight. Since sunlight contains the whole gamut of visible radiations it is referred to as white light. Coloured sensations are produced when less than the complete mixture of radiations strikes the eye. Light rays are not in themselves coloured, but if the longest visible wavelength strikes the eye the sensation we call red is passed on to the brain.

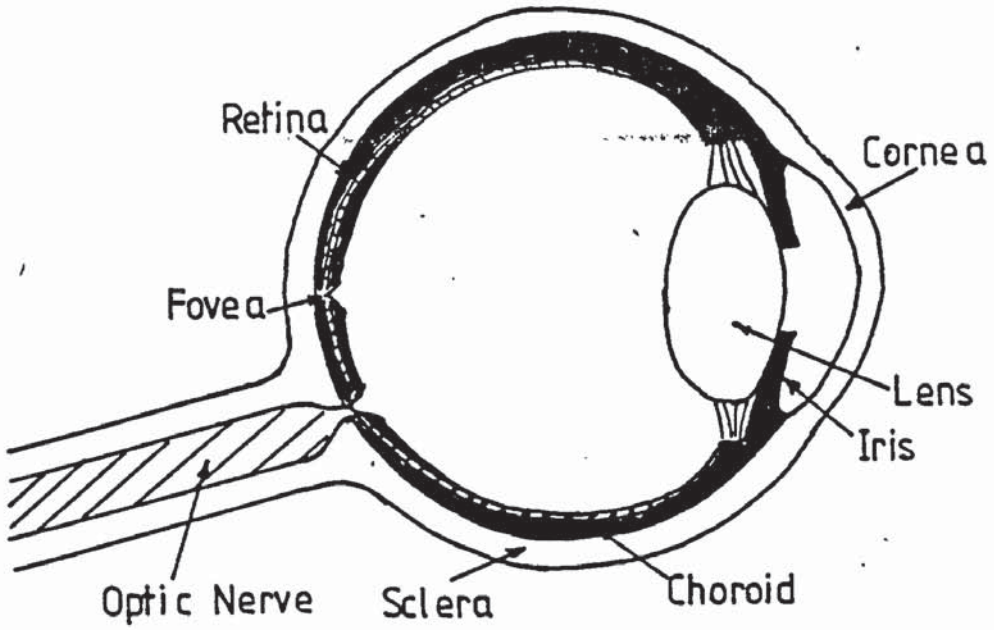

Fig. 1•2

A horizontal section through the eye

Fig. 1•2 shows a horizontal section of the eye. The part of the eye most directly concerned with colour vision is the retina, which is a thin transparent membrane of nerve tissue lining the inner wall of the eyeball. In this region light energy is converted into nervous energy and this in turn produces "colour impulses" in the brain. The retina is a complex assembly of nerve cells and fibres terminating in rods or cone shaped bodies, these are actually light detectors. It is believed that the reaction is of a photochemical nature and that substances within the rods and cones are decomposed by light. The light sensitive chemicals are continuously reformed so that the sensitivity of the eye is maintained. When the level of illumination is high decomposition products accumulate in the eye, thus when we

go from bright sunlight into a darkened room, a short time is required for the eye to adjust, to allow the light sensitive compounds to reform. The rods and cones differ in function; the rods are the light detectors for low intensity light, whilst the cones operate in good light. In intermediate conditions both rods and cones are operational. It has been computed that the eye contains 100 million rods and 5 million cones. The fovea centralis is a very small indentation in the centre of the retina; it is the most sensitive part of the retina giving the best visual acuity. There is the highest concentration of rods in this area, i.e. 100,000. Although it is still the subject of some discussion, it is believed that the colour cones distinguish one colour from another because the eye contains three colour receptors in the cones, one which absorbs mainly red light, one which absorbs mainly green, and another which absorbs mainly blue light.

1·2·3 The Spectrum of White Light

If white light is passed through a diffraction grating, the fine lines in the grating act as barriers to the light causing the light to be slightly bent in such a way that the longer the wavelength the greater the deviation. Thus if the emergent rays are projected on to a screen the rays are split up according to wavelength as shown in Fig. 1·3. It has been calculated that there are about 150 different spectrum colours, but since they merge into each other with only just perceptible differences, it is considered that the fewer colour names used the better. Newton designated seven colours in 1666, but latterly indigo has been dropped, so that the spectrum is now designated violet,

(contd. p. 10)

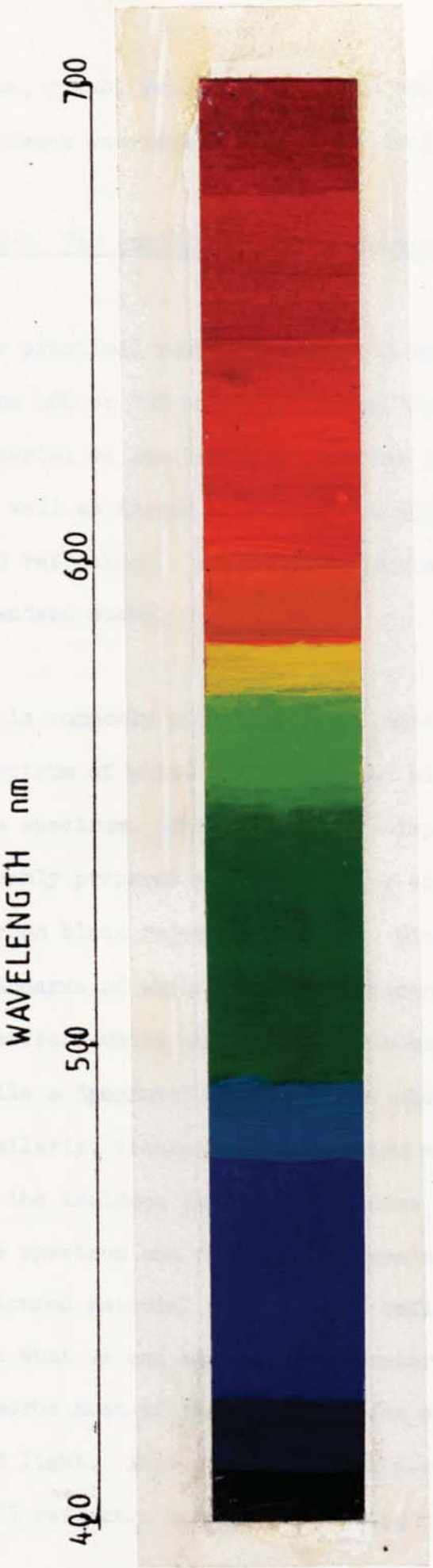

Fig. 1·3

The spectrum of white light

blue, green, yellow, orange and red. The spectrum, together with the relevant wavelengths, is given in Appendix 2.

1·2·4 The Function of Reflectivity and Absorbance

For practical purposes the light wave-band is regarded as extending from 400 to 700 nm. If we look through a coloured transparent material we see its colour by the light transmitted through it. But as well as transmission we must also consider reflection, absorbance and refraction. All these concepts are thoroughly discussed in standard works.

It is commonly said that white materials reflect the whole of the spectrum of white light and that black materials absorb the whole of the spectrum. This is an over-simplification since even a layer of freshly prepared magnesium oxide absorbs 3% of incident light and carbon black rejects about 3%. Since these materials are taken as standards of white and black respectively, it is obvious that a "perfect" white surface reflects most of the light incident upon it, while a "perfect" black surface absorbs most of the incident light. Similarly, transparent colourless materials transmit a high proportion of the incident light. Substances which absorb light from one part of the spectrum and reflect the remainder are said to be coloured. No coloured material exists which reflects light of one wavelength only, but what we can say is that a material of an accepted colour of red absorbs most of the violet, green and yellow light and reflects mainly red light. Thus stated generally we can say that a coloured object will reflect a mixture consisting of light of its apparent colour

together with light of the colours adjacent in the spectrum. Small quantities of other wavelengths may also be present. In some cases the quantity of light other than that which predominates is considerable, e.g. crimson pigments reflect considerable quantities of blue along with the red light. Yellow is rather a special case; these materials selectively absorb violet and blue light from white illumination, and reflect green, orange, yellow, and red rays. Fig. 1·3 shows that yellow covers a very narrow band in comparison to the other colours, hence it follows that the amount of red and green light must be in excess of the yellow. The reason it appears yellow is that a mixture of red and green light produces the visual sensation of yellow. Thus we can see that the measurement of colour is somewhat more complicated than it appears at first sight.

1·3 THE MEASUREMENT OF COLOUR

Colour terminology has been standardised by the British Standards Institution,[13] and the Commission International de l'Eclairage (CIE).[14] The terms include hue, saturation, lightness and dominant wavelength; and these terms are defined in detail in Appendix 3.

1·3·1 Matching Methods

In its simplest form matching is done by comparison with standard charts or cards, but it is obvious that any method depending upon this type of comparison must be subjective. Many systems based on colour matching have been developed including the Nu-Hue, the Colorizor and the Plochere colour systems. Atlases have been

produced, some of them to assess the colours of nature such as the plumage of birds, but which have found uses outside their original field.[15-21]

A series of charts based upon so-called colour solids have been developed including the Ostwald[22] and the Munsell systems.[24]

1·3·1·1 The Ostwald System

This system was developed in the 1920s, and it consists of twelve double triangles (diamonds) as shown in Fig. 1·4a, to form a so-called colour solid (Fig. 1·4b). If we consider each triangle separately for a given hue, the white, black and full colours are situated at the three corners of the triangle. The colours within the triangle are regarded as an additive mixture of white, black and colour, such that: W + B + C = 1. Colours located along lines parallel to the line joining white to the colour, are colours of constant black content and are called Isotones, while colours located along a line parallel to that joining black to the colour are lines of constant white content and are called Isotints. Colours located on a line parallel to that joining white and black are colours of equal full colour content and are called Isochromes. The full single chart consists of two triangles joined base to base, each containing 64 colour patches, the two colours situated at opposite points of the diamond so formed are complementary. If we now rotate the section about WB we obtain a colour solid of double cone shape (Fig. 1·4b). Twelve sections through this solid give us twelve pairs of complementary colours. Colours which have similar amounts of black and white (i.e. they occupy similar positions

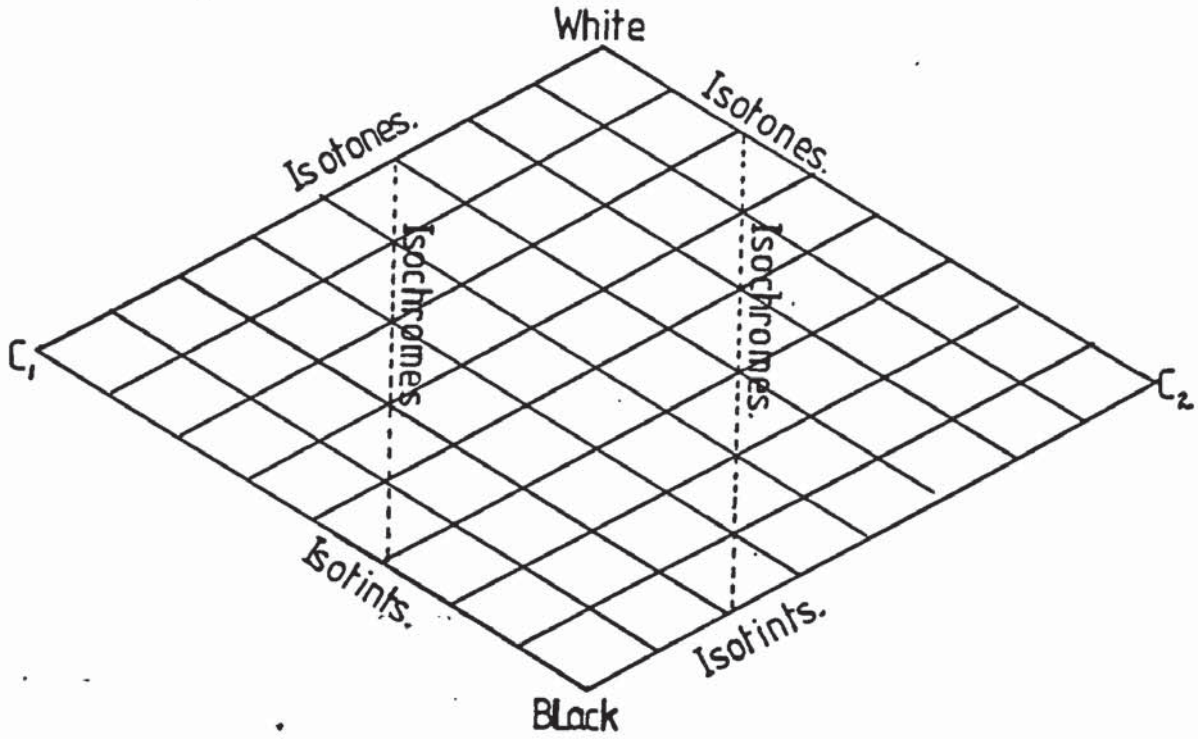

Fig. 1·4a

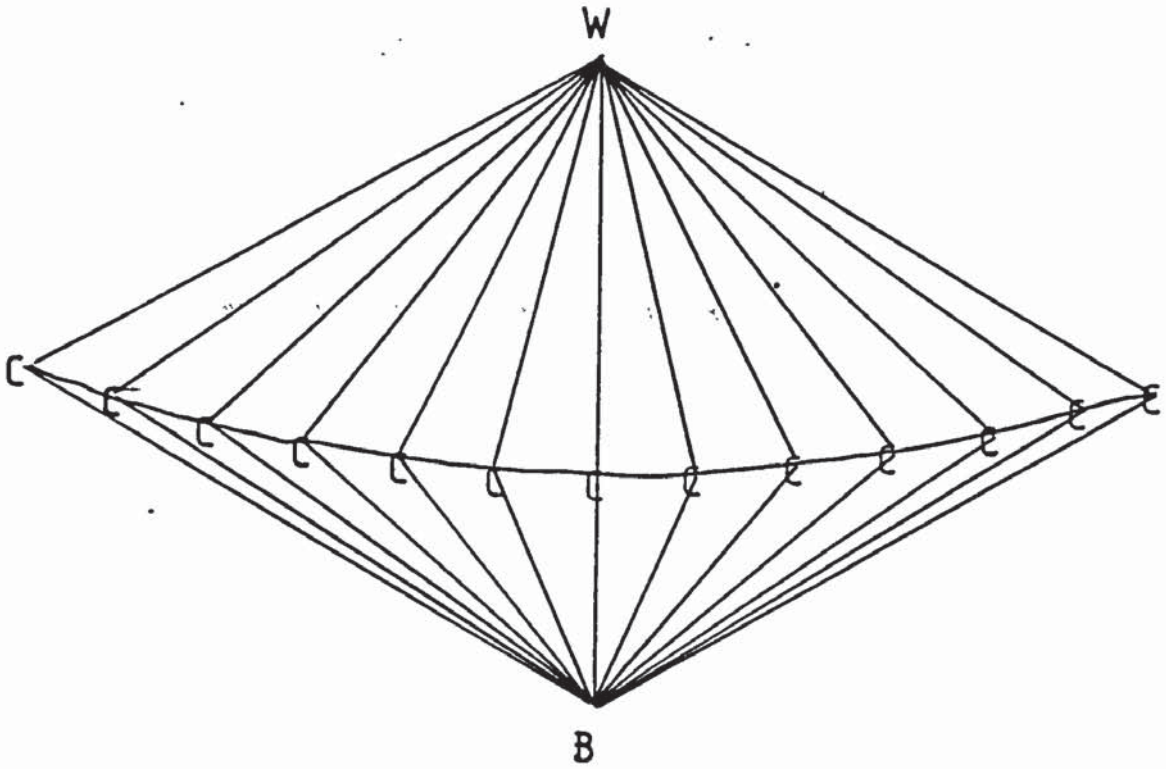

Fig. 1·4b

The Ostwald Colour Solid

on different charts) are called Isovalent colours.

This method of defining colour has drawbacks in that the lettering system is not easy to remember and to relate to a colour. More importantly perhaps, there is no room in the system for any brighter pigments than those already used, so that any new pigments will not be represented. The Container Corporation of America has produced a Colour Harmony Manual based on the Ostwald System.[22]

1·3·1·2 The Munsell System

This colour solid (Fig. 1·5) is irregular in shape, being like a bushy tree. The axis is the "grey scale" which consists of nine steps from white at the top to black at the bottom. The most saturated colours lie on the periphery of the circles. The intermediate colours become increasingly tinted towards the top white, and increasingly darkened downwards to black. The three Munsell properties are "Hue" which indicates its position on the hue circle, R for red, Y for yellow, etc., "chroma" corresponding to saturation or purity and "value" indicating the proportion of white and black. The five principal hues, red, yellow, green, blue and purple occupy the central planes of alternate segments, with intermediate hues being situated in the mid-planes as shown in Fig. 1·5. A closer grading is provided by dividing each segment into ten sections, with the main hue in each segment being numbered 5. A specification for a sample of 10P 5/8 indicates a hue of 10P (a colour between blue-purple and red-purple RP), a value of 5 (equal amounts of white and black), and a chroma of 8 (80% saturated). The complete atlas comprises 960 patterns and

(contd.p.17.)

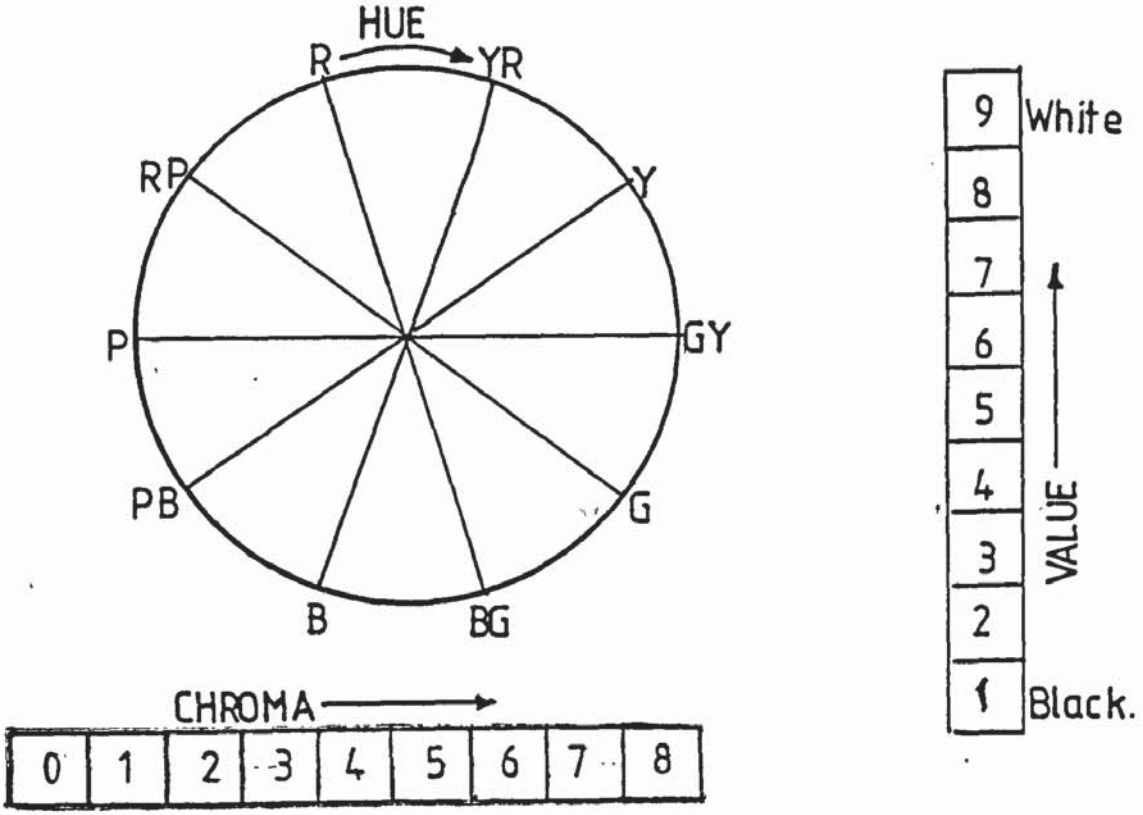

Fig. 1·5a

Elements of the Munsell Colour Solid

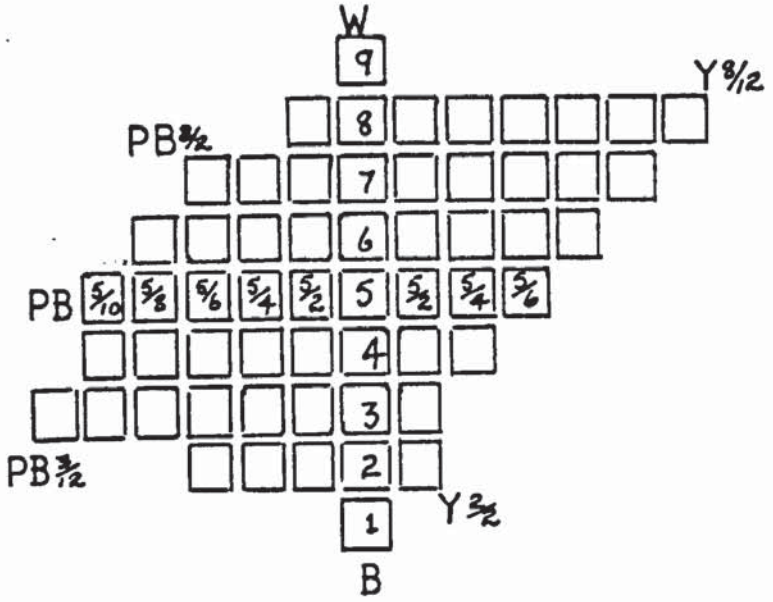

Fig. 1·5b

A vertical section through plane Y-PB of the Munsell solid

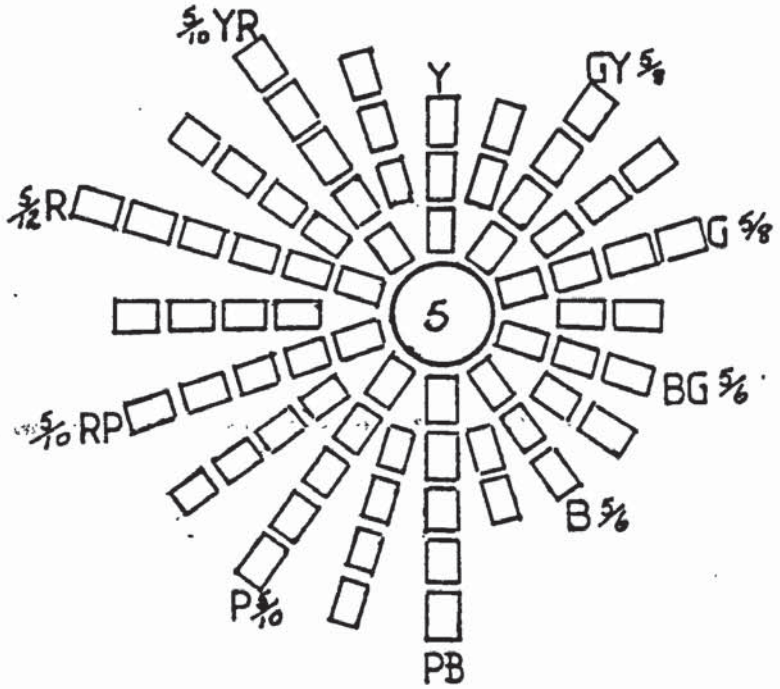

Fig. 1·5c

A horizontal section through the Value 5 plane of the Munsell solid

these have also been given as CIE specifications.

1·3·1·3 The Limitations of the Colour Solid

Any system which depends upon charts of pigment colours may be subject to errors due to soiling or fading. The number of colours which it is possible to include is only a small percentage of the several million surface colours which may be discriminated. Furthermore surface texture (matt, glossy, etc.) would also require an enormous number of extra standards.

1·3·2 Colorimetry

This is a fundamental method of measuring colour and many of the methods depend on the principle that any colour can be matched by the correct mixture of three selected radiations, namely, red, green and blue. Furthermore, if two colours matched by this means are mixed together the resultant will be matched by the sum of their separate matching combinations.[25-30] There are five main types of colorimeters, additive, subtractive, fibre optic, photoelectric and spectrophotometric.

1·3·2·1 Colour Mixing

Additive and subtractive colorimeters depend upon the process of colour mixing. Although it can easily be demonstrated that white light can be produced by mixing together all the coloured lights of the spectrum, it is also possible, because of the response of colour sensitive

cones, to produce white light by combining three selected monochromatic light rays of selected wavelength.

We can show that R + B + G = W(initial letters of colours), and by variation of intensity and amount of each light, the whole range of colour sensations can be obtained. These lights are called "the additive primaries". Binary mixtures of selected light rays also produce white light and these are called complementary colours. Subtractive methods may be considered in an analogous way. If we pass white light through a yellow filter, the blue-purple part of the spectrum is absorbed, and the light emanating appears yellow because the mixture of red and green gives the visual sensation of yellow. If the light is now passed through a cyan filter, red and orange rays are absorbed and the light emanating now contains only yellow and green, which gives the visual sensation of green. If this is now passed through a magenta filter, the remaining yellow-green part of the spectrum is absorbed resulting in complete absorption of the light. The filters which can achieve this are called subtractive primaries.

1·3·2·2 Additive Colorimeters

The diagram given in Fig. 1·6a illustrates the principles of this type of instrument. The instrument allows the three lights (red, blue and green) to be selected to match the colour under test. It is important that the instrument is designed such that the lights must be selected in groups of three members to produce white collectively, and so that no two can be combined to match the third. The diagram shows that in essence the instrument consists of two white screens

(contd. p. 20)

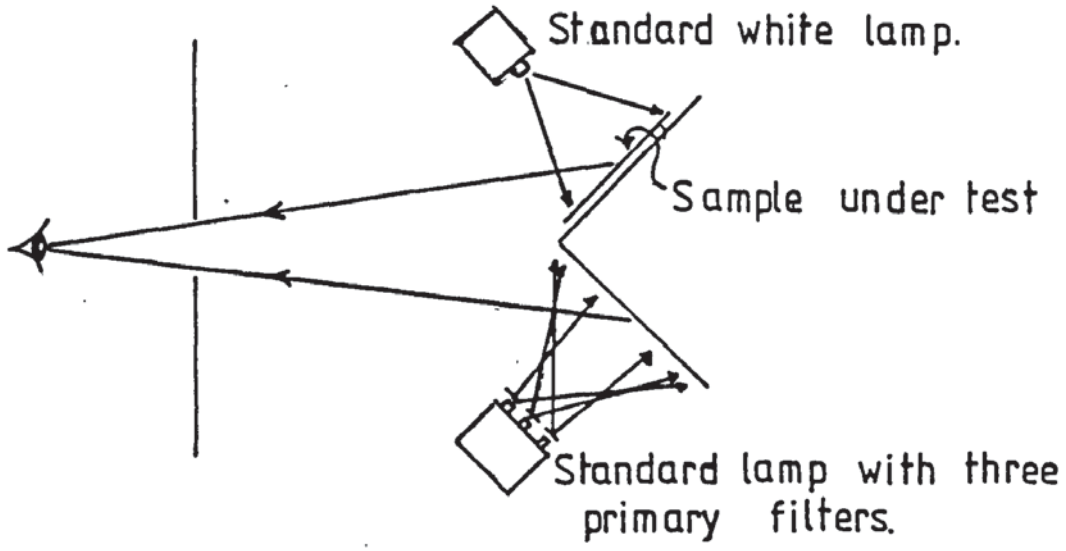

Fig. 1·6a Additive Colorimeter

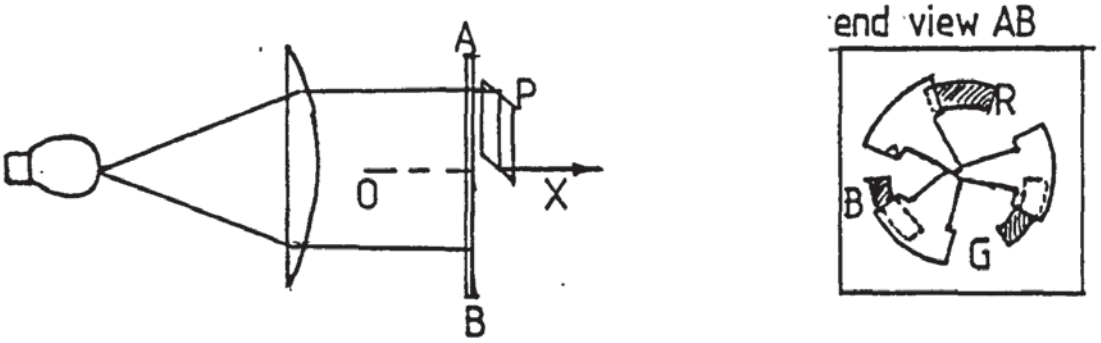

Fig. 1·6b Visual Colorimeter

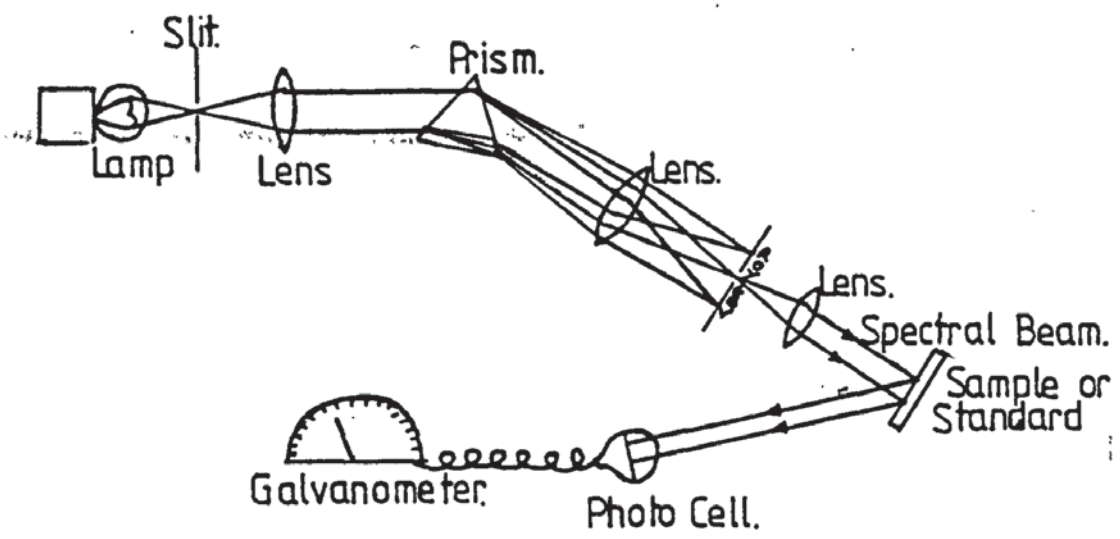

Fig. 1·6c Spectrophotometer

placed at 90° to each other, the coloured specimen is placed on one screen and illuminated by a standard white illuminant, while the three primary light beams are projected on to the other screen and adjusted until a match is obtained by the observer's eye. The controls of the instrument indicate the amounts of the lights required, and these are termed the tristimulus values.

1·3·2·3 Visual Colorimeters

An early type of visual additive colorimeter designed by Guild[31] is shown in Fig. 1·6b. Light is collimated by the lens L into a broad beam and is then passed through three adjustable sector shaped colour filters. The emerging rays are passed through a revolving prism which combines them to give the appropriate colour. The radial shutters are adjusted by the operator until the test colour is matched. A more modern adaptation of this instrument is the Donaldson[32,33] in which the ray mixing is accomplished by passing rays into an integrating sphere, which is a sphere with a matt white interior, which acts as a reflecting screen, in which the rays undergo repeated diffuse reflections and are thus mixed before emerging via a window in the sphere. Visual colorimeters, together with additive and subtractive colorimeters, have the limitation that the results tend to vary from observer to observer.

1·3·2·4 Subtractive Colorimeters

This construction is somewhat similar to the additive colorimeter. In this case the standard white light is projected on to the "matching"

screen via the subtractive primaries, which consist of sets of filters of various intensities. Thus the correct mixture is selected and recorded by the controls of the instrument to give the tristimulus values. The Lovibond tintometer[34,35] is of this type and it has been modified as the Lovibond-Schofield[36] instrument to give units which are easily converted to the appropriate CIE specification.

1·3·2·5 Photoelectric Colorimeters

In order to eliminate the human element, the photoelectric method developed by Hilger and Watts,[37] illuminates the specimen in turn by three primary lights, and the reflected light in each case is picked up by a single photo-electric cell. The photo-electric cell is calibrated against a standard such as magnesium oxide.

1·3·2·6 Fibre Optic Colorimeter

This is an adaptation of the photo-electric colorimeter. Light is transmitted via several fibre optics to a photo-electric photomultiplier.[38] An advantage of the fibre optic colorimeter is that the sensing head may be placed at a distance from the colorimeter, thus it is suitable for automatic production control.

1·3·2·7 Photoelectric Spectrophotometers

Fig. 1·6c indicates the principles of this type of colorimeter. White light is split into its constituent parts, then a moveable screen allows monochromatic light to impinge on to the specimen.

The reflected rays are allowed to fall onto a photocell which transforms the light energy into an electrical impulse. By this means the whole spectrum can be covered and the instrument draws a graph of either reflectivity or absorbance. A similar graph is drawn for the white standard for comparison.

1·3·3 The Commission Internationale de l'Eclairage System (CIE)

There are many possible colour measuring devices, and it was decided internationally in 1931 that efforts should be made to introduce uniformity. This is the basis of the CIE system. This system provides a common basis in which measurements are made on different instruments may be related, without reference to individual judgement. It gives a numerical code which defines the colour exactly. As we would expect, certain standardisations must be made for this exact definition.

1·3·3·1 The Standard Observer

The reaction of individual observers to various colours may well vary, so the CIE defines an imaginery standard observer. The definition is based on an amalgam of the results obtained by a number of non-colour defective observers, when matching colours additively under standardised conditions by means of three selected primary lights of 700, 546·1 and 435·8 nm. By this means the colours may be matched through the spectrum to produce a table of distribution coefficients to represent the colour matching characteristics of the average eye. Guild[39] and Wright[40] have measured distribution

coefficients using groups of observers, and graphs of the form shown in Fig. 1·7 were obtained. In the intervening years since 1931 further measurements have been made particularly for a 10% subtension of angular vision (rather than the usual 2%) by Stiles,[41] Judd[42] and Speranska.[43]

1·3·3·2 The Standard Illuminants

Since colour is perceived according to reflections of various wavelengths from the object in question, the character of the incident light must be very important, hence three standard illuminants were adopted by the CIE in 1931. They comprise S_A (tungsten lamp), S_B (sunlight) and S_C (overcast sky). It was apparent subsequently that these standards were deficient in the ultra-violet region, which is important for fluorescent dyes and pigments. This has led to standards being defined for the wavelength range 300-380 nm, i.e. D_{6500}, D_{5500} and D_{7500}. All the standards referred to are described fully in Appendix 4. Colours may also be related to theoretical equi-energy conditions.

1·3·3·3 The Colour Triangle

The numerical CIE values indicate the amount of redness, greeness and blueness in a colour and these values could be plotted on to a colour triangle in order to indicate the colour. The triangle may be constructed by placing at each apex of an equilateral triangle a spectral primary light (red, green and blue). Fig. 1·8 shows such an artifact. If the lamps are adjusted so that they are at zero

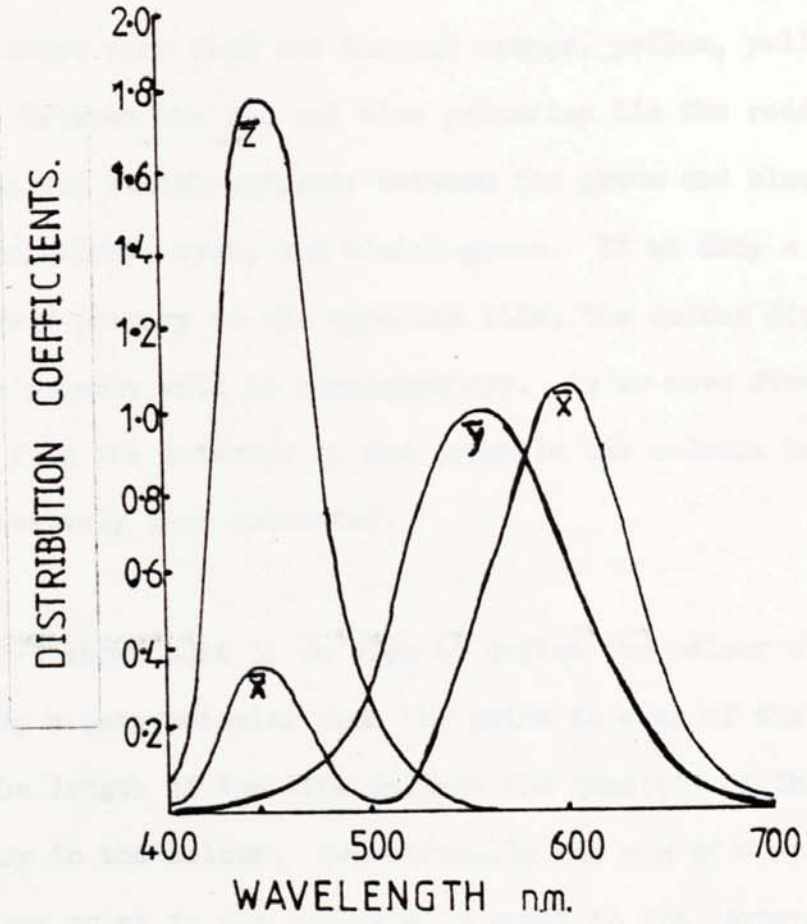

Fig. 1·7 Distribution Coefficients

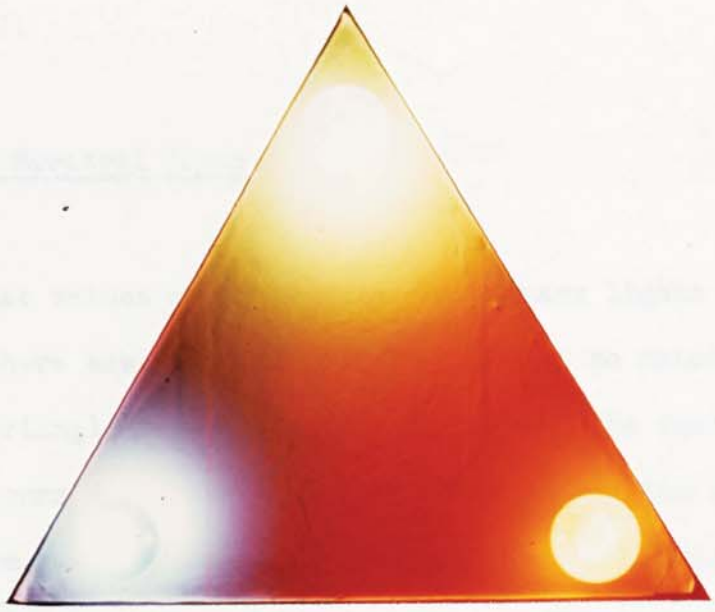

Fig. 1·8 The Light Triangle

intensity when they reach the opposite side, at the centre of the triangle we obtain a white point. Between red and green primaries the colours vary from red through orange, yellow, yellow-green to green; between the red and blue primaries lie the reddish-purples, magenta and bluish-purples; between the green and blue primaries lie greenish-blues, cyan, and bluish-green. If we drop a perpendicular from each primary to the opposite side, the colour directly opposite to the primary will be complementary. As we move from the apex or sides into the interior of the triangle the colours become progressively less saturated.

Fig. 1·9 shows that if we wish to define the colour of the point P we drop a perpendicular from the point to each of the opposite sides and the length of the line defines the quantity of the opposite primary in the colour. Geometrically the sum of the perpendiculars from any point in the triangle is equal to the perpendicular from the apex to the opposite side. If this distance is taken as I then: $r + g + b = I$.

1·3·3·4 The Spectral Locus

No matter what values are taken for the primary lights it has been shown that there are some colours which cannot be matched within the actual triangle. These are the colours of the spectrum, the spectral colours being more saturated than any of the saturated mixtures from any two of the primaries. These spectral colours can only be matched by first mixing some of the third primary with the spectral colour. Thus the spectral colours must lie outside the

(contd. p. 27.)

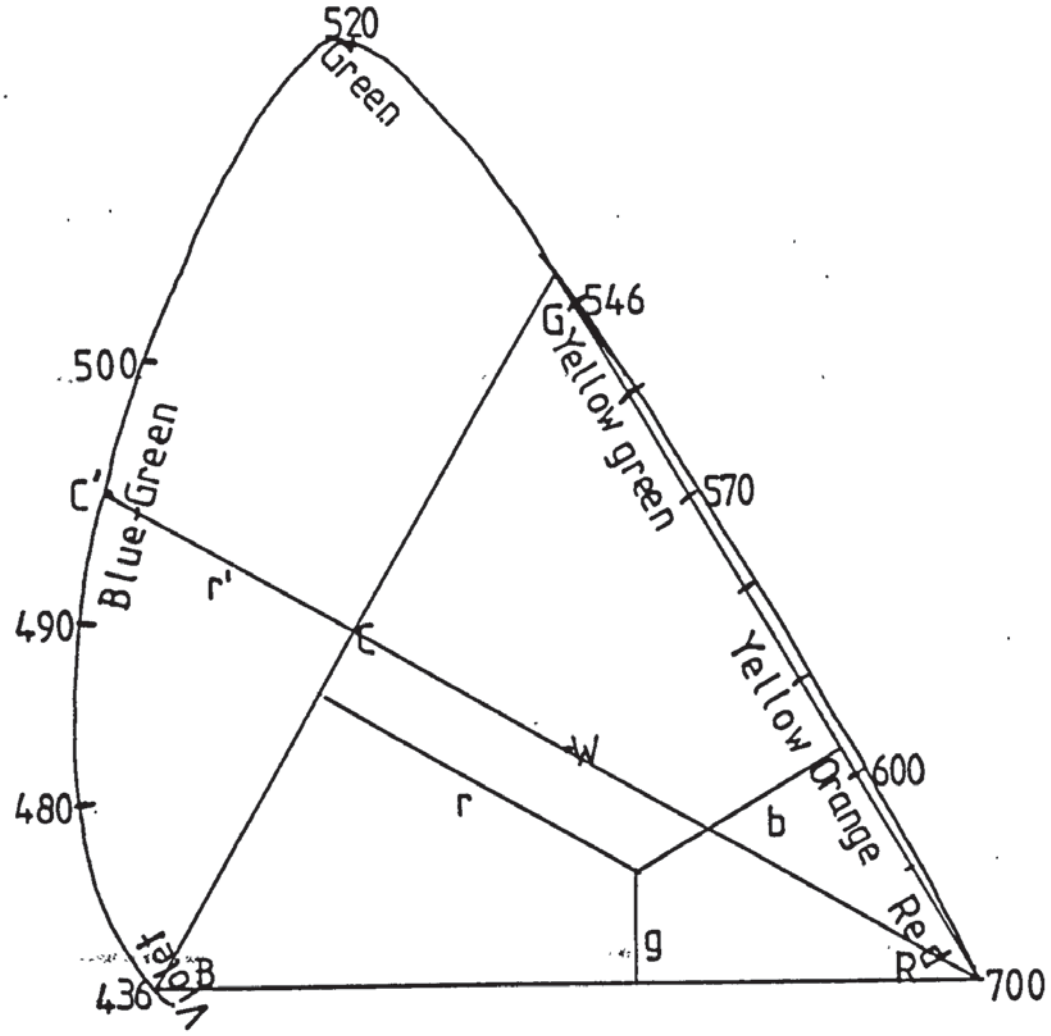

Fig. 1·9 The Colour Triangle and Spectral Locus

triangle and may be plotted as follows. If we wish to match spectral cyan (495 nm) we require to add some red to the blue and green primaries in order to obtain a match. The amount of red added corresponds C-C_1. The equation is now g + b -r = 1. The spectral locus can be plotted in a similar way for other spectral colours, giving the typical flat iron shape as shown in Fig. 1·9. It should be noted that there is no curve around the base of the triangle because purples or magentas are not spectral colours.

1·3·3·5 The CIE Chromaticity Chart

In order to obviate the necessity to consider negative coordinates the CIE postulated three theoretical primaries having a greater degree of saturation than the spectral colours. These theoretical primaries do not physically exist and are therefore referred to as stimuli designated X, Y, Z.

If these stimuli are theoretical they can be designated at any convenient values, and they are chosen so that the triangle with surrounding spectral locus can be accommodated in a right angled triangle so that the chromaticity coefficients may be plotted on ordinary rectilinear graph paper. Only the x and y coordinates need to be plotted since if the sum of x, y and z is 1, the value of z is implicit. Fig. 1·10 shows the spectral locus superimposed on to a right angled triangle with the XYZ stimuli positioned as shown.

(cont'd. p. 29.)

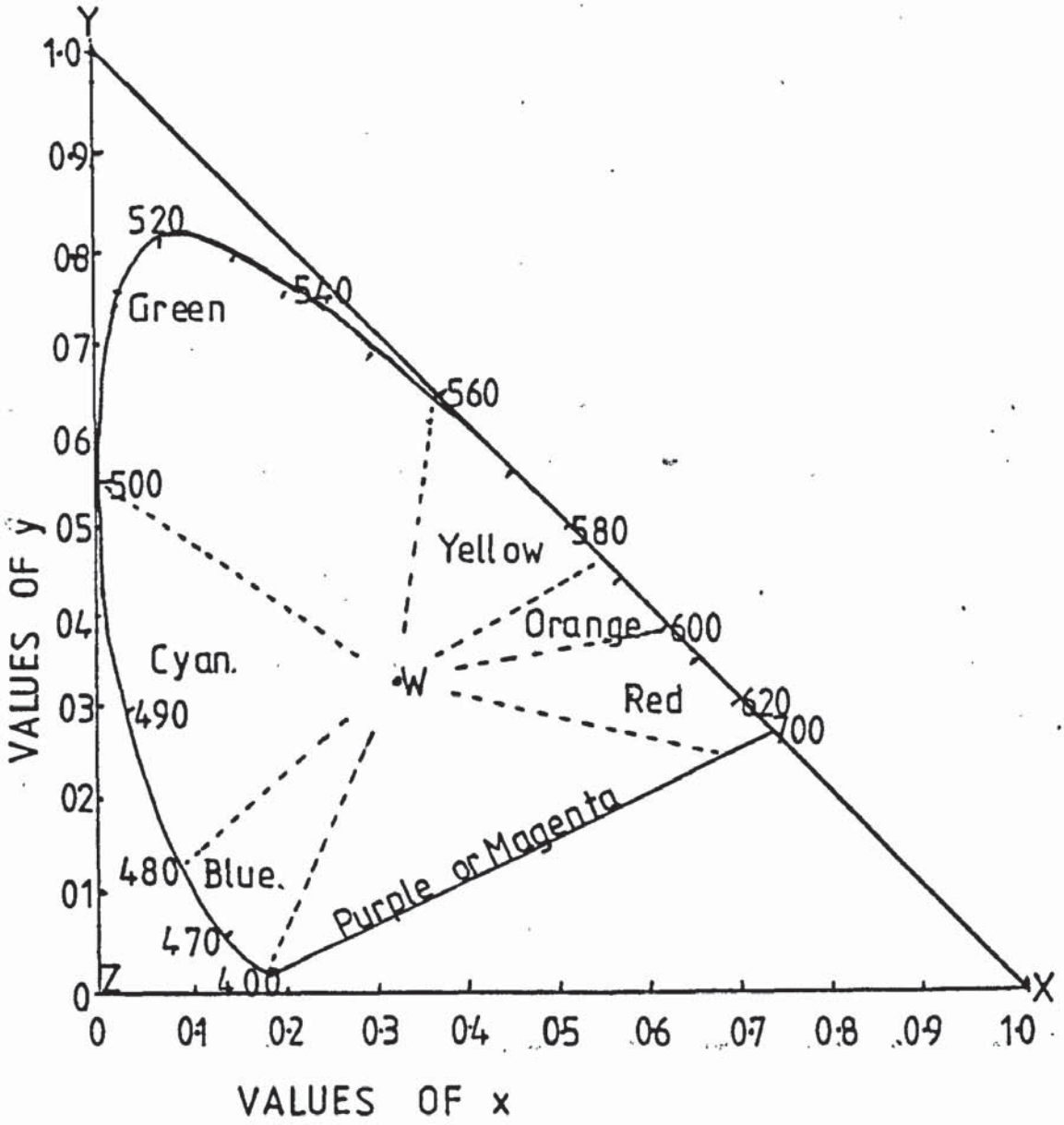

Fig. 1·10

The colour triangle and spectral locus superimposed on a right angled triangle

1·3·3·6 The Conversion of Colorimeter Readings to CIE Tristimulus Values

Providing the values of the three real primaries in an additive colorimeter are known, the measurements for the colours can easily be converted into CIE tristimulus values. A sample calculation is given in Appendix 5.

1·3·4 Spectrophotometer Readings

The end product of a spectrophotometric measurement is a reflectance curve against wavelength of incident light. Although these curves tell us which parts of the spectrum are the most strongly reflected they do not give us an immediate impression of the colour. Thus it is necessary to convert the curves obtained into CIE chromaticity coordinates, and in order to do this tables of distribution coefficients are made use of. These have been determined by standard observers, by measuring the amounts of X, Y and Z stimuli corresponding to each wavelength of the spectrum. The tristimulus values for the spectral wavelengths are designated x, y and z. Fig. 1·7 gives the distribution coefficients for the standard observer under equi-energy conditions. The distribution coefficient for x is multiplied by the reflectance at each wavelength and the sum of these values obtained. Similar calculations are carried out for the y and z values. These totals then express the redness (x), the greeness (y) and the blueness (z) of the sample. The redness, greeness and blueness are expressed as proportions of the total red, green and blue to give numbers between 0 and 1 called the chromaticity coefficients such that $x + y + z = 1$. A sample calculation is given in Appendix 6. By convention the y

total indicates luminosity; it is calculated as a percentage of the total possible for y assuming 100% reflectivity.

The colour position may now be plotted on the CIE chart. From this we can calculate the dominant wavelength and saturation, by the methods given in Appendix 6.

Real light sources do not give an equal energy spectrum so that when we consider standard illuminants such as S_A the distribution coefficients are weighted by considering the actual energy distribution at each wavelength, e.g. E X x = weighted distribution coefficient where E is the actual percentage energy at the wavelength under consideration for the stated illuminant.

1·4 THE INFLUENCE OF ATOMIC STRUCTURE ON THE COLOUR OF METALS AND ALLOYS

Saeger and Rodies[44] have related the colours of gold and its alloys to the effect of energy band structures. They state that the colour is governed by the dependence of its reflectivity upon the energy of the incident light. Thus a material possessing a much higher reflectivity for the low energy end of the visible spectrum (red and yellow light) than for other parts of the spectrum will have a red or yellow colour. It is postulated that the yellow colour of gold is caused by the pronounced step in the reflectivity curve at an energy of incident light of approximately $3{\cdot}7 \times 10^{-19}$ J (2·3e V). This is illustrated in Fig. 6·2. Absorption processes in metals are made possible by band transitions of electrons from the conduction band to energetically higher bands or transitions from lower bands to energy

states of the conduction band situated above the Fermi level. Thus from band calculations we can predict the energy value of incident light which leads to intense absorption. Band calculations are exceedingly complex but these have been carried out by Osborne, Fletcher and Miller[45] and Fong[46] et al, so that calculations are available for most of the pure metals, a number of intermetallic compounds, and a few dilute alloys. Whether or not an electron can be promoted by incident light of a certain energy depends upon the energy gap between conduction band and the next lower energy level. All these conditions are met in gold for an intense absorption process at $3{\cdot}7 \times 10^{-19}$ J from the d band to unoccupied states in the conduction band. If we consider the electronic structure of gold, copper, and silver given in Appendix 7 we see that they are all quite similar, all of them containing a filled d band below the conduction band. Copper gives a step in the reflectivity curve but at slightly lower energy which accounts for the red colouration of copper. On the other hand, the d bands in silver are situated so far below the Fermi level that energy in excess of that found, even at the high energy end of the spectrum, is required to promote the electron. Thus the reflectivity curve for silver is flat, and silver is a white metal. Koster and Stall[47] and Fukutani[48] have shown that as silver is alloyed with gold the reflectivity edge is moved to higher and higher energies; thus not only the red and yellow but green is strongly reflected. Eventually the step is moved out of the confines of the visible spectrum and the alloy is white. This behaviour is quite understandable, since the structure of silver and gold is so similar that we would expect the band structure to be preserved throughout the spectrum, but with a widening of the original gold band gap leading to the

displacement of the reflectivity curve. Another mechanism is postulated for the decolourising effect of nickel or palladium. When monovalent noble metals are alloyed with transition metals virtually bound states occur. Abelès[49,50] showed that the maxima of the relatively broad absorption peaks caused by these virtually bound states lie at energies of $1{\cdot}29 \times 10^{-19}$ J for Au-Ni and $2{\cdot}74 \times 10^{-19}$ J for Au-Pd. Thus absorption processes become possible at energies considerably below those necessary for absorption processes in pure gold. Hence the addition of these transition metals to gold results in markedly decreased reflectivity in the red end of the spectrum and even in the infra red. Thus the step becomes less pronounced and eventually is flattened and the alloy decolourised. Yet another mechanism is responsible for the colours of intermetallic compounds. In the case of intermetallic compounds an entirely new band structure is produced which bears no resemblance to those of the constituent metals, but band calculations can still be carried out for them and it has been shown that band translations can occur at specific energy values over a small energy range. Thus the reflectivity curves of such compounds as $AuAl_2$, $AuIn_2$ and $AuGa_2$, exhibit a dip in the middle of the visible spectrum with a rise towards the violet end. Thus the compounds referred to exhibit a blue colouration, $AuIn_2$ giving the most definite blue colouration. All the forgoing refers to solid thermal alloys.

1·5 THE STRUCTURE AND GROWTH OF ELECTRODEPOSITS

Since the colour of a metal or alloy is closely linked with its internal structure, it should be instructive to consider the growth of an electrodeposit and the mode of substrate coverage.

1·5·1 Epitaxy

When metal atoms arrive at the surface of the substrate during deposition, they tend to occupy positions that continue the grain structure of the substrate even though this structure is not typical of the normal structure of the depositing metal.[51] If the lattices of the substrate and depositing metal are similar, this type of growth can continue indefinitely and it is called "epitaxial". If the two metals differ substantially, the growth pattern usually shifts towards that of the deposit itself and is referred to as "psuedomorphic". Patterns of growth may also be altered by the incorporation of adsorbed material into the growing surface, and this may prevent the formation of normal lattice and inhibit the formation of large grains. The type of metallographic structures commonly found in electrodeposits include columnar, equiaxed and banded.

1·5·2 Crystal Growth of Electrodeposits

Fig. 1·11 illustrates the mode of growth of electrodeposits in a spiral fashion. Cations, which are positively charged, are attracted to the negatively charged cathode, and the hydration sheath is pushed aside and finally removed as the cation is adsorbed on to the surface. The adion then diffuses across the surface to a kink site where it can be bonded in three directions. The result of this is a continual changing of the orientation of the dislocation edge resulting in a spiral growth.[52] This is a rather idealised picture referring to single crystal conditions. It must be remembered that any substrate surface consists of numerous crystal faces of various orientations,

(contd. p. 35)

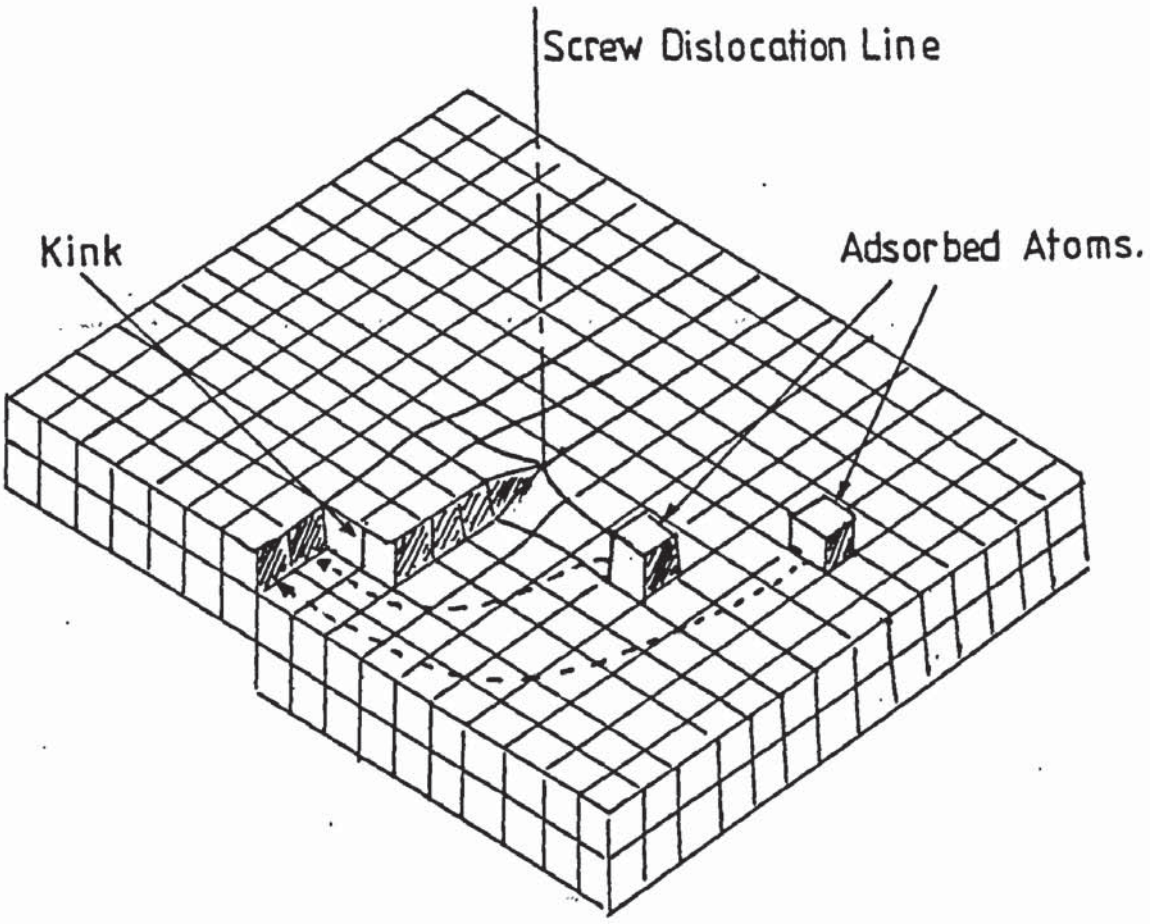

Fig. 1·11

The mode of growth of electrodeposits

and that in the (111) plane for example there will be stronger bonding for the oncoming ion than on the (110) plane.

1·5·3 Studies of the Growth of Silver and Gold by Vacuum Techniques

Vook[53] has shown that the mode of growth for silver and gold on copper is for the formation of small islands which grow to about 4-5 monolayers thick, after which they widen by thin extensions estimated to be about 1 monolayer in height. These extensions tend to thicken as more material is deposited. When the average growth is 5·5 nm for silver and 0·6 to 1·1 nm for gold, the coating is said to be continuous. The mode of growth is illustrated in Fig. 1·12. It must be emphasised that these experiments were carried out by vacuum deposition on (111) copper substrates produced on NaCl covered mica.

1·6 THE ELECTRODEPOSITION OF ALLOYS

1·6·1 The Formation of Alloy Electrodeposits

In order to codeposit two or more metals it is necessary that the decomposition potentials of their ions in solution are close together. Bockris[54] and Potter[55] give an explanation of this summarised as follows. Consider the polarisation curves of two metals A and B as shown in Fig. 1·13. If the potential is held at or more negative than E_1 then only metal A will be deposited and this will continue until all the A which can be deposited at this potential has been removed. It must be remembered that the equilibrium potential (which must be exceeded in a negative direction for electrodeposition) is continually becoming more negative as the activity of the ions

(cont'd. p. 37.)

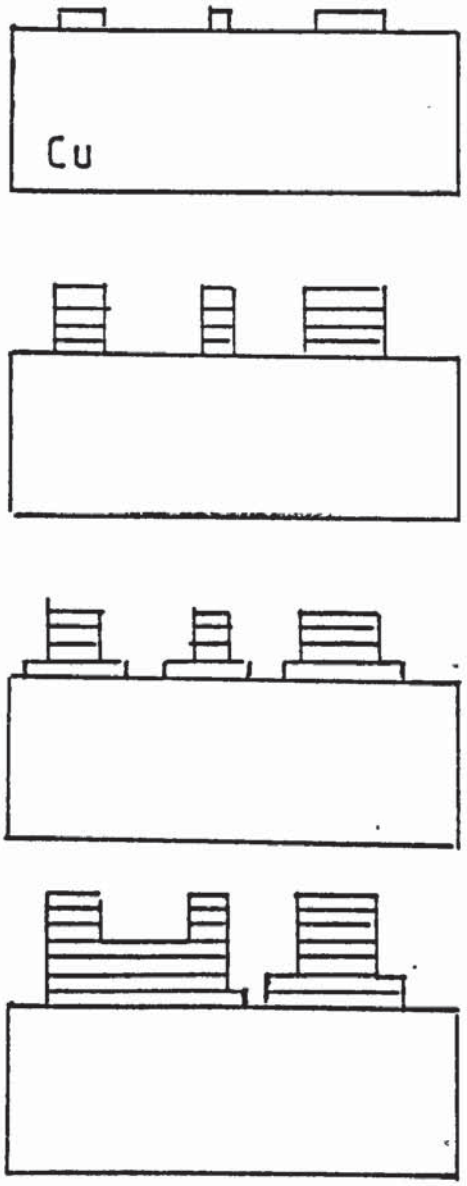

Fig. 1•12

The growth of gold and silver on copper

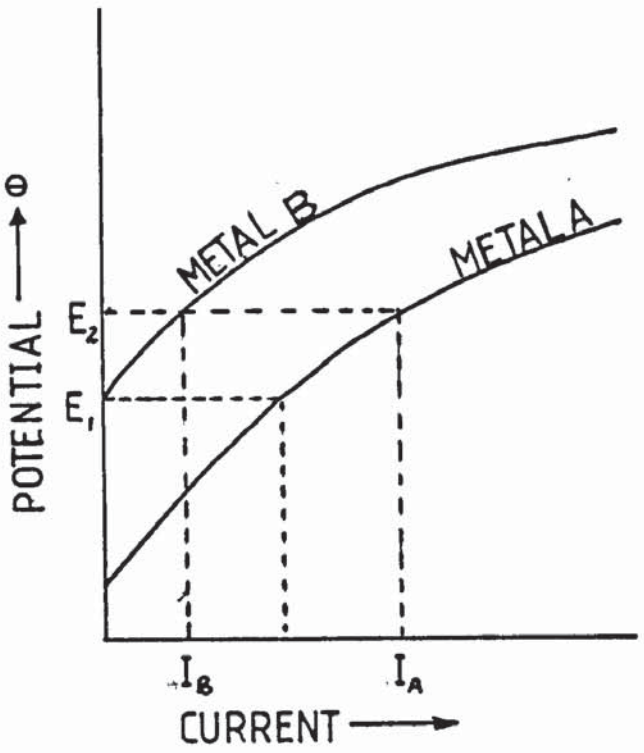

Fig. 1·13

Polarisation curves

decreases according to the Nernst equation:

$$E_{Mz+/M} = E^{o}_{Mz+/M} + \frac{RT}{zF} \ln \frac{a_{Mz+}}{a_{M}}$$

If the potential is now decreased to the more negative potential of E_2 then both metals can be simultaneously electrodeposited.

Current for the deposition of A = I_A

Current for the deposition of B = I_B

From this we can calculate the composition of the resulting deposit:

wt of A deposited = $\frac{I_A t A_A}{F z_A}$ wt of B deposited = $\frac{I_B t A_B}{F z_B}$

where t = time in seconds

A = relative atomic mass of the metal given as subscript

F = Faraday

z = change in charge number of metal given as subscript

$$\text{wt of A in deposit} = \frac{I_A A_A z_B}{z_B(I_A A_A) + z_A(I_B A_B)} \times 100$$

Thus we can see that the polarisation curves must be close together otherwise an unacceptably high current flow will result before the second metal is deposited. In many cases the equilibrium potentials of the two are much too far apart for practical codeposition and hence the ions are complexed by such agents as cyanide. Many alloy electroplating solutions involve codeposition of hydrogen and this also affects the deposition of the polarisation curves, and by inference the composition of the deposit.

Observations on the current density-potential relationships made by Grube,[56] Zvolner,[57] Raub[58] and Krasikov[59] indicate that the difference in potential in the cyanide gold-copper bath is 0·2 volt, and that this gives rise to a diffusion controlled process in which copper is codeposited when the limiting current for gold is reached. The potential gap is even narrower in low pH, free cyanide baths.

1·6·2 The Structure of Electrodeposited Alloys

1·6·2·1 Gold-Copper Alloys

The thermal gold-copper alloys form a single phase face-centred cubic solid solution.[60] At lower temperatures two ordered states of the cubic phase exist (see Fig. 1·14). An intermetallic compound, AuCu, can exist below 424°C (75·5% Au) and $AuCu_3$ (51% Au) below 396°C.

(cont'd p.40.)

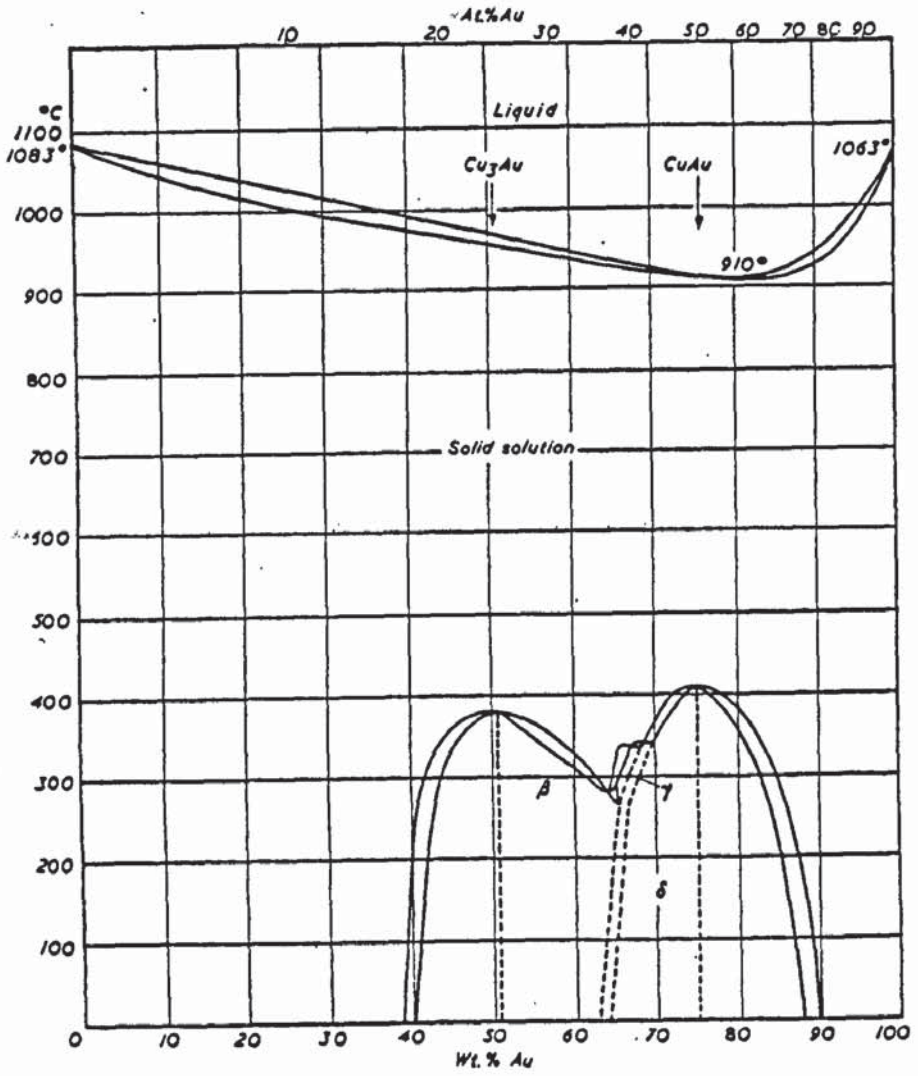

Au-Cu

Fig. 1·14

The gold copper thermal equilibrium diagram

Information on the structure of gold-copper electrodeposited alloys comes mainly from the work of Raub[58,61] and Raub and Sauter[62] and their work showed that the deposits consisted largely of separate crystals of gold and copper. Raub attributed this two phase structure to the gap between the deposition potentials of gold and copper, indicating that the limiting current for gold would have to be exceeded before copper would be deposited. Raub also found that when low free cyanide baths were used the deposit consisted of a mixture of solid solution together with copper and gold crystals. The relative amounts of each phase being dependent upon the copper content of the deposit, the higher the copper content, the greater the proportion of solid solution.

1·6·2·2 Gold-Silver Alloys

The equilibrium diagram for the gold-silver system given in Fig. 1·15 shows that the system consists of a continuous range of solid solutions without any intermetallic compound formation. The liquidus and solidus are very close together indicating a very small melting range. Raub has shown that the structure of the electrodeposited alloy is very similar to that of the thermally prepared alloy, namely a single phase solid solution.

1·7 THE GOLD ELECTROPLATING PROCESS

1·7·1 Introduction

Although it is approximately 130 years since the advent of commercial gold electroplating it was not until the 1950s that the first patent

(contd. p.42.)

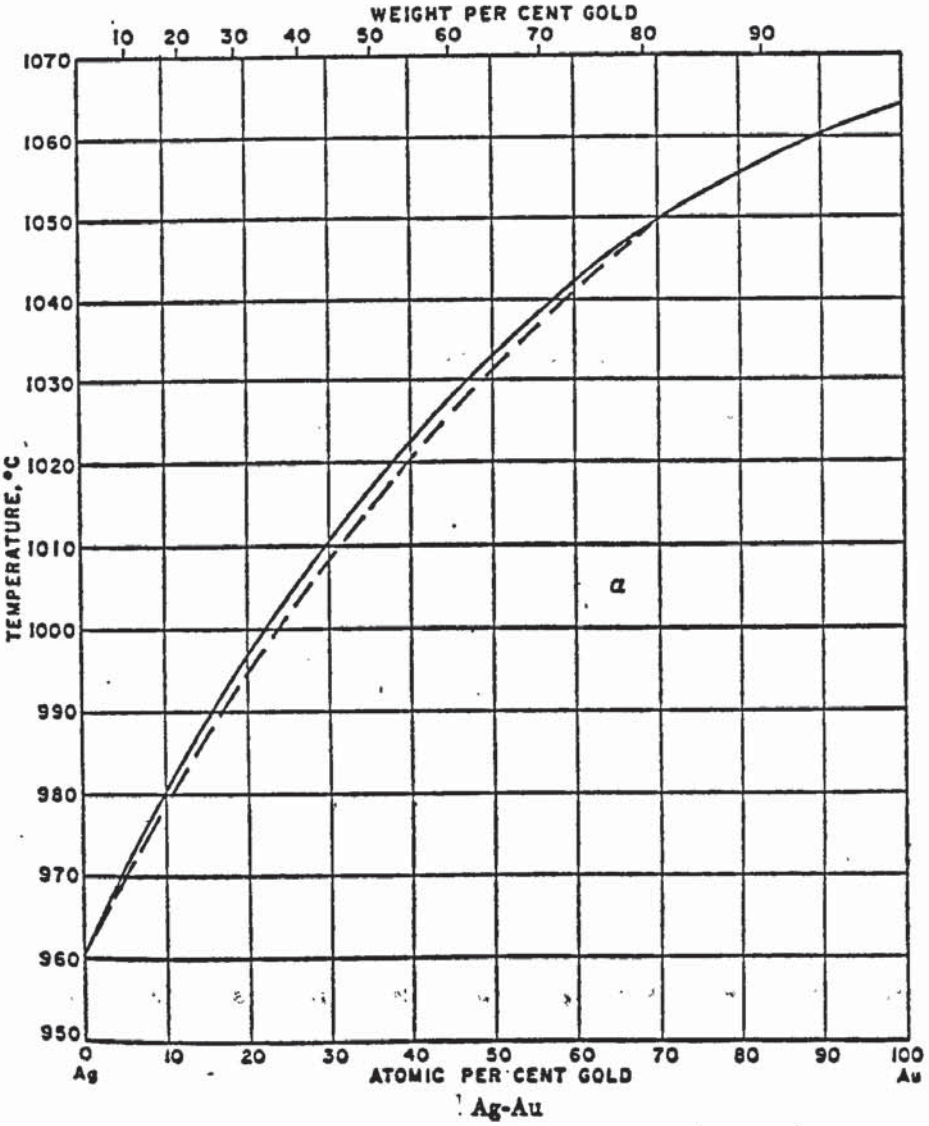

Fig. 1·15

The gold silver thermal equilibrium diagram

for a bright gold bath made its appearance. Until this time much of the literature had been devoted to the regurgitation of recipes. Foulke calls the 1950s the "explosive era" with respect to gold plating, in which low pH cyanide baths were developed. A review of gold electroplating published by Page[63] categorises gold baths as

(i) Alkaline cyanide

(ii) Neutral cyanide

(iii) Acid cyanide

(iv) Non-cyanide (comprising halide, sulphite and organo-metallic)

Clarke and Leeds[64] describe three gold electroplating baths, the alkaline cyanide bath, the acid citrate bath, and the phosphate bath. Thus we can see that there is quite a large selection of types of bath available.

1·7·2 The Chemistry of the Process

Since most of the present work was concerned with the cyanide process, the chemistry of this process will be considered. Much work has been done on the study of complexes in the cyanide solution and an extremely comprehensive survey has been published by Page.[63] He concludes from stability constant values that the stable form of the ion in the cyanide gold electroplating bath is $Au(CN)_2^-$. Although higher coordination complexes are possible, notably $Au(CN)_4^-$, thermodynamic data shows that at potentials below 0·91 volts reduction of the quadrivalent complex will rapidly occur resulting in the stable monovalent form. This is tantamount to saying that as soon as electrolysis commences the higher valent complex will be reduced. The E° value for the $Au(CN)_2^-$ complex is -0·61 volt in comparison with the simple ion value of +1·7 volts,

and this explains the ease with which gold can codeposit with base metals. Free cyanide, i.e. cyanide in excess of that required to form the complex, has the major task of ensuring that the concentration of metal cations remains negligibly small, so that deposition occurs directly from the tetrahedral (sp) cyano-complex. Other functions of the free cyanide include improvement in throwing power and conductivity.

1·7·3 The Electroplating Conditions

1·7·3·1 Anodes

Due to the tendency of gold anodes to dissolve during "down times", it is now the practice to use inert anodes such as stainless steel or platinised titanium.

1·7·3·2 Solutions

From the point of view of economy it is advisable to keep the gold content of the baths as low as possible (gold was quoted at £180·45/ fine ounce on 28/9/1979[65]). The gold is added as gold potassium cyanide, with free potassium cyanide, and various quantities of disodium phosphate and alkali carbonate. Neutral or slightly acid solutions are made possible by the use of citrates or phosphates.

1·7·3·3 Temperature

All the baths are operated in the region of 60-70°C.

1·7·3·4 Current Density

Since the gold contents of the baths are in general low, current densities are also low.

1·8 THE ELECTRODEPOSITED COLOURED GOLDS

A fair amount of information exists in the literature on coloured gold electrodeposits, and although much of it consists of solution "recipes", Brenner[66] gives an impressive distillation of the available information.

1·8·1 The Production of a Desired Colour

Brenner[66] states that the procedures for obtaining a desired colour are established by an operator on the basis of practical experience. The addition of copper to an electroplating bath is the only metal which increases the redness of the gold, other alloying elements lighten the shade to white or greenish colours. Field[71] has shown that 70% of silver is required in the deposit before a truly white deposit is obtained, while Raub[72] has shown that 30% of tin or 15% of nickel is required for this condition. Brenner[66] states that the electroplating time is likely to have an effect on the alloy content of deposits, since with time cathode layer depletion is likely to occur, which because of the relevant electrode potentials leads to flash deposits having a higher gold content than thicker deposits.

1·8·2 Gold-Copper Alloys

Brenner states that workers such as Dole,[67] Raub[62] and Krasikov et al[68] have studied the gold-copper electroplating system in dilute metal cyanide baths and have shown:

(i) Gold is by far the more readily deposited metal.[68,70]

(ii) An increase in free cyanide markedly decreases the copper content of the deposit.[67] As would be expected from this Parker[69] has shown an increase in the free cyanide content of the bath makes the deposit yellower, because it decreases the current efficiency of copper deposition more than that of gold.

(iii) Addition agents such as thiourea give rise to bright deposits,[59] and increase in the copper content of the deposit.

(iv) The copper content of the deposit increases with current density.[62]

(v) The copper content of the deposit increases with increase in temperature.[67,70]

(vi) Agitation of the bath decreases the copper content of the deposit.[62]

All the factors mentioned must have an effect on the colour of the deposit produced, since it is to be expected that with increasing copper content the deposit will be more red. Thus we can see that the baths themselves have been quite thoroughly investigated. Hence it was considered that it would not be fruitful to consider this aspect in the present work.

1·8·3 Other Alloying Metals

Similar investigations have been carried out on other alloy systems notably, silver,[71,56,58] nickel[72,73,74,75] and cobalt.[72,73,74]

1·9 COLORIMETRIC MEASUREMENTS ON VARIOUS METALS AND ALLOYS

Few fundamental colorimetric studies of alloys are reported in the literature although Gardam[76] has measured the spectral reflectivity curves of metals and alloys including gold and gold alloys, sterling silver, platinum, nickel silver and stainless steel. Positions on the colour triangle were calculated. It was found that copper and gold and the alloys of these metals gave red or yellow colours with low saturation values. The remainder were very near to the white point, exhibiting a white or grey colour with zinc, chromium and aluminium exhibiting a bluish tinge. The copper and gold alloys gave rise to reflectivity curves containing a step, whilst the basically white or grey metals gave fairly flat reflectivity curves. Gardam[77] has also studied the dyeing of anodised aluminium by the use of the spectrophotometer, from the results of which he derived spectral reflectivity curves, chromaticity coordinates, and luminosity values. He was able to determine the effect of process variables on the colour of the films produced. He included a brief but very useful summary of the method of converting reflectivity measurements to chromaticity coefficients.

Roberts and Clarke[78] measured the colour characteristics of a number of thermally prepared gold alloys in the binary and ternary gold-silver-copper system. They comment on the paucity of information on fundamental studies on gold alloys and remark that most colour assessment of gold alloys has been carried out in the past by comparison with specially prepared standards (Din 8238). They also comment on other comparison methods such as that by Leuser[79] which

consists of a diagram of many panels of the various gold alloys. Wise[80] reproduced this diagram with slight modifications. Clarke and Roberts used a spectro-ellipsometric technique to measure the optical constants such as relative phase change, relative amplitude change, complex refractive index function, reflectivity function, CIE colour coordinates, luminance, saturation, and dominant wavelength.

A review of the optical properties of gold has been made by Loebich[82] mostly concerning vacuum deposited layers a few nanometres in thickness. Reflectivity values for gold obtained by a number of authors[83-90] are given and although all agree that a reflectivity step is apparent in the visible region some workers have shown it to be much steeper than others. Loebich comments that this may be due to the results of Phillip and Robin being conducted on vacuum deposited films which were not sufficiently free from defects. Loebich also comments that defects in the lattice as well as the presence of alloying atoms tend to aggrevate light absorption by free atoms, at the long-wave end of the spectrum. Any rise in temperature will produce the same effect. It is postulated that absorbed radiation energy is partially re-emitted (possibly involving changes in frequency as soon as excited electrons return to their original state). Part of the absorbed energy is converted into heat as in the case of triple collisions of photon/electron and lattice ions.

1·9·1 Comment

Thus we can see that most of the work which has been done on the

colour of metals and alloys has been directed towards matching of standards. That which has been concerned with the instrumental measurement has been primarily concerned with solid thermally prepared alloys or vacuum deposited metals rather than with electrodeposits.

1·10 THE SCANNING ELECTRON MICROSCOPE

1·10·1 Principles

Electron microscopy depends upon the impingement of a beam of electrons on to a specimen and the interaction of these electrons with the specimen. Although there are similarities between electron optics and light optics there is one vital difference which complicates the construction of the electron microscope, i.e the wavelengths of photon radiation vary between 400-700 nm whilst the electron wavelengths vary between 0·001 and 0·01 nm. This means that electrons are very easily absorbed by many materials, and it is necessary for the optical system to be evacuated to a pressure of less than 10^{-4} Torr.

1·10·2 Production of the Electron Beam

Fig. 1·16 shows the production of the electron beam by means of thermionic emission of a tungsten filament.

1·10·2·1 The Thermionic Triode Electron Gun

The filament F is a piece of tungsten wire bent into a hair pin, and it is heated to 2800 K by the passage of an electric current and at this temperature the tungsten wire emits both light and electrons.

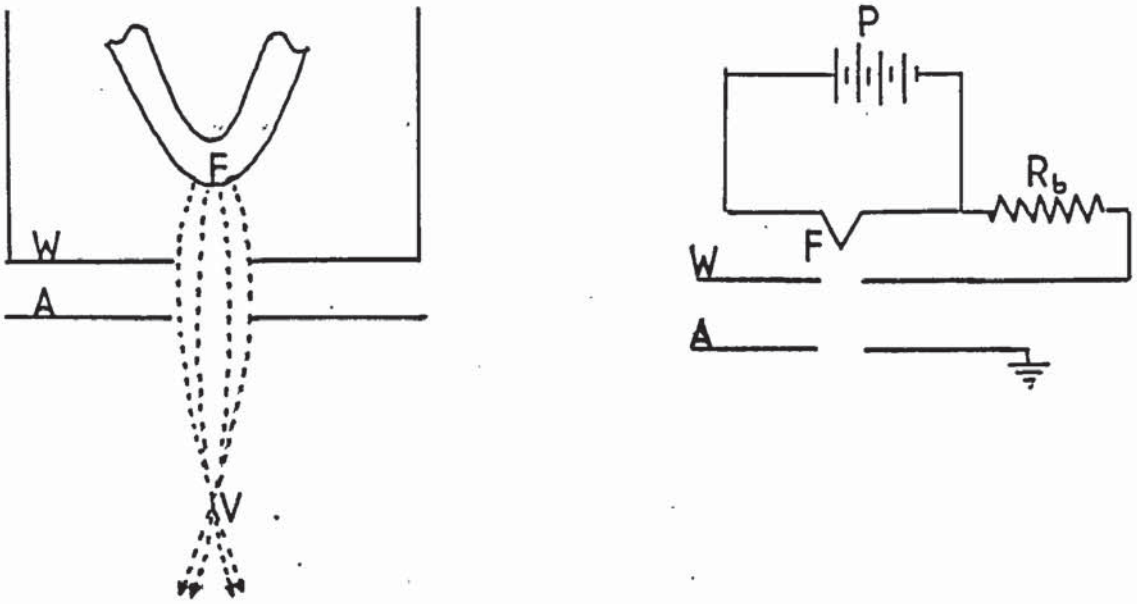

Fig. 1·16

Production of the electron beam

The filament is held at a high negative potential with respect to the anode A, and thus the electrons are accelerated rapidly towards the anode and are emitted through a hole after which they converge to a focus at V. This crossover diameter is effectively the size of the electron source, and this is controlled by the difference in potential between the filament and the grid W by the use of the bias resistor R_b.

1·10·3 The Effect of Lenses on the Electron Beam

When an electron enters a magnetic field it suffers a force Bev, where B is the magnetic field strength, e is the charge on the electron, and v is the electron velocity.

An electromagnetic lens provides a magnetic field almost parallel to the direction of travel of the electrons. An electron entering the lens experiences a magnetic field which may be resolved into the components B_{ax} along the axis of the microscope and B_{rad} in a radial direction. Initially the electron is unaffected by B_{ax} since it is parallel to the direction of movement, but it is subjected to a small force $B_{rad}ev$ from the small radial component which causes the electron to move in a helix along the lens, but immediately the continually changing orientation means that the components of the forces are continually changing, so that the helical path follows a tighter and tighter radius. Thus the beam of electrons entering the lens may be focussed to a spot by adjusting the magnetic field to precisely the right shape and strength. Several lenses of different characteristics may be used to obtain the exact conditions, but they are all basically a coil consisting of a large number of turns of wire on a soft iron core containing an accurately machined air gap.

1·10·4 The Effect of the Electron Beam when it Impinges on a Specimen

The effects are as follows:

(i) The electron may pass through without reacting in any way. This is most unlikely and only occurs in extremely thin specimens.

(ii) The deflection of the electron by attraction of opposite charges when it passes close to the positively charged nucleus of an atom, the angle of scatter lies between 0 and 180°, and virtually no energy is lost in the process, and thus is referred to as elastic scattering.

(iii) The incident electron reacts with an orbital electron and is repelled and it looses some of its energy to the orbital electron. After repeated interactions of this type the electron looses all its incident energy and is absorbed by the specimen, this is inelastic scattering.

(iv) A combination of (ii) and (iii).

The majority of electrons which are knocked out of their orbits wander around the specimen for a short time before being accepted by other excited atoms which have electrons missing from their orbitals. If the electron is near the surface (within 20 nm) it may have enough energy to escape from the surface and then becomes known as a secondary electron to distinguish it from primary or incident electrons. It is the measurement of these secondary electrons which forms the basis of the scanning electron microscope.

1·10·5 The Basic Principles of the Scanning Electron Microscope

Fig. 1·17 is a schematic diagram showing the operation of a scanning electron microscope. The electron beam is focussed on to the scanned specimen S by the condenser lens L_1 and L_2 and moved across it by the deflector coils D. The secondary electrons are converted into a current by the detector, the current is then amplified and used to control the brightness of the cathode ray tube. The fine beam of electrons is scanned across the specimen by the deflector coils D while an electron detector counts the number of low energy secondary electrons given off from each point of the surface. At the same time the spot of the cathode ray tube is scanned across

(contd p 53)

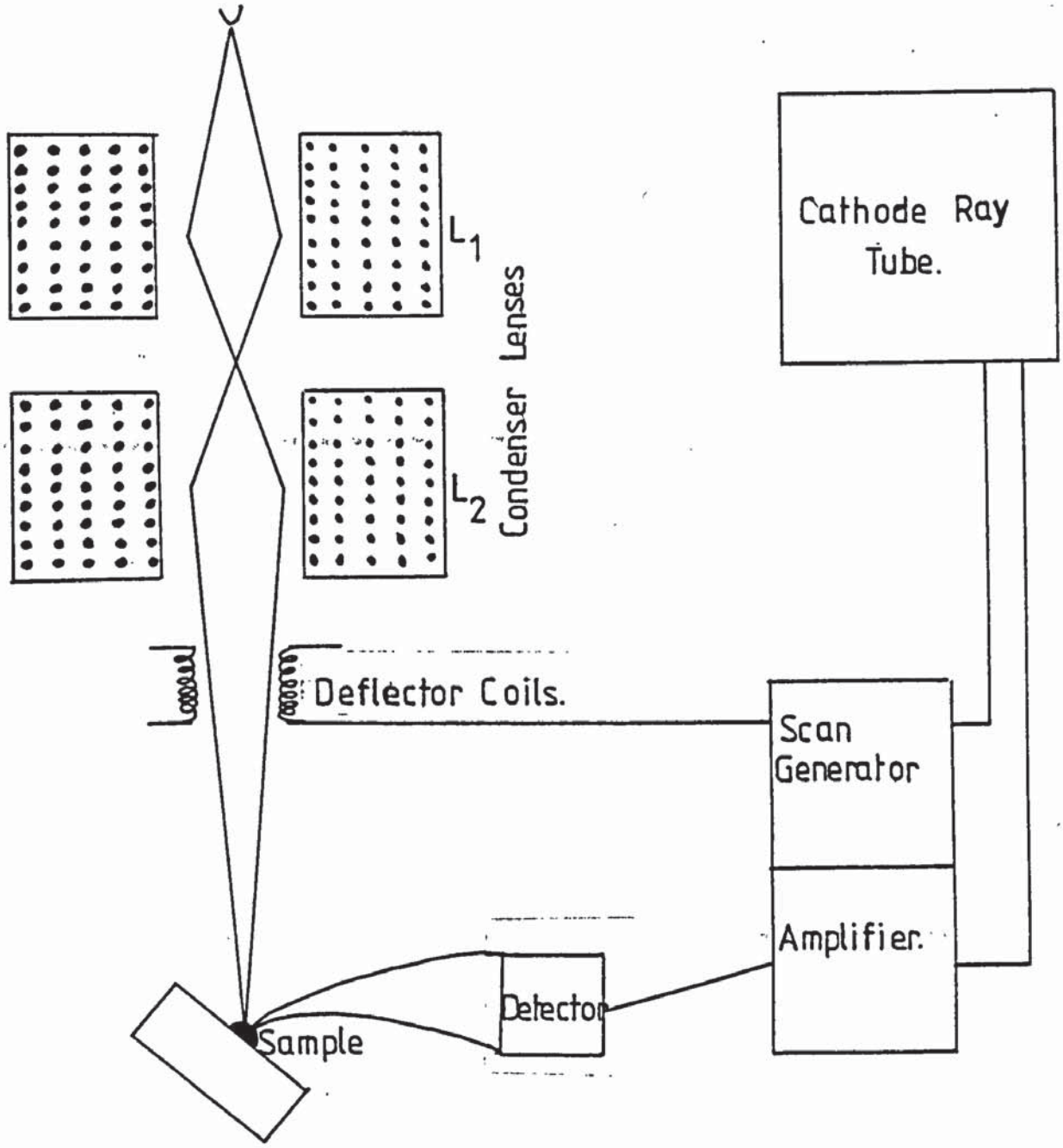

Fig. 1·17

Schematic diagram of the electron microscope

its screen whilst its brightness is controlled by the number of secondary electrons counted. In this way the picture is built up similarly to a television picture, that is in both a rectangular set of lines, known as a raster is scanned in phase across the specimen and the cathode ray tube. A camera is built into the SEM to enable a permanent record of the picture to be retained.

1·10·6 Magnification

The magnification is the side length of the cathode ray tube divided by the side length of the raster. Thus we control the magnification by controlling the size of the raster. Technically it is possible to scan a raster as small as 1 µm x 1 µm to give magnifications of 100 000 and above, but in fact it is the resolution which is the important characteristic. The ultimate resolution is the smallest separation of two points which the microscope can detect as separate entities. This must depend on the diameter of the electron beam, and is 5-10 nm in a typical SEM. The critical electron beam diameter d is influenced by the diameter of the final aperture (A in Fig. 1·16). The larger we can make the final aperture the greater the number of the primary electrons to be concentrated on the scanning spot and by implication the greater the quantity of secondary electrons, thus we can afford to make the scanning spot smaller. But there is a limit to aperture size because of the spherical abberation. Furthermore, the smaller the aperture the greater the depth of field; and since depth of field is one of the great advantages this must be taken into consideration. A typical SEM has the facility to select one of three apertures.

1·10·7 Quantitative Analysis

When an electron fills the vacant electron site in one of the orbitals of an excited atom, the atom changes from a high energy state to a lower one. The excess energy has to be given out and one of the ways in which this can be achieved is by the emission of X-rays of appropriate energy. For example, if one of the electrons had been knocked out of the K shell of the atom and an electron from the L shell jumped in to fill the vacancy, then an X-ray of characteristic wavelength (energy) will be given out, according to the relationship:

$$\lambda\Delta = \frac{hc}{\Delta E}$$

where h = Planck constant

c = velocity of light

ΔE = difference in energy between the two states of the atom

A sample calculation is given in Appendix 8. Fig. 1·18 shows the characteristic spectrum of molybdenum.

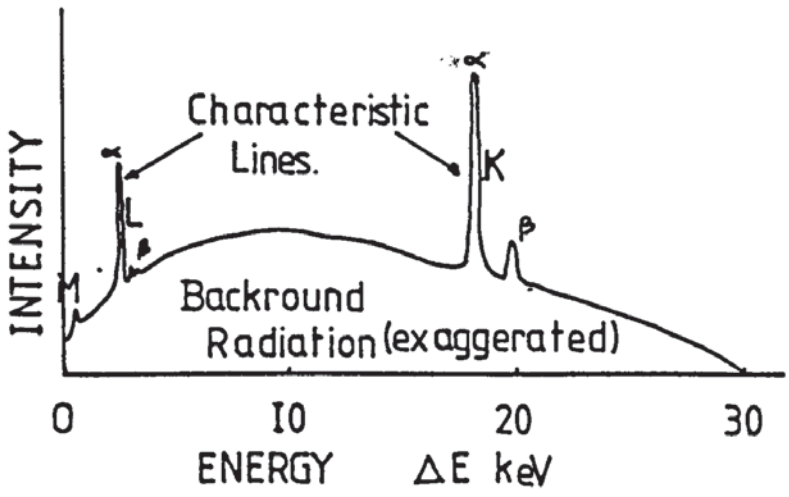

Fig. 1·18

The characteristic spectrum of molybdenum

Thus the different elements give rise to characteristic X-rays and examination of their spectra indicates the presence of a particular element. As well as the discrete electron transitions which give rise to characteristic K, L and M X-rays many other processes cause energy to be emitted as X-rays and this is what gives rise to background radiation. Thus we produce the characteristic spectra for a specimen, select the strongest peak and then compare the intensity of this peak to one produced for a standard specimen of known composition. The Kevex attachment to the SEM counts the X-rays produced, and each X-ray which enters the detector gives rise to a current referred to as a pulse, which is amplified on to a multi-channel analyser which decides which of 1000 channels, each representing a different energy, the pulse should be registered in. Thus a histogram is built up as illustrated in Fig. 1·19 which is displayed on a television screen. The number of counts represented by each peak is recorded (peak integral) and these are the values which are compared to similar peaks obtained from the standard. A sample calculation is given in Appendix 9.

1·11 THE USE OF THE SCANNING ELECTRON MICROSCOPE IN THE STUDY OF ELECTROPLATING PROBLEMS

Richards[81] has used both transmission and scanning electron microscope techniques in the study of gold electroplating. He used a heat treatment which caused blistering of the substrate surface which he found to be mirrored in the subsequently deposited gold. Dark gold deposits were found to be due to slight variations of surface roughness rather than contaminant surface films. Stress cracking of

deposit was observed. In some cases large solid nodules were observed especially towards the edges of the specimen. It was concluded that these nodules were due to the presence of foreign conducting particles in the bath. The forgoing illustrates the usefulness of electron microscope studies in electroplating research.

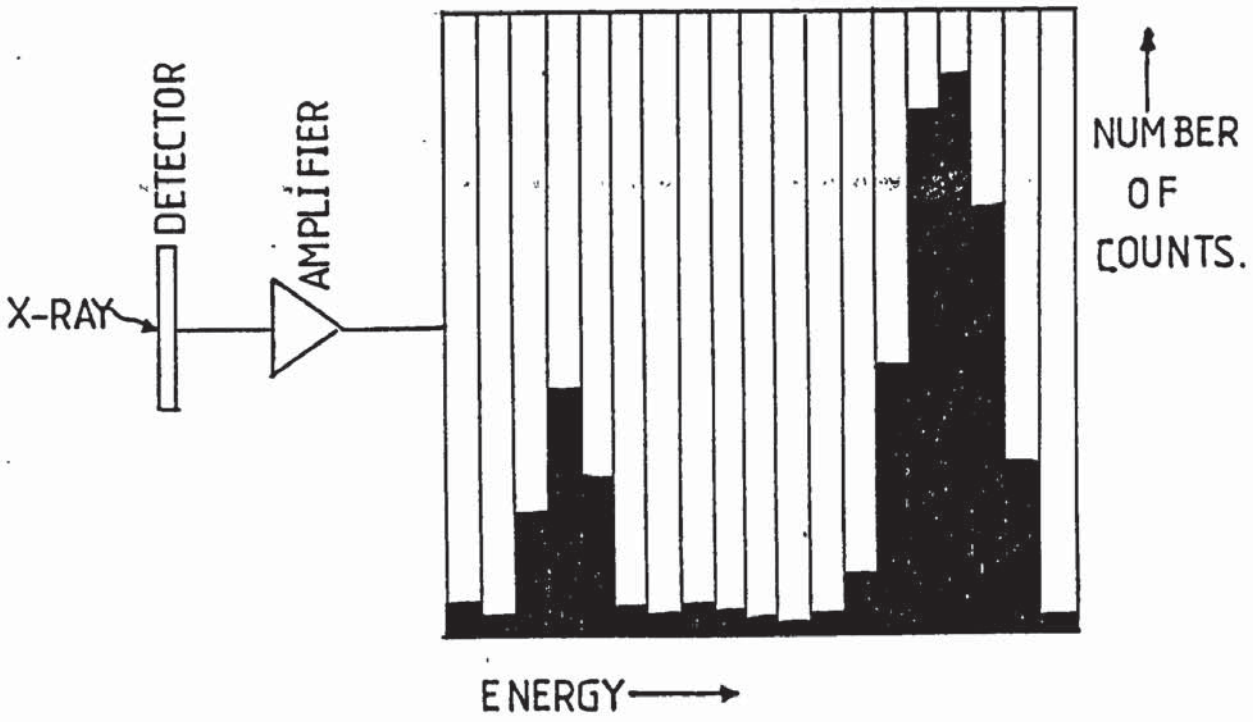

Fig. 1·19

Peak integrals

CHAPTER 2

EXPERIMENTAL APPARATUS, PROCEDURES AND TECHNIQUES

2·1 INTRODUCTION

In this chapter on experimental procedure and techniques the apparatus used is described and also the way in which the experiments were carried out. The compositions of the solutions and their basic operating conditions are given in Appendix 10. The experimental research programme is described.

2·2 EXPERIMENTAL RESEARCH PROGRAMME

The objectives of the programme were as follows:

(i) To determine the thickness of gold electrodeposit required to completely cover the substrate so that the colour of the gold was solely dependent on the deposit itself and not influenced by the substrate.

(ii) To test a spectrophotometric method of measuring the colour of gold and gold alloy deposits.

(iii) To produce gold alloy deposits and to measure their colour and where possible to relate the colour obtained to deposit and solution composition.

(iv) To examine the electrodeposits obtained by scanning electron microscope techniques to determine if there was any correlation between colour and the physical state of the deposit surface.

2·3 THE SPECIMENS USED IN THE EXPERIMENTS

2·3·1 The Pre-Treatment of the Nickel Discs

Much of the work was done on nickel discs produced by parting off by

means of a lathe from a nickel bar. The discs were approximately 1·75 mm in thickness and 32 mm in diameter except for the first group of discs which were 25 mm in diameter.

Several different pretreatments were applied to the discs, as described in the appropriate tables, and they include:

(i) Abrading by normal metallographic techniques (i.e. abrading on silicon carbide papers of increasing fineness, turning through 90° on changing grade) both with and without water lubrication. This process was carried out both on static papers supported on glass plates and on rotating wheels.

(ii) Machined lapped down to 600 grit.

(iii) Polished on a diamond wheel down to either 1 or 6 µm diamond. Either hand held or utilising the automatic apparatus attached to the wheel.

During the process stages (i) and (iii) the discs were secured to bakelite metallographic mounts by means of Araldite. The surface topography of selected discs was measured using a Talysurf machine and these results are given in Appendix 11.

Other substrates used in the preliminary experiments included cold rolled copper, aluminium, brass and nickel. The Hull cell plates were cut from rolled nickel sheet.

2·3·2 Electroplating of Nickel Discs

Regardless of the mechanical surface treatment all the discs were electroplated in the same way:

(i) An identifying number was engraved on the back of the disc.

(ii) Cleaned ultrasonically for five minutes in dilute Teepol solution.

(iii) Washed in distilled water.

(iv) Washed in acetone.

(v) Dried with hot air.

(vi) Supported around the periphery by a loop of thin copper wire as shown in Fig. 2·1a.

(vii) Degreased cathodically in the alkaline degreaser.

(viii) Washed in distilled water.

(ix) Dipped in dilute hydrochloric acid.

(x) Washed in distilled water.

(xi) Nickel struck in Wood's nickel bath.

(xii) Washed in distilled water.

(xiii) Washed in acetone.

(xiv) Dried with hot air.

(xv) Weighed accurately (four decimal places).

(xvi) Stopped off as shown in Fig. 2·1b with Canning's Lacomit stopping off medium in order to achieve maximum economy in the use of gold.

(xvii) Steps (vii) to (x) repeated.

(xviii) Electroplated in the designated gold electroplating bath, under the conditions given in the appropriate Tables and Appendix 10.

(xix) Washed in distilled water.

(xx) Washed in methylated spirits.

(xxi) Dried with hot air.

(xxii) Jigging wire removed together with as much Lacomit as it was possible to remove.

(xxiii) Washed in three changes of acetone to remove traces of Lacomit.

(xxiv) Dried with hot air.

(xxv) Weighed.

Figs. 2·2a and b show the apparatus used in the electroplating of the discs. The hot plate was thermostatically controlled and incorporated a magnetic stirrer. When low currents were required an external circuit consisting of a 185 ohm series resistor and a milliameter was used in conjunction with the 12 volt rectifier.

(contd. p. 63.)

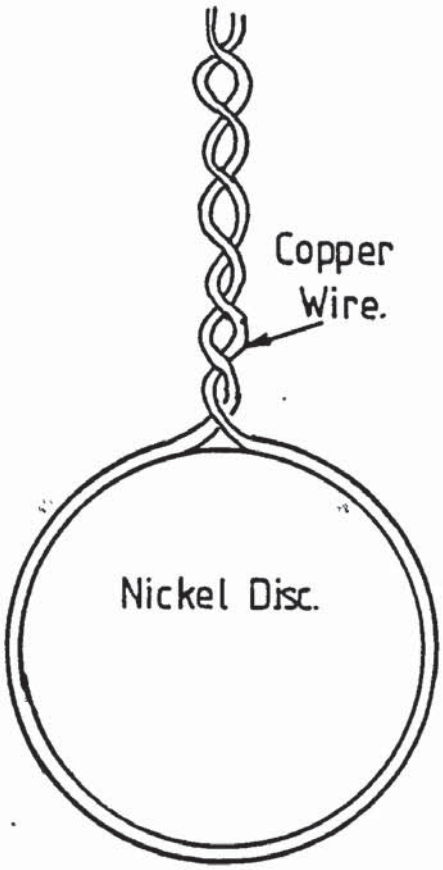

Fig. 2·1a

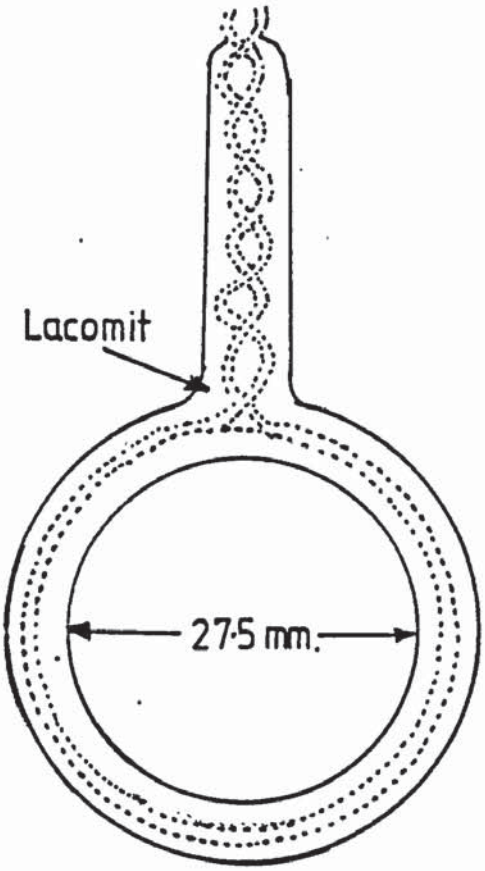

Fig. 2·1b

The mode of support and stopping off of the nickel discs

Fig. 2·2a

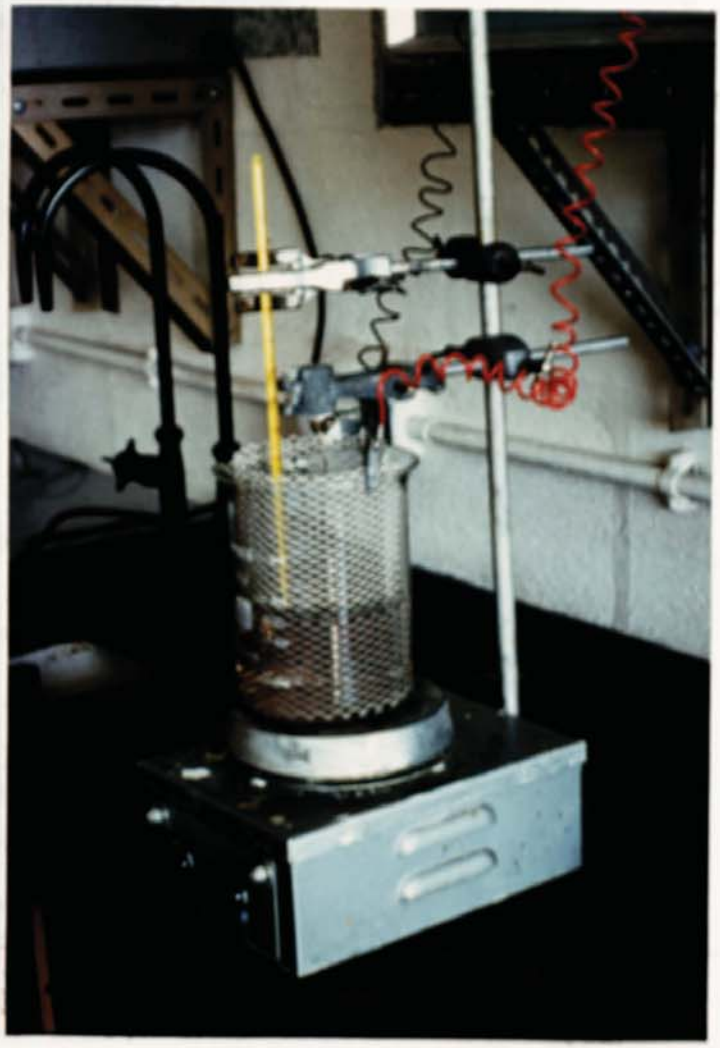

Fig. 2.2b

The Electroplating Cell

2·4 HULL CELL EXPERIMENTS

2·4·1 The Miniature Hull Cell

In order to promote economy in the use of gold, a miniature Hull cell was constructed which could be immersed in the 250 cc of solution normally used in the experiments. The construction of the cell is shown in Figs. 2·3a and b. The cell was constructed from Perspex sheet, perforated as shown to allow circulation of the solution. A stainless steel anode was used and the cathodes were cut from nickel foil to the dimensions shown in Fig. 2·3c.

Fig. 2·3a

The miniature Hull cell

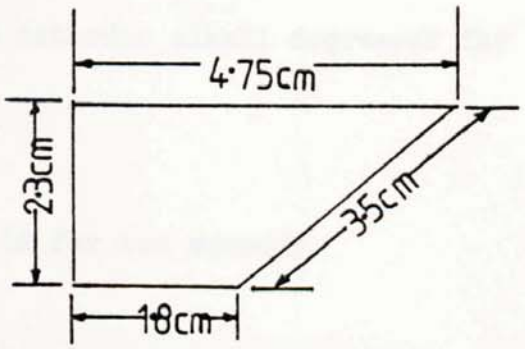

Fig. 2·3b

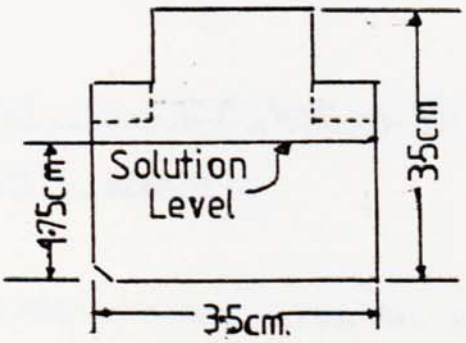

Fig. 2·3c

The Hull cell plate

2·4·2 Experimental Procedure for Hull Cell Plates

The Hull cell tests were confined to work on either the addition of indium to a gold bath or to the addition of gold to an indium bath. The indium was added to the gold bath X as solid indium chloride, while a gold cyanide stock solution was used to add gold to the indium electroplating solution. The composition of these solutions are given in Appendix 10.

2·4·3 Electroplating of Hull Cell Plates

The Hull cell plates were electroplated as follows:

(a) Degreased at 10 a.s.d. in the cathodic alkali degreaser for five minutes.

(b) Washed in distilled water.

(c) Dipped in 10% hydrochloric acid for ten seconds.

(d) Washed in distilled water.

(e) Electroplated using the conditions given in Table 9·3.

(f) Washed in distilled water.

(g) Washed in acetone.

(h) Dried with hot air.

2·5 THE COLOUR MEASUREMENTS

2·5·1 Apparatus

A Unicam spectrophotometer type SP 800 fitted with a diffuse reflectance attachment type SB 890 was used in the experiments. The optical system was as shown in Fig. 2·4, and a photograph of the equipment is given

(contd. p. 66)

in Fig. 2·5.

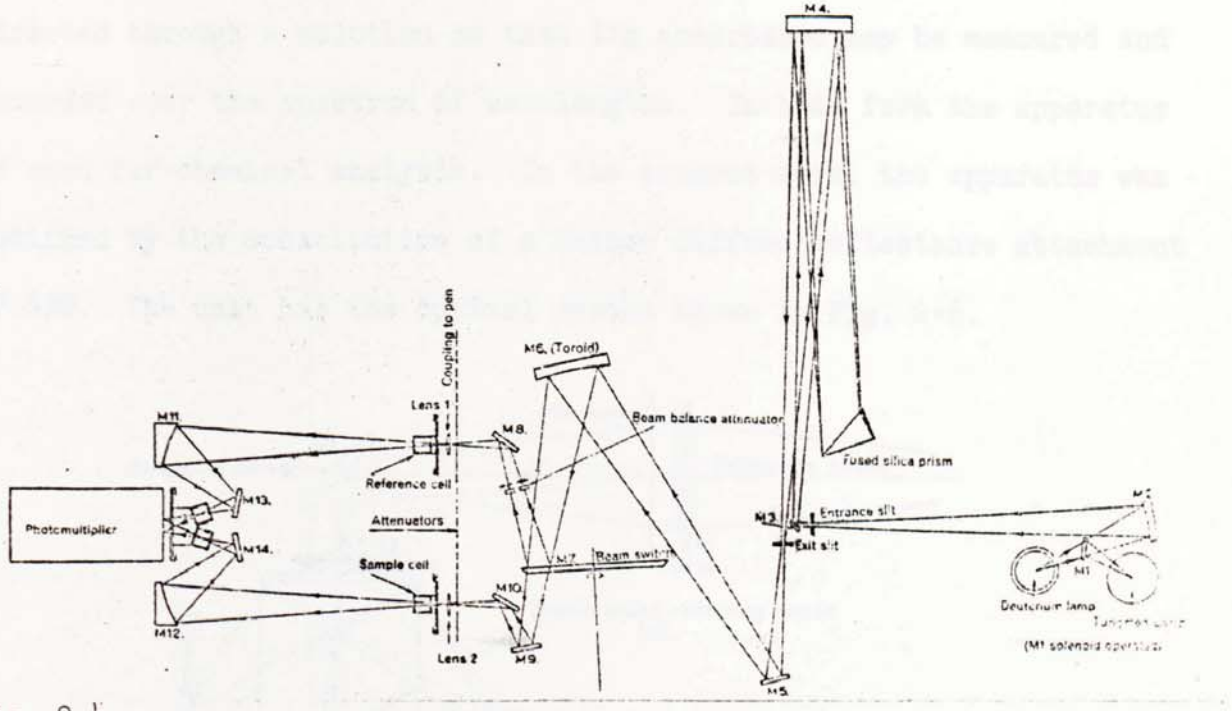

Fig. 2·4

The optical system of the Unicam SP 800

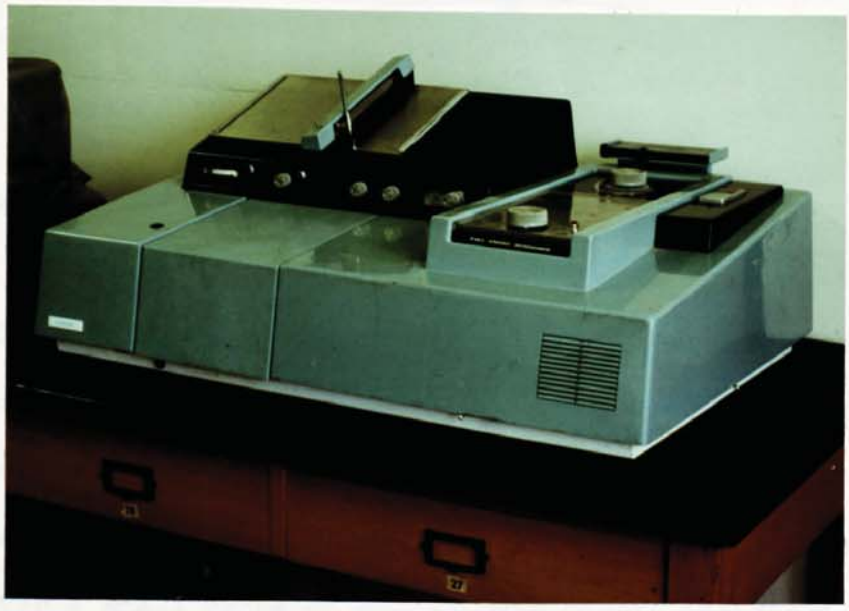

Fig. 2·5

The SP Unicam SP 800

As can be seen from the diagram, light from the tungsten lamp source is split into its constituent wavelengths each increment then being directed through a solution so that its absorbance may be measured and recorded over the spectrum of wavelengths. In this form the apparatus is used for chemical analysis. In the present work, the apparatus was modified by the substitution of a Unicam diffuse reflectance attachment SP 890. The unit has the optical system shown in Fig. 2·6.

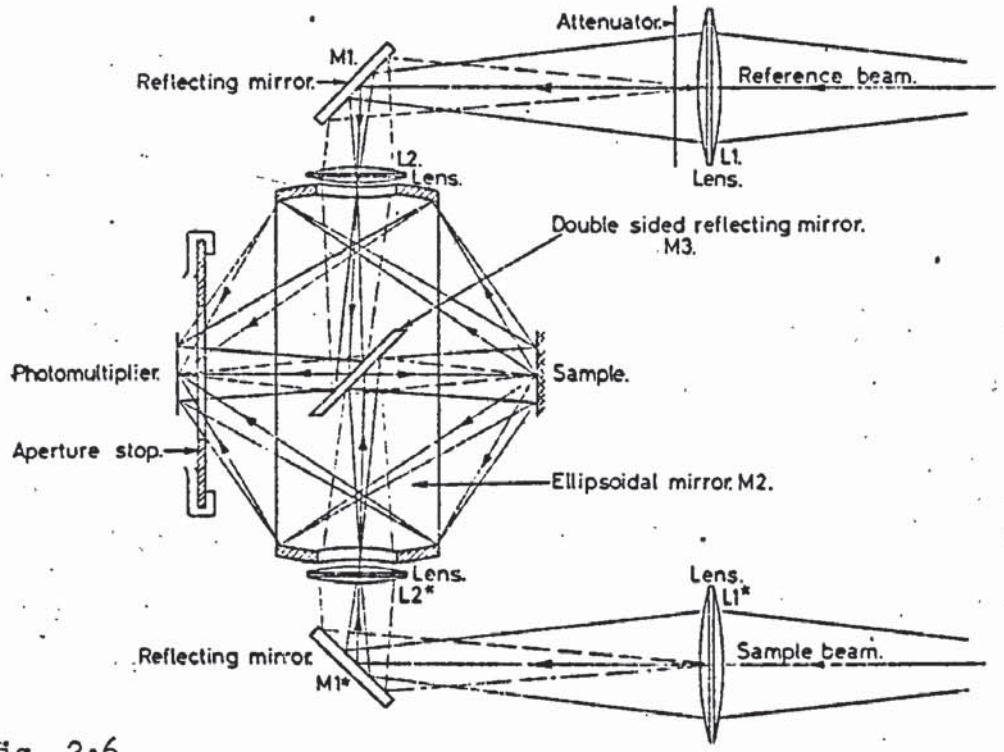

Fig. 2·6

The optical system of the diffuse reflectance attachment

Light from the sample and reference beams of the SP 800 is focussed by the lenses L1* and L1 to form images of the monochromater slit at the apertures in the side of the ellipsoidal mirror M2. Light from the sample beam falls upon one side of mirror M3 and then illuminates the sample over a small range of angles near normal incidence. An image of the prism is formed on the sample by lens L2* thus ensuring even illumination of the sample.

Light from the reference beam is reflected by the rear of mirror M3 on to the face of the photomultiplier.

The light which is diffusely reflected by the sample is collected by the ellipsoid mirror over a range of angles of reflection between approximately 35° and 55° and is focussed on to the face of the photomultiplier. The ellipsoidal mirror collects about 30% of the total diffusely reflected light and to compensate for this, an attenuator is fitted in the reference beam.

2·5·2 Method

The colour measurement was carried out as follows:

(i). The diffuse reflectance attachment (Figs. 2·7a and b) was substituted for the MT3 to M14 section of the spectrophotometer.

(ii) Analar magnesium oxide was pressed into the hollow disc provided with the jig (Fig. 2·8a). A glass microscope slide was used to apply the pressure so that a smooth surface was obtained.

(iii) The magnesium standard was placed in the jig which was then placed in the diffuse reflectance attachment (Figs. 2·7b, 2·8b).

(iv) The zero of the instrument was then adjusted and the absorbance of the standard measured over the spectrum of wavelengths, resulting in a graph as shown in Fig. 2·9.

(v) The disc under test was then substituted for the standard and the absorbance measured.

(vi) The difference in absorbance between the standard and the disc was then derived from the graph at 10 nm intervals. From

(cont'd. p.70.)

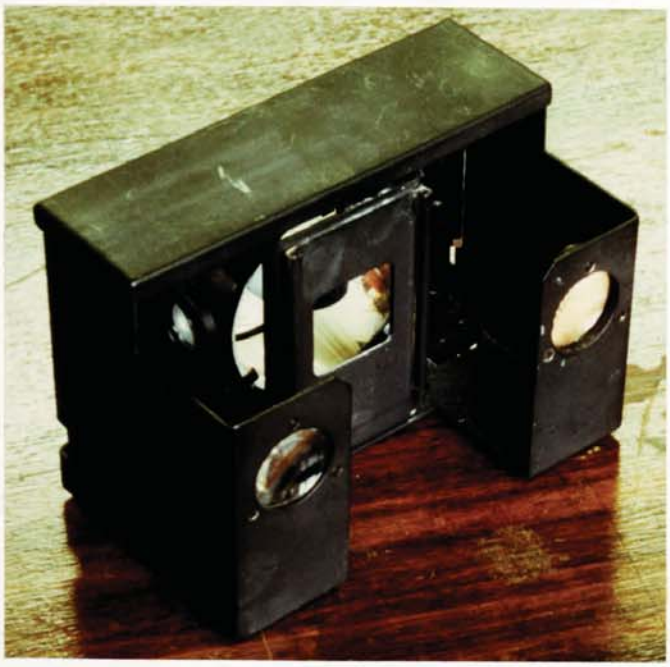

Fig. 2·7a

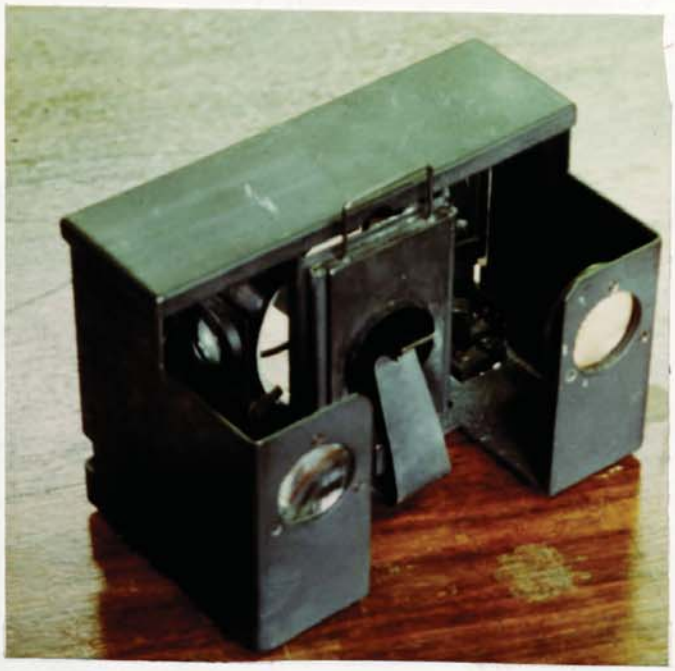

Fig. 2·7b

The Diffusion Reflectance Attachment

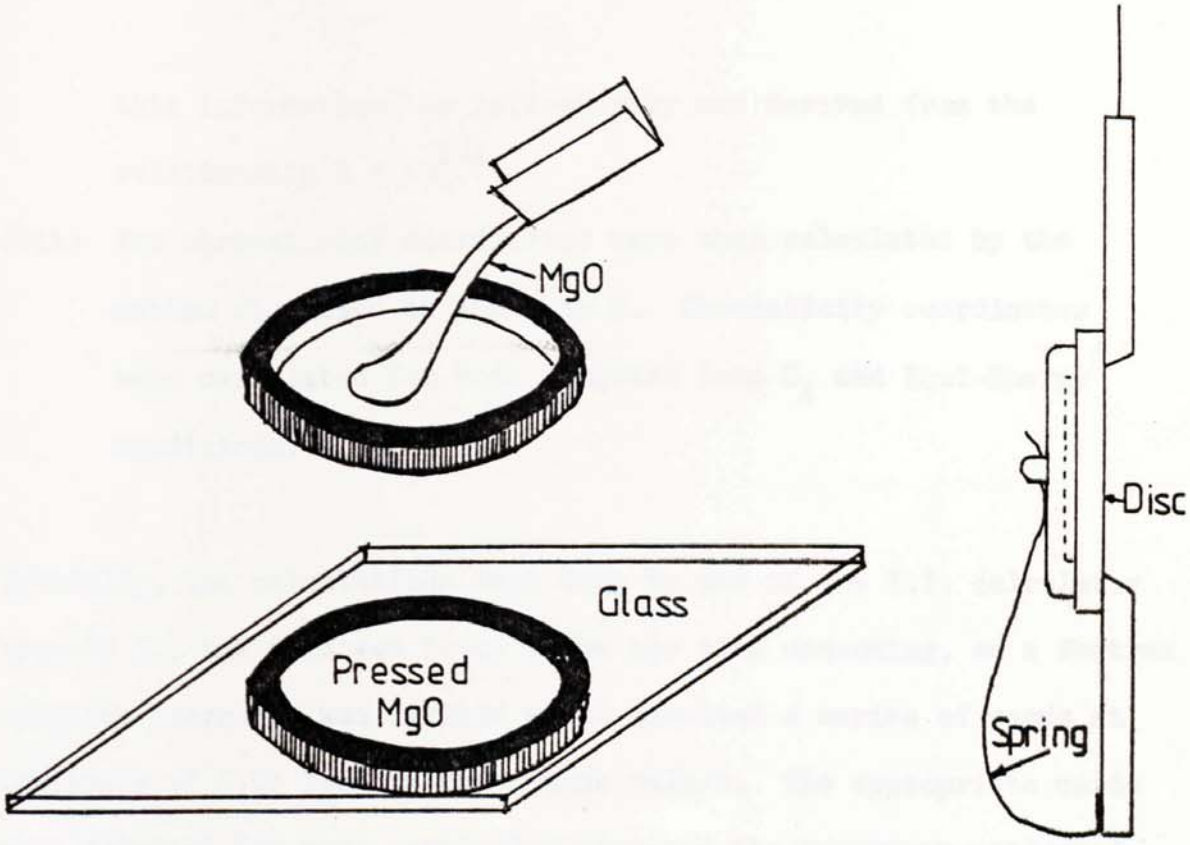

Fig 2·8a

Fig. 2·8b

The preparation of the standard, and the sample and standard holder

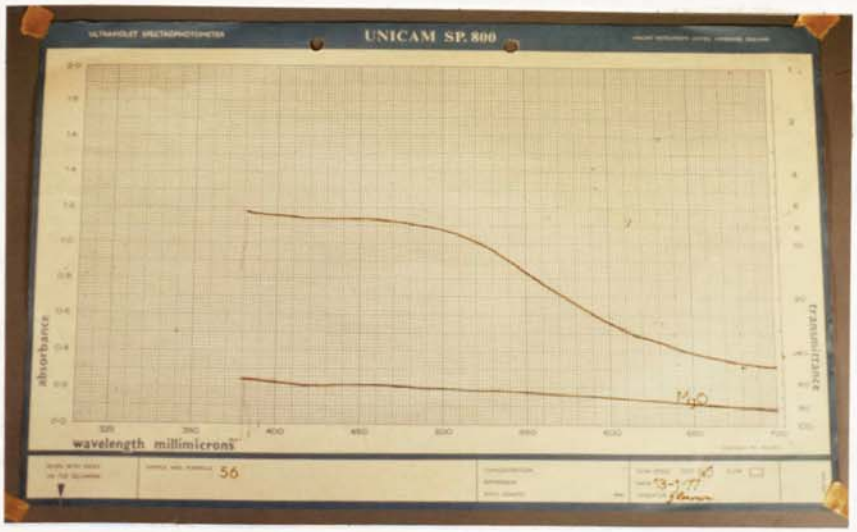

Fig. 2·9

The Absorbance graph

this information the reflectivity was derived from the relationship $R = 10^{2-A}$.

(vii) The chromaticity coordinates were then calculated by the method discussed in Appendix 6. Chromaticity coordinates were calculated for both Tungsten Lamp S_A and Equi-Energy conditions.

Initially, the calculations were done by use of the T.I. calculator type SR 50, but this was found to be too time consuming, so a Fortran computer programme was devised which involved a series of cards at intervals of 0·01 for the absorbance values. The appropriate cards were selected for each particular disc and the programme activated with these cards. Even this was rather a cumbersome method and when a T.I. programmable calculator type TI 59 became available it was utilised. The programme for deriving reflectivity values and multiplying these with the appropriate distribution coefficients to obtain the x, y and z product totals formed the basis of one programme, while the final calculation to obtain the x, y and z chromaticity coefficients formed the basis of another one. The advantage of this method over the Fortran programme was that the results were immediately available. The programmable calculator programmes used are given in Appendix 12.

In order to facilitate saturation and dominant wavelength calculations large charts as shown in Figs. 2·10 and 2·11 were prepared.

(contd. p. 73)

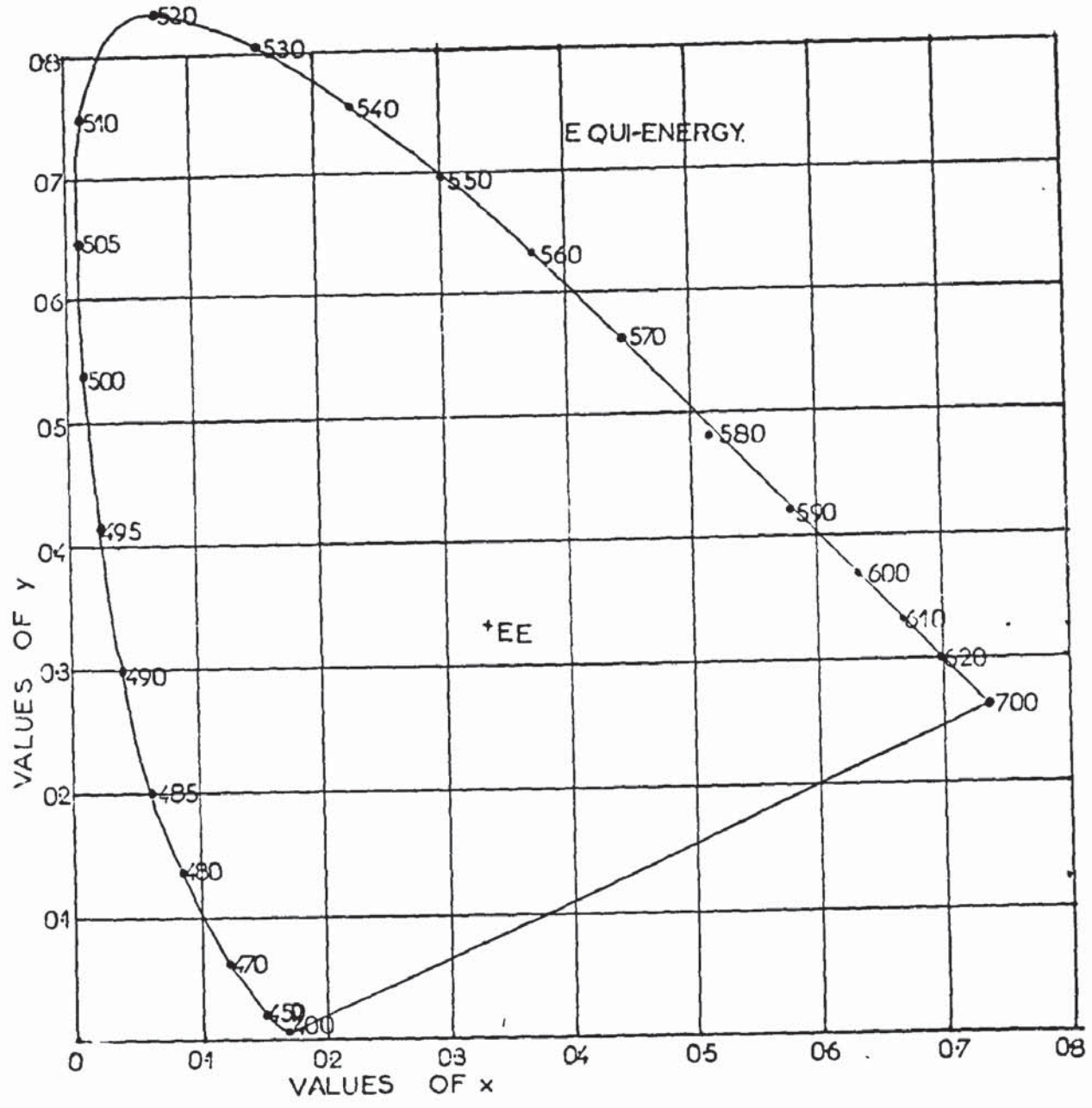

Fig. 2·10

The CIE Chromaticity Chart for Equi-Energy Conditions

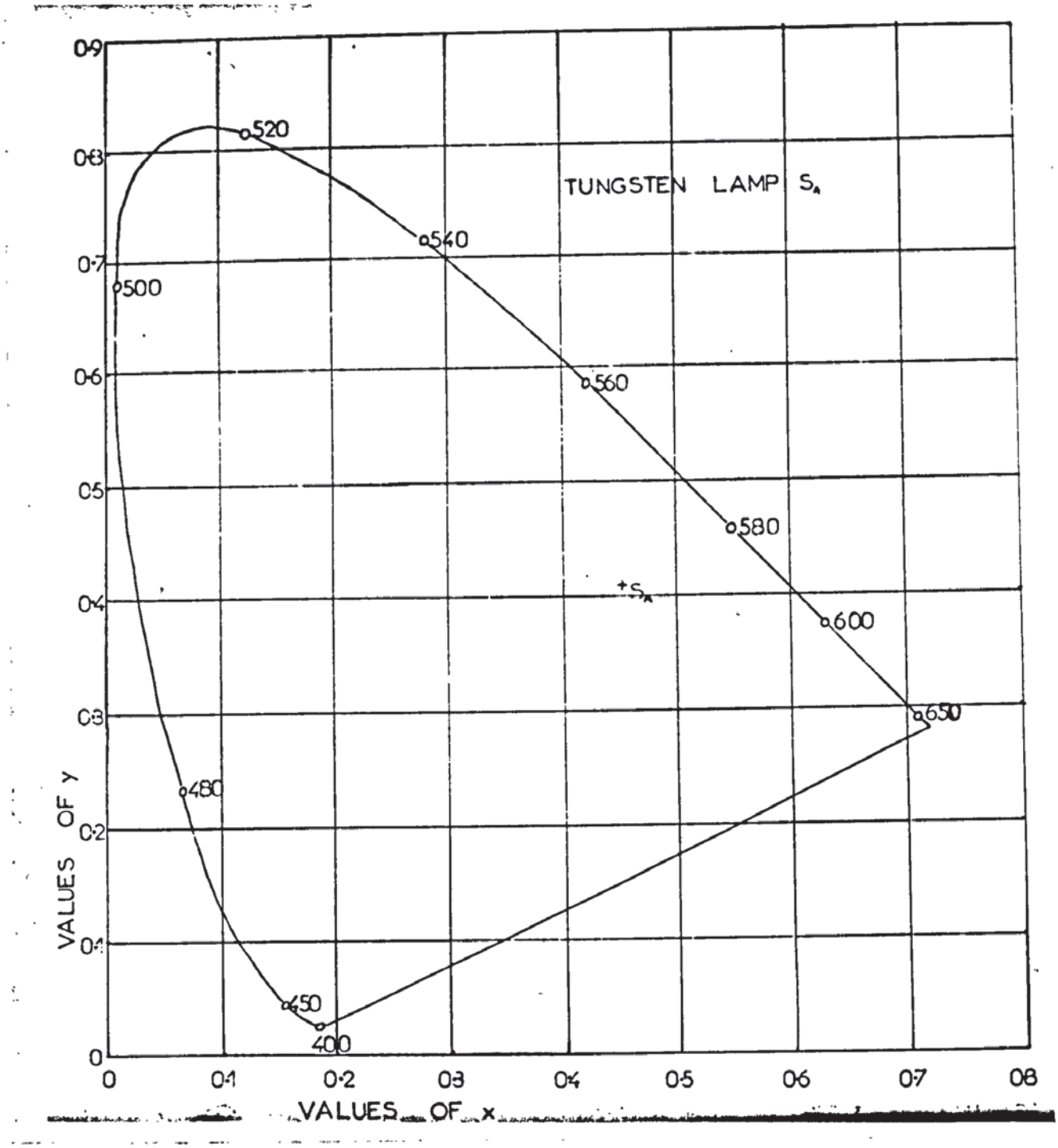

Fig. 2·11

The CIE Chromaticity Chart for Tungsten Lamp S_A Conditions

2·6 THE USE OF THE SCANNING ELECTRON MICROSCOPE IN THE PRESENT WORK

2·6·1 Instruments Used

Most of the SEM work was carried out using a Cambridge Spectroscan type 2A instrument, and in the later stages a type S150 became available and this was then utilised. The Kevex attachment was used in the analysis work.

2·6·2 Preparation of Samples

Small fragments (10-20 mm) were cut from selected discs by means of a jewellers saw. The samples were cut in various shapes (triangles, squares, oblongs, etc.) so that they could be readily identified when several were put in the vacuum chamber together. The samples were held in tweezers while the burrs were removed from the underside with silicon carbide paper, then cleaned ultrasonically in three changes of acetone. A piece of double-sided Sellotape was then placed on an SEM stud, and the samples secured to the stud as shown in Fig. 2·12. In order to secure electrical continuity the sides of the samples were painted with Aquadag which was continued over the Sellotape to the bare aluminium sides of the stud.

When cross-sections were required, the disc fragments were electroplated with thick nickel deposits, for edge preservation, metallographically polished and etched in an acetic acid-nitric acid solution.

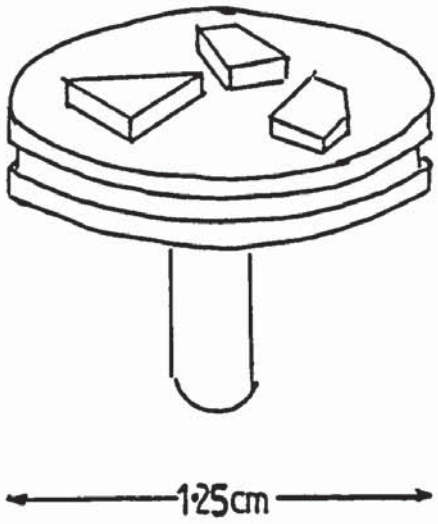

Fig. 2·12
Samples for the Scanning Electron Microscope

2·6·3 Preparation of Standards

Gold, silver and nickel standards were prepared by electroplating nickel discs with 2-4 μm of electrodeposit using the normal pretreatment and the solutions and conditions listed in Appendix TO. Small samples were cut from these discs and treated as described in Section 2·6·2.

2·6·4 The Measurements

The loaded studs were placed in the vacuum chamber and the pressure reduced to TO^{-4} Torr. The samples were observed at various magnifications, and photographs taken where it was deemed advisable. Most of the work was done with the sample at 45^{o} to the electron beam, and thus when thickness measurements were carried out the samples were oriented so that the angle did not affect the measurement.

2·6·5 The Kevex Determinations

The selected standard was focussed under a magnification of 1 or 5 K and an area 2·5 x 2·5 cm was selected, and the energy spectrum collected and displayed on the television screen. The peak selected for the metal standard was associated with a spare channel, and the background set to a datum judged to be average for the surroundings. The channel width was then adjusted until the peak was entirely covered, and the peak integral measured. These conditions of energy position and channel width were set so that other samples could be measured under the same conditions. All the standards used were set in a similar fashion. The spectra of the disc samples were then collected and displayed in turn on the television screen. The spectrum of each was surveyed and compared to preset windows to determine those elements present. The peak integrals of metals such as copper and nickel were measured. From these values the alloy metal content was assessed; a sample calculation is given in Appendix 9.

CHAPTER 3

COLOUR MEASUREMENT OF RANDOMLY SELECTED MATERIALS

3·1 INTRODUCTION

The object of the first series of experiments was to measure the colour of randomly selected materials so that the method of colour measurement could be tested. In addition, two gold plated nickel discs were also subjected to the colour measuring process.

3·2 ESTABLISHMENT OF A STANDARD

Before these experiments were carried out, it was necessary to establish a "white" standard; various materials were tried in order to determine the most satisfactory from the point of view of reproductibility and convenience.

Fig. 3·1 shows the absorbance graphs obtained for various standards. The spectrophotometer was zeroed at 700 nm and the graphs drawn over the range of 700-380 nm. The results show that the general shape of the graphs obtained was very similar except that white paper showed slightly greater absorbance at the violet end of the spectrum and that there was negligible difference between the graph for pressed magnesium oxide and condensed magnesium oxide, and thus it was considered that for all subsequent experiments a pressed magnesium oxide standard would be satisfactory. A fresh standard was prepared for each batch of discs measured and the spectrophotmeter was zeroed using the standard before each disc was measured.

(contd. p.79.)

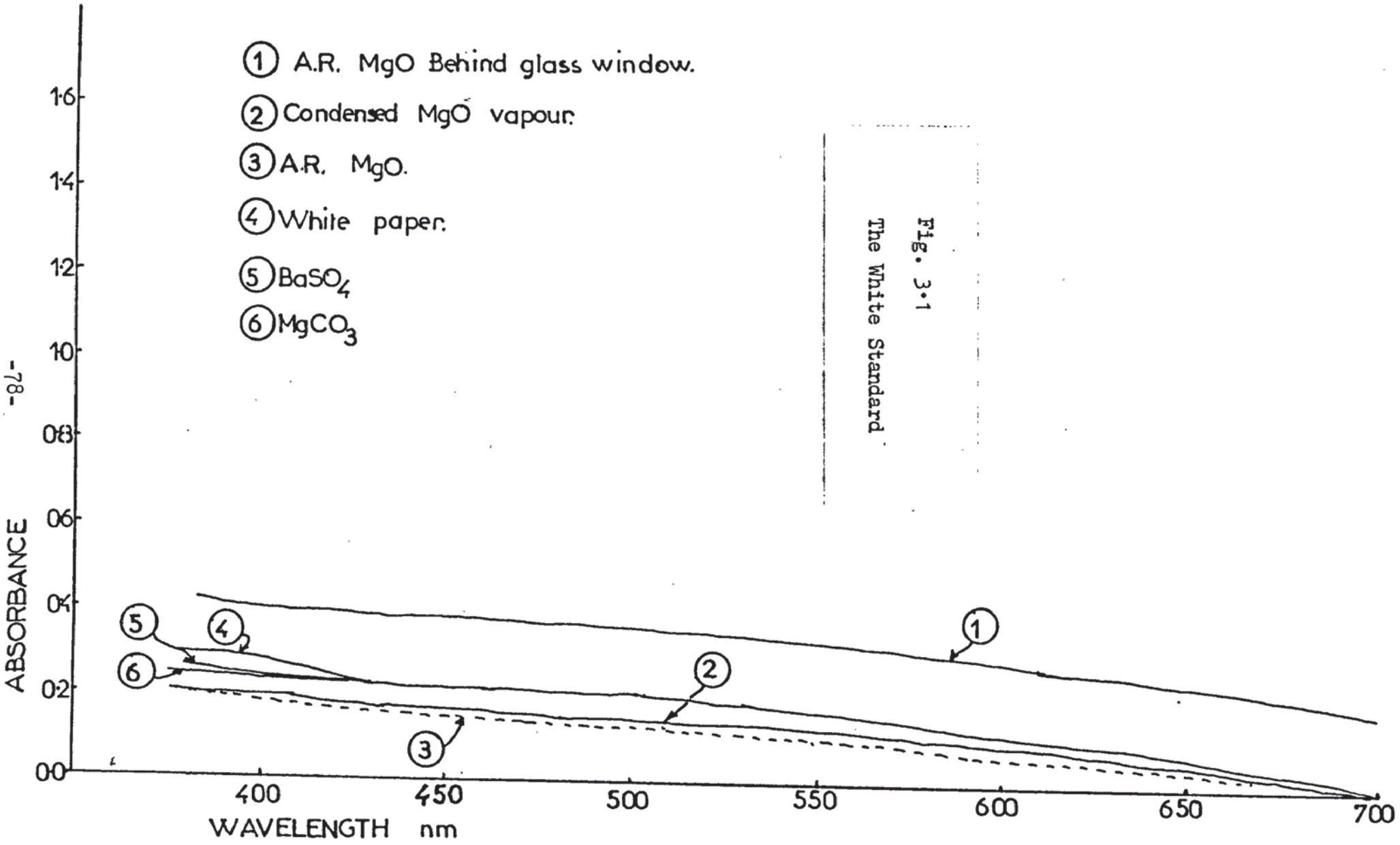

Fig. 3·1
The White Standard

3·3 COLOUR MEASUREMENTS

The results of the preliminary experiments are given in Table 3·1A-C. The chromaticity coordinates were calculated both for equi-energy conditions and for a tungsten light source (S_A). Dominant wavelengths, % saturation and % luminosity were also calculated.

3·3·1 Reflectivity Curves

The reflectivity curves given in Fig. 3·2 show that for rolled aluminium and nickel foil smooth reflectivity curves were obtained with a slight progressive increase in reflectivity on moving from the high energy (380 nm) to the low energy (700 nm) end of the spectrum. A nickel disc polished to 6 µm diamond gave very similar results to the rolled nickel foil, but with slightly lower reflectivity at each wavelength. A silver disc polished to 6 µm diamond gave a reflectivity curve in which reflectivity decreased slightly from the high energy to the low energy (700 nm) end of the spectrum. No steps were observed in the spectral relectivity curves of these specimens. A bright rolled copper foil sample showed a pronounced step starting at 540 nm. Similarly, the gold electroplated samples showed a pronounced step but at a somewhat lower wavelength. This indicates that both copper and gold reflect the red end of the spectrum strongly. The curves for the copper and gold electroplated samples were redrawn (Fig. 3·3) with reflectivity plotted against the energy of the incident light instead of wavelength. These graphs showed that for both of the gold electroplated samples a pronounced absorption process occurred at $3{\cdot}66 \times 10^{-19}$ Joules

(contd. p. 84.)

Disc No.	Material	Treatment
2	Bright rolled copper foil	None
3	Rolled aluminium foil	None
4	Rolled nickel foil	None
6	Nickel disc	Polished to 6 μm diamond then pretreatment A
7	Nickel disc	As 6 then electroplated in bath X for 5 seconds at at 7 a.s.d. Temp. 65°C
8	Nickel disc	As 7 but time in bath 10 seconds
10	Silver disc	Polished to 6 μm diamond

Table 3·1A

Materials and Treatment for Preliminary Experiments

Disc No.	Chromaticity Coordinates					
	Equi-Energy			Tungsten Lamp		
	x	y	z	x	y	z
2	0·420	0·367	0·213	0·520	0·402	0·078
3	0·344	0·342	0·314	0·461	0·408	0·131
4	0·358	0·350	0·292	0·472	0·409	0·119
6	0·366	0·348	0·286	0·475	0·408	0·117
7	0·426	0·396	0·178	0·519	0·418	0·063
8	0·435	0·399	0·166	0·528	0·415	0·057
70	0·321	0·321	0·358	0·440	0·402	0·158

Table 3·1B

Disc No.	Equi-Energy			Tungsten Lamp		
	D.W. nm	S %	L %	D.W. nm	S %	L %
2	589	36	30	596	41	32
3	580	7	30	594	7	30
4	583	12	24	589	15	24
6	587	13	21	591	16	22
7	583	46	34	587	52	35
8	583	49	38	589	56	39
70	477	5	13	459	2	13

Table 3·1C

D.W. = Dominant Wavelength

S = Saturation

L = Luminosity

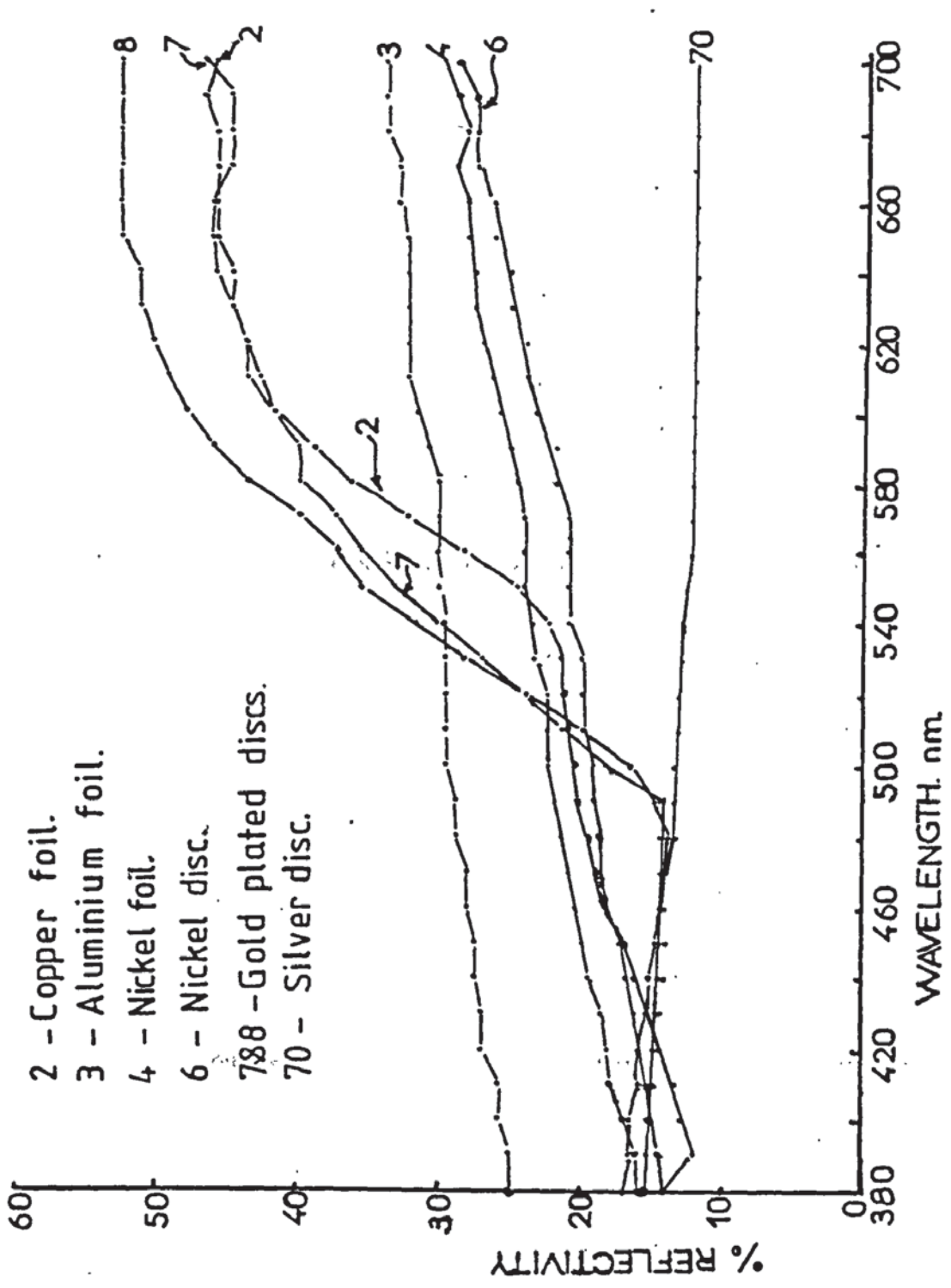

Fig. 3·2

Reflectivity Curves (against wavelength of incident light)

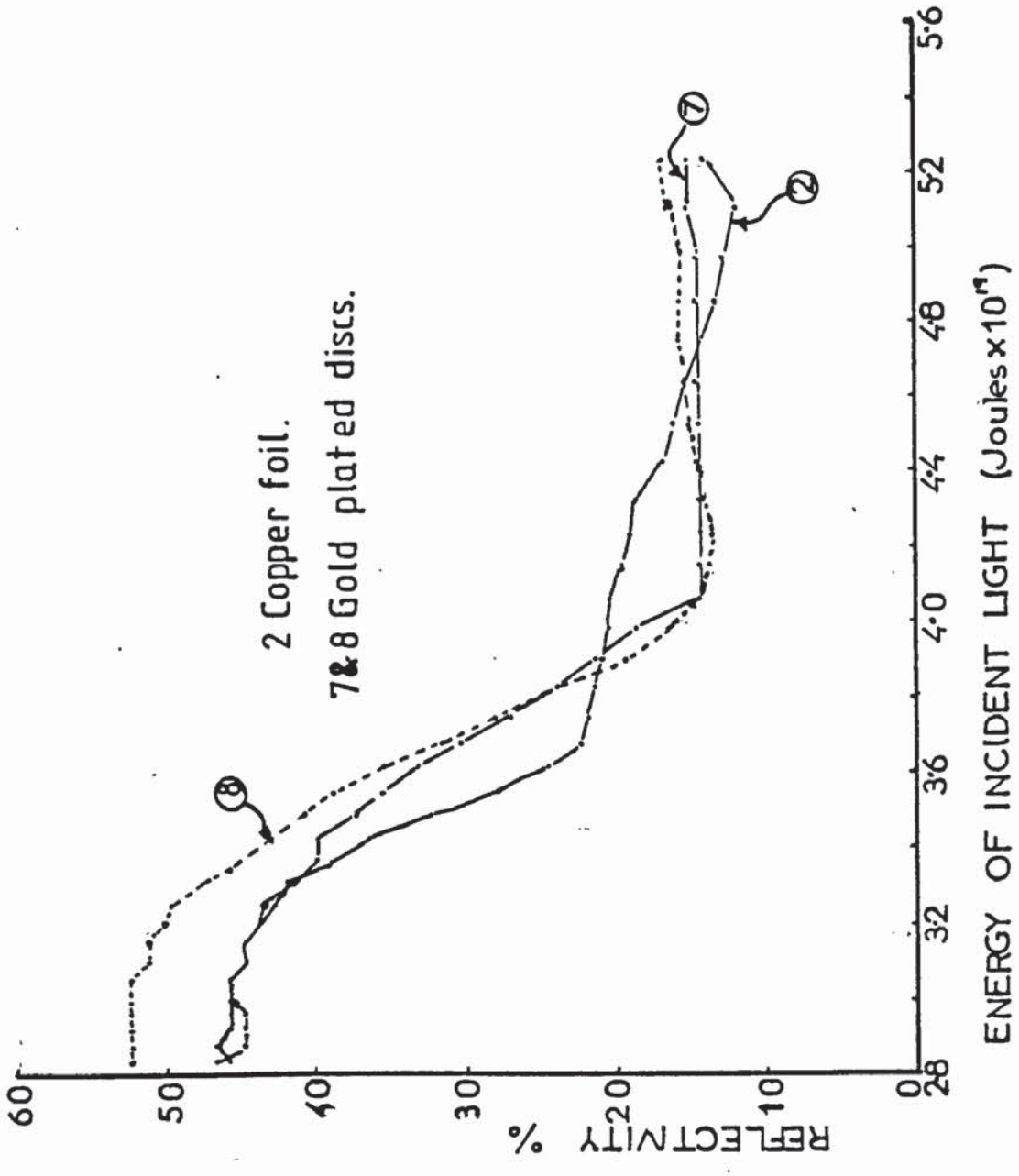

Fig. 3·3

Reflectivity Curves (against energy of incident light)

(2·28 eV) incident light energy, while for copper the intense absorption process occurred at $3{\cdot}46 \times 10^{-19}$ Joules (2·16 eV). The results conform very closely to those obtained by Saeger and Rodies[44] in which such steps were found in the gold curve at $3{\cdot}68 \times 10^{-19}$ Joules (2·30 eV) and the step for copper was stated as being somewhat lower although actual values were not given. The steps were due to a decrease in reflectivity from the high values characteristic of free electrons because absorption processes are made possible by transitions of electrons from the conduction band to energetically higher bands. Thus it was considered that the colour measuring method was adequate since the expected curves were obtained.

3·3·2 Chromaticity Coordinates

In Fig. 3·4 the chromaticity coordinates for the samples (measured with respect to tungsten lamp illuminant) have been plotted on the relevant portion of the CIE chromaticity chart. This shows that the colours for rolled aluminium foil, rolled nickel foil and a nickel disc polished to 6 μm diamond were fairly close to the white point (S_A), the rolled aluminium foil being the nearest and the least saturated (7%) while the rolled nickel foil and the polished nickel disc had very similar chromaticity coordinates.

The gold plated discs were nearer to the yellow-orange part of the chart than the copper which was nearer to the red-orange. A similar relationship was exhibited under equi-energy conditions as shown in Fig. 3·5. (contd.p.87)

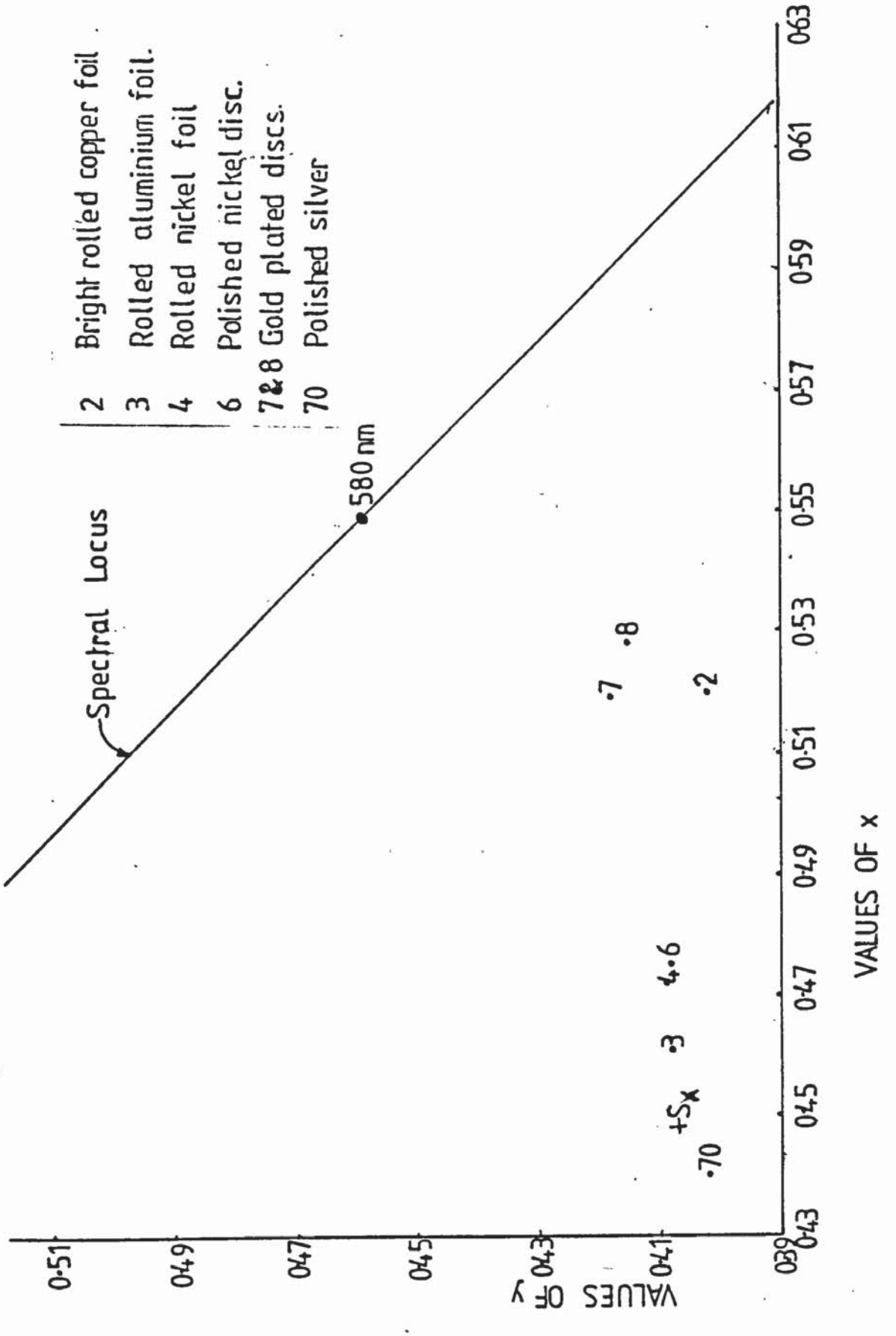

Fig. 3·4

The Chromaticity Coordinates - Positions on the CIE Chart (Tungsten Lamp)

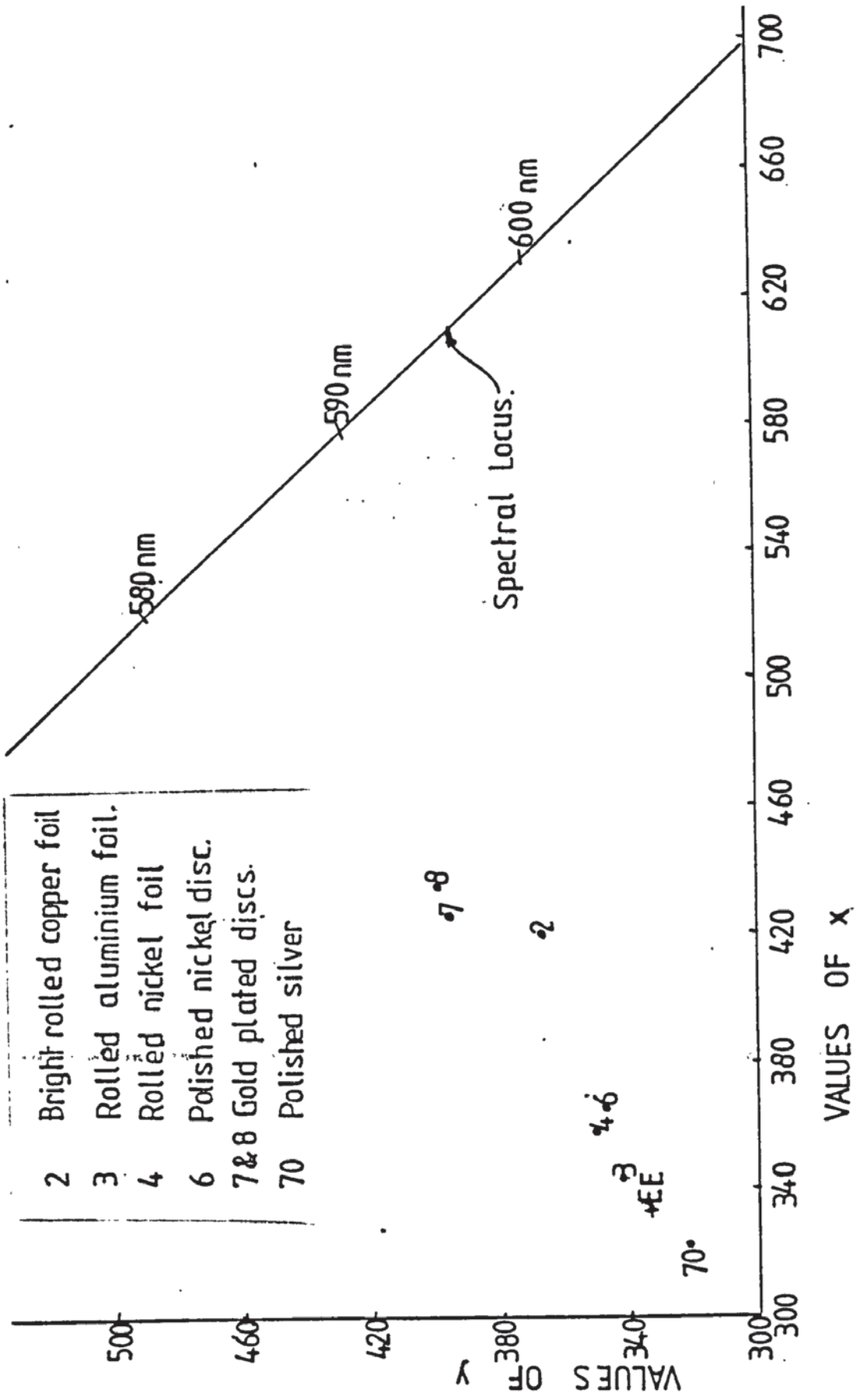

Fig. 3·5

The Chromaticity Coordinates - Positions on the CIE Chart (Equi-Energy)

Only two gold electroplated samples were tested in the first series of experiments and it was thus not possible to know if a stable colour had been obtained. Fig. 3·6 shows that under both equi-energy and tungsten lamp conditions there was considerable increase in x parameter for the gold electroplated discs in comparison with the unplated nickel disc but only a slight increase in the y parameter, there was a considerable decrease in the z parameter. This means that with gold electroplating the samples become more red and less blue which is to be expected. In all cases the x and y tungsten lamp values were numerically higher than the equi-energy values while the z values were lower.

3·3·3 Luminosity Dominant Wavelength and Saturation

Fig. 3·7 shows that the dominant wavelength for silver was in the blue region of the spectrum with only a very small saturation value as would be expected from a value so near the white point. On the other hand aluminium which also appeared white gave a dominant wavelength in the orange region (tungsten lamp) and in the yellow region (equi-energy). Again the saturation value was very low due to the aluminium being so close to the white point.

Unexpectedly the dominant wavelength for the gold plated samples exhibited slightly less red than the bare nickel disc when calculated with respect to both illuminants, but this may be explained by the greater saturation of the gold electroplated samples. As expected the dominant wavelength for the copper sample was nearer to the red end of the spectrum than any other sample measured.

(contd. p. 92.)

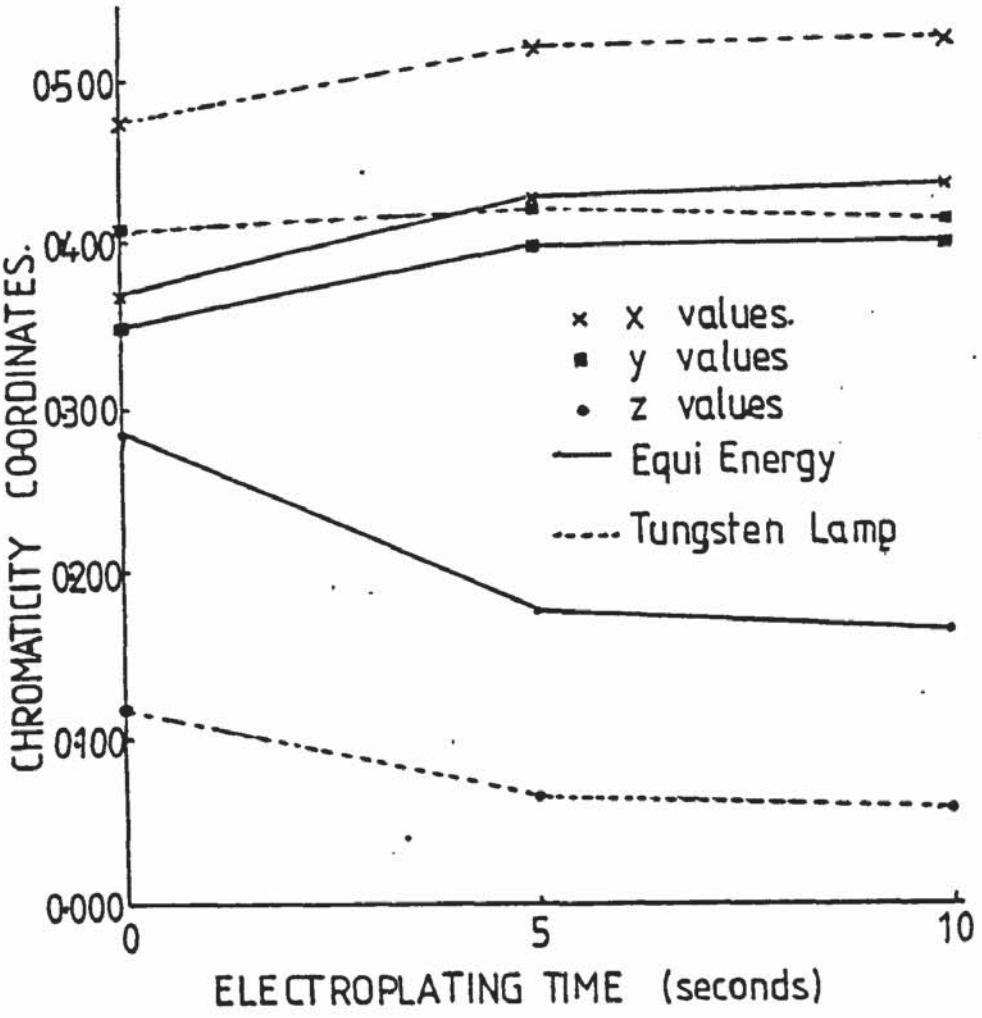

Fig. 3·6

Chromaticity Coordinates for Gold Electroplated Nickel Samples

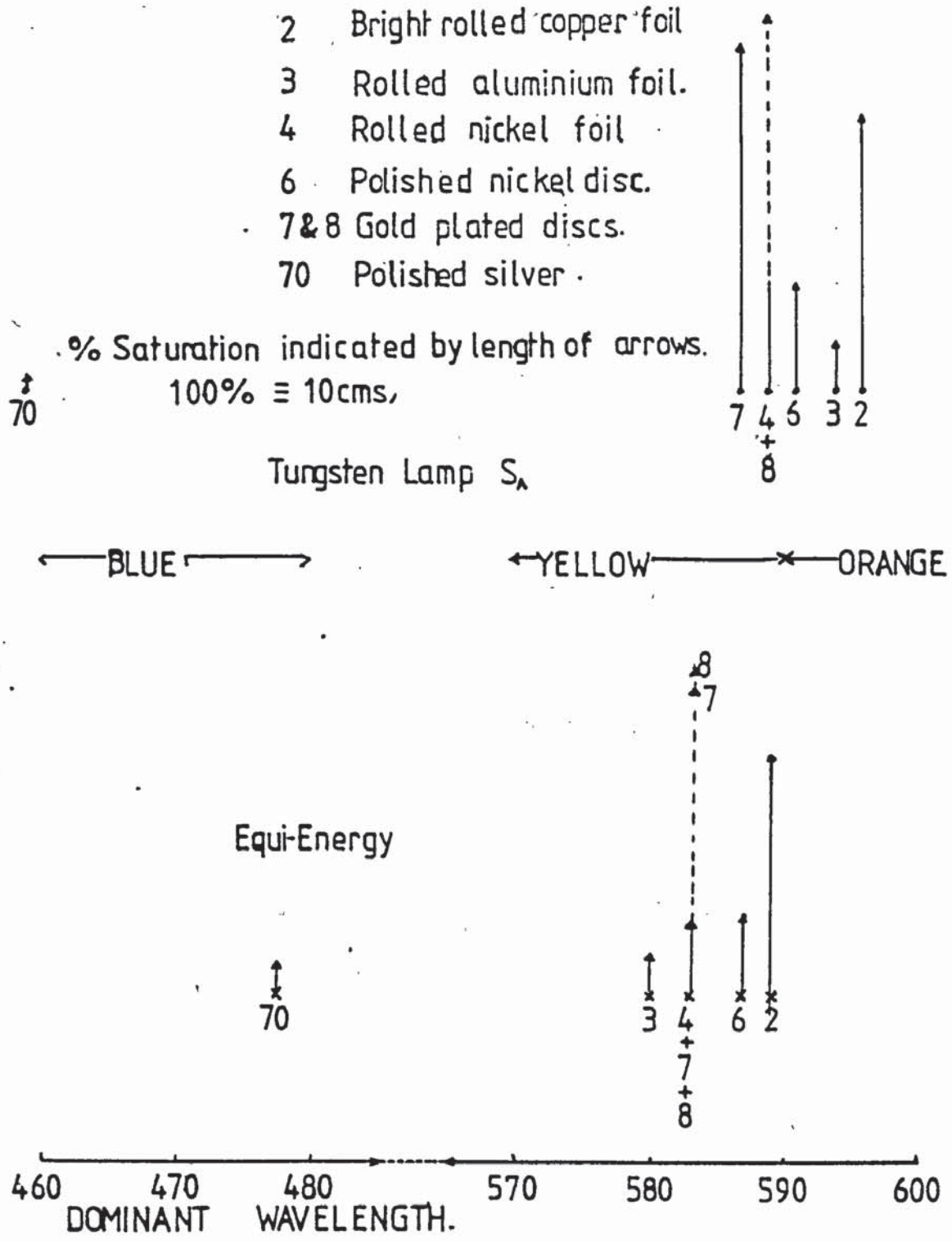

Fig. 3·7

Dominant Wavelength and Saturation Values for the Randomly Selected Materials

Figs. 3·8 and 3·9 show that gold electroplating of the discs resulted in a considerable increase in both luminosity and percentage saturation, the values for tungsten lamp conditions being very slightly higher than those for equi-energy.

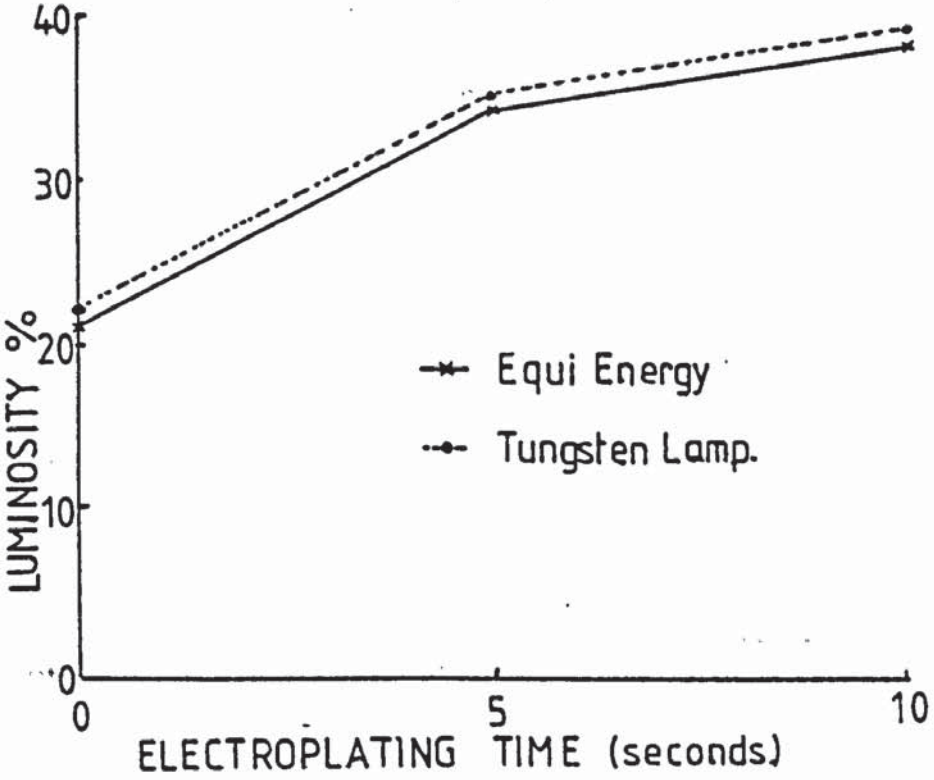

Fig. 3·8

Effect of electroplating time on luminosity

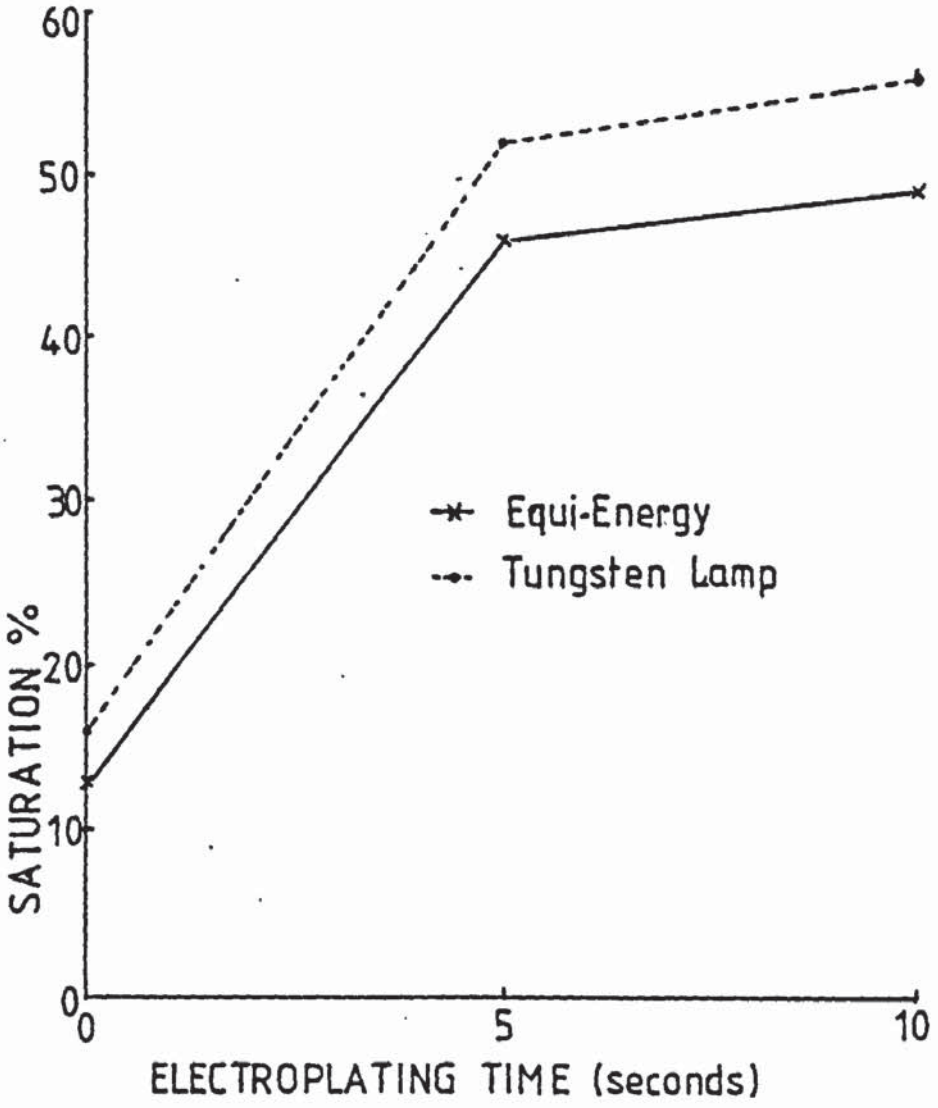

Fig. 3·9

Effect of electroplating time on saturation

CHAPTER 4

THE INFLUENCE OF SURFACE PREPARATION ON COLOUR MEASUREMENT

4·1 INTRODUCTION

The object of the second series of experiments was to determine the best pre-treatment for the nickel discs prior to the gold electroplating process. The pre-treatment chosen was required to provide a clean and even surface with reproducible colour values in order to provide a datum for colour changes when gold was electrodeposited on to the surface. The results of this series of experiments are given in Table 4·1A-C.

4·2 REFLECTIVITY AND COLOUR MEASUREMENTS

4·2·1 Reflectivity

Fig. 4·1 shows the reflectivity of the various surfaces over the wavelength range tested (380-700 nm). These results show that no steps were obtained in any of the graphs. This is expected since it has been shown on the basis of the Fermi level in nickel that a step is not to be expected in the visible range. Most of the graphs exhibited a slight positive slope indicating a slightly greater reflectivity of the red end of the spectrum.

Samples ground to 600 grit on a lapping machine and followed by a nickel "strike" deposit all gave very similar reflectivity curves and these 600 grit samples gave the highest reflectivity of any of the samples measured. Furthermore, the reflectivity curves exhibited a much greater slope than any of the others, indicating a relatively greater reflectivity of the red end of the spectrum.

(contd. p. 98.)

Disc No.	Treatment
11a	Mounted in plastic and ground on a 100 grit wheel. Turned continually to prevent bevelling.
9a	Hand ground on 80c grit silicon carbide paper. No lubrication.
6b, 9b, 10b, 11b, 12b, 13b	As 9a but silicon carbide paper was grade 180c.
9c, 10c, 11c, 12c, 13c	Hand ground on 320 grit paper with water lubrication. Turned continually to prevent bevelling.
9d, 10d, 11d, 12d	As the above "c" samples followed by pretreatment A.
5α, 14α	Original machined surface given pretreatment A.
15, 16, 17, 18	Machine lapped to 600 grit then given pretreatment A.
60, 43, 92	Metallographically polished to 1 μm diamond. Metallographically polished to 6 μm diamond.

Table 4·1A

The Effect of Pre-Treatment on the Optical Properties of Nickel Discs

All the discs were parted off from a solid nickel bar.

Disc No.	Chromaticity Coordinates					
	Equi-Energy			Tungsten Lamp		
	x	y	z	x	y	z
11a	0·342	0·343	0·315	0·458	0·409	0·133
9a	0·347	0·345	0·308	0·463	0·409	0·128
6b						
9b	0·347	0·345	0·308	0·462	0·410	0·128
10b	0·350	0·346	0·304	0·465	0·409	0·126
11b	0·344	0·343	0·313	0·460	0·408	0·131
12b	0·346	0·345	0·309	0·462	0·409	0·129
13b	0·345	0·345	0·310	0·460	0·410	0·130
9c	0·341	0·341	0·318	0·457	0·409	0·134
10c	0·342	0·339	0·319	0·459	0·406	0·135
11c	0·343	0·340	0·317	0·459	0·408	0·133
12c	0·348	0·347	0·305	0·463	0·409	0·126
13c	0·345	0·342	0·312	0·461	0·408	0·131
9d	0·322	0·324	0·354	0·441	0·403	0·156
10d	0·334	0·333	0·333	0·451	0·406	0·143
11d	0·335	0·333	0·332	0·453	0·403	0·144
12d	0·328	0·327	0·345	0·447	0·404	0·149
5 α	0·343	0·342	0·315	0·459	0·408	0·133
14α	0·349	0·347	0·304	0·465	0·409	0·126
15	0·357	0·352	0·291	0·471	0·410	0·119
16	0·361	0·356	0·283	0·473	0·412	0·119
17	0·360	0·355	0·285	0·473	0·411	0·116
18	0·359	0·355	0·286	0·471	0·412	0·117
60	0·337	0·333	0·330	0·455	0·405	0·140
43	0·320	0·322	0·357	0·440	0·403	0·158
92	0·329	0·328	0·343	0·448	0·403	0·148

Table 4·1B

Disc No.	Equi-Energy			Tungsten Lamp		
	D.W. nm	S %	L %	D.W. nm	S %	L %
11a	577	6	5	590	5	5
9a	579	8	16	590	8	16
6b						
9b	580	8	10	589	9	10
10b	580	8	14	592	10	14
11b	578	6	10	594	5	10
12b	577	8	19	589	9	19
13b	577	8	12	589	8	12
9c	577	6	4	587	5	4
10c	581	6	4	623	4	4
11c	582	6	4	592	5	4
12c	580	8	3	591	9	3
13c		5	13	592	8	14
9d	481	4	7	462	2	5
10d	N.M.	N.M.	5	N.M.	N.M.	5
11d	N.M.	N.M.	5	513	2	5
12d	475	2	5	454	2	5
5 α	580	6	21	591	7	21
14α	578	9	21	591	10	21
15	580	13	29	590	16	29
16	580	15	29	588	17	30
17	580	15	30	590	16	30
18	579	15	32	588	16	32
60	588	2	8	515	1	8
43	480	5	8	460	2	8
92				451	2	7

Table 4·1C

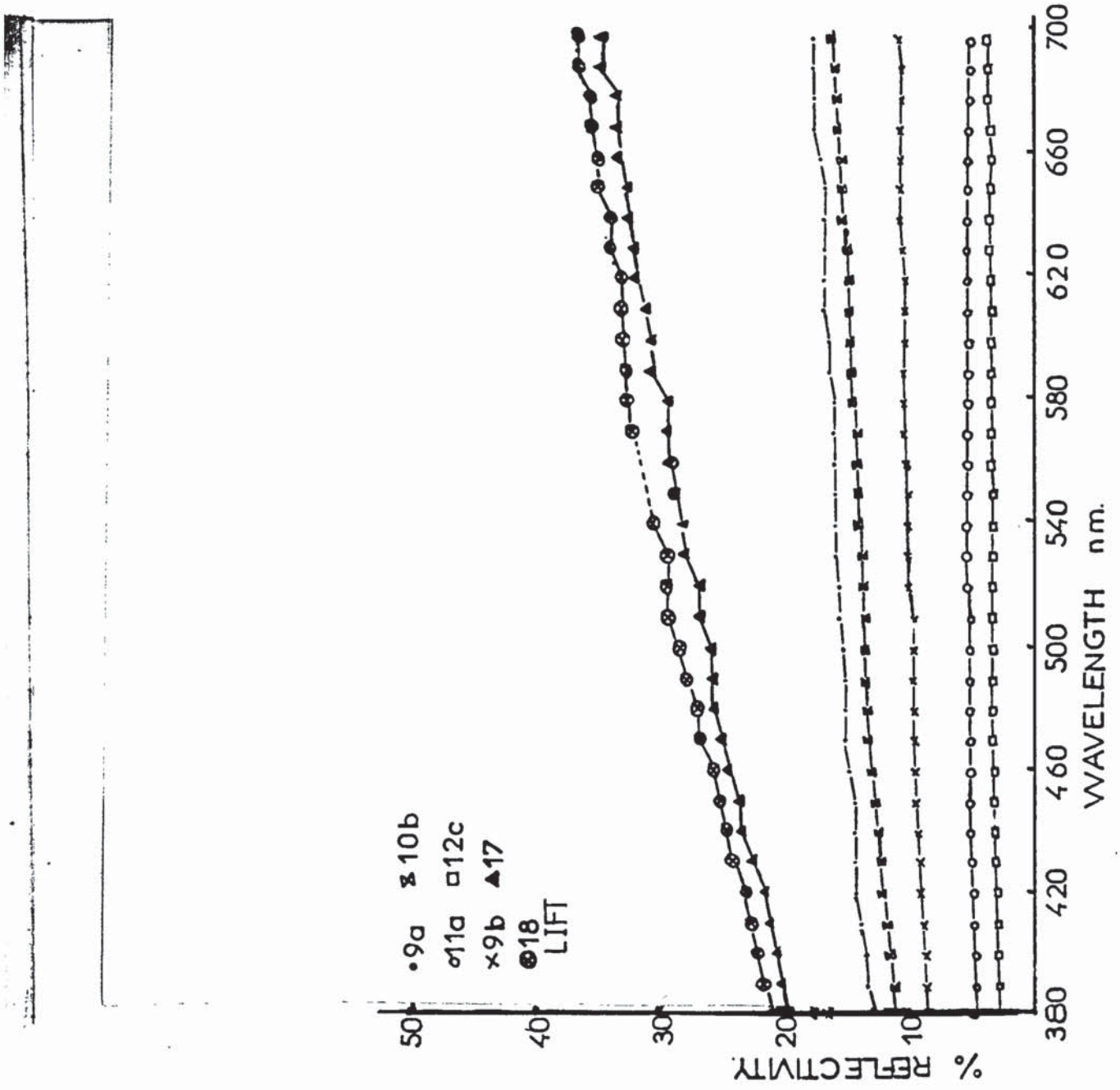

Fig. 4·1

Reflectivity curves for nickel discs with various types of pre-treatment

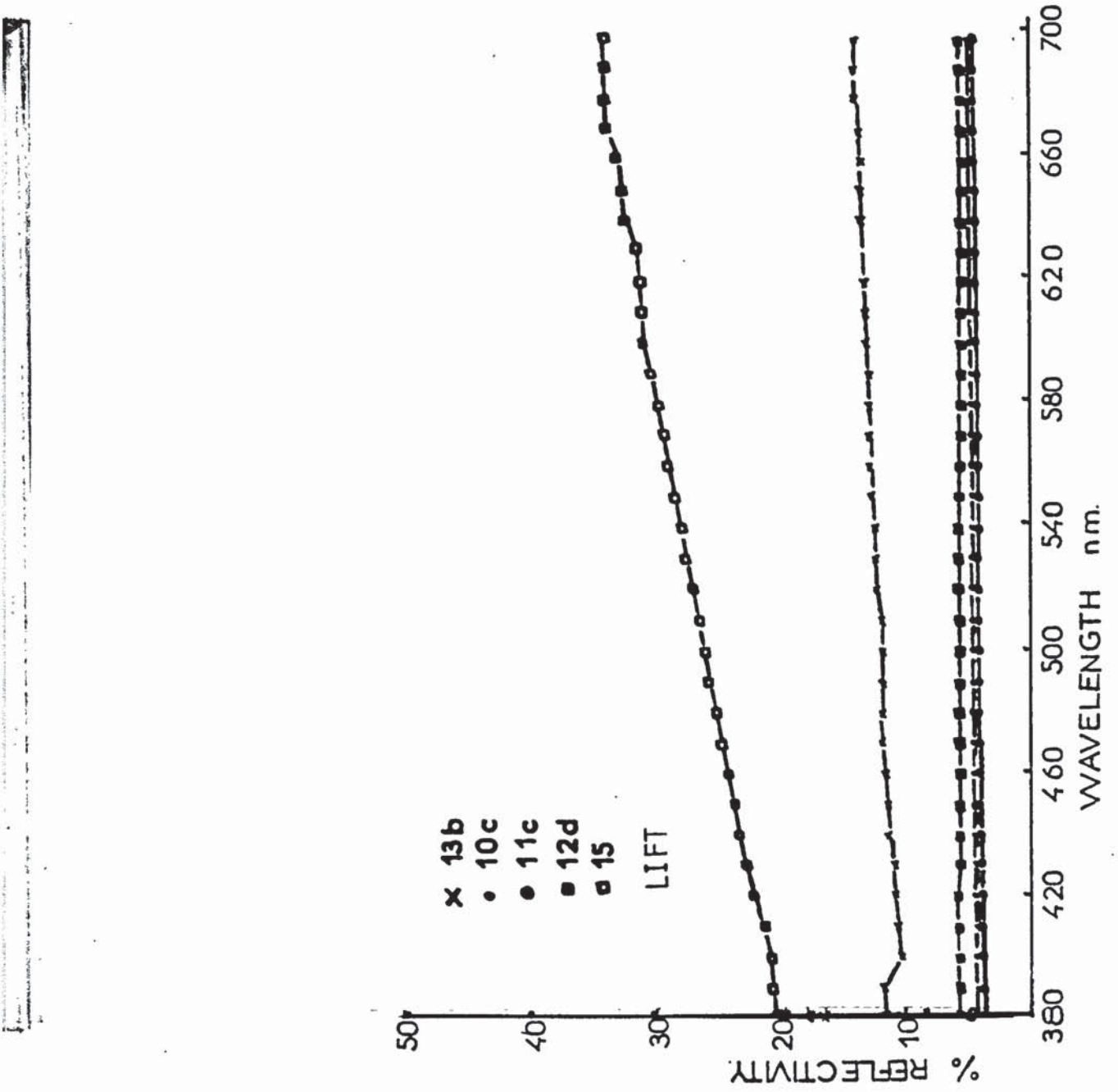

Fig. 4.1

Reflectivity curves for nickel discs with various types of pre-treatment

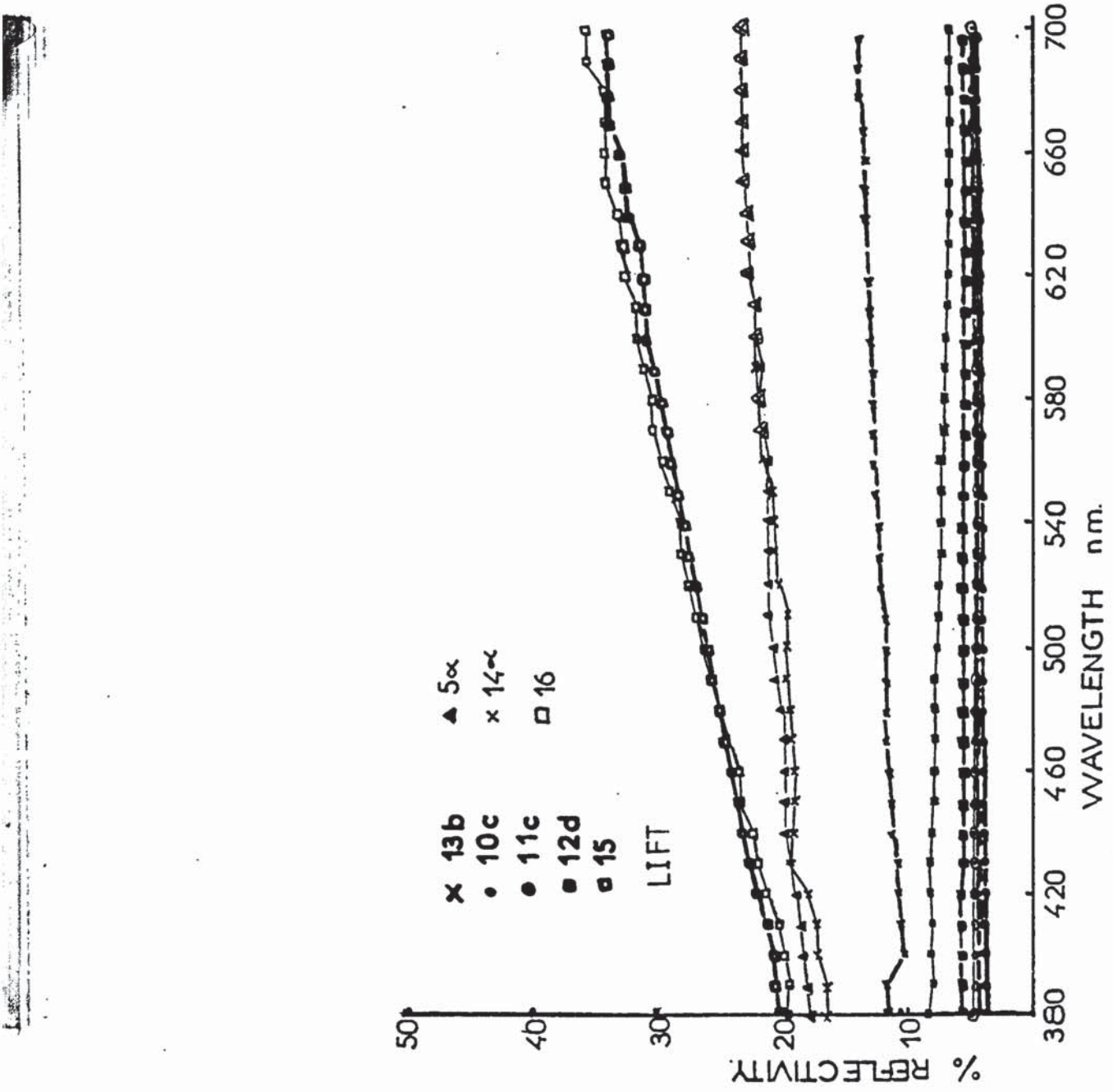

Fig. 4·1

Reflectivity curves for nickel discs with various types of pre-treatment

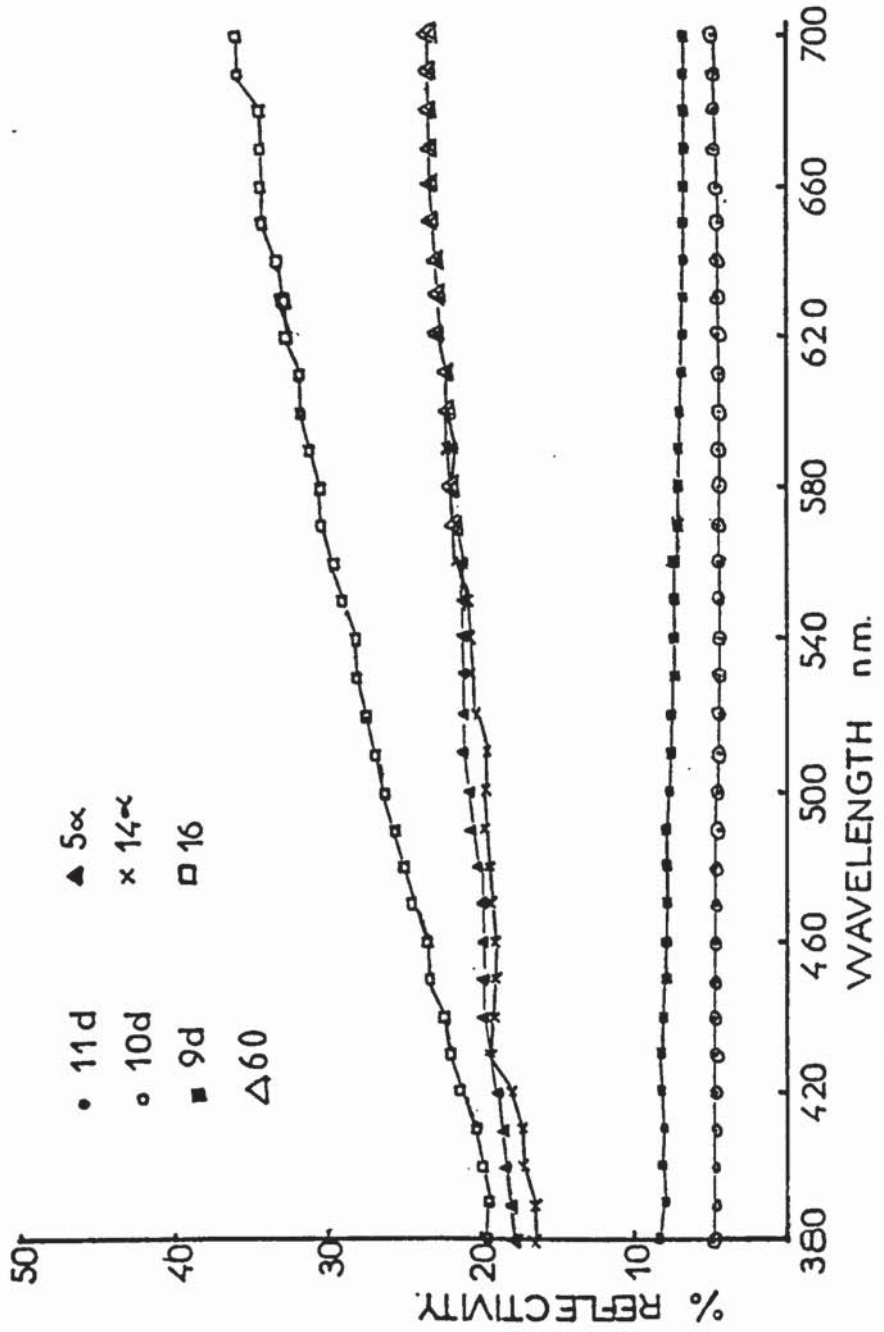

Fig. 4·1

Reflectivity curves for nickel discs with various types of pre-treatment

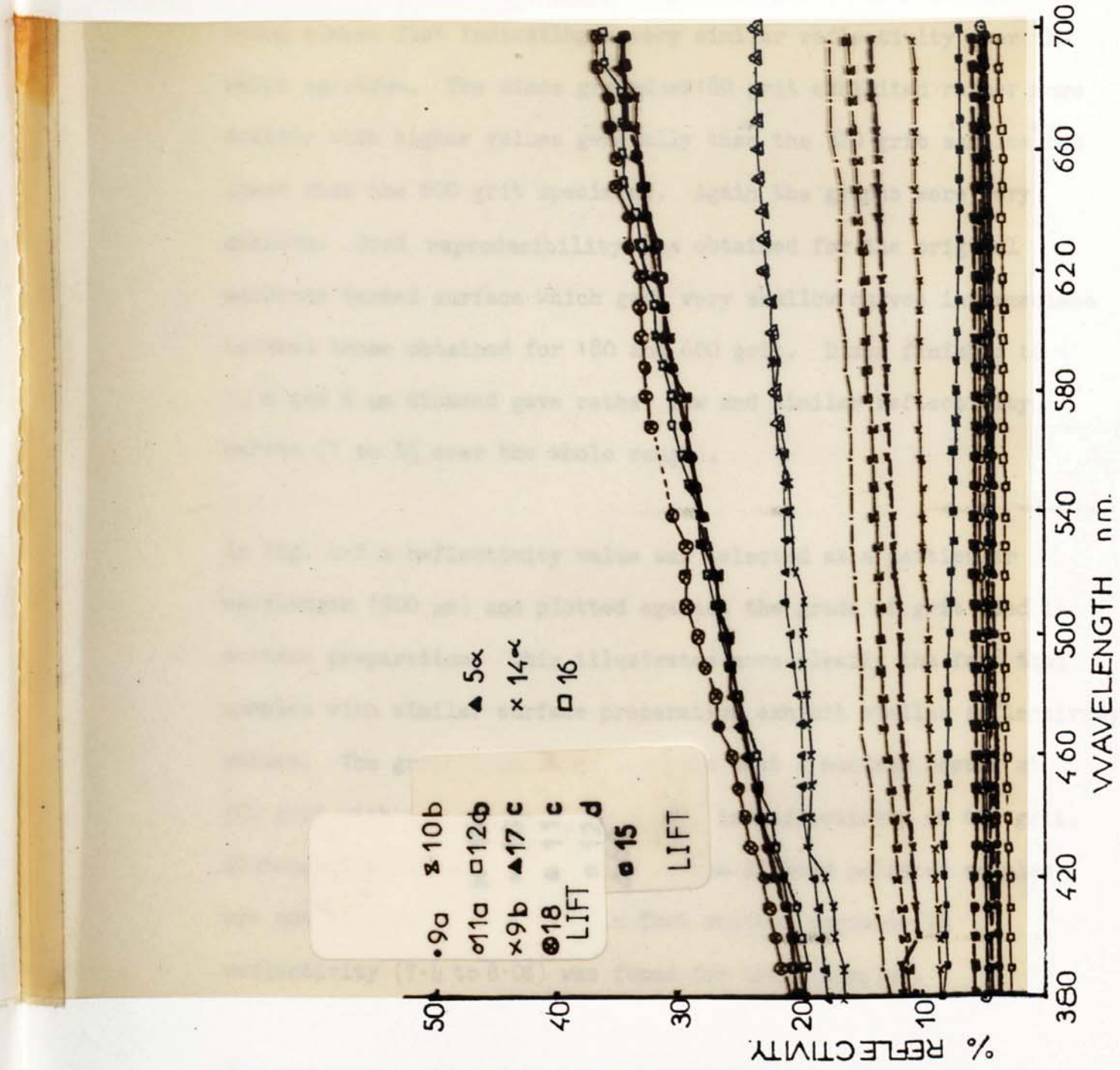

Fig. 4·1

Reflectivity curves for nickel discs with various types of pre-treatment

Most of the hand ground 320 grit discs both with and without a nickel "strike" gave very low (3-5%) reflectivity values, the curves being almost flat indicating a very similar reflectivity over the whole spectrum. The discs ground on 180 grit exhibited rather more scatter with higher values generally than the 320 grit samples but lower than the 600 grit specimens. Again the graphs were very shallow. Good reproducibility was obtained for the original machined turned surface which gave very shallow curves intermediate between those obtained for 180 and 600 grit. Discs finished to 1 μ m and 6 μm diamond gave rather low and similar reflectivity curves (7 to 8% over the whole range).

In Fig. 4·2 a reflectivity value was selected at a particular wavelength (500 μm) and plotted against the grade of grit used in surface preparation. This illustrates more clearly the fact that samples with similar surface preparation exhibit similar reflectivity values. The graph appears to indicate that a minimum occurs at 320 grit with a considerable increase in reflectivity at 600 grit. Although the reflectivity values of the diamond polished samples are not plotted in Fig. 4·2, in fact another decrease in reflectivity (7·4 to 8·0%) was found for these samples.

Thus it was considered that changes in reflectivity were not due entirely to grinding grit size but to the effect on the surface of different preparation methods.

The coarser grit sizes were prepared by hand (and thus scratches might be expected to be cut across approximately at right angles).

(contd.p.100.)

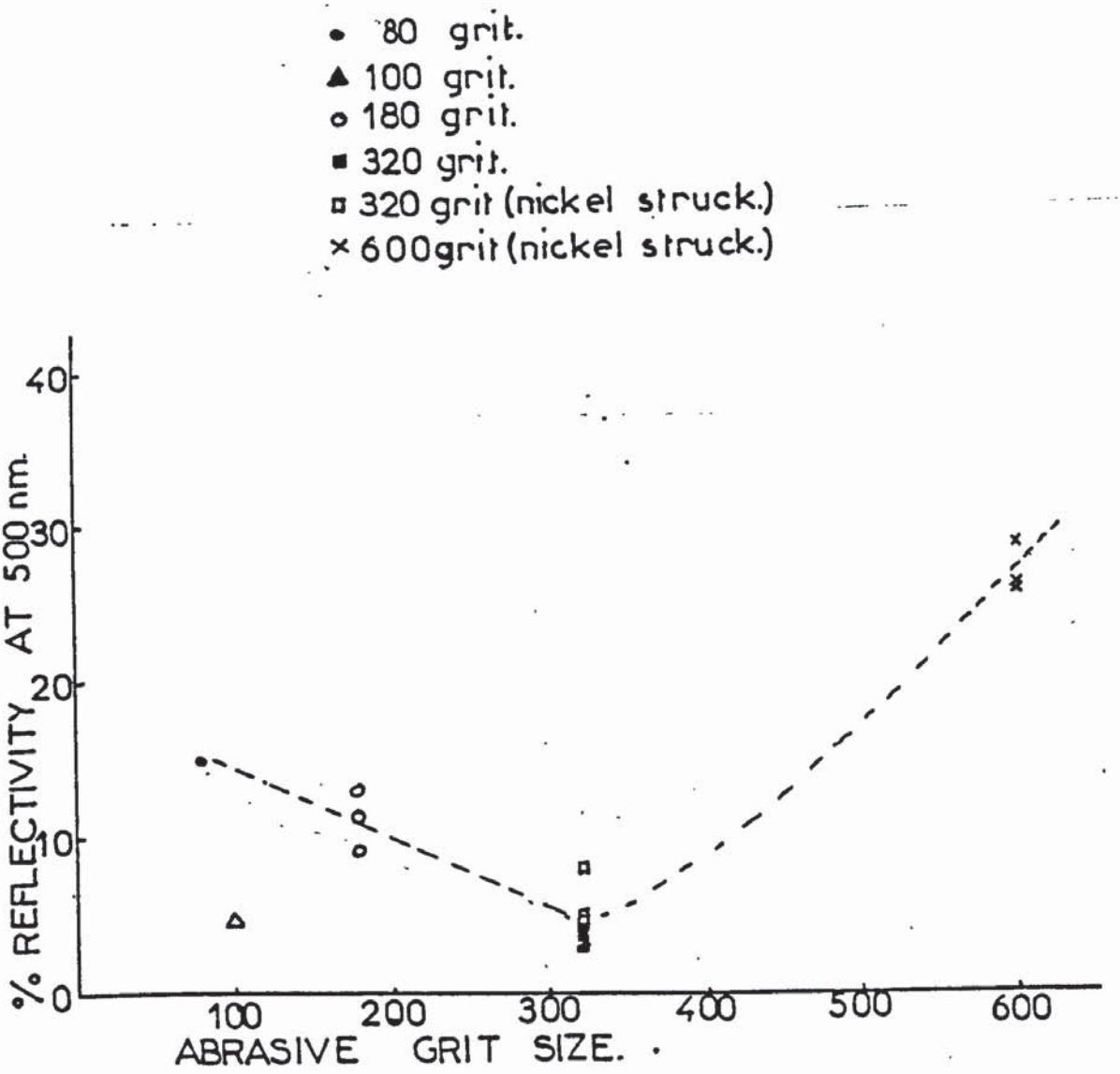

Fig. 4·2

Reflectivity at 500 nm plotted against grit size

The 600 grit was lapped by machine in which the discs slowly rotated in opposition to the grinding plate and thus any scratch was of continuously changing orientation. The diamond polished samples were prepared by normal metallographic techniques, finished by hand on a diamond wheel being rotated at 250 rpm and one might thus expect to obtain a "glassy" amorphous surface.

Examination of the surfaces by scanning electron microscope showed that the surface of the 600 grit machine lapped sample exhibited entirely different topography to hand ground 320 grit specimens. Figs. 4·3 and 4·4 show that the 600 grit surface was far more even in character. The 600 grit sample had a rippled appearance without any grit scratches being identifiable whilst the scratches on the 320 grit samples were very plainly seen at relatively low magnification (x 1K). The scratches appeared to be oriented at approximately 30° to more deeply seated scratches. Furthermore, many fissures and defects were present which had obviously pre-existed in the original surface. Increase in magnification to 5K (Fig. 4·5) showed that the 600 grit surface appeared to have been formed by being gouged out from the surface and then turned back, rather like ploughing on a micro-scale. Since the discs were being rotated in opposition to the grinding plate the ridges were continually being formed at different orientations resulting in the formation of broken rounded furrows.

The increase in reflectivity with the 600 grit was not continued with the even finer surface finish of the diamond finished samples.

(contd.103)

Fig. 4·3

machine lapped 600 grit x1 K

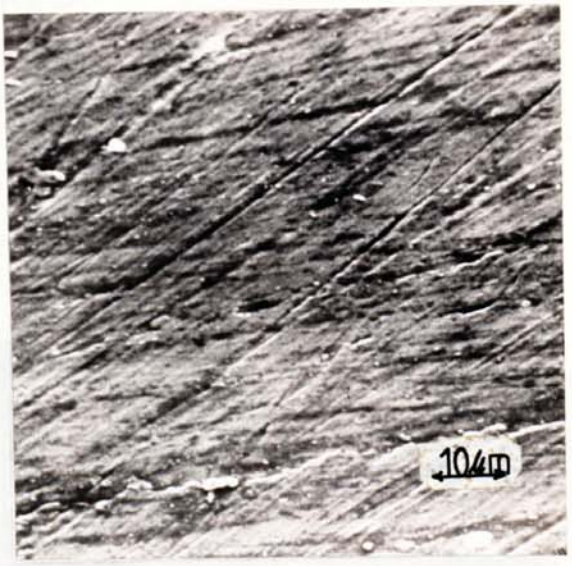

Fig. 4·4

hand ground 320 grit x1 K

Fig. 4·5

machine lapped 600 grit x5 K

Fig. 4·6

hand ground 320 grit x5 K

1 μm diamond : 1K

Fig. 4·7

1 μm diamond : 5K

Fig. 4·8

It was considered that this could be due to the formation of an amorphous "glassy" layer on the surface. Inspection of the SEM photomicrographs (Figs. 4·7 and 4·8) show that a rather featureless surface was obtained with black spots whose size indicated that they could have been embedded diamond particles.

Thus since the character of the surface was so entirely different as a result of different surface preparation it is quite understandable that reflectivities should be different.

4·2·2 Chromaticity Coordinates

Within each group of similar pre-treatments the chromaticity coordinates were generally very close to each other. Coordinates calculated for both tungsten lamp S_A and equi-energy (Figs. 4·9 and 4·10) showed that the values were quite near to the white point, those for 600 grit being furthest away, and thus to be expected to exhibit a more saturated colour than those discs nearer to the white point. The diamond polished samples gave rather variable results from the point of view of chromaticity coordinates but in general were fairly close to the white point.

Since it had been observed that fairly flat curves of between 7 and 8% reflectivity had been obtained for the diamond finished samples it was considered that the chromaticity coordinates should have been more reproducible, but plotting the reflectivities on an extended vertical scale (Fig. 4·11) showed that within the narrow range of reflectivities there was considerable difference in the

(contd. p. 107.)

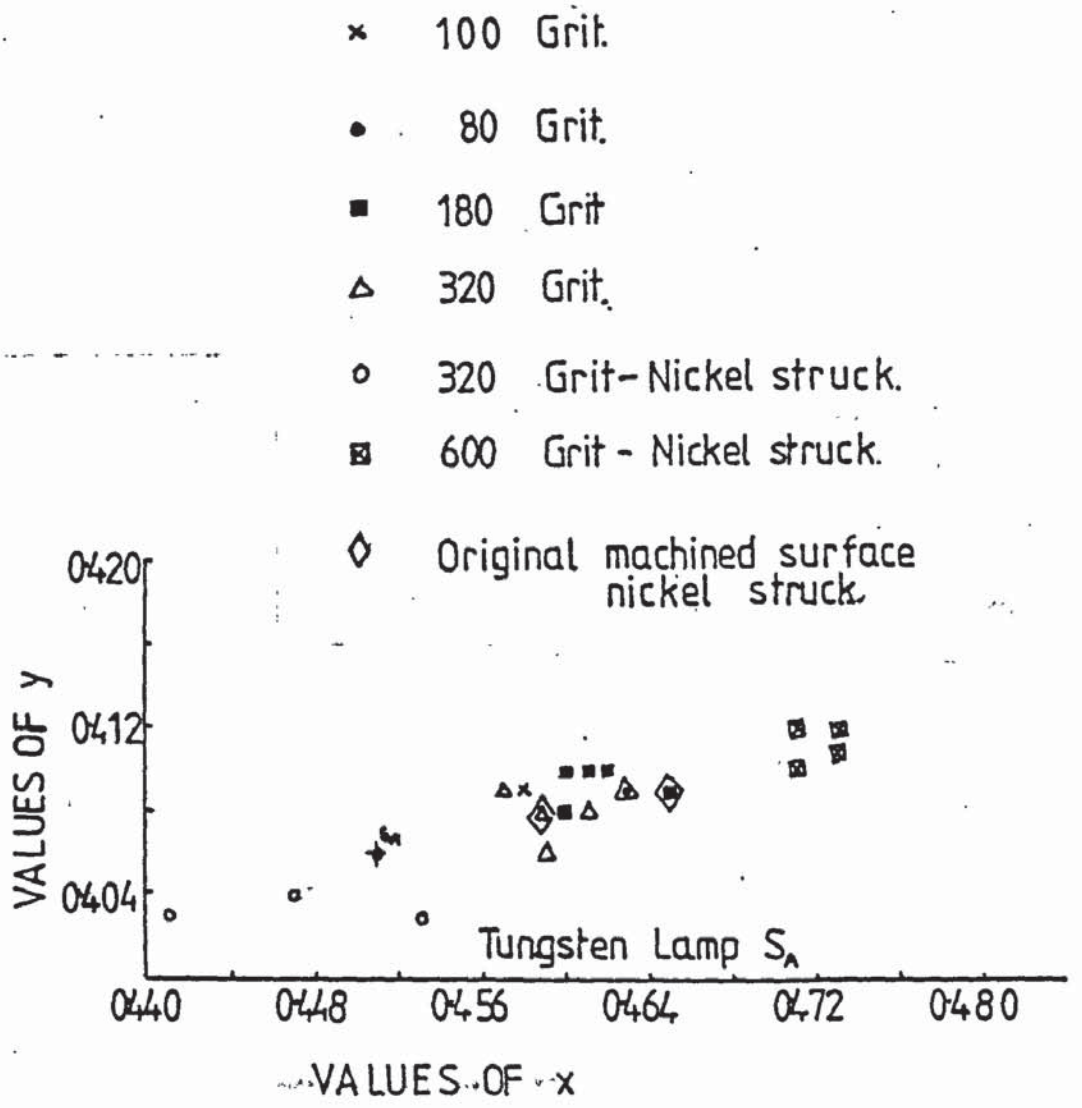

Fig. 4·9

The effect of surface treatment on Chromaticity Coordinates (Equi Energy)

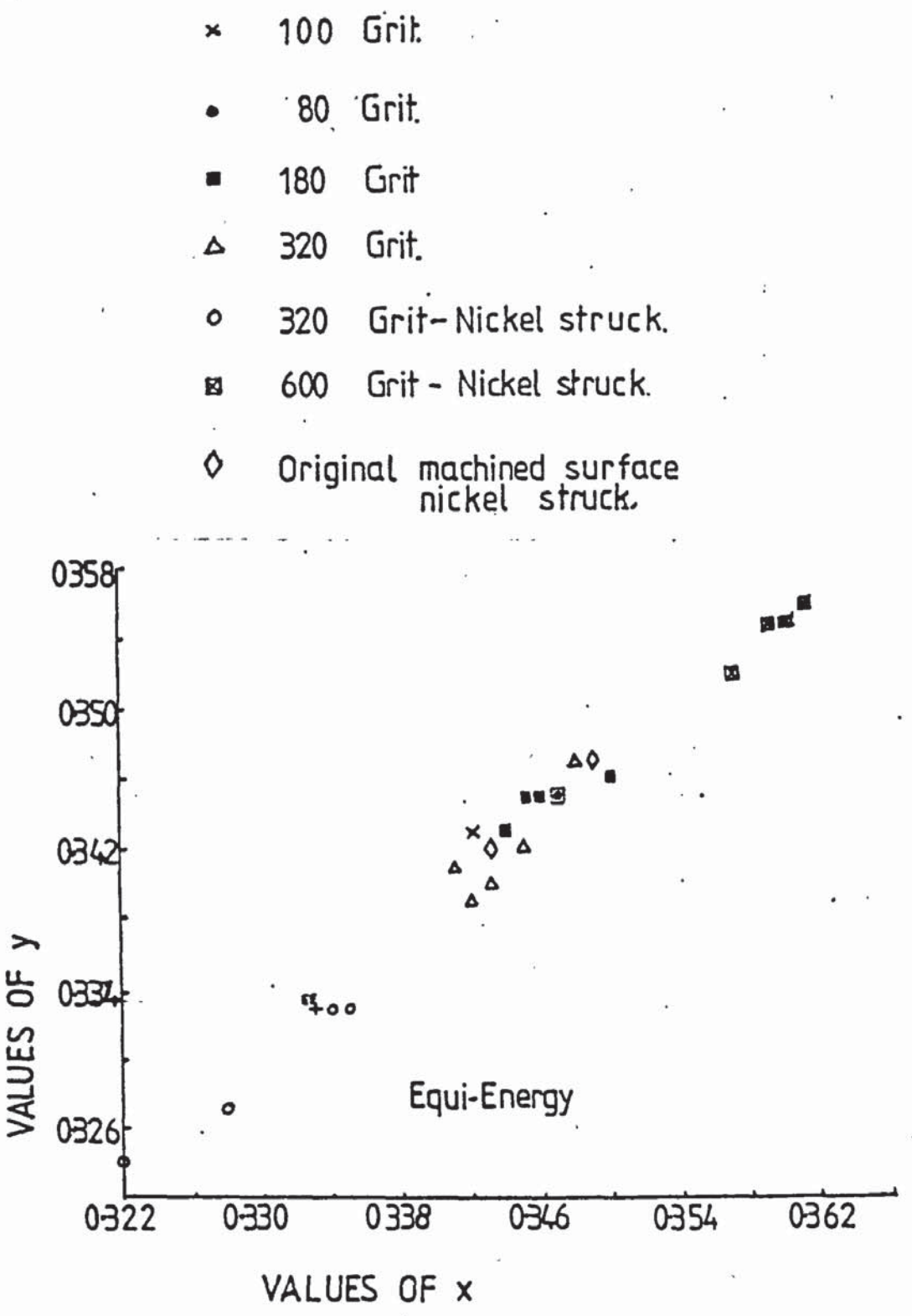

Fig. 4·10

The effect of surface treatment on Chromaticity Coordinates (Tungsten Lamp)

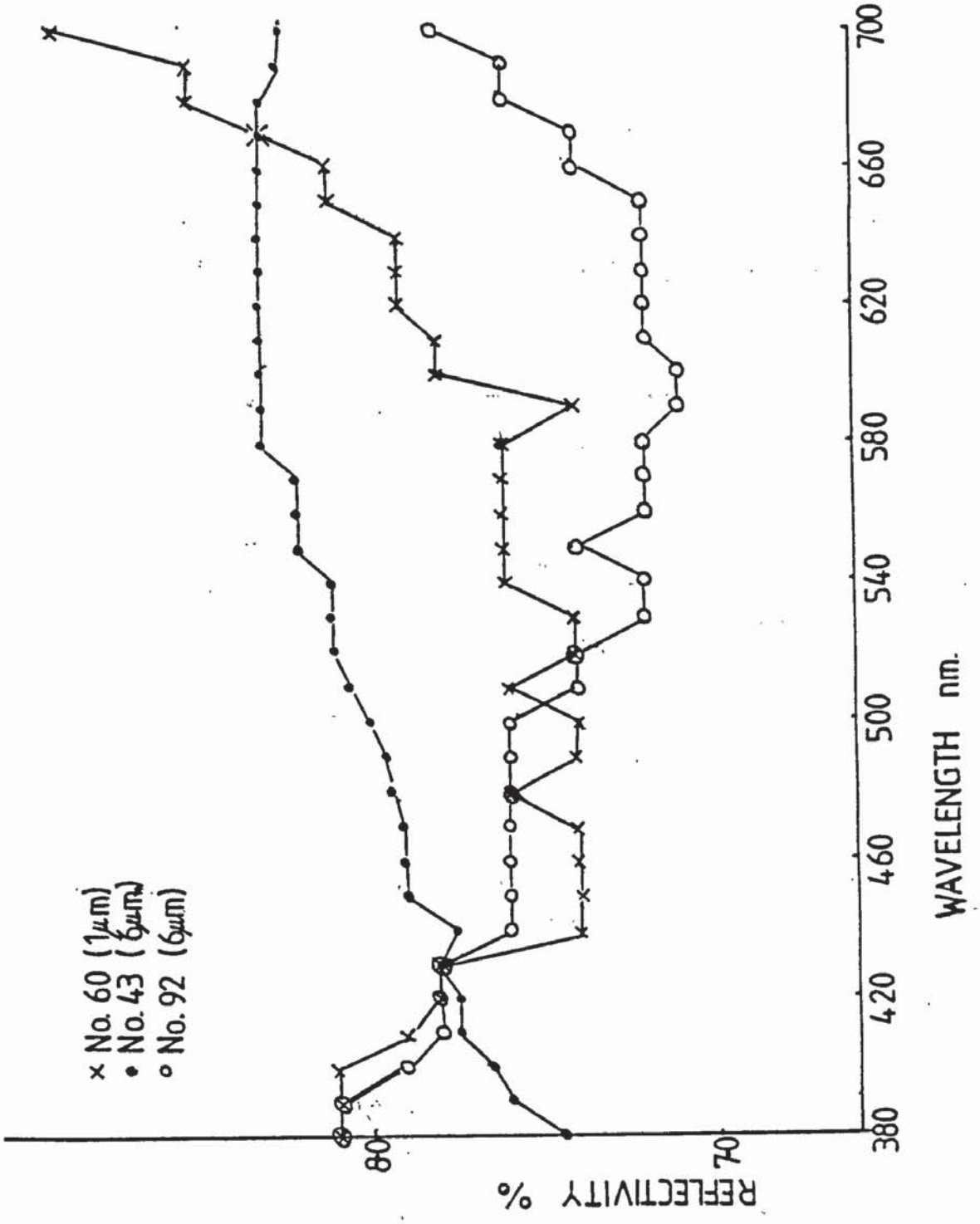

Fig. 4·11

Reflectivity for diamond finished samples plotted on an extended scale

shape of the graphs and, by implication, considerable difference in colour.

4·2·3 Dominant Wavelength and Saturation

The results given in Table 4·1C show very good reproducibility of dominant wavelength values for all silicon carbide grit finished samples with the exception of the 320 grit nickel struck samples which exhibited much lower values. The average values were 579 nm under equi-energy conditions and 592 nm under tungsten lamp conditions. From values given by Wright (Appendix 1) this would appear to suggest yellow to orange, but it must be remembered that the saturation values were low so that all the colours were very much diluted with white. The highest saturation was observed with the 600 grit nickel struck samples (15% average). It is considered that the drop in dominant wavelength values for the 320 grit nickel struck samples may have been due to slight tarnishing of the nickel samples prior to colour measurement, but again the saturation values were so low (3% average) as to make visual correlation meaningless.

The diamond finished samples gave rather variable wavelength results (591 nm-480 nm equi-energy and 506 nm-460 nm tungsten lamp) but the saturation values were so low (near to the white point) that the dominant wavelengths were difficult to derive accurately.

Most of the dominant wavelengths measured were in the blue or blue-green part of the spectrum (Appendix 2). It is probable that the glassy amorphous layer produced by the diamond finishing process

is more resistant to slight tarnishing than the coarser finishes.

4·2·4 Luminosity

Since the calculation of luminosity values depends on the sum of the products of the reflectivity and the distribution coefficients at each wavelength compared with the sum of the products at 100% reflectivity, it is to be expected that luminosity values would follow a similar trend to reflectivity values. This is confirmed, a minimum being shown at 320 grit with the highest luminosity values being exhibited by the 600 grit discs. Very similar values were calculated for equi-energy conditions. The luminosity values for the diamond finished samples were as expected very near to their reflectivity values (7-8%).

4·2·5 Comment

On the basis of these experiments it was decided that provided a pre-treatment was standardised for each series of experiments satisfactory comparisons could be made. Since at this chronological moment the lapping process was not available, two types of surface preparation were selected (namely, nickel struck 320 grit and machine turned) for the next section of experimental work. Subsequently a set of discs was gold plated for the 600 grit machine lapped type of surface.

CHAPTER 5

THE HIDING POWER OF GOLD ELECTRODEPOSITS

5·1 INTRODUCTION

The object of the third series of experiments was to determine the thickness of gold required on a nickel surface in order to obviate the effect of the colour of the underlying surface. Various types of pre-treatment were used and the influence of different thicknesses of gold tested, the gold being deposited in increments on some discs and in different thicknesses on separate discs. The results of these experiments are given in Table 5·1A-C.

Subsequently a series of experiments was carried out in which the 600 grit pre-treatment was used exclusively and the results of these experiments are given in Table 5·2A-C. In Fig. 5·1 the discs are arranged in order of electroplating time and show that the very short plating times did not alter the appearance of the disc, but that gradually the gold spread over the disc until at 20 seconds a clear yellow gold was exhibited. (contd. p. 114.)

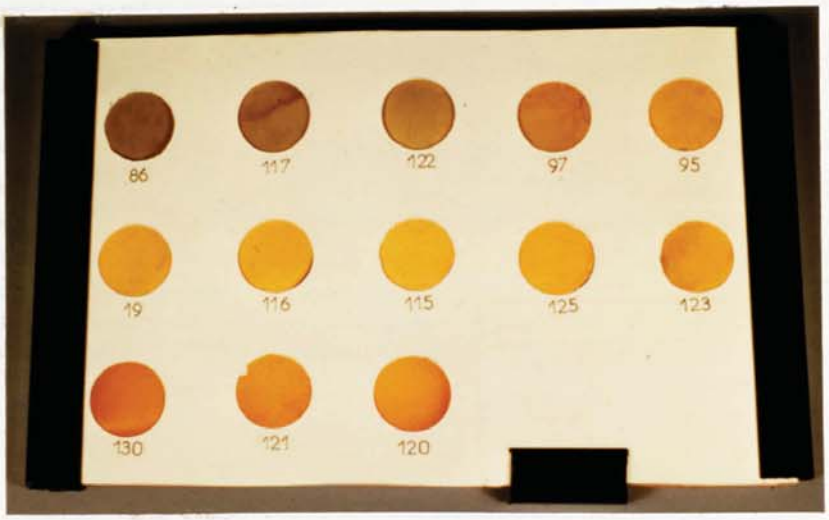

Fig. 5·1

Gold electroplated nickel discs (600 grit machine lapped finish)

Disc No.	Pre-Treatment	Current Density a.s.d	Time secs	Temp. °C	Calc. Thickness µm
9d(i)	(a) 320 grit by hand (b) Treatment A	2·5	1·4	65	0·0206
10d(i)	" " " " " "	2·5	5	65	0·0515
12d(i)	" " " " " "	2·5	30	65	0·278
11d(i)	" " " " " "	2·5	60	65	0·5773
5	original machined	2·5	30	65	0·4845
5(i)	continued by incremental electroplating	2·5	30 Total 60	65	0·773 total
5(ii)	" " " " " " " " "	2·5	60 Total 120	65	1·26 total
5(iii)	" " " " " " " " "	2·5	120 Total 240	65	2·25 total
5(iv)	" " " " " " " " "	2·5	240 Total 480	65	2·402 total
14e(i)	(a) original machined surface (b) Treatment A	1·25	30	65	0·38
14e(ii)	continued by incremental electroplating	1·25	60 Total 90	65	0·423 total
13d(i)	as 9(i)	2·5	120	65	0·608
13d(ii)	continued by incremental electroplating	2·5	120 Total 240	65	1·144 total

Table 5·1A

The Effect of Electroplated Gold Thickness on the Optical Properties of Gold Electrodeposits.

Disc No.	Chromaticity Coordinates					
	Equi-Energy			Tungsten Lamp		
	x	y	z	x	y	z
9d(i)	0·332	0·331	0·337	0·447	0·405	0·148
10d(i)	0·389	0·374	0·237	0·495	0·415	0·090
12d(i)	0·417	0·388	0·195	0·513	0·417	0·070
11d(i)	0·456	0·401	0·143	0·540	0·412	0·048
5	0·446	0·399	0·155	0·532	0·415	0·053
5(i)	0·460	0·401	0·139	0·542	0·411	0·047
5(ii)	0·487	0·405	0·108	0·559	0·406	0·035
5(iii)	0·507	0·407	0·086	0·571	0·402	0·027
5(iv)	0·502	0·409	0·089	0·567	0·405	0·028
14e(i)	0·449	0·404	0·147	0·534	0·416	0·050
14e(ii)	0·443	0·405	0·152	0·530	0·418	0·052
13d(i)	0·463	0·408	0·129	0·543	0·414	0·043
13d(ii)	0·463	0·409	0·128	0·544	0·413	0·043

Table 5·1B

Disc No.	Equi-Energy			Tungsten Lamp		
	D.W. nm	S %	L %	D.W. nm	S %	L %
9d(i)	457	1	8	450	1	8
10d(i)	580	28	7	587	33	7
12d(i)	583	41	11	586	47	12
11d(i)	585	57	25	590	63	27
5	585	53	38	589	45	42
5(i)	585	59	41	591	64	44
5(ii)	587	66	38	593	73	42
5(iii)	588	74	31	594	77	35
5(iv)	588	72	39	593	77	44
14e(i)	584	55	39	589	60	42
14e(ii)	583	54	48	588	60	51
13d(i)	585	61	54	590	66	58
13d(ii)	585	62	55	590	66	59

D.W. = Dominant Wavelength

S = Saturation

L = Luminosity

Table 5·1C

Thicknesses of gold were estimated by weighing before and after electroplating.

5·2 OPTICAL MEASUREMENTS ON THE FIRST SERIES OF EXPERIMENTS - VARIOUS PRE-TREATMENTS

5·2·1 Reflectivity

Four representative curves were plotted (Fig. 5·2) and these show that the characteristic step was not exhibited when the plating time was 1·4 seconds, and even after 5 seconds there was only the suggestion of a step, but after 30 seconds a step with a mid-energy of $3·6 \times 10^{-19}$ joules was obtained. After two minutes the mid-step energy was $3·5 \times 10^{-19}$ joules. Thus it is obvious that a minimum thickness of gold was required before the characteristic curve was obtainable. Insufficient samples were available in this series to determine the precise onset of an energy step.

5·2·2 Chromaticity Coordinates

Figs. 5·3a and b show the effect of gold thickness on the values of x, y and z, calculated with respect to equi-energy and tungsten lamp conditions. These results show that the x and y values calculated under both conditions increased with gold thickness on a smooth ascending decelerating curve, which eventually became almost horizontal. The z values decreased with gold thickness and became almost horizontal.

It was noticed that although two different pre-treatments were

(contd. p.118.)

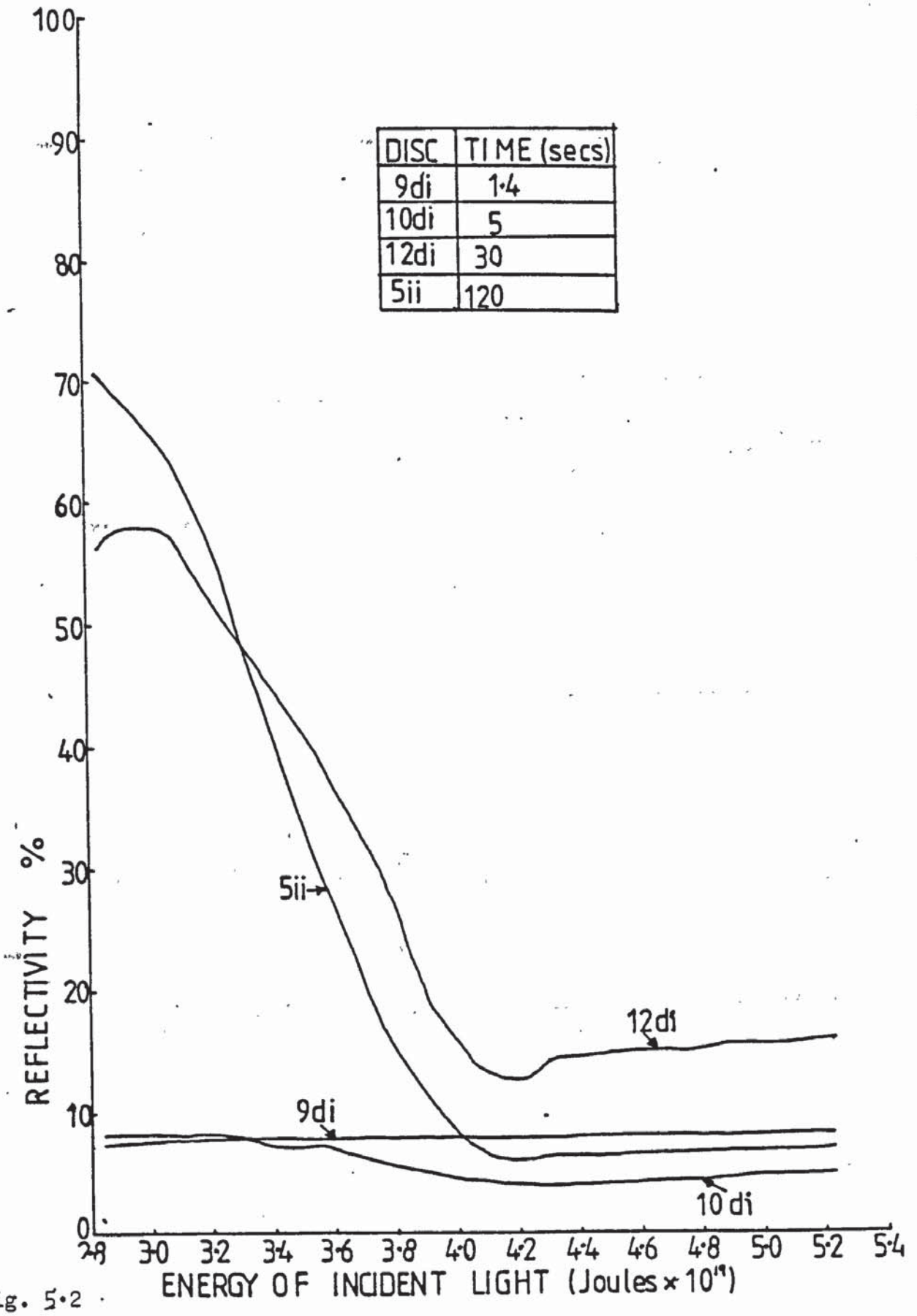

Fig. 5·2

Representative reflectivity curves

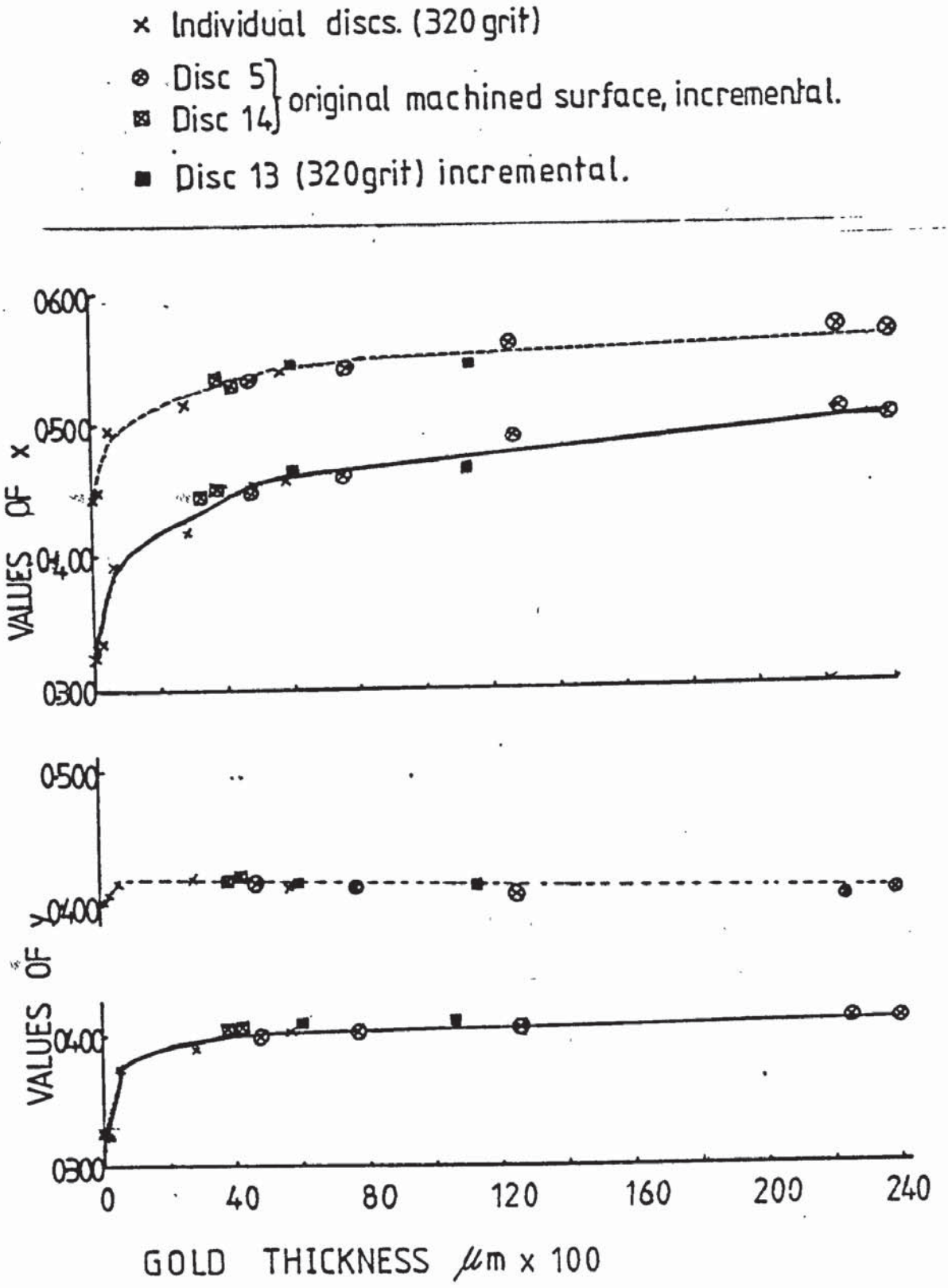

Fig. 5·3a

Effect of gold thickness on x and y chromaticity coordinates

× Individual discs. (320 grit)

⊗ Disc 5
⊠ Disc 14
} original machined surface, incremental.

■ Disc 13 (320grit) incremental.

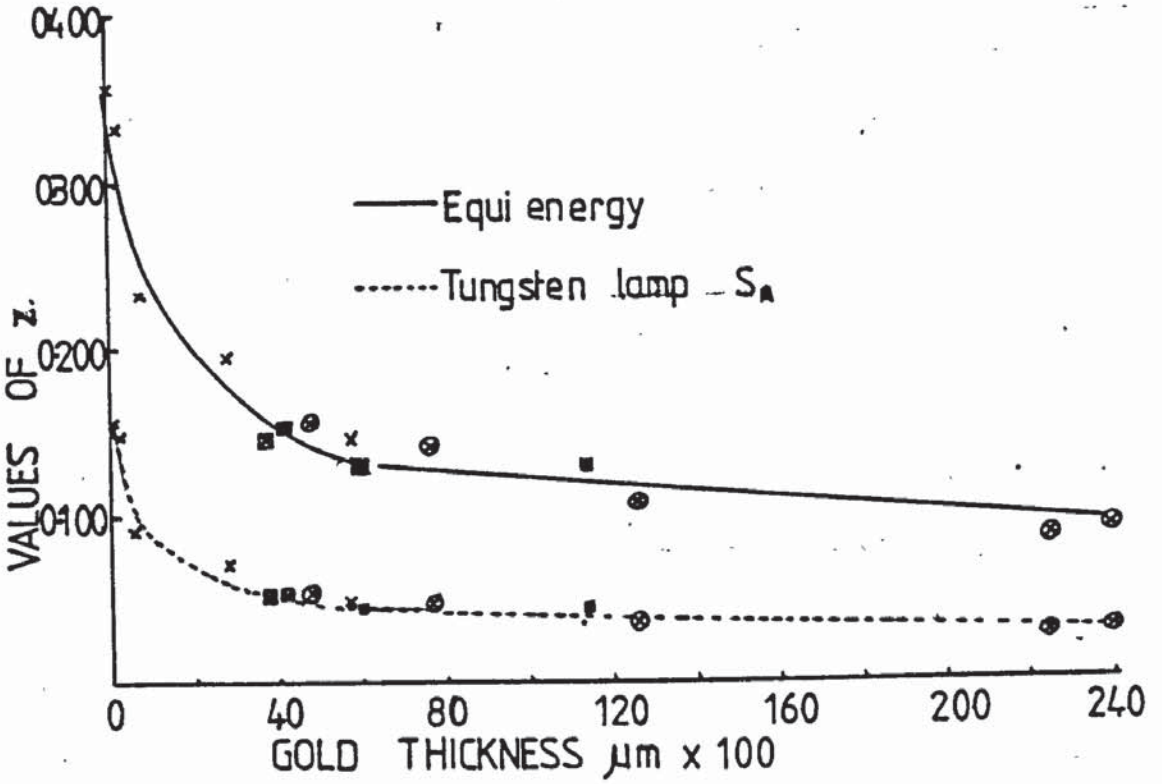

Fig. 5·3b

Effect of gold thickness on z coordinates

tried, and some of the gold was deposited in increments, the chromaticity coefficients fitted on to smooth curves, in general regardless of the practical details of the electrodeposition process. Thus it seemed that the colour of the samples was mainly dependent on the thickness of the gold, although the pre-treatment could have affected the thinner deposits.

The x parameter increased with thickness and became virtually stable at a thickness of 0·6 μm. Similarly with respect to the y parameter, except that stability appeared to be achieved at lower thicknesses (0·2-0·4 μm). The z parameter decreased with thickness, stability being achieved at approximately 0·6 μm. These results indicate that as the thickness of gold builds up, there is an increase in the amount of red and green in the colour and a decrease in blue.

The use of the term stability in this context infers little change in parameter with increase in thickness. This was achieved but it must be remembered that in no case was a completely horizontal graph obtained. On the other hand, if the electroplating process was operated in the region where all the graphs showed a tendency to flatten out, it is believed that for all practical purposes reproducible colours would be obtained. It seems likely that any changes in the relatively flat portion of the curve are likely to be due to the deposit itself rather than the underlying nickel. Thus it appears that greater than 0·6 μm of gold is required to cover the original surface. Examination of the graphs given in Fig. 5·3 show that for the x and y parameters, the parameters calculated under tungsten lamp conditions gave greater numerical

values than those for equi-energy conditions, and vice versa for the z parameter. This suggests that colours viewed under tungsten lamp conditions contained more red and green and less blue than under equi-energy conditions.

5·2·3 Luminosity

The luminosity values plotted in Fig. 5·4 show that as the thickness of gold increased the luminosity increased on a smooth curve, until at a thickness of 0·58 μm, the luminosity was 25% (equi-energy) and 27% (tungsten lamp). The pre-treatment for these initial discs was 320 grit, and subsequent thicknesses on the original machined surface gave somewhat higher luminosity values which then declined with increasing thickness. It was inferred that the probable shape of the luminosity curve if unaffected by different pre-treatments would be of the form shown in Fig. 5·5. (contd. p.121.)

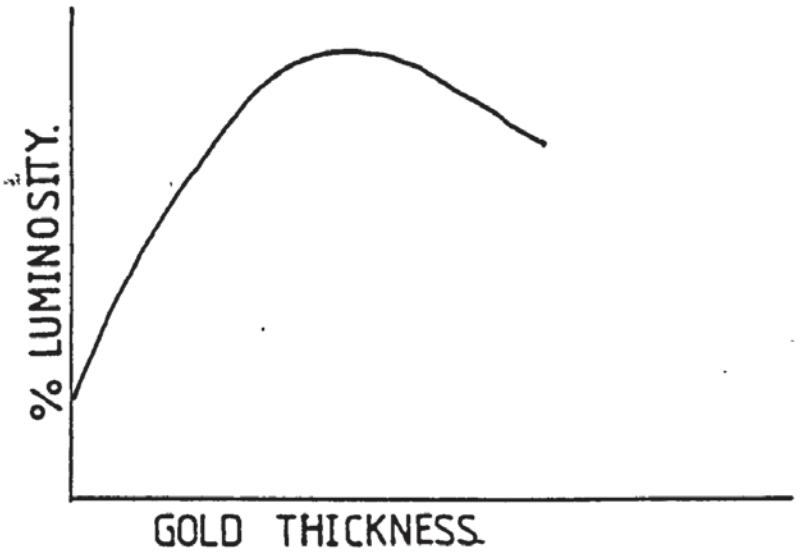

Fig. 5·5

Probable form of the luminosity curve

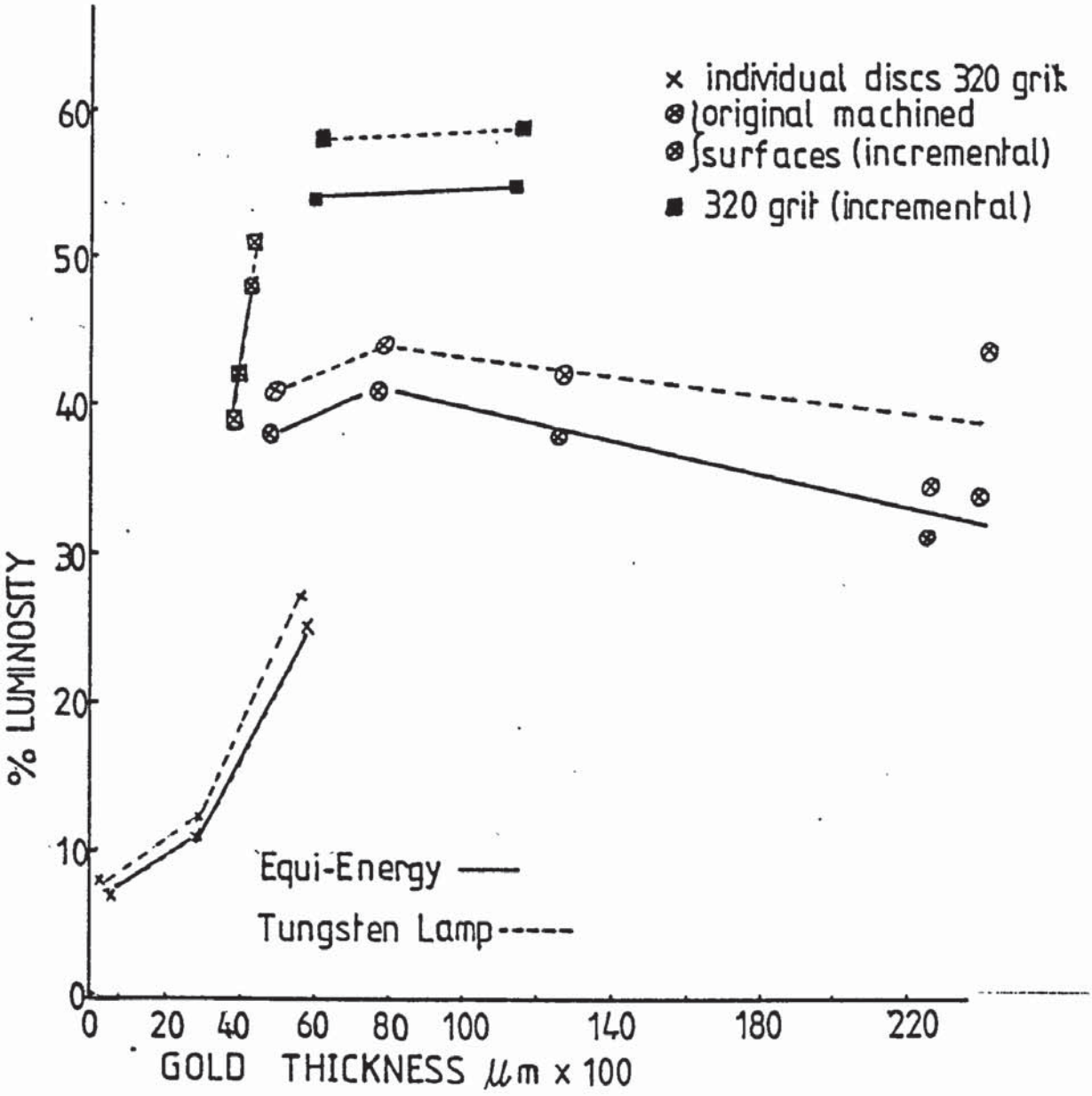

Fig. 5·4 Effect of gold thickness on luminosity

The luminosity values were very similar for each sample whether calculated for equi-energy or tungsten lamp conditions, with those for tungsten lamp conditions giving slightly higher values.

5·2·4 Dominant Wavelength and Saturation

Fig. 5·6 shows that there was a sudden increase in dominant wavelength from 457 nm (EE), 450 nm (S_A) to 580 nm (EE), 587 nm (S_A) when the thickness of the gold was increased from 0·0206 to 0·052 μm and thereafter as the gold thickness increased the dominant wavelength increased, but only slightly. Thus after 0·38 μm we can claim to be on the stable part of the curve. It would seem that there was very little change in the dominant wavelength after the deposition of a very thin gold coating, but it was obvious from visual examination that the colour was still changing considerably as the thickness increased. The chromaticity coordinates given in Fig. 5·3 confirm this. But if we examine the saturation curves for equi-energy and tungsten lamp conditions given in Fig. 5·7 we see that for both equi-energy and tungsten lamp the saturation increased dramatically initially, but then the rate of change decreased until at a thickness of 0·8 μm the slope was quite shallow. Thus we are in a range of relative stability beyond 0·8 μm of gold.

5·2·5 The Effect of Surface Quality

Three discs were electroplated together as a batch in Bath X, and the gold was built up in increments, with the colour being measured after each increment. Two discs in the batch were finished to 1 μm

(contd. p.124.)

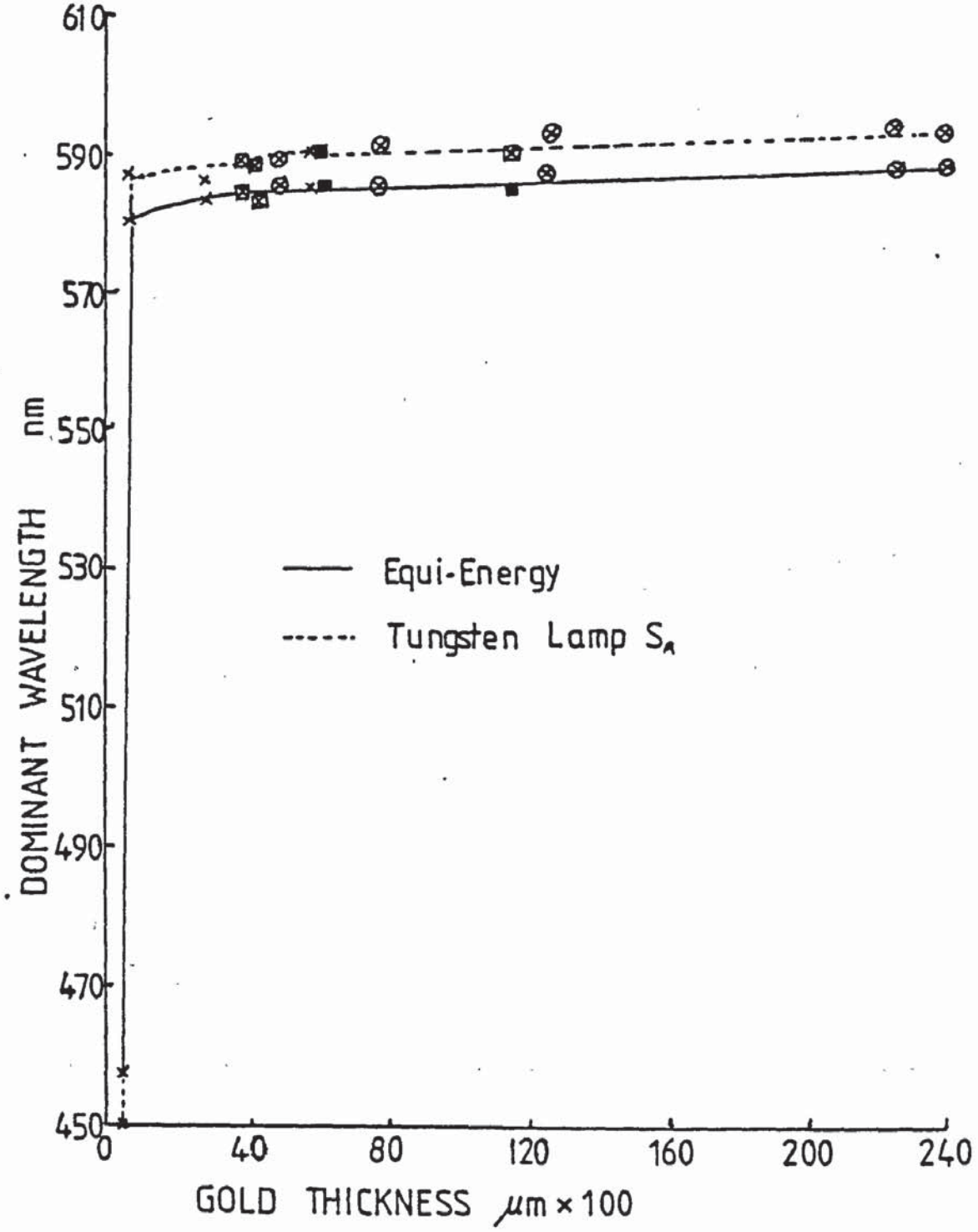

Fig. 5·6

Effect of gold thickness on dominant wavelength

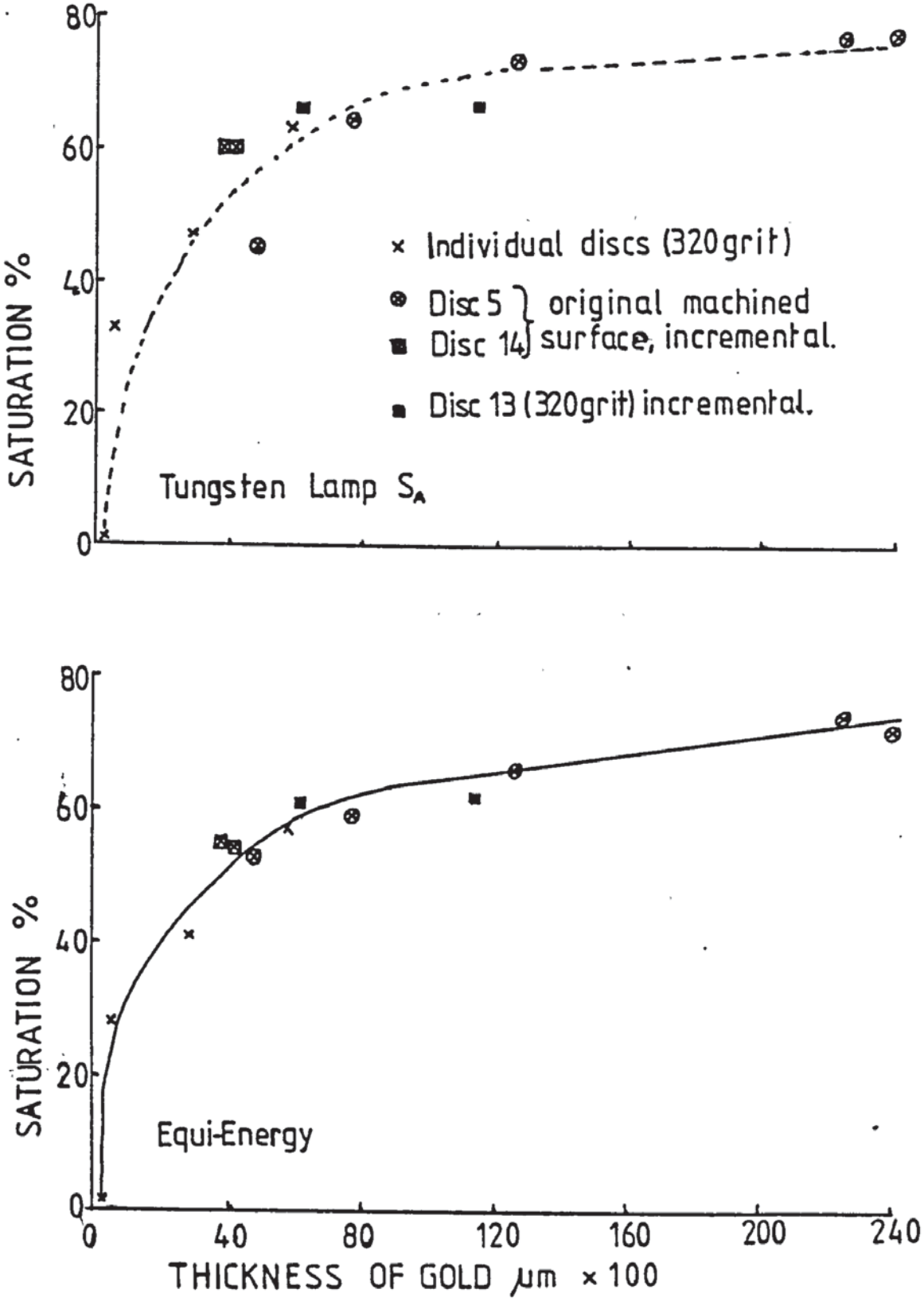

Fig. 5·7

The effect of thickness of gold on saturation

diamond, and the third was machine lapped to 600 grit. One of the diamond finished samples was repolished after each increment, whilst the other diamond finished disc and the 600 grit finished disc were untouched between increments. The results of these experiments given in Tables 5·2A-C show that the chromaticity coordinates of the two diamond finished discs were identical, and very near to the white point (saturation 2% dominant wavelength 588 nm), while the 600 grit sample was much further from the white point (saturation 11% dominant wavelength 579 nm). Thus it would appear that the grit finished disc was somewhat more yellow than the diamond finished, tending to confirm that the diamond finished tends to give protection from very slight, almost invisible tarnish films. Fig. 5·8 shows that after the deposition of the first increment all the discs moved away from the white point as was to be expected since they were all now definitely gold coloured. The dominant wavelength of the grit finished increased while the diamond finished fell slightly, but they all remained within the yellow region. The grit finished disc the greatest distance from the white point (57% S), the untouched diamond having a saturation value of 38% while the repolished gold had a saturation value of 33%. Thus we can see that the untouched diamond finished sample had moved somewhat nearer to the grit finished. This was confirmed as the deposits thickened, the untouched diamond finished sample getting progressively nearer to the grit finished sample. The measurements for these two conditions were very close. On the other hand, the values for the repolished sample remained very close together, and quite far away from the other two surface conditions (saturation for 600 grit 54%, untouched diamond finished 52%, interim diamond finished 30%). Luminosity values were

(contd. p.129.)

Sample No.	Description
64(o)	Disc surface finished to 600 grit, then nickel struck
64(i)	Disc surface finished to 600 grit, nickel struck, gold plated for 1 minute, then colour measured
64(ii)	A further increment of gold (2 minutes, total 3 minutes)
64(iii)	A further increment of gold (5 minutes, total 8 minutes)
42(o)	Disc finished to 1 µm diamond then nickel struck
42(i)	Disc surface finished to 1 µm diamond, nickel struck, gold plated for 1 minute
42(ii)	A further increment of gold (2 minutes, total 3 minutes)
42(iii)	A further increment of gold (5 minutes, total 8 minutes)
60(o)	Disc finished to 1 µm diamond then nickel struck
60(i)	Disc surface finished to 1 µm diamond, gold plated for 1 minute, then refinished on the diamond wheel to original brightness, judged by eye, prior to colour measurement
60(ii)	A further increment of gold (2 minutes, total 3 minutes), again refinished to 1 µm diamond
60(iii)	A further increment of gold (5 minutes, total 8 minutes), again refinished to 1 µm diamond

Table 5·2A

Batch incremental electroplating (different pre-treatments)

Disc No.	Chromaticity Coordinates					
	Equi-Energy			Tungsten Lamp S		
	x	y	z	x	y	z
64(o)	0·354	0·351	0·295			
64(i)	0·449	0·390	0·161	0·537	0·407	0·056
64(ii)	0·461	0·391	0·148	0·545	0·405	0·050
64(iii)	0·453	0·394	0·153	0·530	0·417	0·053
42(o)	0·337	0·333	0·330	0·456	0·404	0·140
42(i)	0·408	0·381	0·211	0·509	0·414	0·077
42(ii)	0·441	0·379	0·180	0·530	0·407	0·063
42(iii)	0·447	0·394	0·159	0·535	0·410	0·055
60(o)	0·337	0·333	0·330	0·456	0·404	0·140
60(i)	0·396	0·381	0·223	0·499	0·418	0·083
60(ii)	0·400	0·379	0·221	0·503	0·415	0·082
60(iii)	0·391	0·372	0·237	0·496	0·414	0·090

Table 5·2B

Disc No.	Equi-Energy			Tungsten Lamp S		
	D.W. nm	S %	L %	D.W. nm	S %	L %
64(o)	579	11	35			
64(i)	586	51	42	592	57	45
64(ii)	587	56	33	594	62	36
64(iii)	586	54	34	588	58	36
42(o)	588	2	8	515	1	8
42(i)	583	38	11	588	43	11
42(ii)	588	46	22	592	53	23
42(iii)	585	52	35	590	58	37
60(o)	588	2	8	515	1	8
60(i)	580	33	9	586	36	9
60(ii)	582	33	8	588	38	9
60(iii)	582	30	9	587	34	9

D.W. = Dominant Wavelength

S = Saturation

L = Luminosity

Table 5·2C

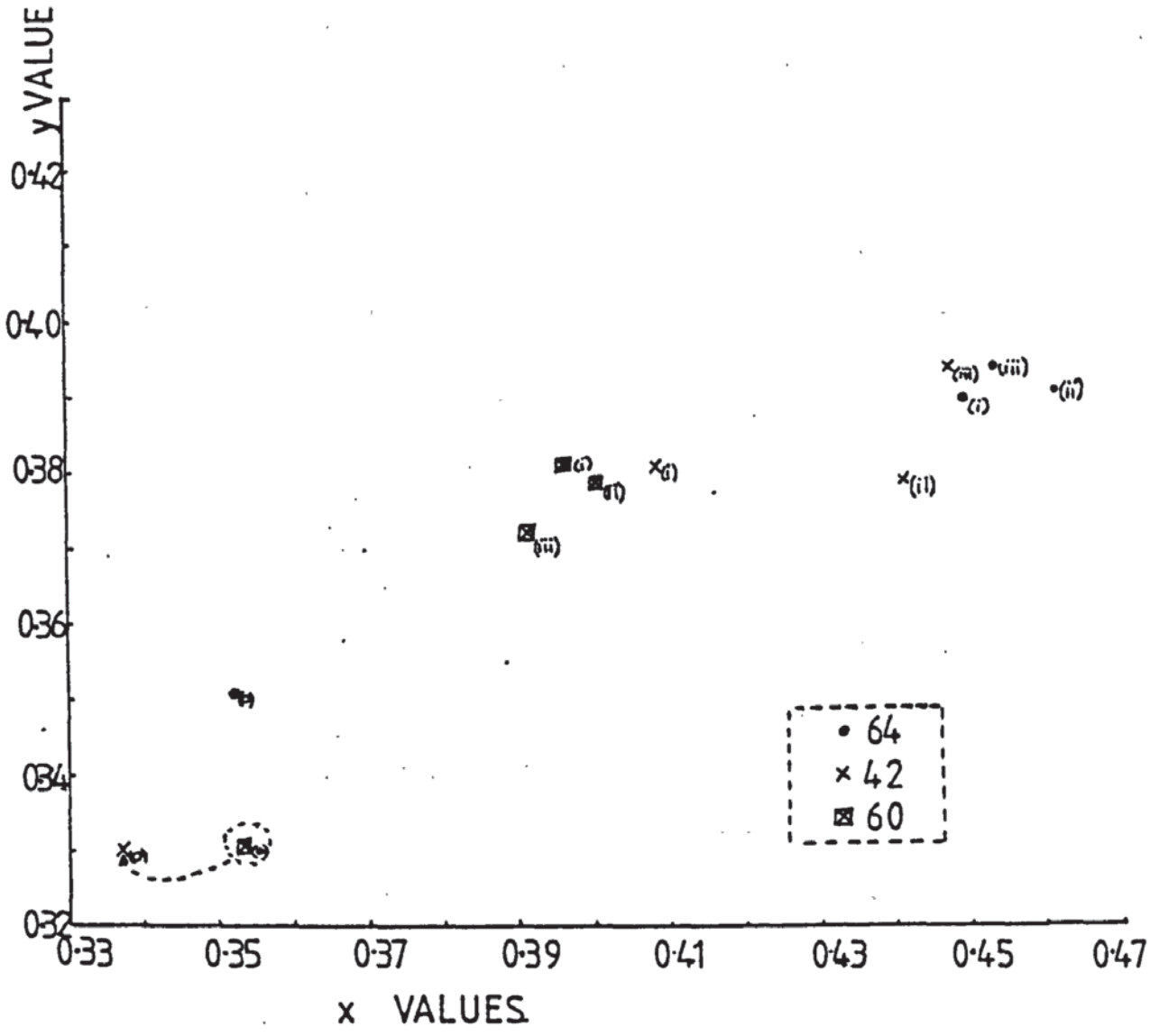

Fig. 5·8

Chromaticity coordinates showing the effect of pre-treatment and interim treatment (Equi-energy)

higher for the grit finished samples, and the untouched diamond finished ones increased to conform, but the interim diamond polished remained low.

5·2·6 Comment

At this stage it was considered that further information was required with respect to the thinner deposits and also thicknesses lying outside those already produced. It was decided therefore to increase the gold thickness gradually in increments, and to measure the colour at each increment.

5·3 OPTICAL MEASUREMENTS ON MACHINE LAPPED 600 GRIT SURFACES

5·3·1 Incremental Electroplating

Table 5·3 gives the increase in weight with time for disc TT9.

These results reveal that in the early samples (0·6 and 1·3 seconds) the increase in weight values, and from these the thickness values, were not to be relied upon, since they infer greater than 100% current efficiency. It may be that with such small plating time periods inaccuracies are bound to occur since the technique of incremental plating involves stripping and re-stopping off at each increment. Thus the unexplained increase in weight could be due to precipitation of nickel hydroxides in the roughly engraved numbers at the back of the disc. After a 3·6 second increment a loss in weight was actually experienced, and it was considered possible that this could have been due to the interstage acid dip causing

(cont'd. p. 131)

Increment No.	Time for this Increment (secs)	Increase in weight for this Increment (grams)	Increase in thickness for this Increment (μm)	Appearance
1	0·6	0·0012	0·18	No visible change, still an even grey colour
2	1·3	0·0019	0·17	A blotchy appearance not readily identified as gold
3	3·6	0·0025	none	Gold seems to be creeping in from the edges but still nickel showing through
4	2·9	0·0008	0·07	Perhaps a little more definitely gold, but still nickel showing through
5	5·1	0·0009	0·08	More definitely gold but still an odd nickel spot

Table 5·3

Results of incremental electroplating

bimetallic corrosion, since it was observed that bare areas of nickel were visible together with the gold deposit. It is realised that if nickel had entered the solution anodically an electronically equivalent amount of gold must have been cathodically deposited, but this could have been on the copper jig wire so that it would not be included in the final weighing. Subsequent increments of 2·9 and 5·7 seconds did not give weight increases consistent with time. Thus thicknesses based on weight increase did not seem likely to be accurate for extremely thin deposits, because any inaccuracies due to the reasons mentioned would be too great a proportion of the total. Hence it was decided to prepare a set of separate discs and to measure and calculate the various parameters with respect to the electroplating time. By reference to weight increase with thicker deposits a calculated thickness for even the very thin deposits could be obtained by calculation.

Since it was found that the very thin deposits up to an electroplating time of 5 seconds gave weight increases which were obviously too high, these samples, marked with an asterisk in the table, were not included in the following weight/thickness calculation:

Total electroplating time for those discs described in Table 5·4A-C	= 2860 seconds
Total increase in weight	= 0·2596 grams
Average increase in weight per second	= 0·00009076 grams
Average increase in thickness per second	= 0·008 µm

This factor was used to relate electroplating time to thickness measurements.

(contd.p. 135.)

Disc No.	Time in Bath X (seconds)	Appearance of Deposit	Thickness calculated from weight change (μm)
1T7	1·3	Still grey	0·0963*
97	5	Yellow but thin	0·0175*
1T6	30	Golden yellow	0·28
120	1200	Yellow but some darkening around the edges	8·79
130	480	Clear golden yellow but some darkening around the edges	2·79
T23	300	Golden yellow with darkening around the edges. The dark area easily rubbed off giving a clear yellow	2·905
1T9	0·6	No visible change	0·105*
95	10	Shadows of grey but mostly golden yellow	0·0788
115	60	Golden yellow	0·7875
122	3	Blotchy gold but much grey showing	0·13*
126	10	Thin gold with nickel coloured patch in the centre	0·20
19	20	Clear yellow gold	0·28
125	150	Clear yellow gold with slight darkening around edge	1·0675
121	600	Rather darker, not so smooth	5·53
121 α		Very light burnishing. removed powder giving a clear yellow colour	
1T5	0	Grey	0

Table 5·4A

The Effect of Thickness of Gold on Machine Lapped Discs

(All the discs were machine lapped to 600 grit before being electroplated at 2·5 a.s.d. at a temperature of 65°C in Bath X)

	Chromaticity Coordinates					
Disc No.	Equi-Energy			Tungsten Lamp		
	x	y	z	x	y	z
117	0·355	0·351	0·294	0·470	0·410	0·120
97	0·407	0·382	0·211	0·508	0·414	0·078
116	0·441	0·395	0·164	0·530	0·413	0·057
120	0·475	0·404	0·121	0·552	0·408	0·040
130	0·467	0·404	0·129	0·546	0·411	0·043
123	0·447	0·403	0·150	0·534	0·415	0·051
119	0·349	0·348	0·303	0·464	0·410	0·126
95	0·418	0·391	0·191	0·515	0·416	0·069
115	0·441	0·401	0·158	0·529	0·416	0·055
122	0·360	0·354	0·286	0·473	0·411	0·116
126	0·400	0·382	0·218	0·502	0·416	0·082
19	0·435	0·394	0·171	0·526	0·414	0·060
125	0·449	0·401	0·150	0·535	0·414	0·051
121	0·476	0·419	0·105	0·548	0·418	0·034
121 α	0·457	0·403	0·140	0·540	0·413	0·047
115	0·349	0·346	0·305	0·464	0·409	0·127

Table 5·4B

Disc No.	Equi-Energy			Tungsten Lamp		
	D.W. nm	S %	L %	D.W. nm	S %	L %
117	580	13	34	590	13	35
97	580	37	42	589	41	44
116	585	51	52	590	56	56
120	586	63	37	592	67	40
130	586	61	45	590	67	49
123	584	54	43	589	61	45
119	579	9	33	588	10	34
95	582	43	50	588	47	53
115	584	52	58	589	58	61
122	581	15	38	588	18	38
126	582	33	49	587	39	51
19	584	48	50	590	53	53
125	584	54	53	590	60	57
121	584	68	29	588	72	31
121 α	585	57	41	590	63	44
115	580	9	32	590	9	32

Table 5·4C

5·3·2 Gold Deposition on Separate Discs Machine Lapped to 600 Grit

The results of these experiments for lapped discs are given in Tables 5·4A-C.

5·3·2·1 Reflectivity Curves

Representative curves are plotted in Fig. 5·9 and show that the first curve to exhibit an energy step was a 5 second electroplating time, no steps being apparent with 1·3 and 3 second electroplating times. The energy steps were in the 3·6-3·7 x 10^{-19} J. region. The 5 second sample was described as yellow but thin whilst the 1·3 second sample was categorised as still grey. The emergence of the energy step indicated that the low energy end of the spectrum was being strongly reflected. The reflectivity percentage in this region increased with electroplating time (and thus with thickness) but then declined (10 minute sample) and this coincided with a darkening of the deposit.

5·3·2·2 Chromaticity Coordinates

Initially these were plotted for fairly short time periods (up to 60 seconds electroplating time, 0·47 μm calculated thickness). These results (Fig. 5·10) showed that for equi-energy values the x values lay on a fairly shallow ascending curve up to 3 seconds, but at 5 seconds there was a sudden increase in the parameter and there after the curve reverted to a fairly shallow ascending curve until at 30 seconds (0·23 μm) it appeared to have flattened, i.e. to have

(contd.p.138)

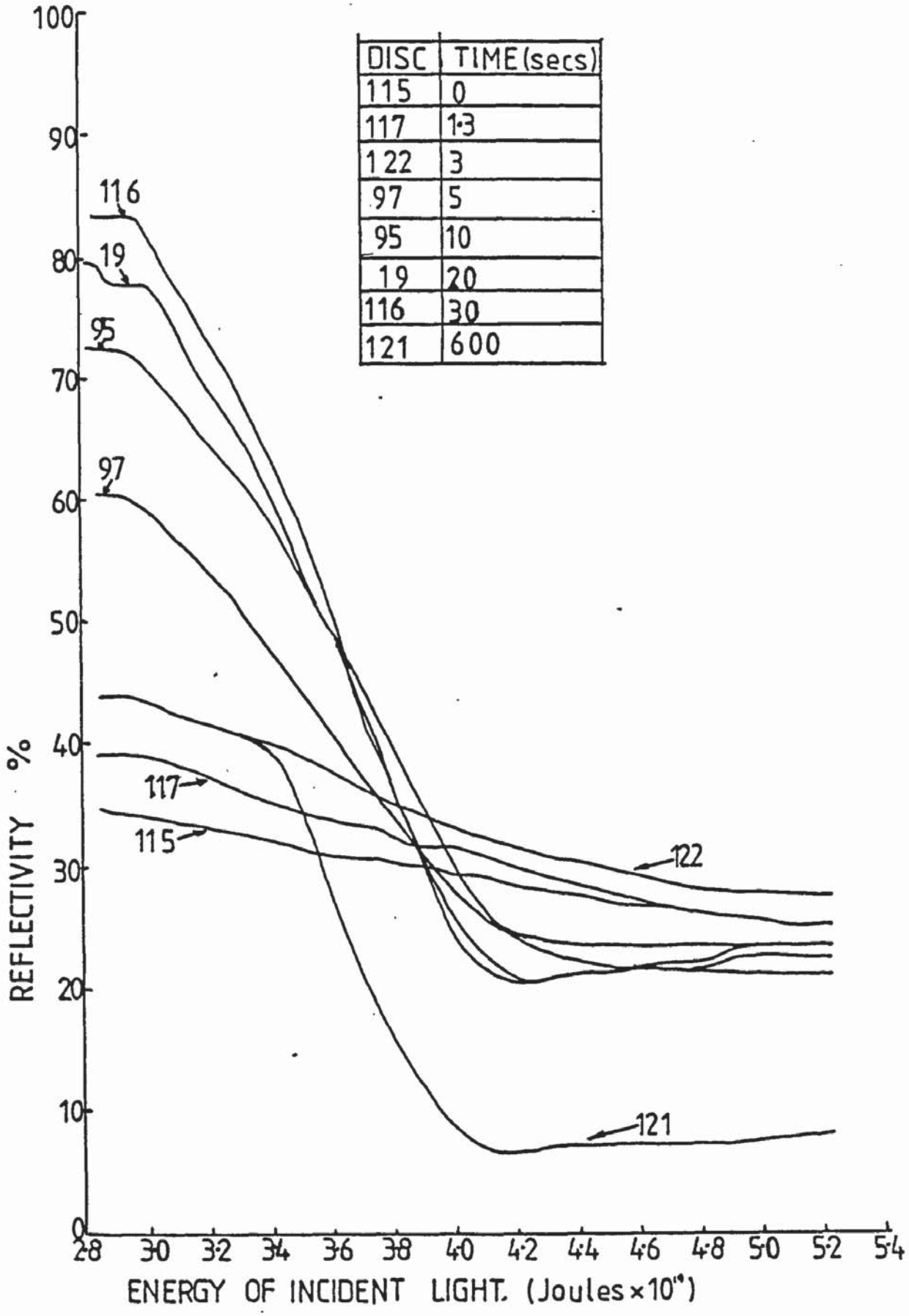

Fig. 5·9

Reflectivity Curves

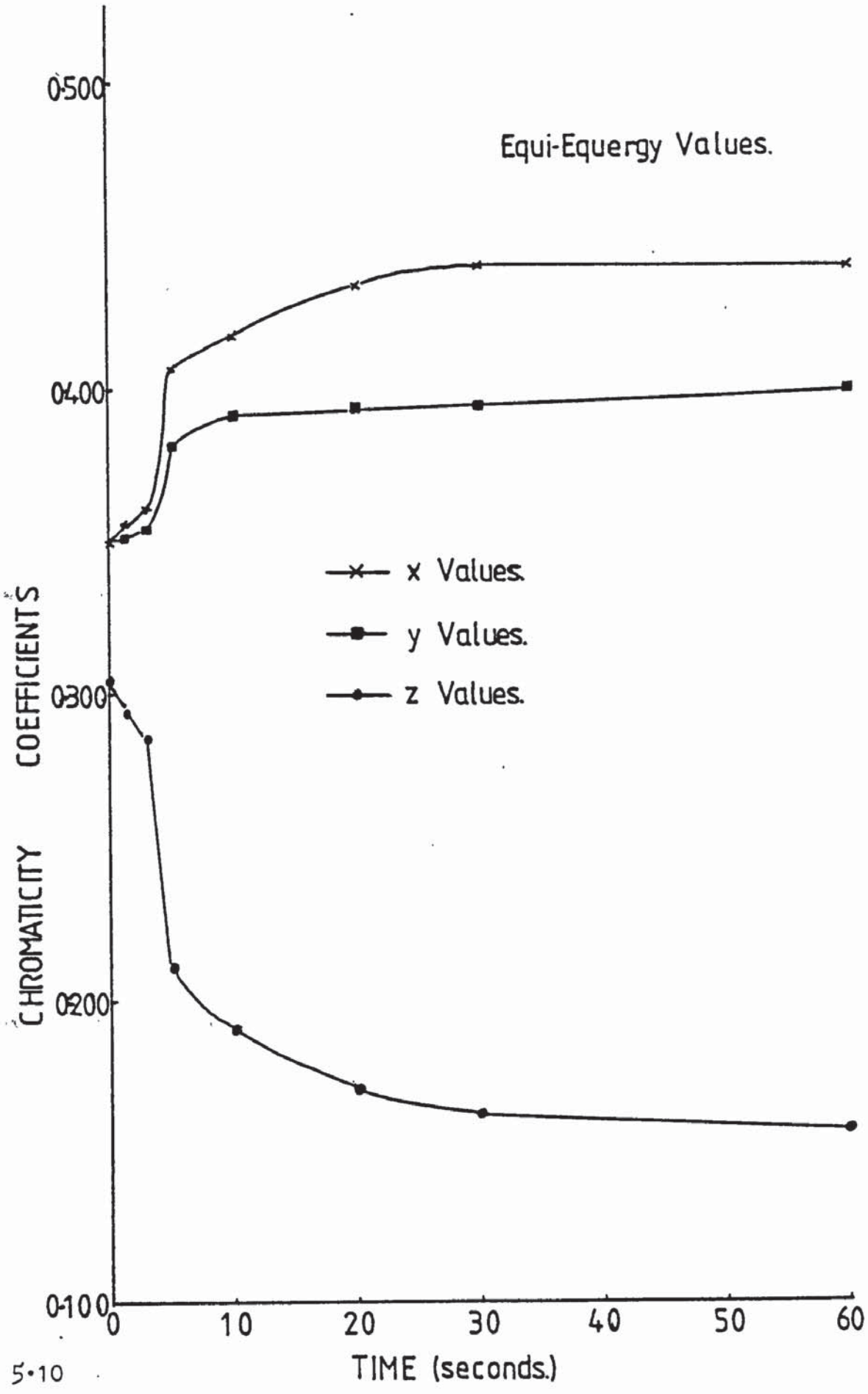

Fig. 5·10

Effect of electroplating time on chromaticity coordinates in discs lapped to 600 grit (Equi-energy)

become stable. If we examine the comments made about the deposit at the time we find that there was no visible change in the nickel surface at 0·6 seconds, it was still grey at 1·3 seconds, at 3 seconds blotchy with nickel showing through, at 5 seconds yellow but thin, whilst at 10 seconds it was mostly golden yellow with shadows of grey. At 20 seconds a clear yellow gold was exhibited. These comments then appear to conform to the chromaticity results. The y parameter followed a similar pattern to the x values except that stability was achieved after 10 seconds. The z values exhibited a downward trend with time until at 10 seconds there was a sudden descent and thereafter the rate of change declined until at 30 seconds stability was achieved.

A very similar pattern of results (Fig. 5·11) was obtained for the tungsten lamp S_A values except that the x and y values were numerically higher for any specified time period, while the z values were numerically lower.

In order to illustrate the effect of long time periods, the graph given in Fig. 5·12 was plotted, in which the parameters were plotted against logarithm of time in seconds, showing that colour stability continued from 30 seconds (0·23 μm) to 5 minutes (2·34 μm) after which there was a step up in the x parameter curve and a step down in the z parameter curve. The step also occurred in the y curve but at 8 minutes (3·74 μm). These steps appeared to conform to a darkening of the deposit which coincided with a slight powderiness of the deposit. Thus it seems that the growth of the deposits may be considered in three parts:

(contd p 141)

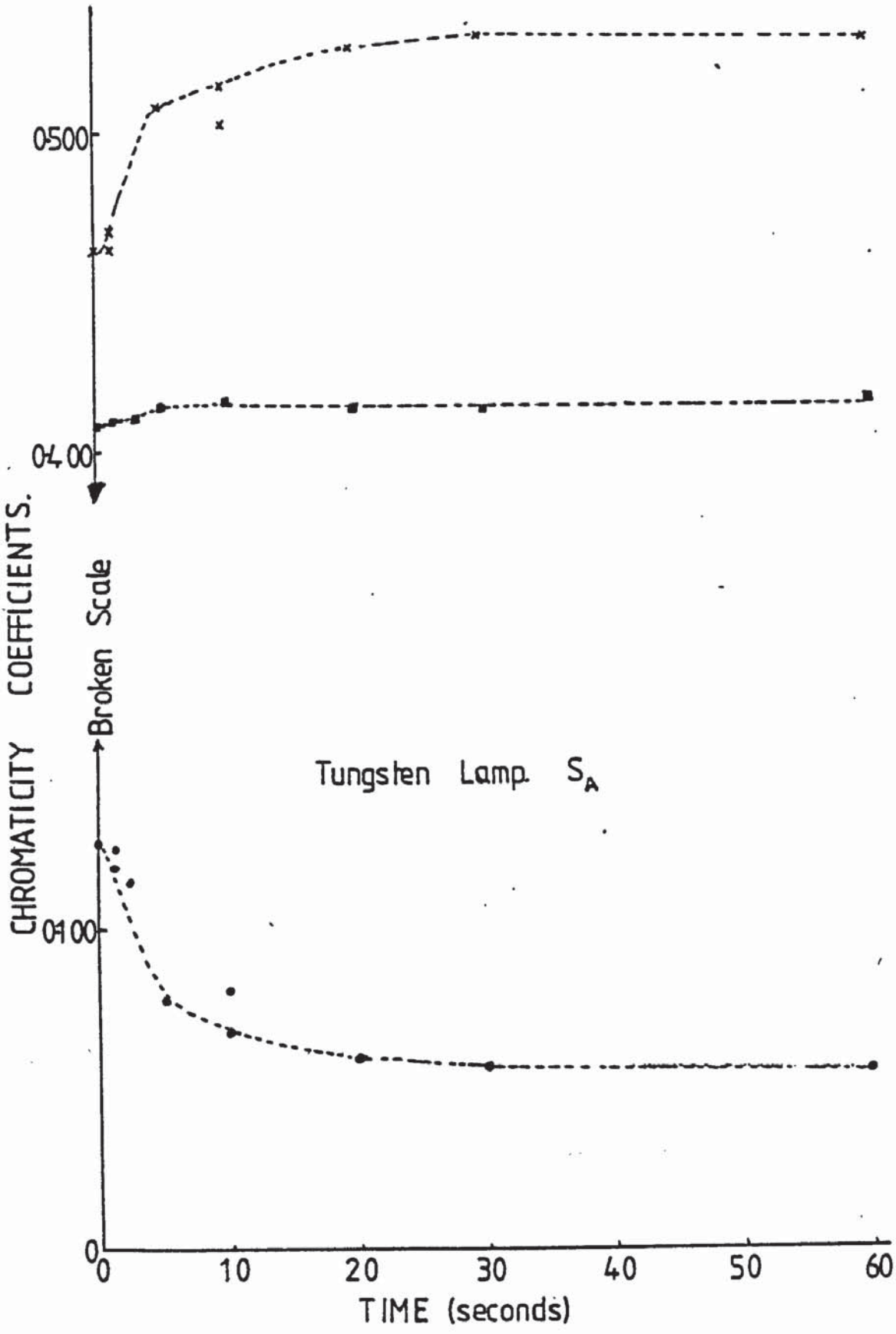

Fig. 5·11

Effect of electroplating time on chromaticity coordinates in discs lapped to 600 grit (Tungsten lamp)

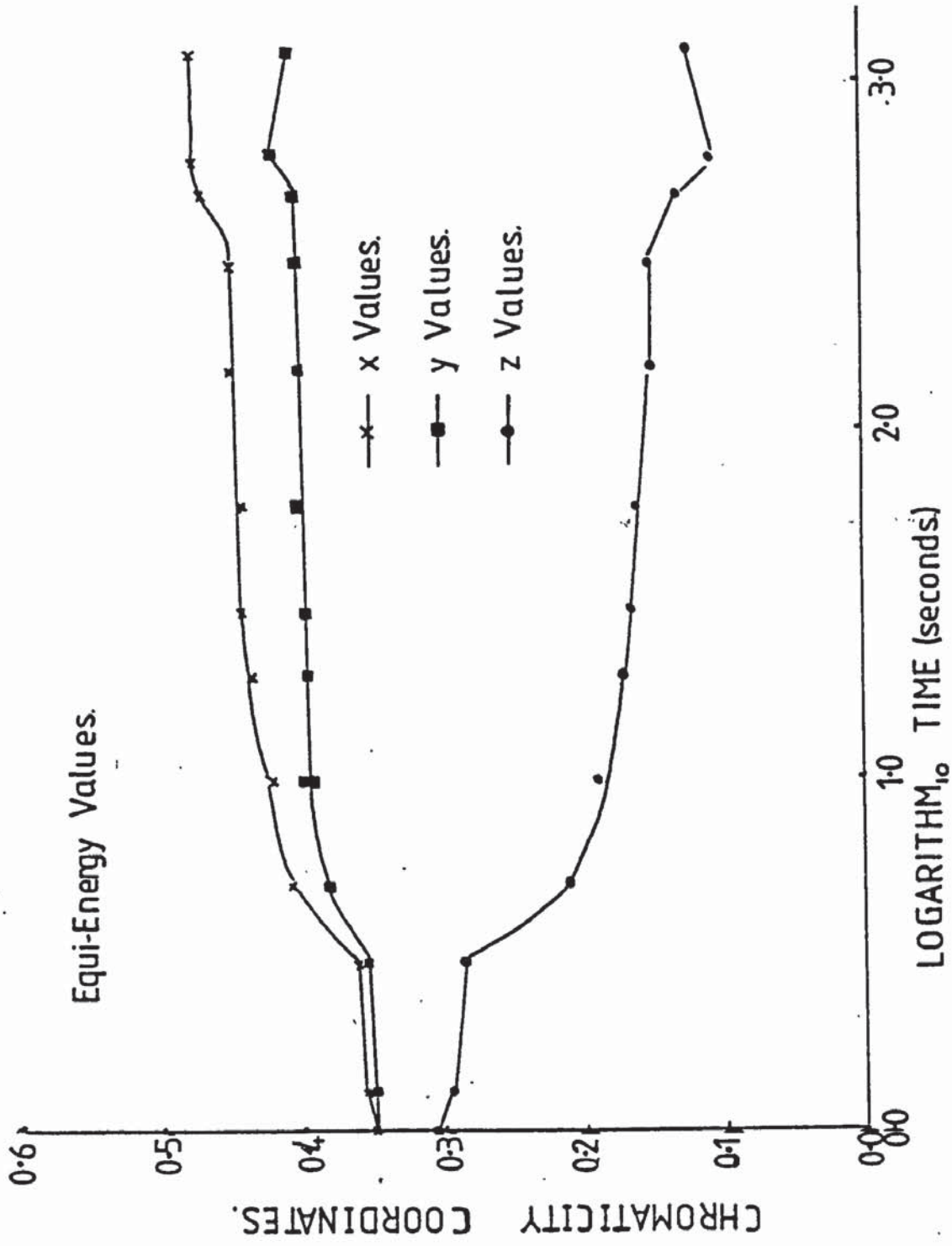

Fig. 5·12

Effect of plating time on chromaticity coordinates (Equi-energy)

(i) Gradual covering of the original colour of the nickel until the full gold colour is established.

(ii) Continuation of this colour with thickness.

(iii) Onset of powderiness and continuation of powdery growth.

This would appear to suggest that at the current density used there was a metal deficit in the catholyte which was not completely made up by diffusion from the main bulk of the solution. Eventually as the deficit continues to grow we reach a position (somewhere between 5 and 8 minutes electroplating time) where the gold content of the catholyte is so low that much hydrogen is evolved along with the gold. If we look at the increase in weight of a 5 minute sample and a 20 minute disc this appears to be substantiated, the increase in weight of the 20 minute sample only being approximately three times that of the 5 minute sample.

Curves of very similar shape were obtained for the tungsten lamp S'_A determinations (Fig. 5·13) except that the numerical values of the x and y parameters were somewhat higher and the z parameters somewhat lower.

5·3·2·3 Luminosity

The luminosity values for this set of experiments are given in Fig. 5·14 and show that with odd exceptions the luminosity increased with increase in the logarithm of time as a straight line relationship, reaching a peak after 70 seconds of electroplating, after which the luminosity decreased with time. Thus as the surface became increasingly gold-like the luminosity increased. The decrease in

(contd.p.144.)

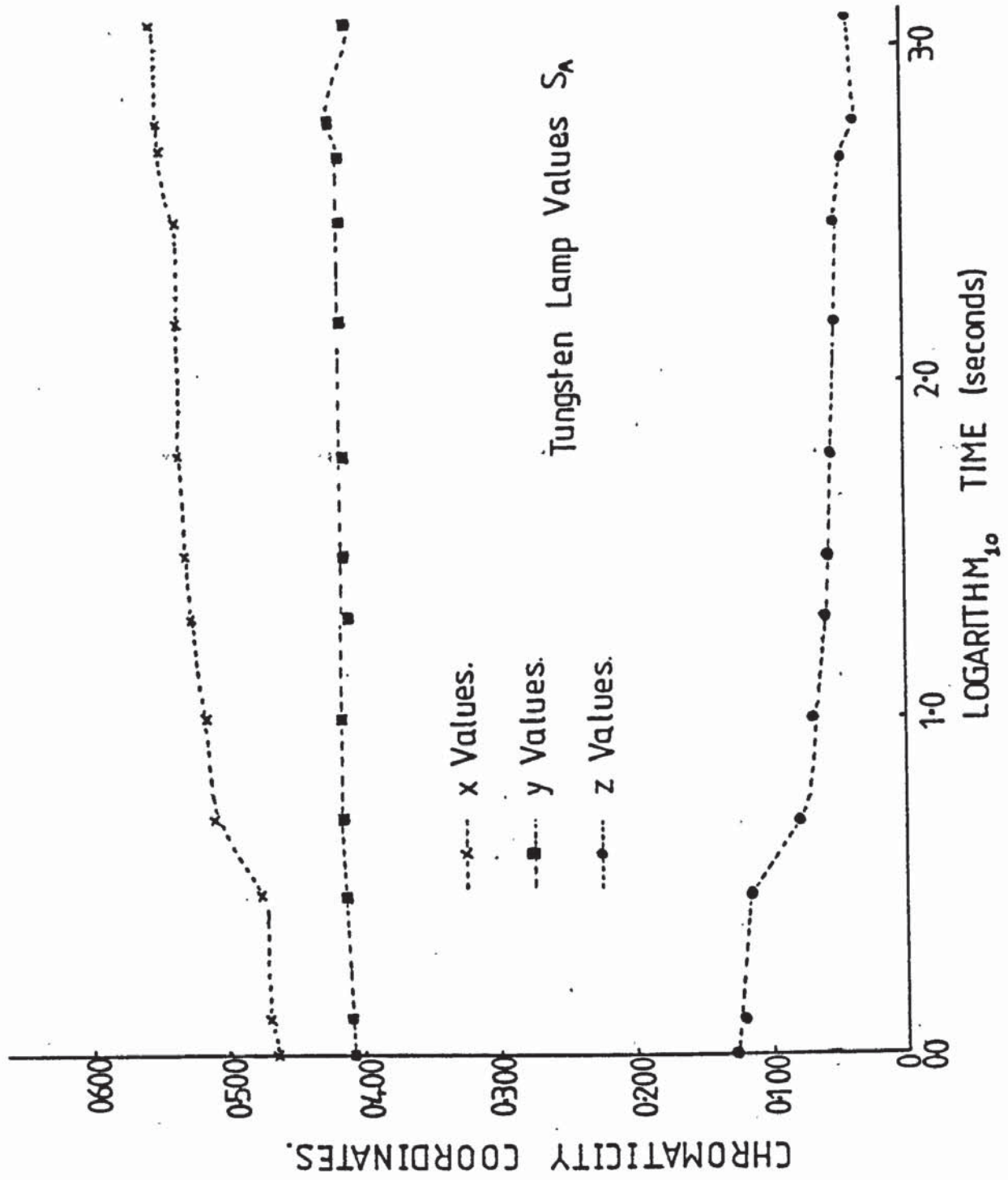

Fig. 5·13

Effect of plating time on chromaticity coordinates (Tungsten lamp)

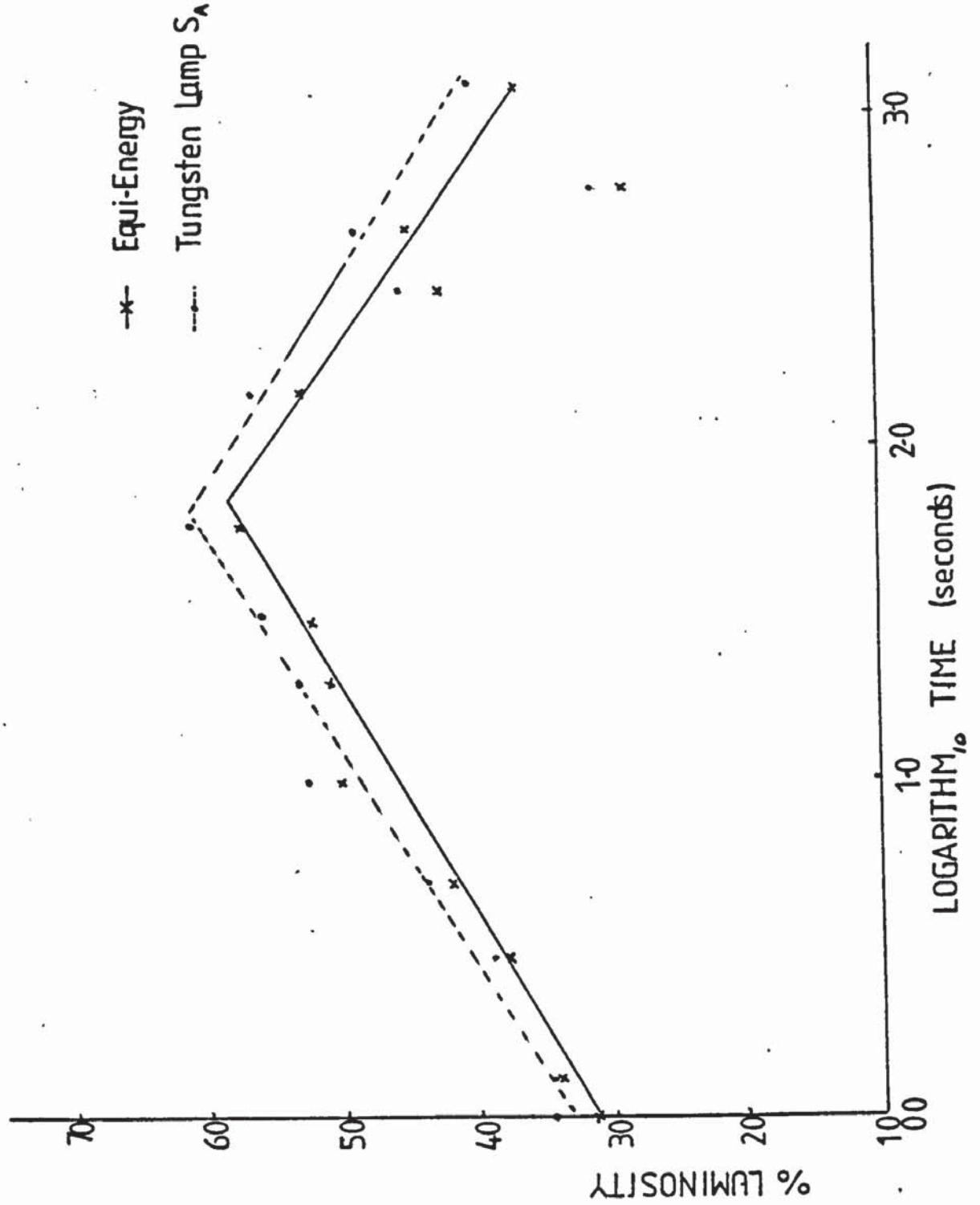

Fig. 5-14

The effect of plating time on luminosity values

luminosity appeared to correlate to the increasingly dark appearance of the gold associated with powderiness, the first fall in luminosity being noticed when the gold had only just started to darken at the extreme edges of the disc. Thus it appears that the spectrophotometer measuring process detected a change in luminosity before it was apparent to the eye, since the edges of the sample were not in the measurement area.

Luminosity values for equi-energy conditions conformed well with those calculated for tungsten lamp conditions, the tungsten lamp values being slightly higher at each time period.

5·3·2·4 Dominant Wavelength and Saturation

The dominant wavelength increased in value until after a time period of 20 seconds dominant wavelength stability was obtained (Fig. 5·15 equi-energy). This increase from 579 to 584 nm indicated that the colour was becoming more red. At 8 minutes there was a sudden increase in dominant wavelength which coincided with a darkening of the deposit growing in from the edges.

The same trends were noticed in those values calculated for tungsten lamp S_A, although the values were numerically higher and rather more scatter was observed. Increase in saturation followed a similar pattern for both illuminants which indicated that the colour stability was closely followed by saturation stability (Fig. 5·16).

(contd. p. 147.)

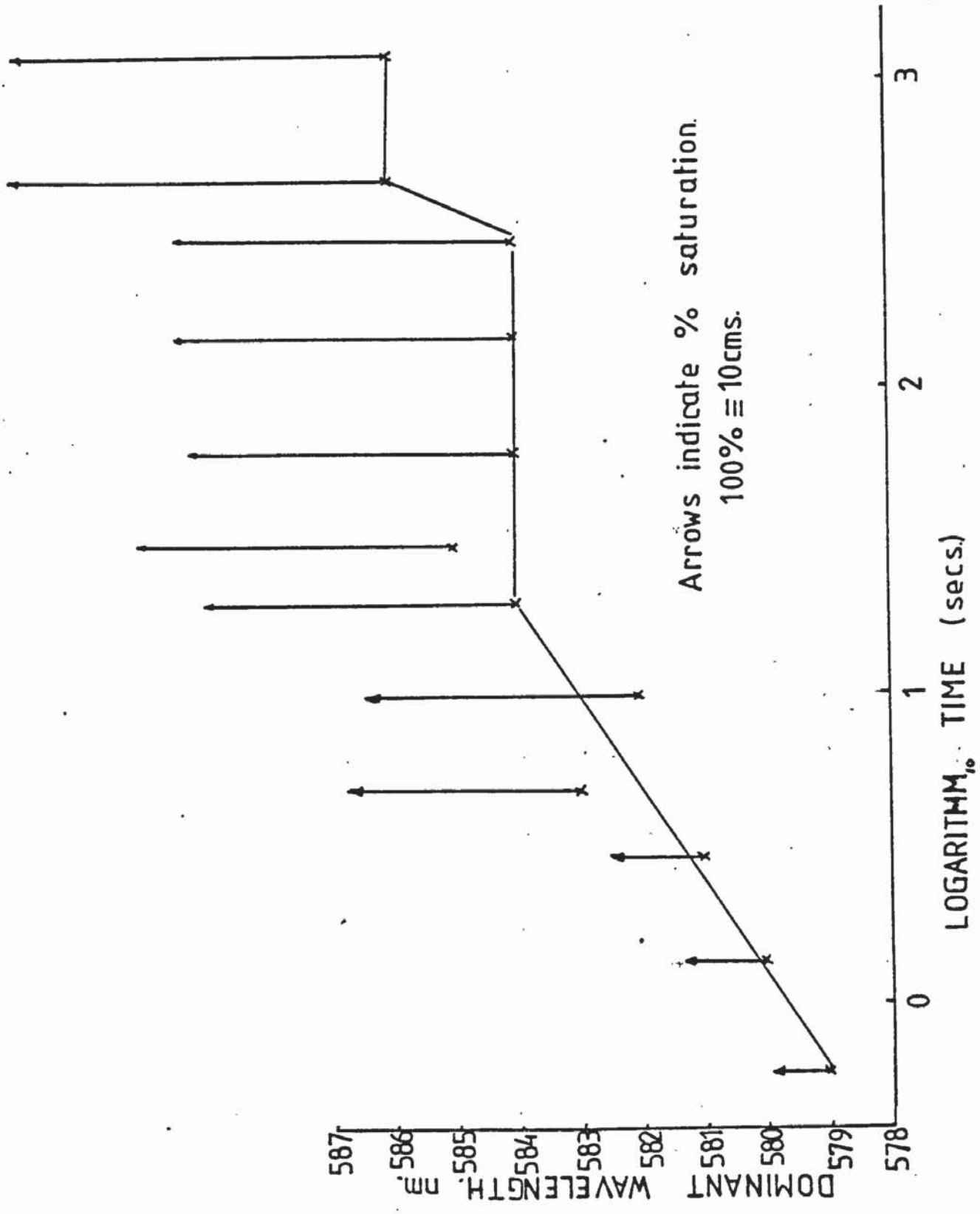

Fig. 5·15

The effect of electroplating time on Dominant Wavelength (Equi-energy)

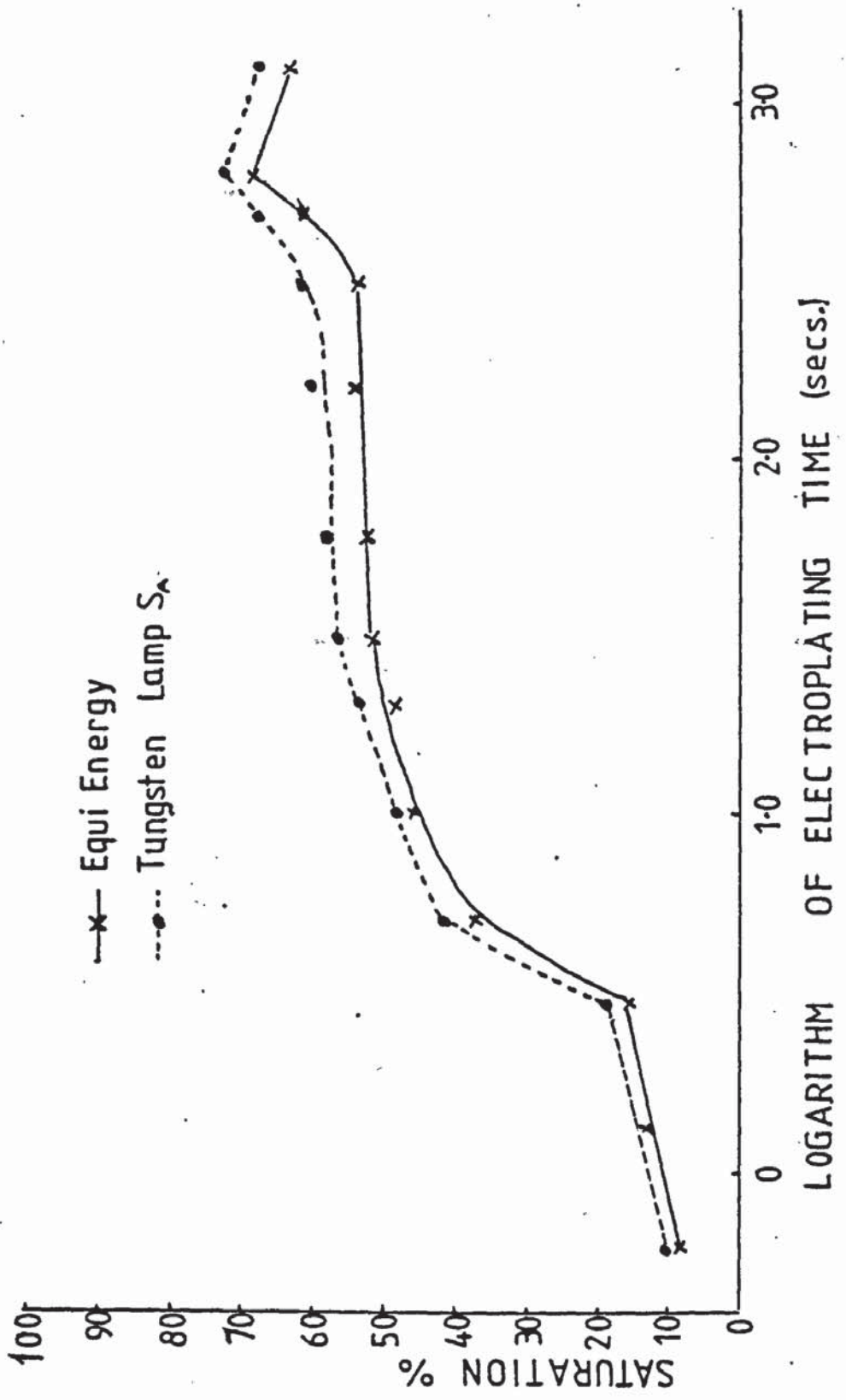

Fig. 5·16

The effect of electroplating time on saturation values

5·4 COMPARISON OF FIRST SET OF GOLD ELECTROPLATED SAMPLES - VARIOUS TYPES OF PRE-TREATMENT - WITH THE SECOND SET (LAPPED 600 GRIT)

5·4·1 Chromaticity Coordinates

Colour stability was obtained in the initial samples (320 grit and original machined) after a thickness of 0·6 μm of gold had been deposited, but for the 600 grit samples stability was obtained when 0·234 μm of gold (average value calculated from electroplating time) had been deposited. This is 0·23 μm if the individual weighed value is taken. Thus whichever value we consider, stability was obtained for the 600 grit samples at approximately half the thickness required for the initial samples. The shape of the curves obtained were very similar with the colour stability x values for the initial samples being slightly numerically higher than for the 600 grit samples, the y values being almost identical, and the z values being almost identical.

5·4·2 Luminosity

The luminosity curves for both series of experiments were similar, i.e. rising to a peak and then falling off with thickness. Although it was not possible to be absolutely accurate, the peak appeared to be in the region of 0·7 μm for the initial samples (320 grit and original machined) and at 0·55 μm for the 600 grit samples. Thus it seems that as colour stability is approached luminosity increases and continues to increase even when the colour is stable. The actual luminosity values were similar at

peak but the initial values were much lower for the initial samples which is probably related to the fineness of the surface finish. The falling part of the curve appears to conform to the slight darkening of the deposit with increasing thickness.

5·4·3 Dominant Wavelength and Saturation

The dominant wavelengths were very similar in numerical value in both series of experiments, with near stability being noted for very thin deposits. In both cases it was observed that the dominant wavelength became stable before the chromaticity coordinates. It must be remembered that dominant wavelength, as the name implies, refers to the dominant wavelength only, and tells us nothing about the distribution of the other wavelengths. This explains why the dominant wavelength reaches stability before the chromaticity coordinates.

5·5 SCANNING ELECTRON MICROSCOPE STUDIES ON THE GOLD ELECTROPLATED 600 GRIT FINISHED DISCS

The photographs given in Figs. 5·17-5·23 show that the usual "ploughed" surface was obtained for the 1·3 second disc (117), and that gold was not detected by the Kevex measurements. When the electroplating time was increased to 3 seconds, colonies of light coloured material believed to be gold, appeared to be growing, mostly from side faces of the "furrows". Gold was detected by the Kevex measurements. A similar topography was obtained for the 10 second disc (95) which exhibited a blotchy gold patch in the centre. A

20 second disc (19) which was described as clear yellow gold was shown to be of similar character to the original nickel surface, but rather more "feathery", that is, the outcrops of the furrows seemed to be more broken, obviously consisting of fine colonies of gold. This sample was also photographed with the effect of sample tilt eliminated, which made little difference except that the structure appeared to be somewhat elongated in a vertical direction. As we would expect from a sample described as "clear yellow gold", gold was detected in the Kevex measurement. The 150 second sample (125) exhibited a well defined granular appearance. Each granule appeared to consist of an aggregate of smaller granules.

(contd. p. 152)

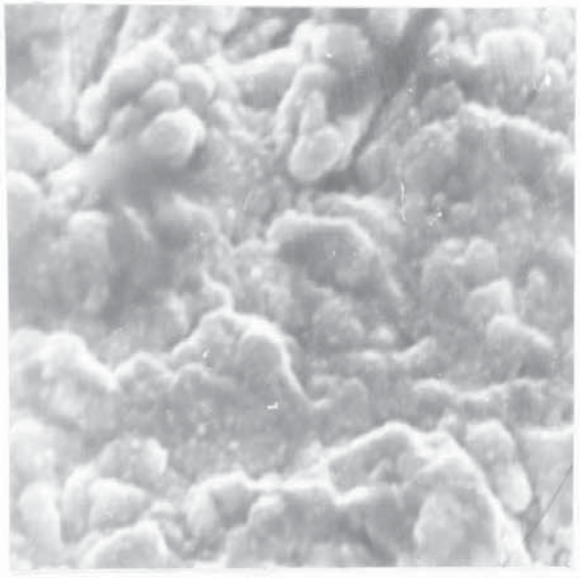

No. 117 1·3 seconds
Still grey. Gold not detected by Kevex (5K)

Fig. 5·17

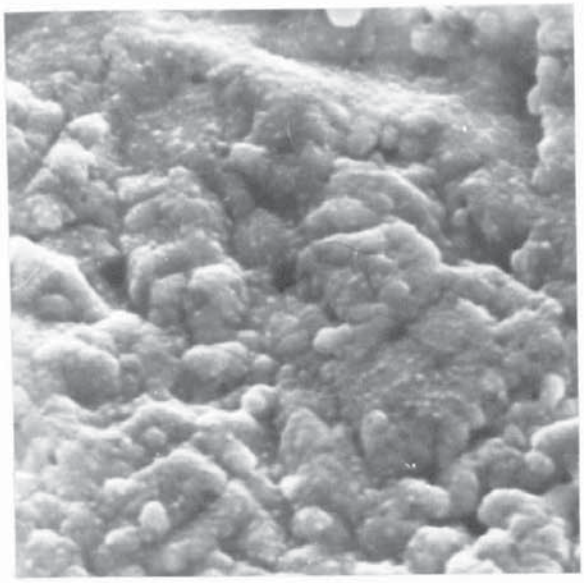

No. 97 5 seconds
Yellow but thin gold detected by Kevex (5K)

Fig. 5·18

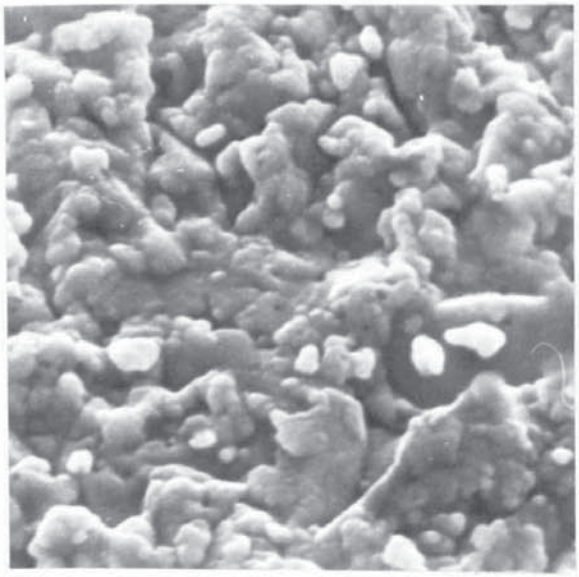

No. T22 3 seconds
Blotchy gold but much grey showing. Gold detected but small peak (5K)

Fig. 5·19

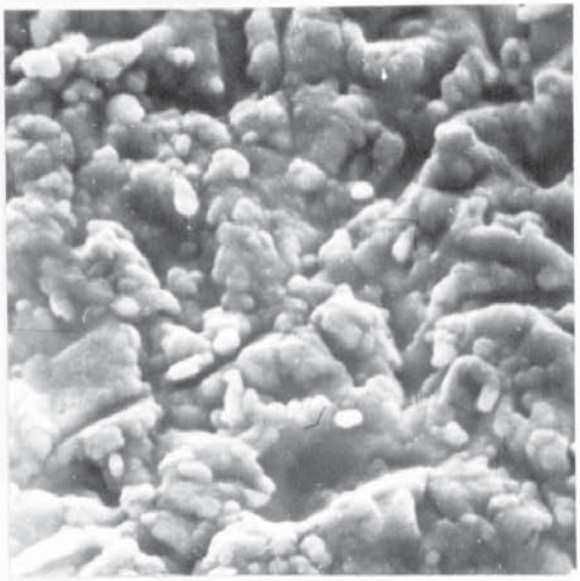

No. 95 10 seconds
Thin gold with nickel coloured patch in centre. Gold detected by Kevex (5K)

Fig. 5·20

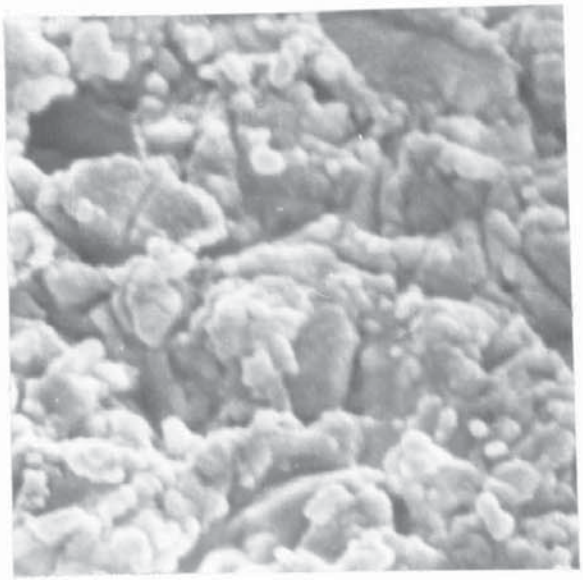

No. 19 20 seconds
Tilt not eliminated. Clear yellow gold detected by Kevex (5K)

Fig. 5·21

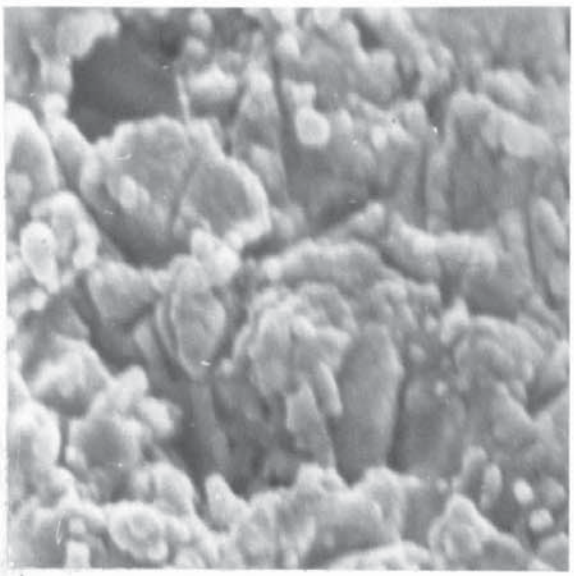

No. 19 20 seconds
Tilt eliminated (5K)

Fig. 5·22

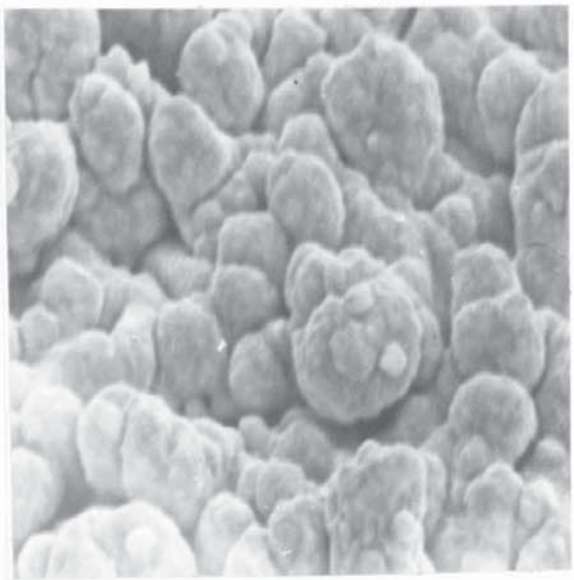

No. 125 150 seconds
Clear yellow gold with slight darkening around edges. Gold detected by Kevex. Tilt correction (5K)

Fig. 5·23

CHAPTER 6

THE ADDITION OF COPPER TO THE GOLD ELECTROPLATING BATH

6·1 INTRODUCTION

In this series of experiments the object was to add copper to a simple gold bath and to measure any changes in optical properties produced, and if possible to relate these changes to bath and deposit compositions. The numerical results of these experiments are given in Tables 6·1A-C, and a photograph of the discs produced is given in Fig. 6·1.

6·2 OPTICAL MEASUREMENTS

6·2·1 Reflectivity Curves

The shape of the curves measured on the spectrophotometer gave reason to suppose that all the reflectivity curves would exhibit a step and the curves are plotted in Fig. 6·2. These curves show that for low copper contents, as the copper content of the gold bath increased, the step occurred at progressively lower energies, but that for the higher copper contents the situation became somewhat confused. The reflectivity curves though, still exhibiting a step, changed in character in that the step became somewhat rounded, whilst the maximum reflectivity decreased. Plotting of the high, low and mid point energies (Figs. 6·3 and 6·4) confirm the impression gained from the reflectivity curves. The graphs show that as the copper content of the baths increased the energy value of the step fell on a smooth curve until around 7 gm/dm^3 of copper the energy again started to increase, becoming relatively stable between 10 and 16 gm/dm^3, and thereafter falling on a smooth curve. The value for a copper electrodeposit (which had the lowest energy step measured)

(contd. p.161.)

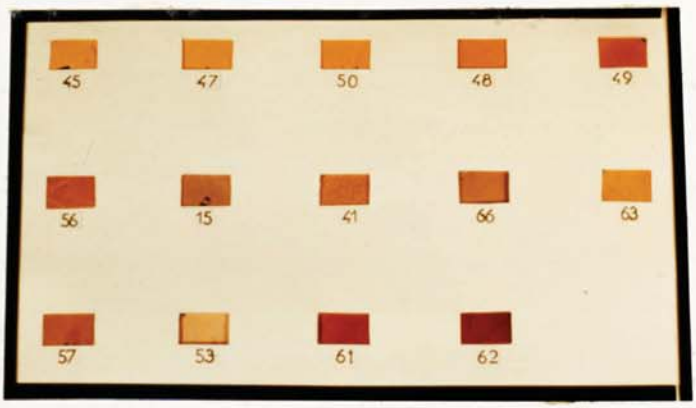

Fig. 6·1

The effect of copper additions to a gold bath

Disc No.	Addition of copper to bath (gm/dm^3)	Time (min)	Appearance	Notes
15) 16)	6·9	28	Pale smooth pinkish fawn	Stirred with magnetic stirrer
17) 18)	6·9	28	As above but colour slightly more red	No stirring for this and subsequent discs
45	0·0	20	Yellow	
47	0·45	20	Yellow	
50	0·90	20	Yellow	
48	1·8	20	Slightly darker yellow	
49	3·6	20	A reddish tone to the gold	
41	10·70	20	Fawn	
53	17·90	20	Pink	
62		20	Copper coloured	A copper cyanide bath
56	7·2	20	Reddish	
66	12·5	20	Putty coloured	
63	14·32	20	Reddish-fawn	
57	16·10	20	More red in the fawn than 63	
61	21·48	20	Copper-coloured	

Table 6·1A

The Effect of the Addition of Copper to Gold Bath Y

Temperature of bath = 25°C

Disc No.	Chromaticity Coordinates					
	Equi-Energy			Tungsten Lamp		
	x	y	z	x	y	z
15	0·385	0·358	0·257	0·494	0·406	0·100
16	0·386	0·359	0·255	0·495	0·406	0·099
17	0·398	0·360	0·242	0·505	0·403	0·092
18	0·401	0·361	0·238	0·507	0·403	0·090
45	0·456	0·400	0·144	0·540	0·411	0·049
47	0·453	0·394	0·153	0·539	0·409	0·052
50	0·457	0·396	0·147	0·542	0·408	0·050
48	0·458	0·391	0·151	0·543	0·406	0·051
49	0·458	0·379	0·163	0·546	0·399	0·055
41	0·418	0·371	0·211	0·518	0·405	0·077
53	0·387	0·353	0·260	0·498	0·402	0·100
62	0·450	0·350	0·200	0·548	0·382	0·070
56	0·457	0·374	0·169	0·547	0·395	0·058
66	0·408	0·377	0·215	0·509	0·412	0·080
63	0·408	0·365	0·227	0·513	0·403	0·084
57	0·383	0·361	0·256	0·492	0·409	0·099
61	0·417	0·356	0·227	0·522	0·394	0·084

Table 6·1B

Disc No.	Equi-Energy			Tungsten Lamp		
	D.W. nm	S %	L %	D.W. nm	S %	L %
15	586	23	42	594	31	43
16	586	24	32	594	31	33
17	587	28	39	595	32	41
18	588	28	48	596	33	50
45	585	56	49	591	62	53
47	586	53	49	591	60	52
50	586	55	45	592	61	49
48	587	55	38	593	61	42
49	590	51	33	596	57	36
41	588	37	35	594	42	37
53	589	22	46	597	27	48
62	598	40	21	607	50	23
56	591	49	27	597	56	30
66	584	36	38	590	41	40
63	588	31	36	595	38	38
57	585	23	33	592	26	34
61	593	31	27	602	37	29

Table 6•1C

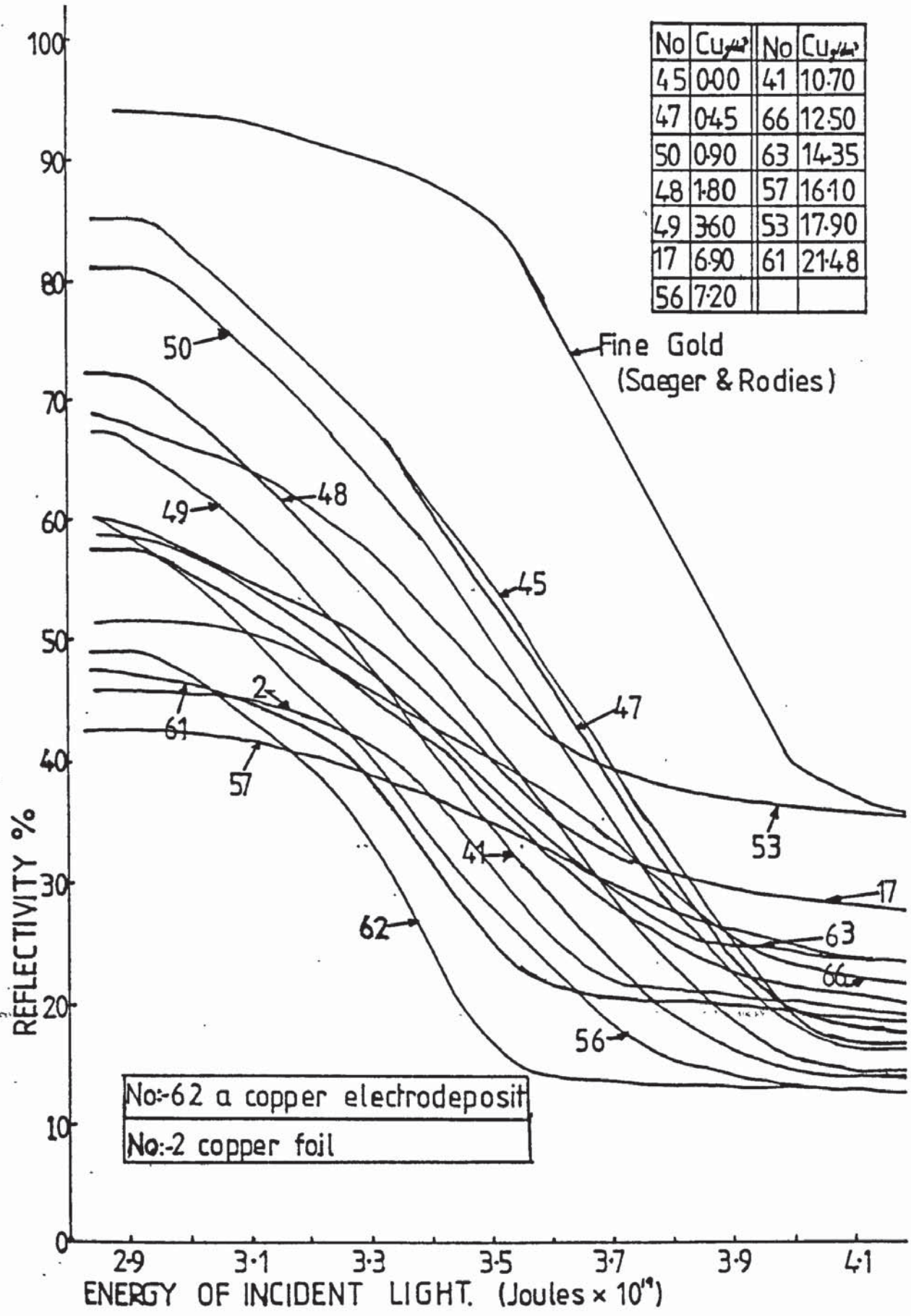

Fig. 6·2

Reflectivity Curves

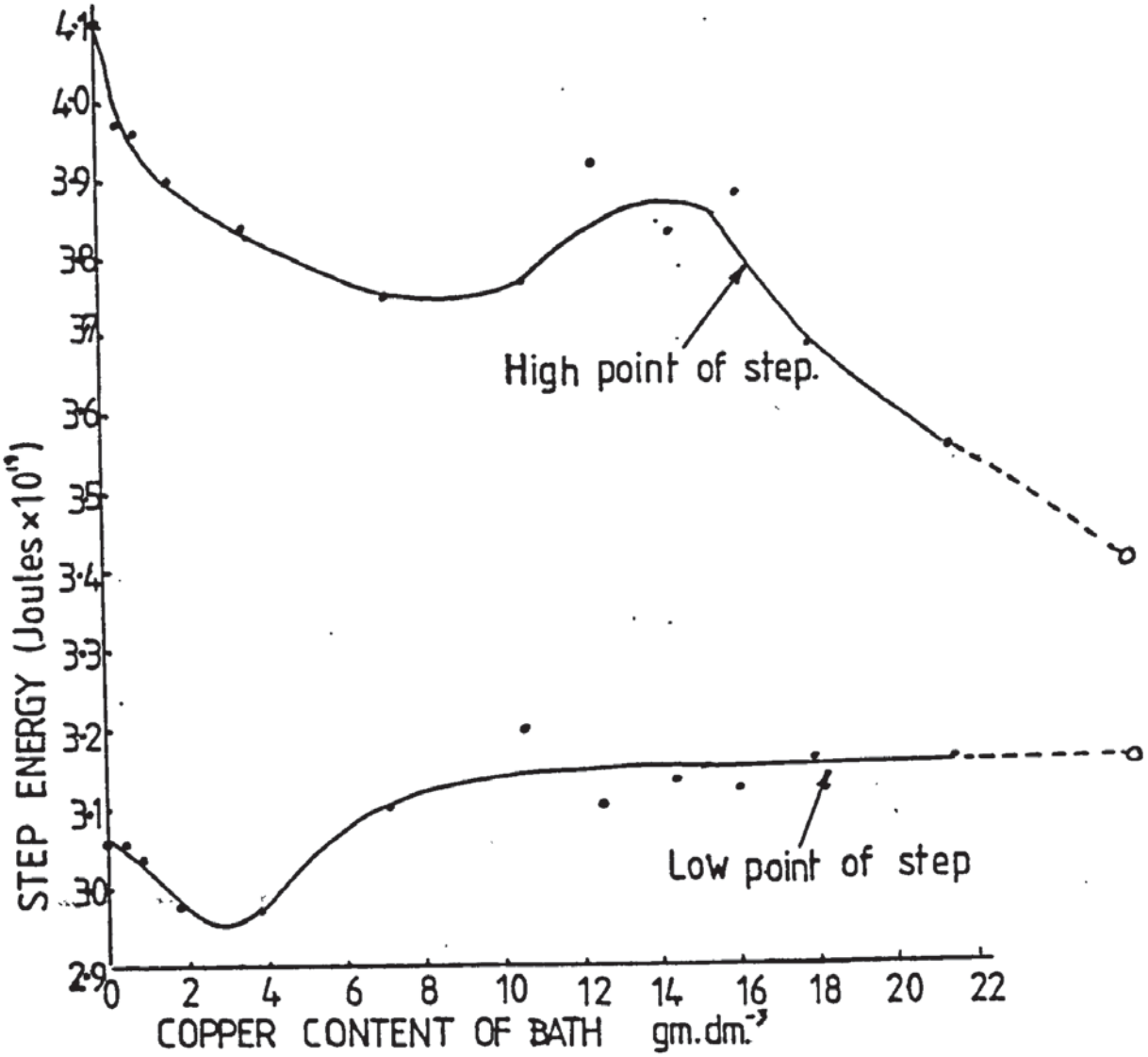

Fig. 6·3

High and low point step energies

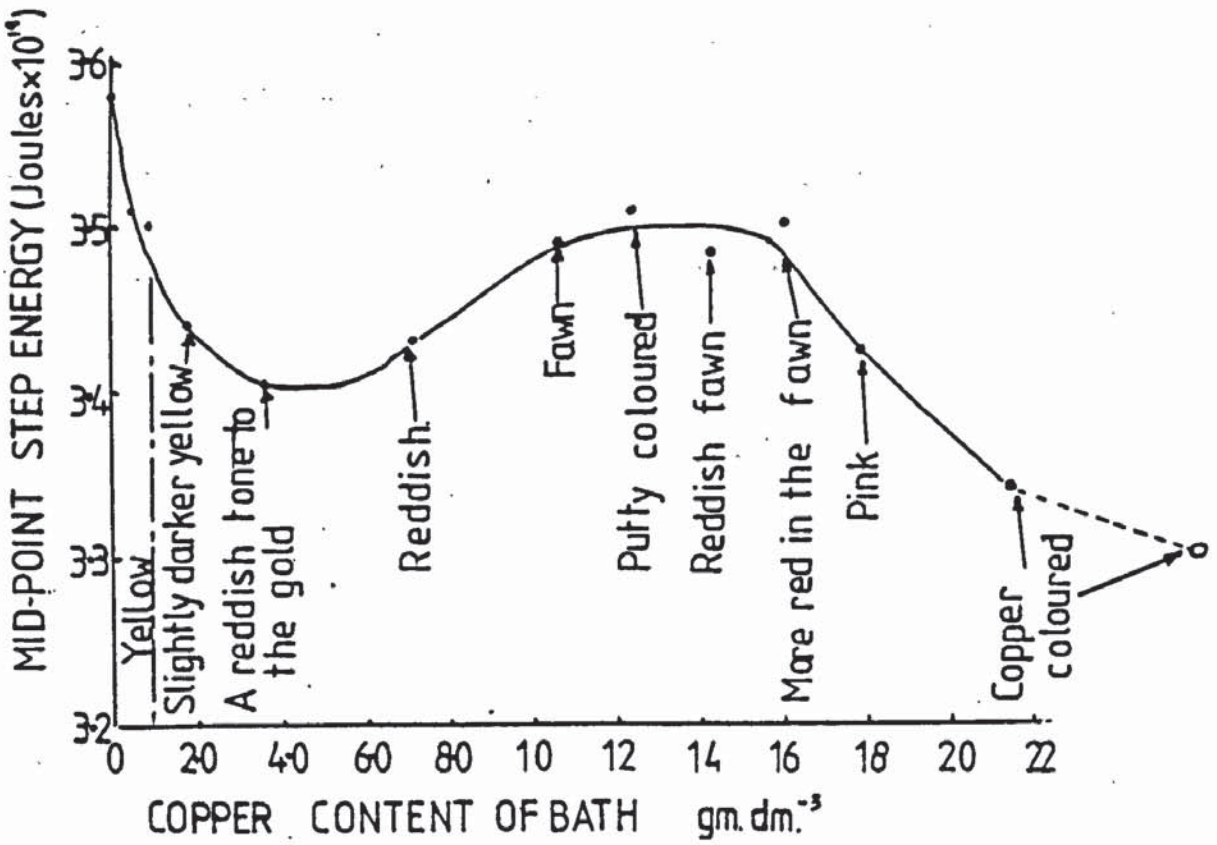

Fig. 6·4

Mid-point energies

was also plotted for comparison and it confirmed the continuing downward trend of the graph. The visual comments made on the samples immediately after electroplating have been superimposed on the graph in Fig. 6·4. It is interesting to note that the first three samples were all assessed as yellow and yet the reflectivity graph appeared to pick up nuances of colour not apparent to the eye since the descending trend of the graph was very evident. The lowest part of this first section of the graph corresponded to the establishment of a reddish tone to the gold, and the rising second section appeared to conform to a decolourising of the gold, it being described as fawn. As the copper content increased, red tones appeared in the fawn, and as the graph again descended the copper was described as pink and then copper coloured. From this it would appear that increasing "redness" of the colour conforms to a fall in the numerical value of the energy step. Since the red end of the spectrum is at the low energy end of the spectrum this is to be expected.

6·2·2 Chromaticity Coordinates

6·2·2·1 The x Value

The graph of equi-energy values given in Fig. 6·5a shows that as the copper content of the bath increased, the x value increased very slightly. With the copper content up to 7·2 gm/dm^3 the graph was extremely shallow, showing only a very slight increase in x value, and the values for tungsten lamp conditions were similar but with a slightly greater slope, and all values being higher than for equi-energy conditions. This slight increase in x value corresponded to a slight darkening of the original yellow, and subsequently to the

(contd. p.163.)

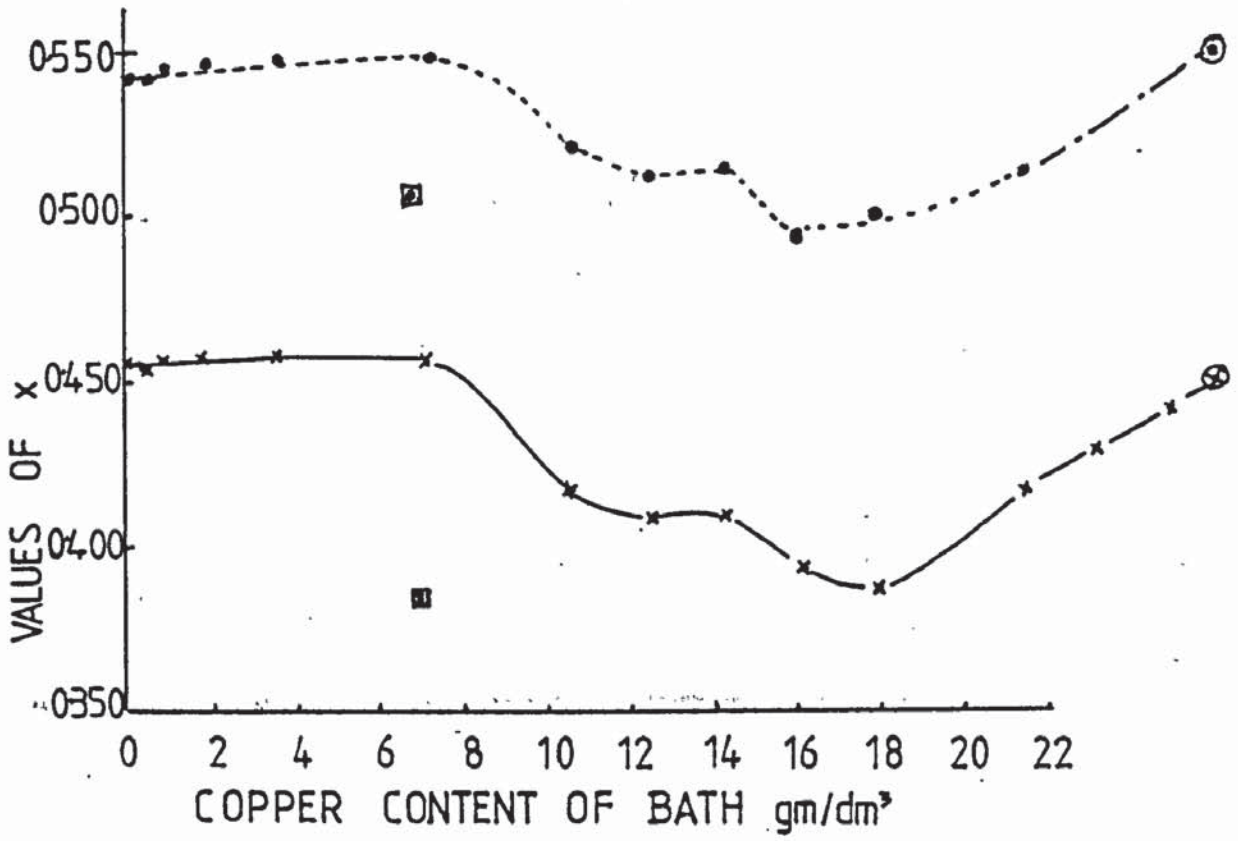

Fig. 6·5a

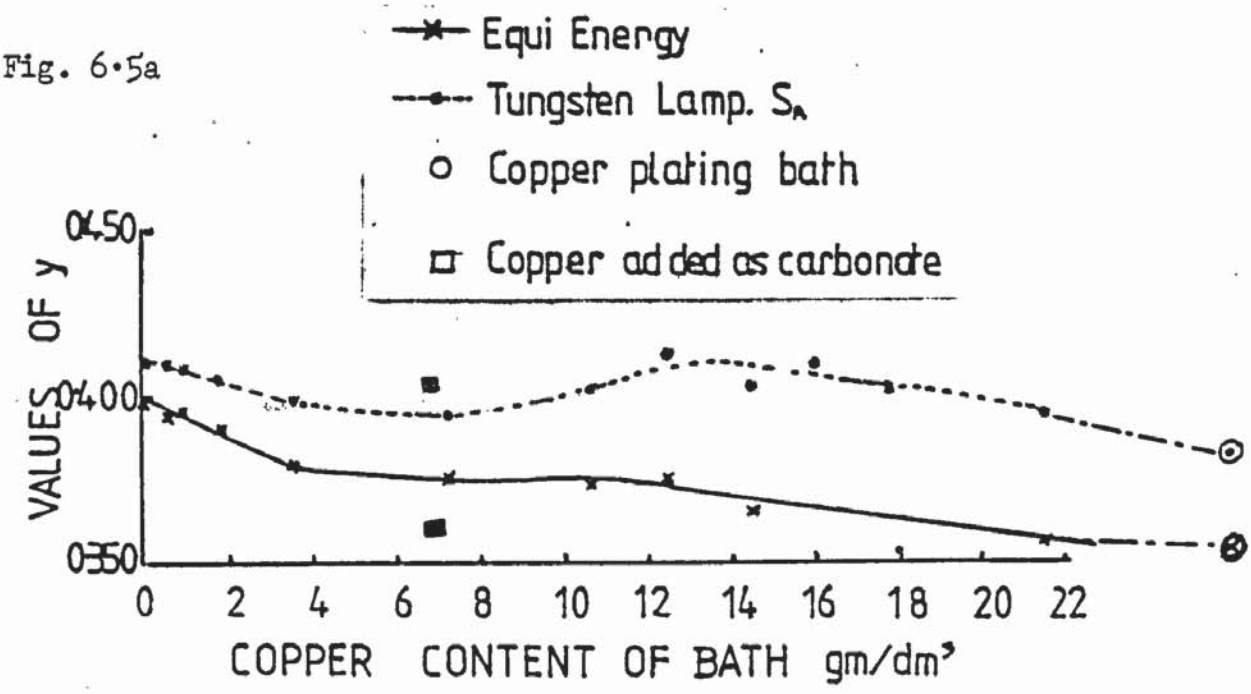

Fig. 6·5b

The effect of copper content on the x and y coordinates

emergence of a reddish tone to the gold. It would be quite reasonable to refer to this as "rose gold". One group of discs, all containing 6·9 gm/dm^3 of copper, did not fit on to the graph, the values being much lower than expected. On checking it was found that in the case of these discs the copper had been added in the form of copper carbonate, whilst in other cases the copper had been added as cuprous cyanide. Thus it seems that the particular complex affected the colour of the gold very greatly. As the copper content increased above 7·2 gm/dm^3, the x value fell and the gold appeared to become decolourised, being described as putty coloured. When the "redness" started to be re-established it was noted that the x value again rose, the highest value being obtained for a gold-free bath. Thus we can say that the x value indicated the increasing or decreasing redness of the deposit.

6·2·2·2 The y Value

Fig. 6·5b shows that the y value also gave an undulating graph when plotted against copper content, in this case a fall in value as the copper content (and redness) increased, whilst increase in the value indicated decolourisation, and when the value again fell redness was re-established.

6·2·2·3 The z Value

Both the equi-energy and tungsten lamp conditions gave a similar shaped curve with the tungsten lamp giving lower numerical values than the equi-energy, and the peak of the curve being slightly less

(cont d. p. 165.)

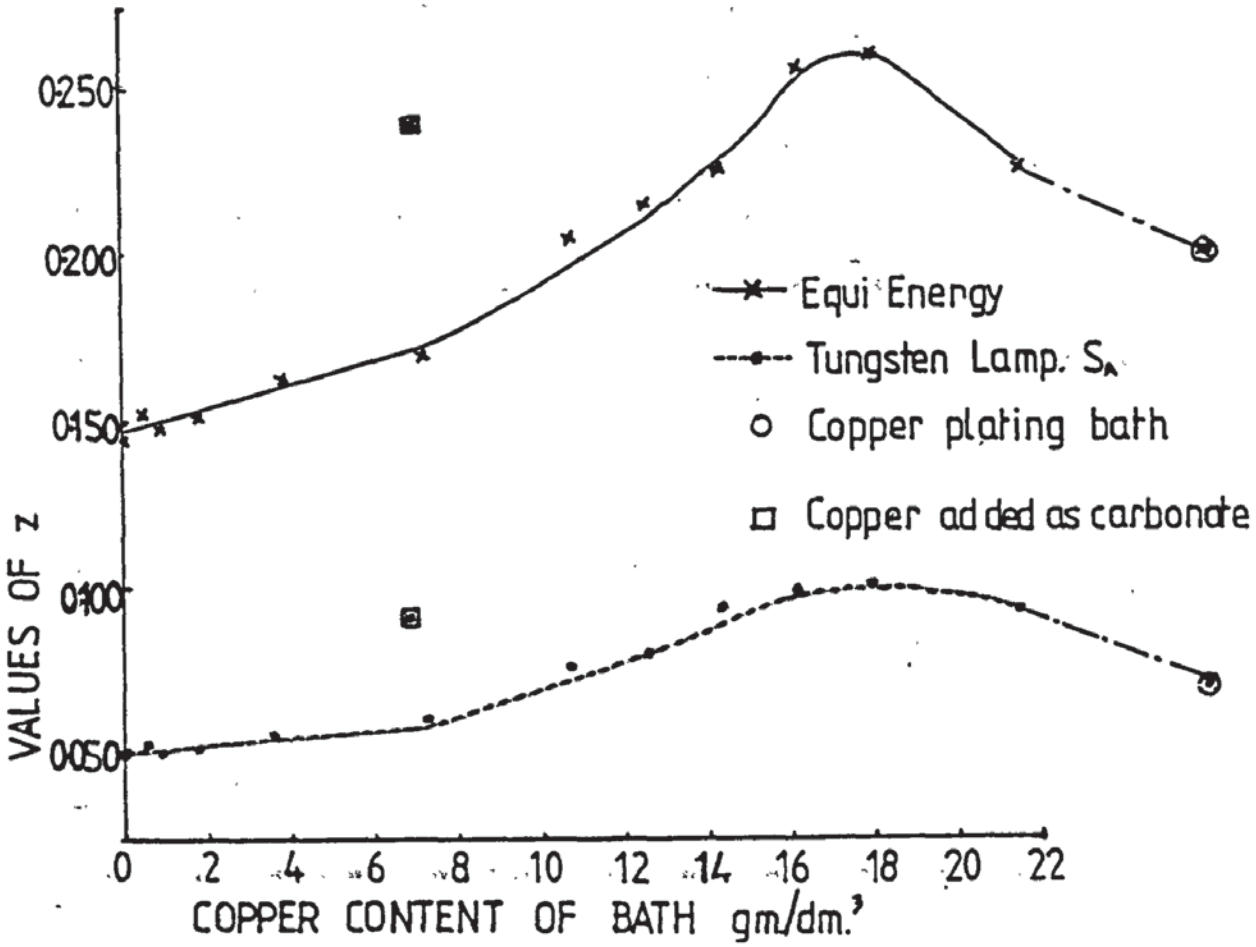

Fig. 6·5c

The effect of copper content on the z coordinates

well defined. The samples in which copper was added as copper carbonate were again typical, being higher numerically than the prevailing curve (Fig. 6·5c).

6·2·3 Luminosity

Fig. 6·6 shows that as the copper content of the bath increased, the luminosity decreased to a minimum at 7·2 gm/dm^3 of copper. Thereafter the luminosity increased to a peak at 12·5 gm/dm^3 followed by a fall. Thus we can say that as the redness of the deposit increases the luminosity falls and as the deposit is decolourised the luminosity increases, and when redness re-emerges luminosity again falls. Again the solution in which the copper was added as carbonate did not conform to the curve.

Luminosity values were very similar for both equi-energy and tungsten lamp, those for tungsten lamp being very slightly higher.

6·2·4 Dominant Wavelength and Saturation

Fig. 6·7 shows that the dominant wavelength curves are very similar in shape with the tungsten lamp conditions exhibiting higher values. The first part of the curve is parabolic in shape with again a maximum at 7·2 gm/dm^3 of copper. As would be expected the dominant wavelength increased in value as redness increased and decreased as decolouring occurred. When the second stage redness emerged, the values appeared more scattered, but there was no doubt of the ascending nature of the curve. Trends were well established in the

(cont'd. p. 168)

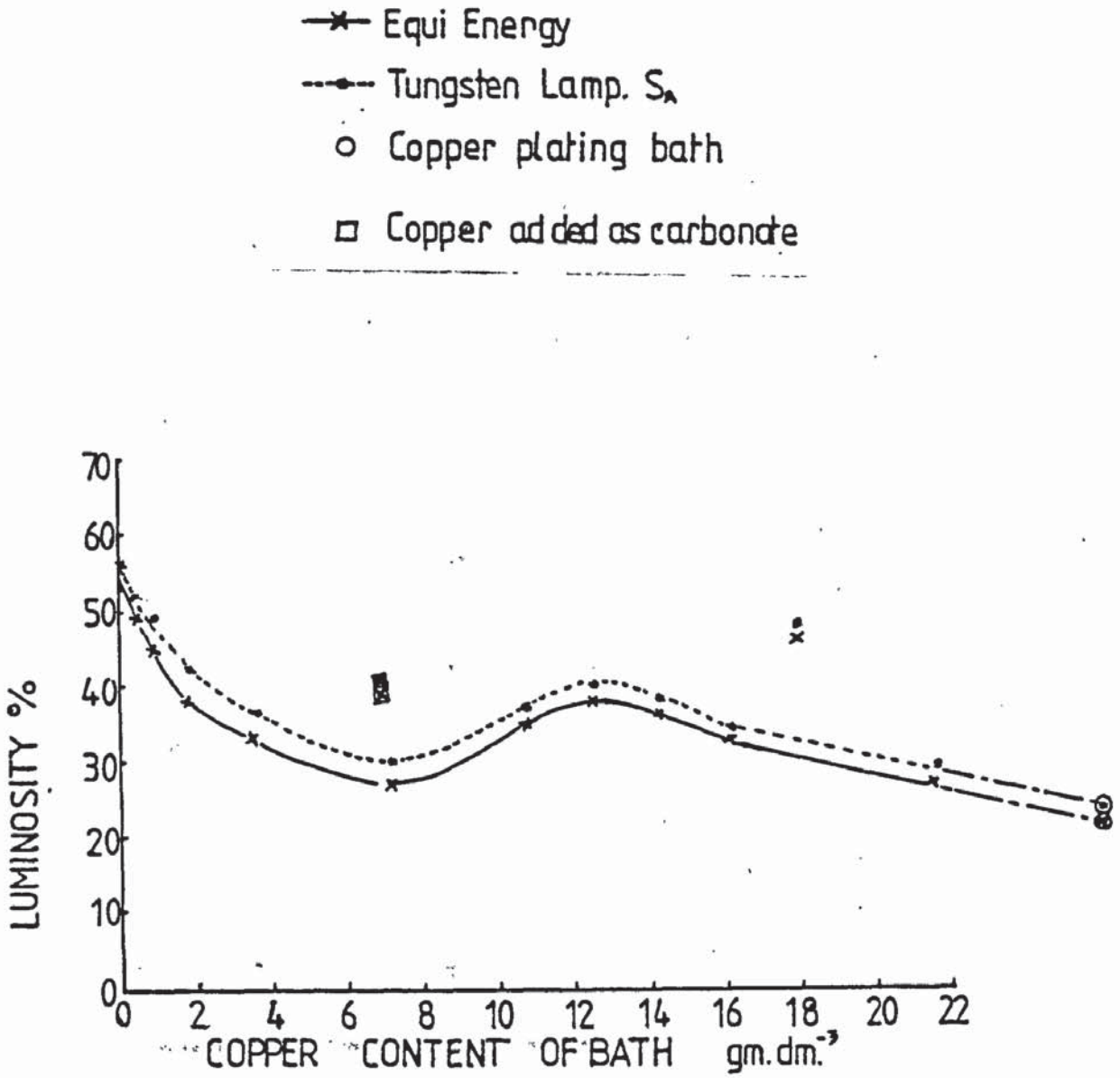

Fig. 6·6

Effect of copper content on luminosity

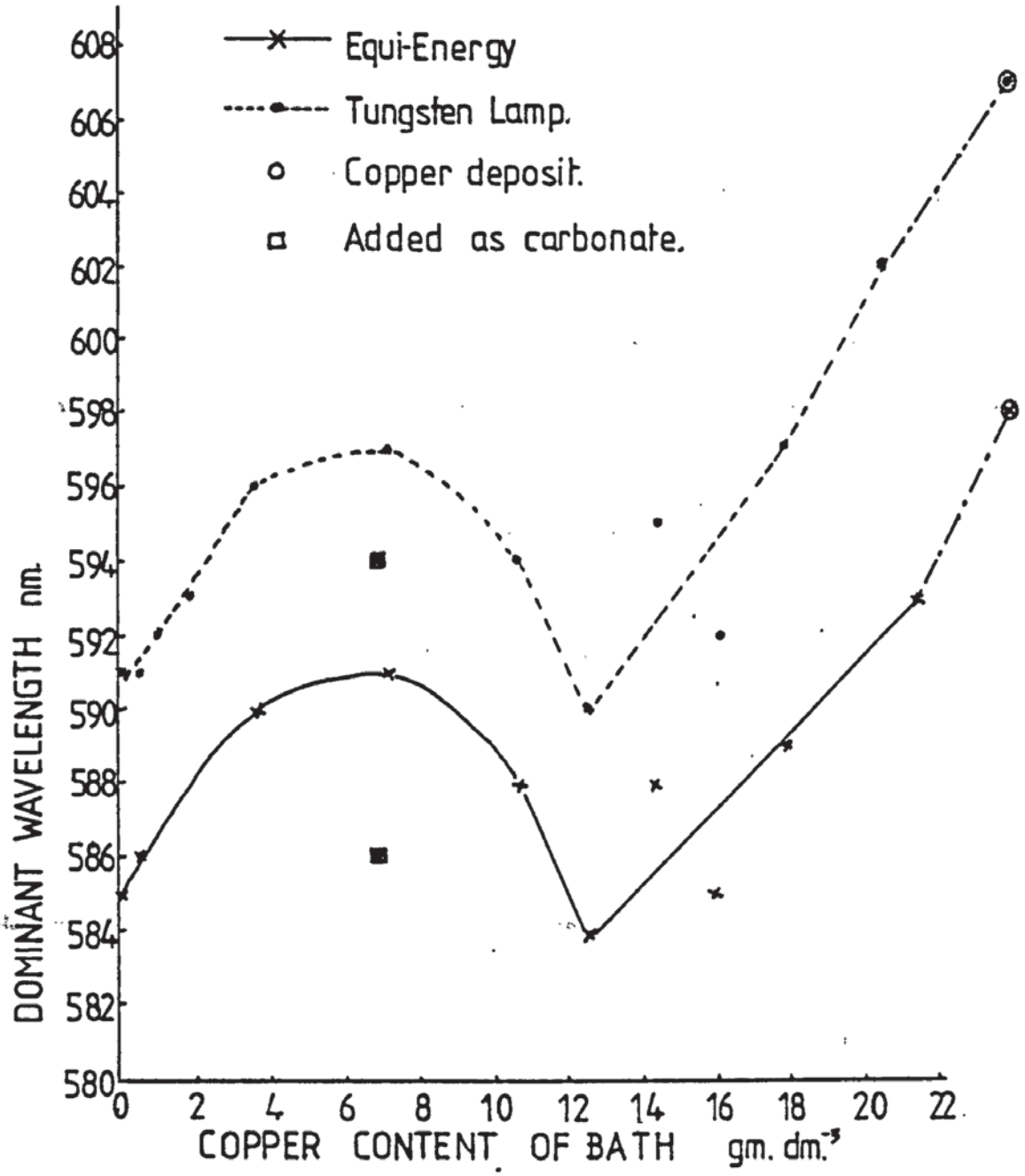

Fig. 6·7

Effect of copper content on dominant wavelength

saturation curves (Fig. 6·8) in that saturation gradually fell to a minimum at 17·9 gm/dm^3 of copper in the solution. There appeared to be no relationship to the decolourisation of the deposit or to the second stage redness. Saturation values for the two conditions were quite similar with the tungsten lamp values being slightly higher.

6·3 THE SCANNING ELECTRON MICROSCOPE

6·3·1 The Copper Content of the Deposit

Experiments carried out by the use of the Kevex attachment to the electron microscope are given in Table 6·2. It was found that an angle of incidence of 45° was the most satisfactory from the point of view of the collection of secondary X rays. Although it was realised that the accuracy of analysis would not be great if was hoped to obtain some idea of the range of copper content of the deposit by this means. The results given in Table 6·2 indicate that there was a considerable interference from the nickel substrate and it was decided to account for this by means of a "nickel modification" technique as described in Appendix 13.
Certain representative discs were selected and submitted to the measuring process and these results are graphically represented in Fig. 6·9.

6·3·1·1 Analysis Results

The best curve drawn through the first series of results shows that although there is considerable scatter, a trend can be established.

(cont'd p 176)

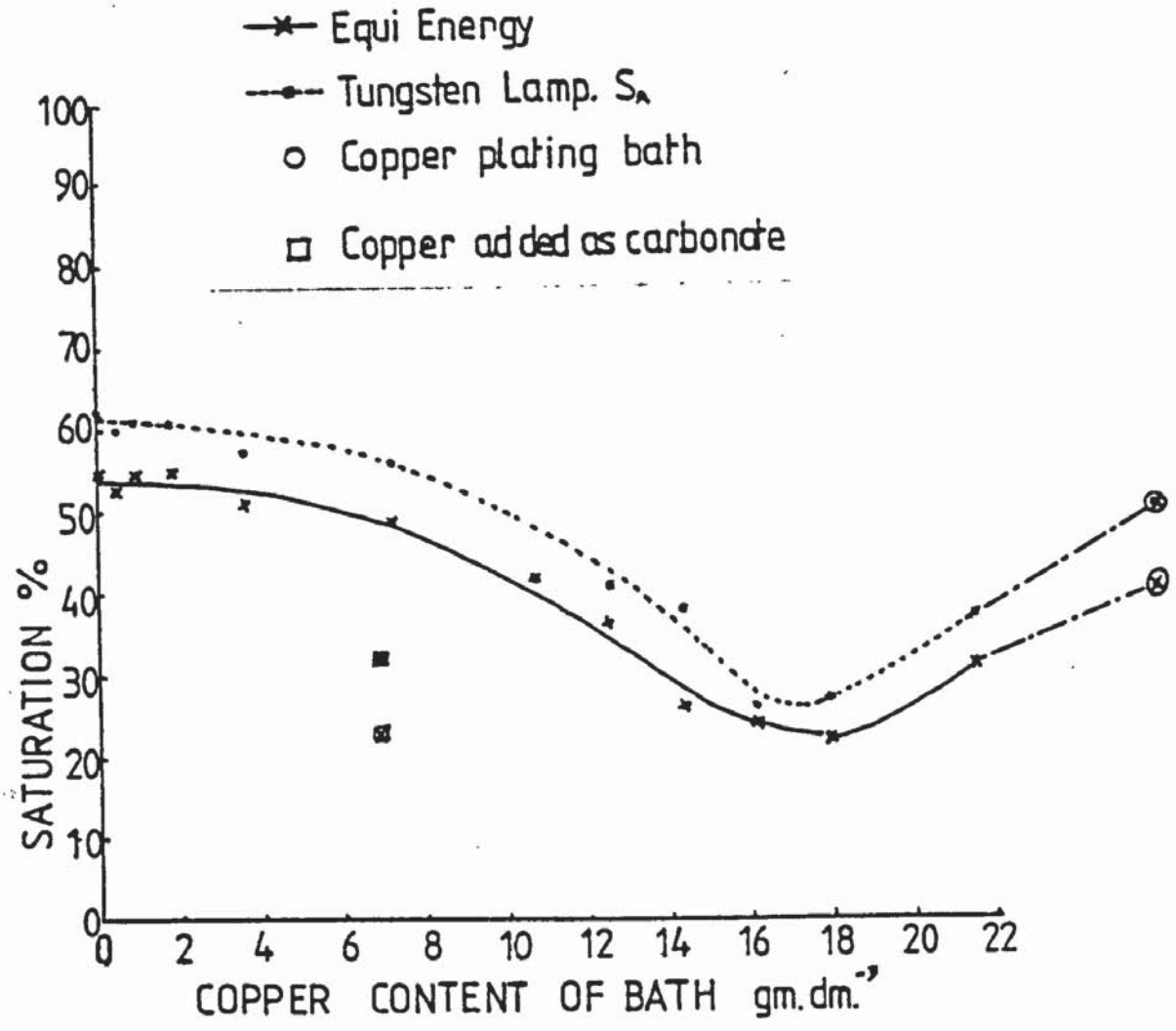

Fig. 6·8

Effect of copper content on the saturation value

TABLE 6.2

RESULTS OF KEVEX MEASUREMENTS

Key

Column 1 : Disc number

2 : Copper content of solution

3 : Copper peak integral (standard)

4 : Nickel peak integral (standard)

5 : Copper peak integral (disc)

6 : Nickel peak integral (disc)

7 : Copper content of deposit

8 : Nickel content of deposit

9 : Modified copper content (disc)

10 : Estimated thickness μm

11 : Magnification

12 : Notes

1	2	3	4	5	6	7	8	9	10	11	12
53C	17·9	118703	-	55081	D	46·4	-	-	1·84	1K	Copper only measured
63E	14·32	221103	182989	26886	2303	12·16	1·26	12·32	1·49	5K	
53C	17·9	126444	-	35102	ND	27·76	0	-	1·42	1K	
53C	17·9	28078	-	11358	ND	40·45	0	-	1·78	1K	Standards reset
53C	17·9	24687	-	9764	ND	39·55	0	-	1·82	1K	Standards reset
63	14·32	9878	-	899	ND	9·10	0	-	1·45	1K x 1·16	Standard and disc average of 3
47	0·45	-	-	ND	ND	0	0	-	1·12	1K x 1·16	
50	0·9	-	-	ND	ND	0	0	-	1·11	1K x 1·16	Standard and disc average of 5
48	1·8	-	-	ND	ND	0	0	-	1·26	1K x 1·16	Average of 4 for disc
50	0·9	11974	13323	ND	236	0	1·77	-	1·11	1K x 1·18	
48	1·8	11974	13323	ND	367	0	2·75	-	1·26	1K x 1·18	
63	14·3	11974	13323	865	ND	7·2	0	-	1·43	1K	
47	0·45	-	-	-	-	0	0	-	-	1K x 1·05	
41	10·7	91857	105390	6768	3253	7·37	3·09	3·19	1·14	1K x 1·05	
66	12·5	91857	105390	4671	3446	5·09	3·27	5·26	1·43	1K x 1·05	
49	3·6	91857	105390	878	5001	0·96	4·75	1·0	1·08	1K x 1·05	
61	21·5	91857	105390	89644	3117	97·59	2·95	101	2·79	1K x 1·05	
61	21·5	71067	95379	80948	1487	114	1·56	116		1K x 1·16	
61	21·5	71067	95379	82267	1747	116	1·83	118		1K x 1·11	Remeasured, spot moved

1	2	3	4	5	6	7	8	9	10	11	12
49	3·6	71067	95739	ND	4086	0	4·3	-		1K x 1·05	
49	3·6	71067	95379	ND	3489	0	3·66	-		1K x 1·05	Remeasured, spot moved
49	3·6	71067	95379	ND	4747	0	4·9	-		1K x 1·05	Disc removed and refocussed
66	12·5	71067	95379	ND	1877	0	1·97	-		1K x 1·06	
41	10·7	71067	95379	ND	2098	0	2·19	-		1K x 1·05	
66	12·5	70078	-	9695	ND	13·83	0	-		1K x 1·06	
41	10·7	70078	-	11835	ND	16·89	0	-		1K x 1·06	
61	21·5	70078	-	83637	ND	119	0	-		1K x 1·15	
49	3·6	70078	-	8605	ND	12·28	0	-		1K x 1·05	
63	14·3	85868	-	16271	ND	18·95	0	-		1K x 1·16	
47	0·45	85868	-	6710	ND	7·8	0	-		1K x 1·32	
50	0·90	85868	-	5329	ND	6·21	0	-		1K x 1·50	
48	1·80	85868	-	7873	ND	9·15	0	-		1K x 1·16	
50	0·90	26412	35174	ND	1876	0	5·3	-		1K x 1·18	
50	0·90	26412	35174	ND	749	0	2·13	-		1K x 1·18	Spot moved
50	0·90	26412	35174	ND	1692	0	4·81	-		1K x 1·18	Spot moved
47	0·45	26412	35174	ND	ND	0	0	-		1K x 1·05	
47	0·45	26412	35174	ND	ND	0	0	-		1K x 1·05	Spot moved
47	0·45	26412	35174	ND	29	0	0·08	-		1K x 1·05	Spot moved
47	0·45	26412	35174	ND	ND	0	0	-		1K x 1·05	Spot moved

1	2	3	4	5	6	7	8	9	10	11	12
63	14•3	26412	35174	3161	1043	11•96	2•97	12•32		1K x 0•96	
63	14•3	26412	35174	2999	1725	11•35	4•9	11•93		1K x 0•96	Spot moved
48	1•8	26412	35174	ND	1294	0	3•7			1K x 1•07	
48	1•8	26412	45576	ND	97	0	0•28			1K x 1•07	Spot moved
61	21•5	27120	37550	30497	787	112	2•1	114		1K x 1•16	
61	21•5	27120	37550	29918	719	110	1•9	112		1K x 1•16	Spot moved
49	3•6	27120	37550	ND	141	0	0•38			1K	
49	3•6	27120	37550	ND	1016	0	2•7			1K	Spot moved
66	12•5	27120	37550	458	479	1•69	1•27	1•71		1K	
66	12•5	27120	37550	944	263	3•48	0•70	3•5		1K	Spot moved
41	10•7	27120	37550	1677	1273	6•18	3•39	6•40		1K	
41	10•7	27120	37550	1994	1609	7•35	4•28	7•68		1K	Spot moved
56	7•2	99872	118133	9964	4784	9•98	4•05	10•40		1K x 1•08	
56	7•2	99872	118133	7002	4323	7•01	3•66	7•28		1K x 1•08	Spot moved
56	7•2	99872	118133	9802	5657	9•81	4•79	10•30		1K x 1•08	Spot moved
57	16•1	99872	118133	11274	6314	11•3	5•30	11•93		1K x 1•12	
57	16•1	99872	118133	12146	7785	12•2	6•60	13•06		1K x 1•12	
57	16•1	99872	118133	11278	8183	11•3	6•90	12•14		1K x 1•12	

1	2	3	4	5	6	7	8	9	10	11	12
56	7•2	90706	109117	9726	5324	10•72	4•88	11•27		1K x 1•05	
56	7•2	90706	109117	9105	5519	10•03	5•06	10•56		1K x 1•05	Spot moved
57	16•1	90706	109117	14032	10992	15•46	10•07	17•19		1K	
57	16•1	90706	109117	15379	8878	16•95	8•14	18•15		1K	Spot moved

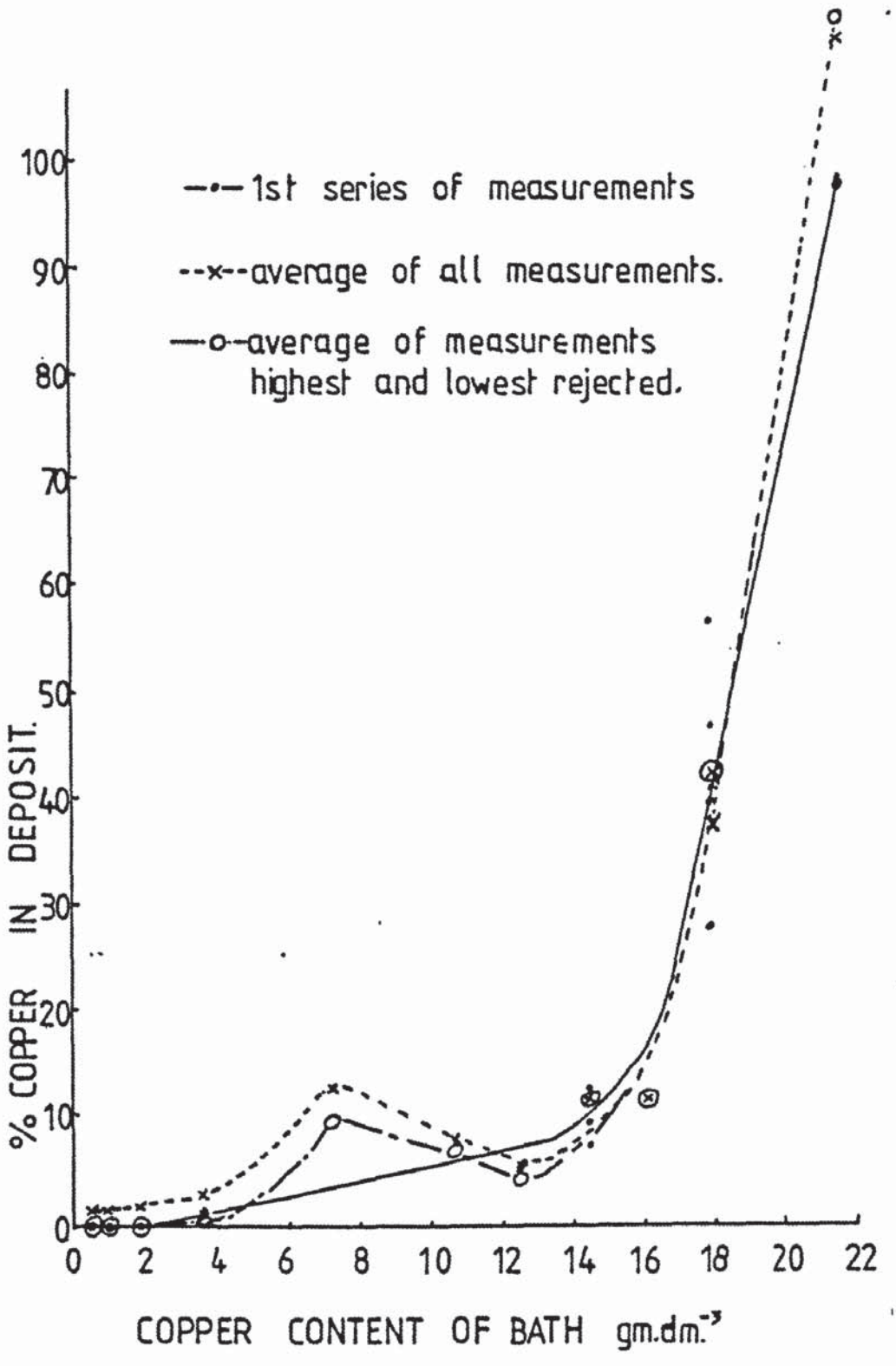

Fig. 6·9

Kevex Analysis Results

Up to 1·8 gm/dm^3 of copper in the bath no copper was present in the deposit, after which copper was detected gradually increasing in amount up to 14·3 gm/dm^3 of copper in the bath. Thereafter the amount of copper present in the deposit rose very sharply, and when 21·5 gm/dm^3 of copper was present in the bath the deposit was substantially copper. Thus although a trend was established it was decided to carry out more tests to determine if this trend could be relied on. The averages of these values are plotted in Fig. 6·9. Although it appeared from this average curve that the low copper content baths gave meaningful amounts of copper in the deposit, closer examination of the results revealed that the copper content of the average results was due to one estimation for each disc and that it was accompaned by several zero results on the same disc. Further, all the high results were obtained during one experimental run, i.e. they were all in the vacuum chamber together. Although electrodeposits are not necessarily homogeneous, it was decided on the available evidence that it would be safer to reject these "high" results on the assumption that they were due to a Kevex malfunction. Accordingly, a curve was plotted in which the highest and lowest results for a particular disc were rejected. (If there were several zeros one of them was rejected). These results showed that copper was only evident in the deposit with a bath copper content of 3·6 gm/dm^3 . The results are given in Table 6·2 and indicate that the copper contents were only altered slightly by the nickel modification of the results. Although it must be conceded that scatter in the results was present even in the modified average curve, the original trend of a sudden upsurge in the copper content of the deposit was substantiated. But since more intermediate samples

were available for the subsequent measurements, a small peak became evident at a bath composition of 7·2 gm/dm^3 of copper. It was not considered that this was due to one atypical sample since the adjacent copper contents lay on the curve

6·3·2 The Topography of the Electrodeposit

The topography of the lower copper contents, Figs. 6·10-6·15 (0·45 to 1·8 gm/dm^3 copper metal bath content) were all very similar in appearance. At 1K magnification an even pebble-like surface was apparent but at 5K it was seen that the surface consisted of cauliflower-like growths varying in size from approximately 0·5 µm to 4 µm diameter. It was noted that the larger growths appeared to consist of smaller growths aggregated together. The deposit was obviously very soft since in some cases flat portions were observed on the growths. They were probably caused by samples resting under their own weight on filter paper during drying. The surfaces of the growths were not smooth but rather dimpled. A deposit produced from a solution of much higher copper content (Fig. 6·21, 14·3 gm/dm^3 copper content of bath) exhibited similar cauliflower-like growths but in this case the growths were much smoother and rounder, the dimpled effect being absent. The range of growth sizes were similar to the lower copper contents.

The topography of disc 18 (from a set in which copper had been added as carbonate, i.e. 6·9 gm/dm^3 of copper) given in Figs. 6·16-6·19 showed that the character of the surface was very similar to the higher copper contents. At the edges of the sample large growths

(cont'd p 181)

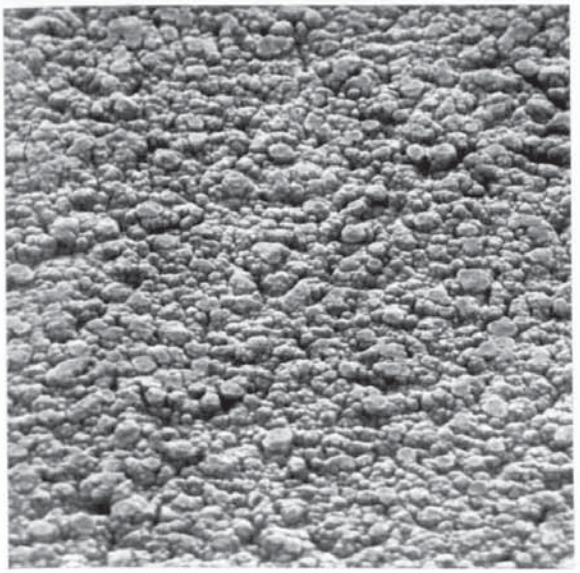

Fig. 6·10 No. 47 Mag. 1K

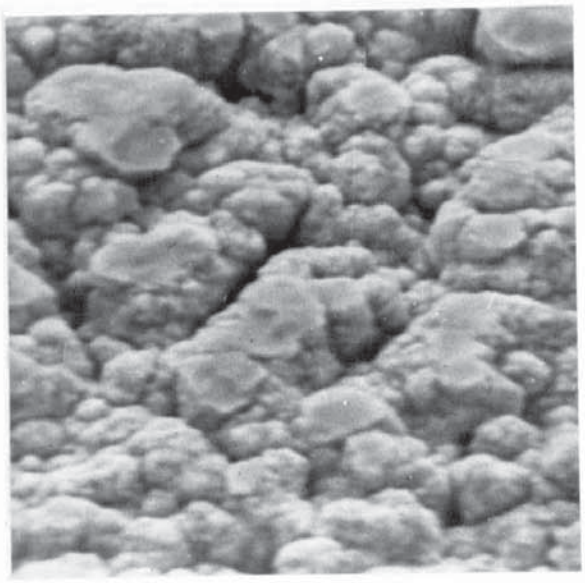

Fig. 6·11 No. 47 Mag. 5K

Fig. 6·12 No. 50 Mag. 1K

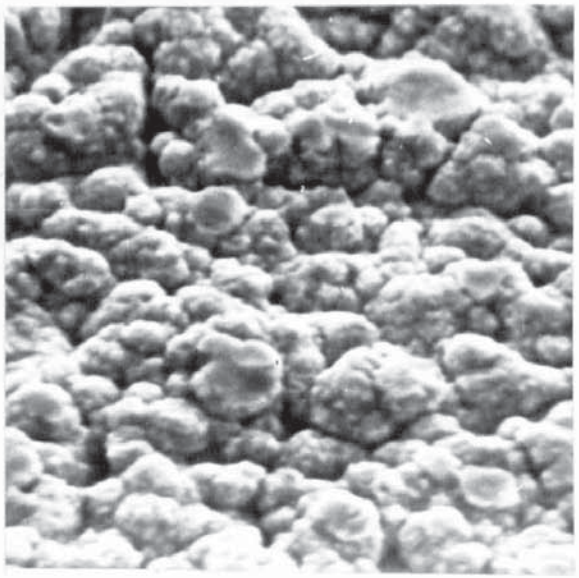

Fig. 6·13 No. 50 Mag. 5K

Fig. 6·14 No. 48 Mag. 1K

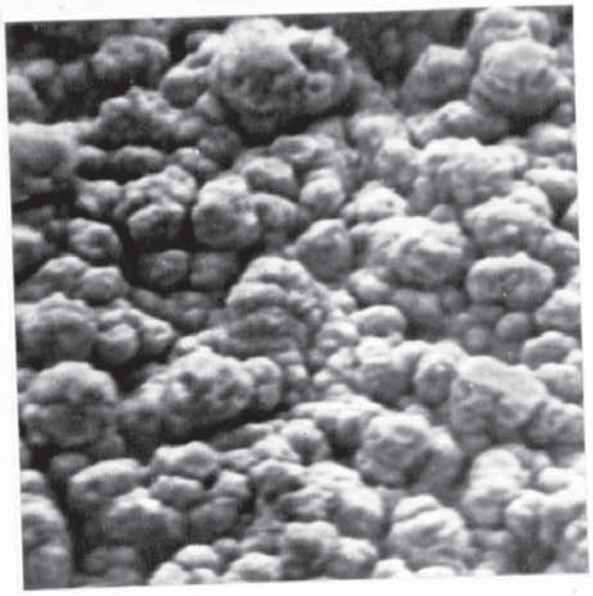

Fig. 6·15 No. 48 Mag. 5K

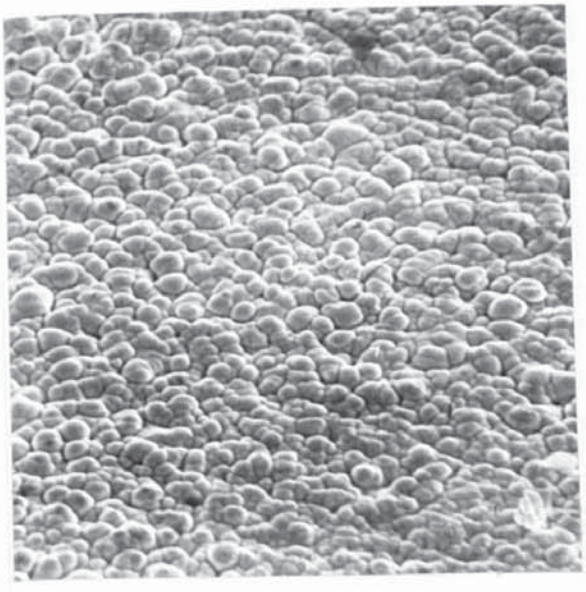

Fig. 6·16 No. 18 (centre) Mag. 1K

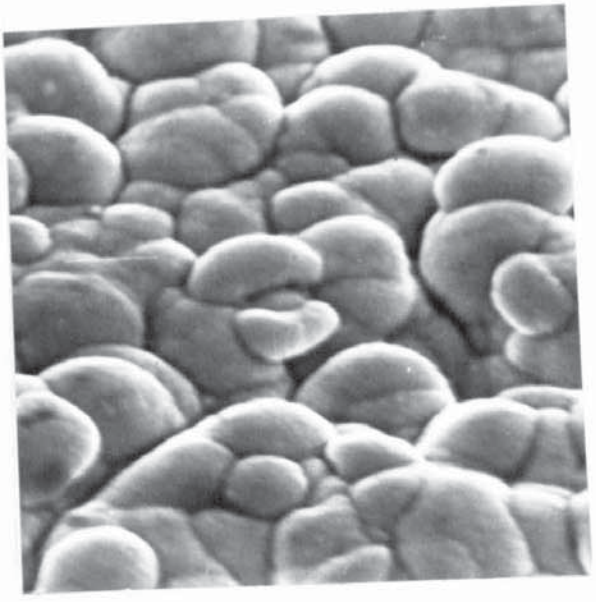

Fig. 6·17 No. 18 Mag. 5K

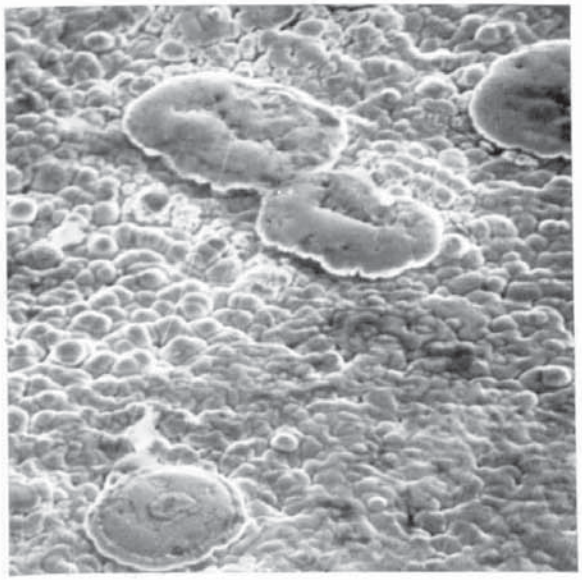

Fig. 6·18 No. 18 Mag. 1K

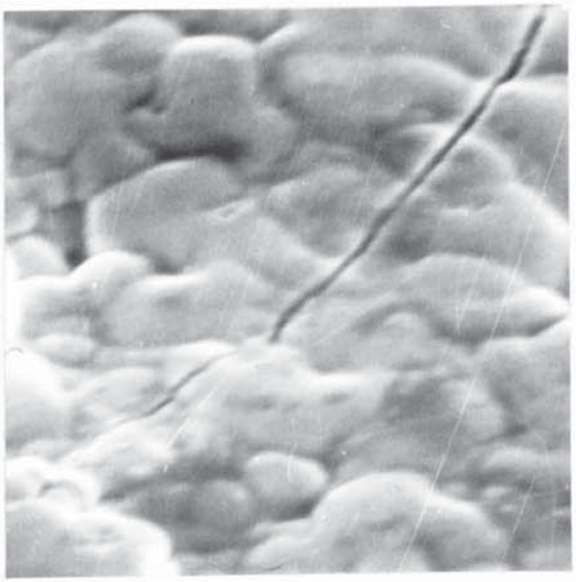

Fig. 6·19 No. 18 (edge) Mag. 5K

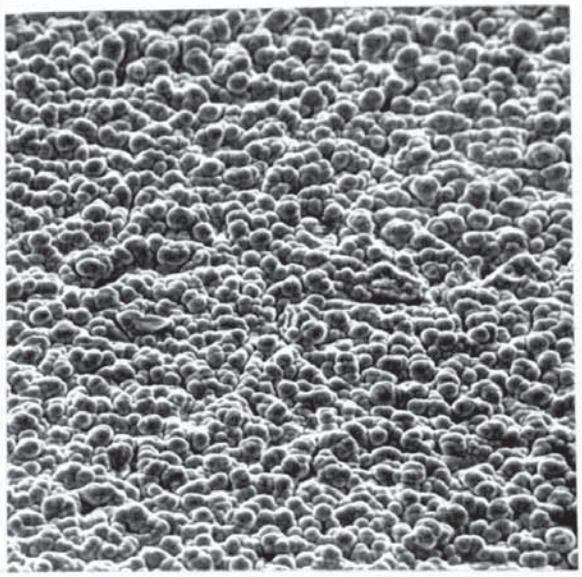

Fig. 6·20 No. 63 Mag. 1K

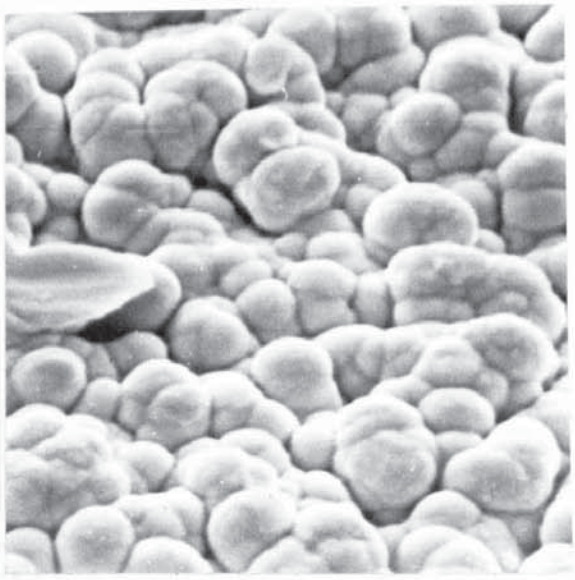

Fig. 6·21 No. 63 Mag. 5K

approximately 30 μm diameter were present. These appear to be fast growing nuclei due to the higher current densities obtaining at the edges of the disc. Cracks approximately 10^{-1} μm in width were also present, and it can be seen that they traverse some of the growths indicating that they occurred due to stress in the deposit, after it had built up to a certain thickness.

CHAPTER 7

THE ADDITION OF SILVER TO A GOLD ELECTROPLATING BATH

7·1 INTRODUCTION

In this series of experiments silver was added to a simple gold bath in order to determine the effect of silver on the colour and texture of the electrodeposits produced. Fig. 7·1 shows a set of discs produced in this series of experiments, and the variation of colour with silver content of the electroplating solution is clearly shown. The results of these experiments are given in Table 7·1A-C.

7·2 THE GENERAL APPEARANCE OF THE DISCS

The colour of the discs was commented on immediately after washing and drying, and it was observed that the first intimation of a green tinge was when 0·42 g/dm^3 of silver was added to the basic gold bath. This greenish appearance was still apparent as the silver content was increased, until when 1·7 g/dm^3 was present the deposit was buff coloured, this changed to cream and finally off-white as the silver content was further increased.

7·3 THE OPTICAL PROPERTIES

7·3·1 The Reflectivity Curves

Fig. 7·2 shows that as the silver content of the gold electroplating bath was increased the adsorption edge moved progressively to the high energy end of the spectrum. This is confirmed by Fig. 7·3 which shows a progressive increase in mid-point step energy with increasing silver content of the bath. Fig. 7·4 shows that as the silver content of the bath was increased the slope of the

(contd. p. 191.)

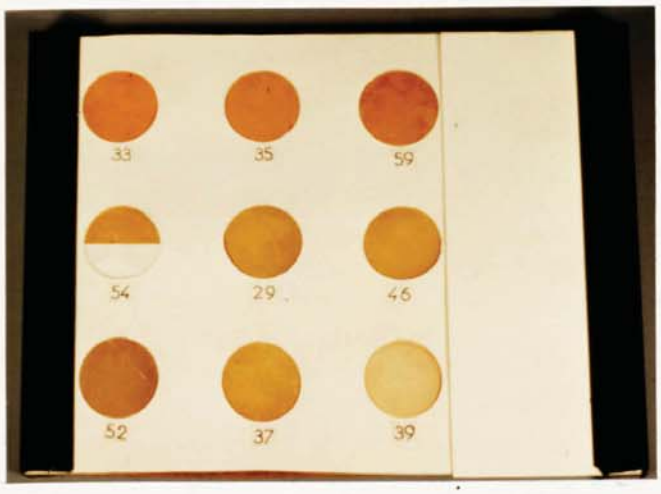

Fig. 7·1

The addition of silver to a gold electroplating solution

Sample	Addition of silver metal to bath g/dm^3	CD amps/sq dm	Time mins	Gain in Weight (grams)	Description
25	0·1	1·0	10	0·0047	Pale yellow
26				0·0058	Pale yellow
27	1·0	1·0	11	0·014	Greenish yellow
28				0·0198	Greenish yellow
29	1·0	1·0	20	0·0367	Greenish yellow
30				0·048	Greenish yellow
33	0·21	1·0	10	0·0162	Yellow
34				0·0191	Yellow
35	0·42	1·0	10	0·0184	Yellow with a slight green tinge
36				0·0190	
37	2·1	1·0	10	0·0176	Cream
38				0·0224	Cream
39	4·2	1·0	10	0·0241	Off-white
40				0·0224	Off-white
59	0·6	1·0	10	0·0206	Pale yellow
54	0·81	1·0	10	0·0251	Yellow with a definite green tinge
46	1·37	1·0	10	0·0253	Greenish yellow
52	1·7	1·0	10	0·0212	Buff coloured

Table 7·1A

Addition of silver to a gold electroplating bath

Initial gold bath: 2·9 g/dm^3 $KAu(CN)_2$ 40 g/dm3 KCN
Temp. 50°C ; pH 10-11 ; silver added as AgCN

Machine lapped to 600 grit

Sample No.	Chromaticity Coefficients					
	Equi-Energy			Tungsten Lamp S_A		
	x	y	z	x	y	z
25	0·451	0·416	0·133	0·532	0·420	0·048
26	0·451	0·416	0·133			
27	0·402	0·414	0·184	0·498	0·432	0·070
28	0·401	0·412	0·187			
29	0·409	0·413	0·177	0·503	0·430	0·067
30	0·410	0·413	0·177	0·504	0·429	0·067
33	0·464	0·427	0·109	0·539	0·423	0·037
34	0·466	0·426	0·108	0·541	0·422	0·037
35	0·447	0·430	0·122	0·528	0·429	0·043
36	0·446	0·432	0·122	0·527	0·430	0·043
37	0·387	0·394	0·219	0·489	0·425	0·086
38	0·387	0·391	0·222	0·489	0·425	0·086
39	0·383	0·384	0·233	0·488	0·421	0·091
40	0·382	0·385	0·233	0·487	0·422	0·091
59	0·422	0·427	0·131	0·525	0·428	0·047
54	0·426	0·424	0·150	0·514	0·431	0·055
46	0·399	0·406	0·195	0·497	0·428	0·075
52	0·389	0·394	0·217	0·491	0·425	0·084

Table 7·1B

	Equi-Energy			Tungsten Lamp S_A		
Sample No.	DM nm	S %	L %	DM nm	S %	L %
25	582	59	42	587	63	44
26	582	59	47			
27	576	44	51	580	46	52
28	576	44	57			
29	577	46	43	582	50	44
30	577	46	40	582	49	42
33	582	68	46	587	68	49
34	582	67	41	587	70	44
35	580	63		584	64	49
36	580	63	47	584	66	49
37	576	35	51	581	36	51
38	577	33	50	581	36	51
39	577	30	45	582	33	46
40	577	30	47	581	33	48
59	579	60	45	584	63	47
54	578	54	43	583	56	44
46	576	41	48	581	44	49
52	577	35	44	581	38	46

Table 7·1C

DM = dominant wavelenth

S = saturation

L = luminosity

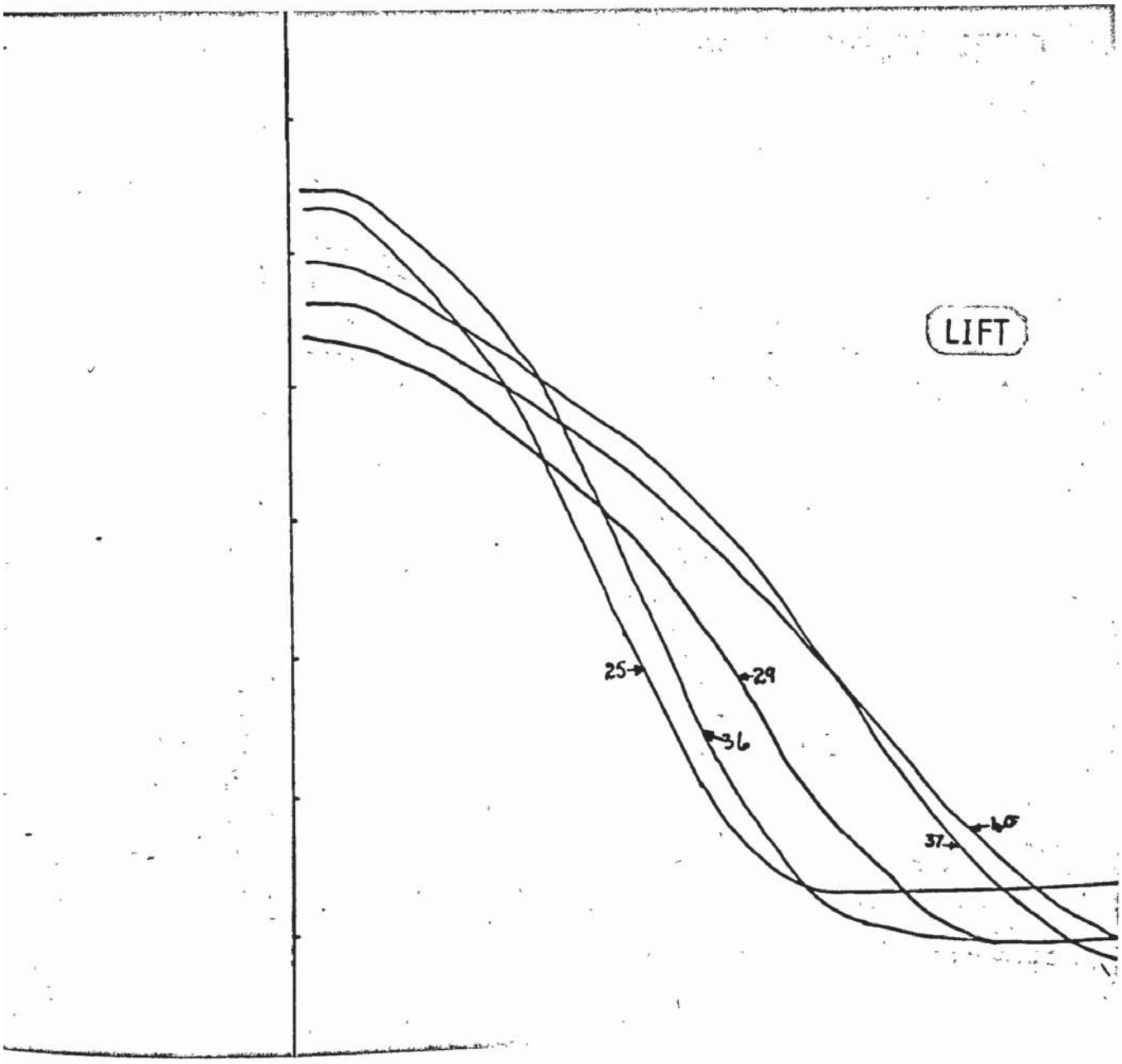
LIFT
25
29
36
37
45

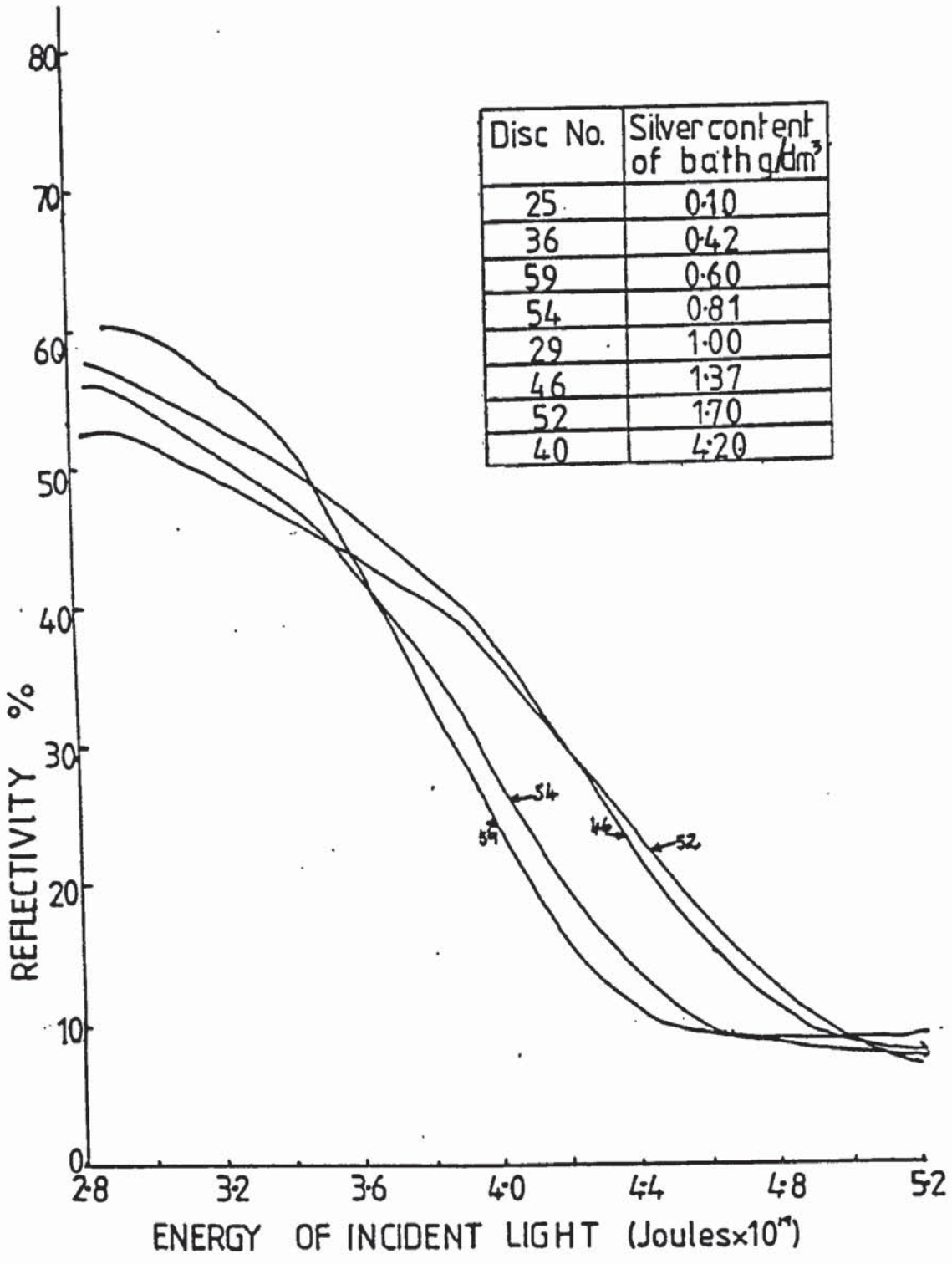

Fig. 7·2

The effect of bath silver content on the reflectivity curves

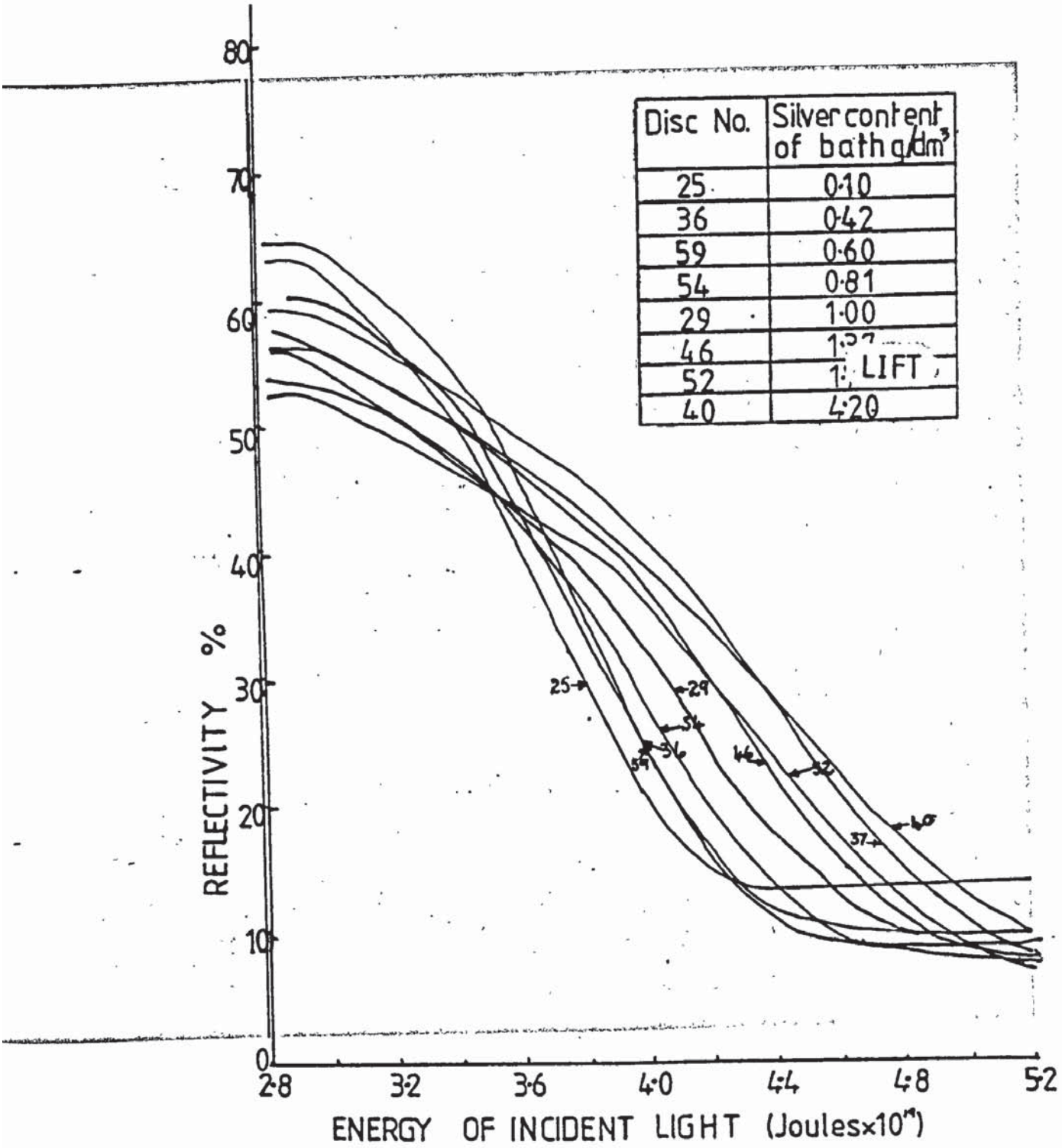

Fig. 7·2

The effect of bath silver content on the reflectivity curves

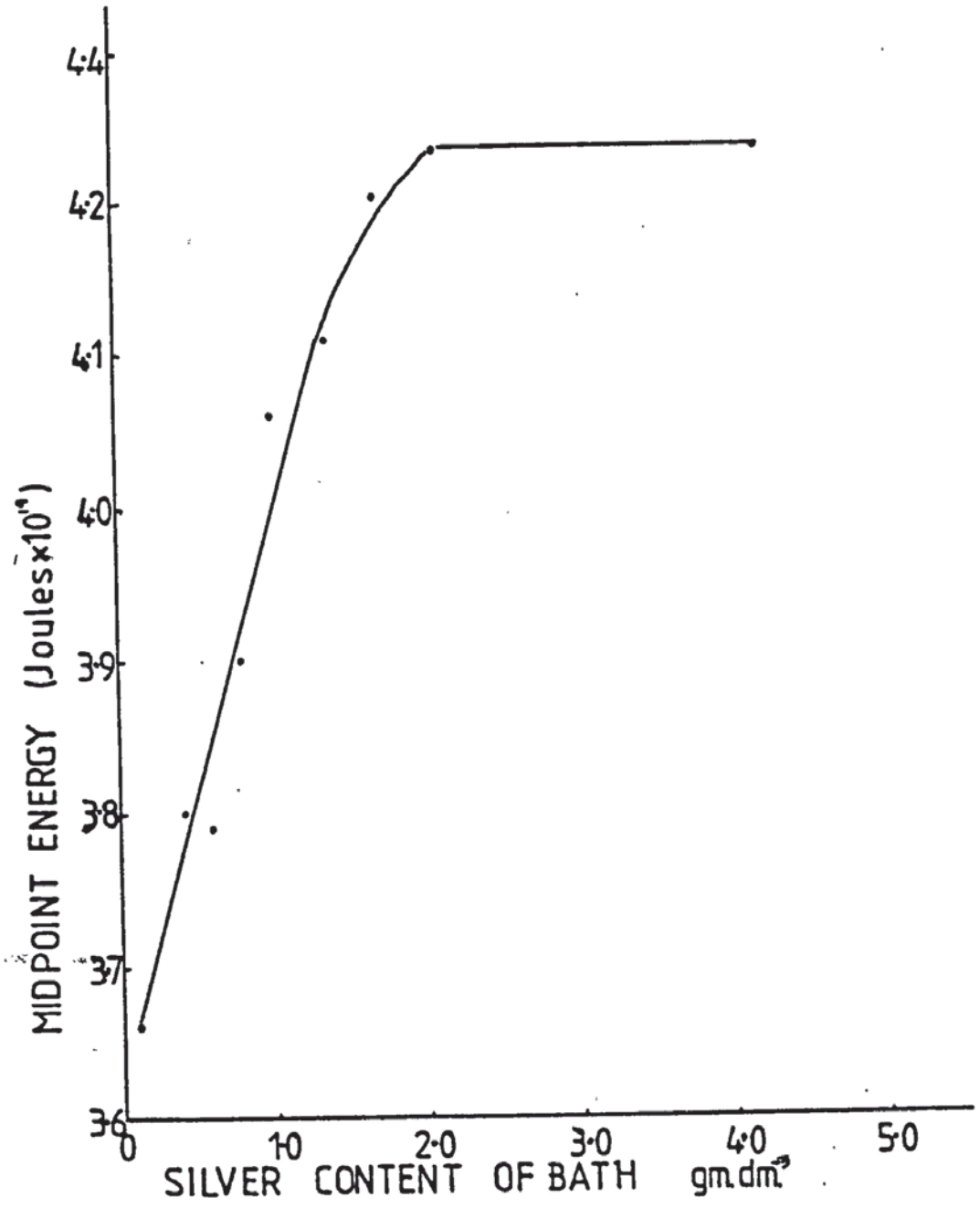

Fig. 7-3

The effect of bath silver content on the mid point energy

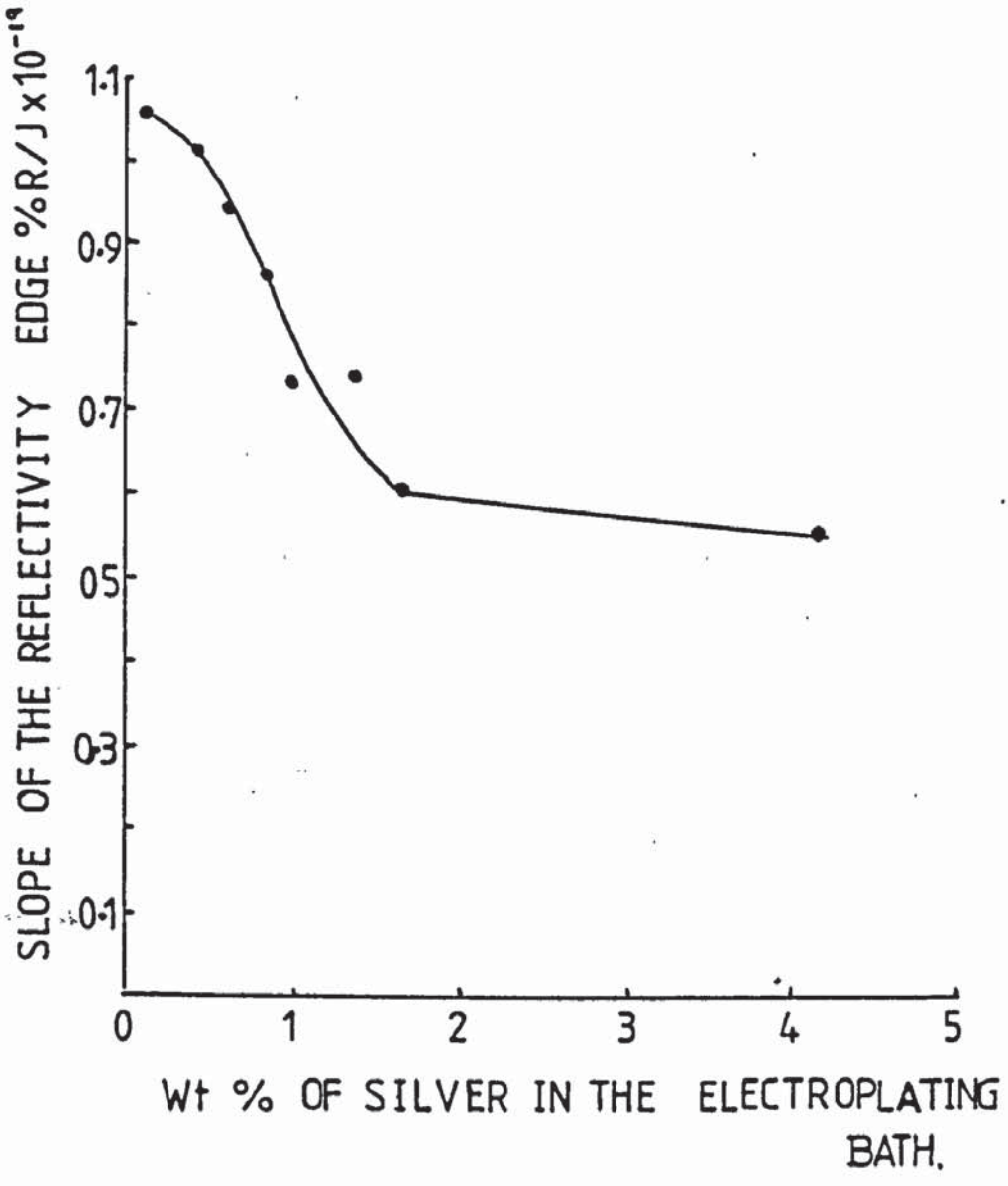

Fig. 7·4

The effect of bath silver content on the slope of the reflectivity edge

reflectivity edge decreased but at a decelerating rate as we approach the higher silver contents. As the visual assessment of colour changed from pale yellow through yellow to greenish-yellow the mid-point step energy changed linearly with increasing silver content of the bath, but as the deposit became decolourised and changed from buff to cream to off-white the graph curved over and then became horizontal. Thus we can say that as the deposit became decolourised the energy step moved towards the ultra-violet end of the spectrum.

7·3·2 The Chromaticity Coordinates

7·3·2·1 The x Value

Fig.7·5a shows that as the observed colour changed from pale yellow to yellow to greenish-yellow the equi-energy x curve rose initially and then fell very steeply with increasing bath silver content, starting to flatten out at 1·7 g/dm^3, when the colour was observed to be buff. Further increase in bath silver content gave an observed colour of cream and then off-white, the x value becoming very shallow and almost horizontal. Good reproducibility was obtained when more than one disc was prepared, in some cases coincident numerical values being obtained.

7·3·2·2 The y Value

The range of numerical values was smaller for the y values than the x value (equi-energy) but again the pattern was one of rising to a peak, in this case at 0·42 g/dm^3 of silver (slight green tinge). This was followed by a fairly steep fall, then at the onset of a

(contd. p.194.)

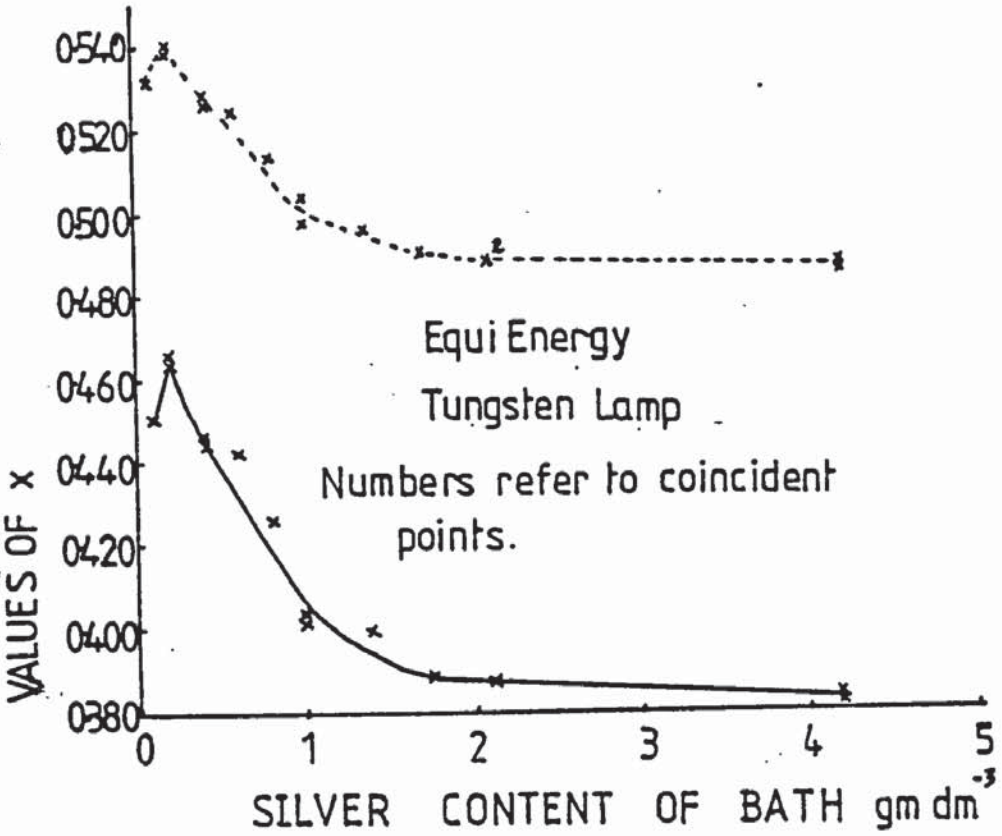

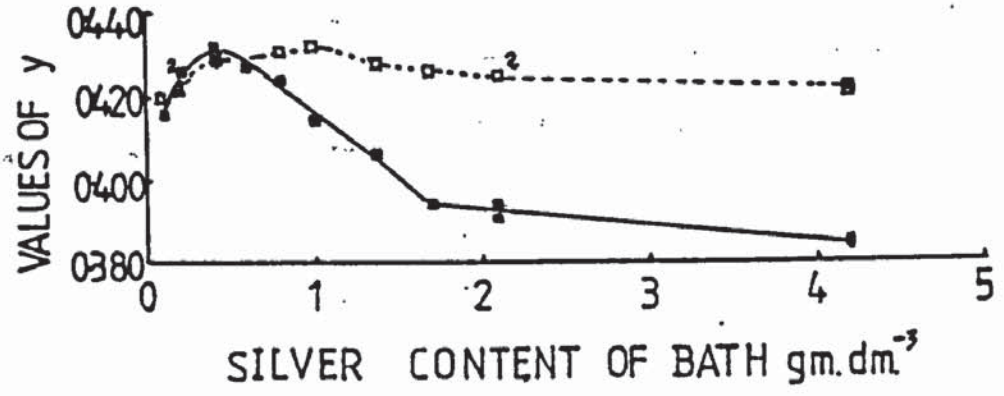

Fig. 7·5a-c

The effect of silver content on the chromaticity coordinates

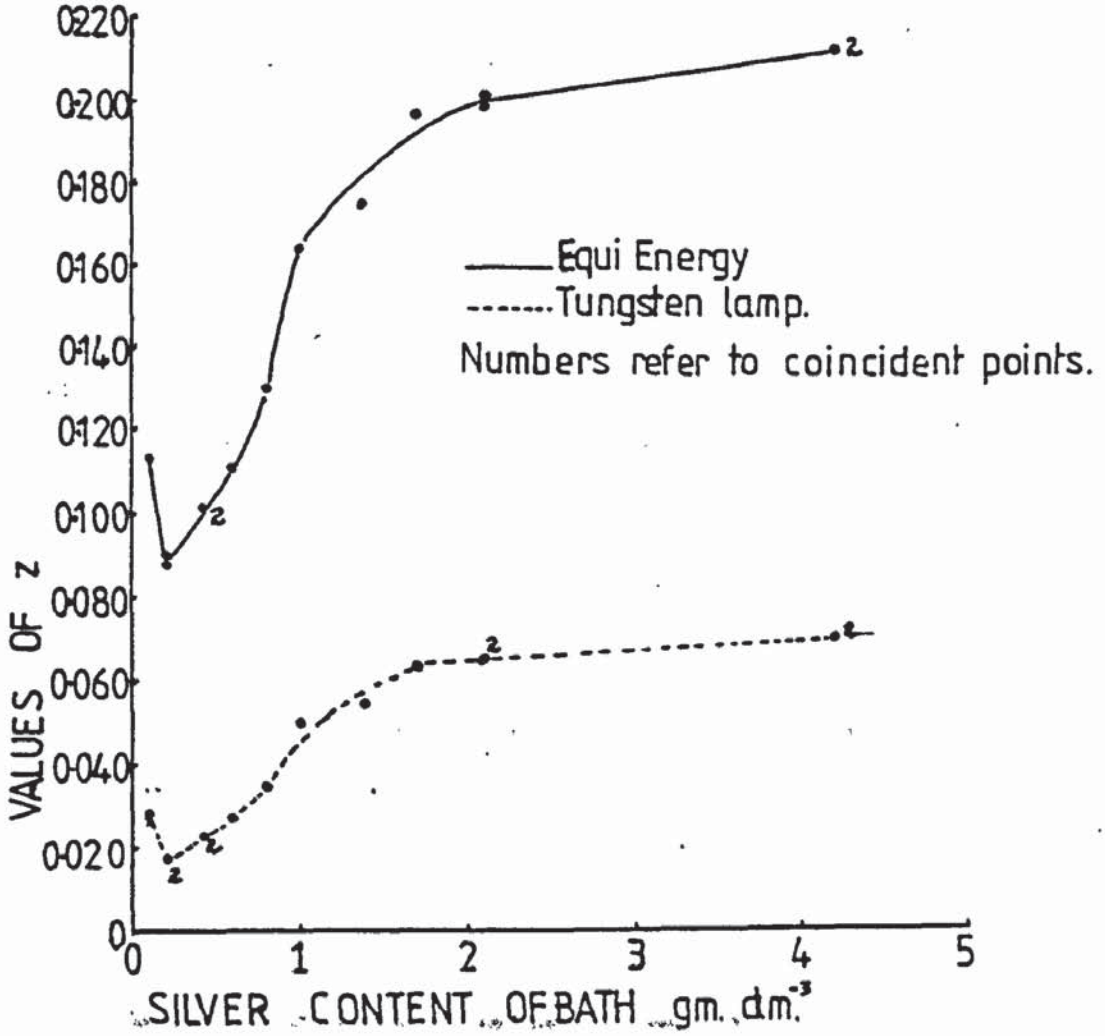
0·220
0·200
0·180
0·160
0·140
0·120
0·100
0·080
0·060
0·040
0·020
0
VALUES OF z
0
1
2
3
4
5
SILVER CONTENT OF BATH gm. dm.⁻³
Equi Energy
Tungsten lamp.
Numbers refer to coincident points.

Fig. 7·5c

buff colour a change to a very shallow slope (Fig. 7·5b).

7·3·2·3 The z Value

The shape of this curve (equi-energy) was rather like the x curve in reverse, i.e. an initial fall followed by a steep rise and subsequently almost horizontal (Fig. 7·5c).

7·3·3 Dominant Wavelength, Saturation and Luminosity

Fig. 7·6 which shows the variation of dominant wavelength with silver content of the bath, indicates that under equi-energy conditions as the silver content increases the dominant wavelength falls and at 1·0 gm/dm^3 of silver becomes constant. As the dominant wavelength falls the percentage saturation also falls and then the curve flattens at the higher silver contents (Fig. 7·7). Luminosity values were in the band 44-51% but they did not follow any definable pattern.

7·3·4 Comparison of Optical Properties under Equi-energy Conditions and Tungsten Lamp Conditions

The graphs derived for the x and z values under tungsten lamp conditions were very similar in shape to those derived for equi-energy except that numerically the tungsten lamp x values were higher while the z values were lower than for equi-energy conditions. Furthermore the range of numerical values was slightly less. The y value under

(contd. p. 197.)

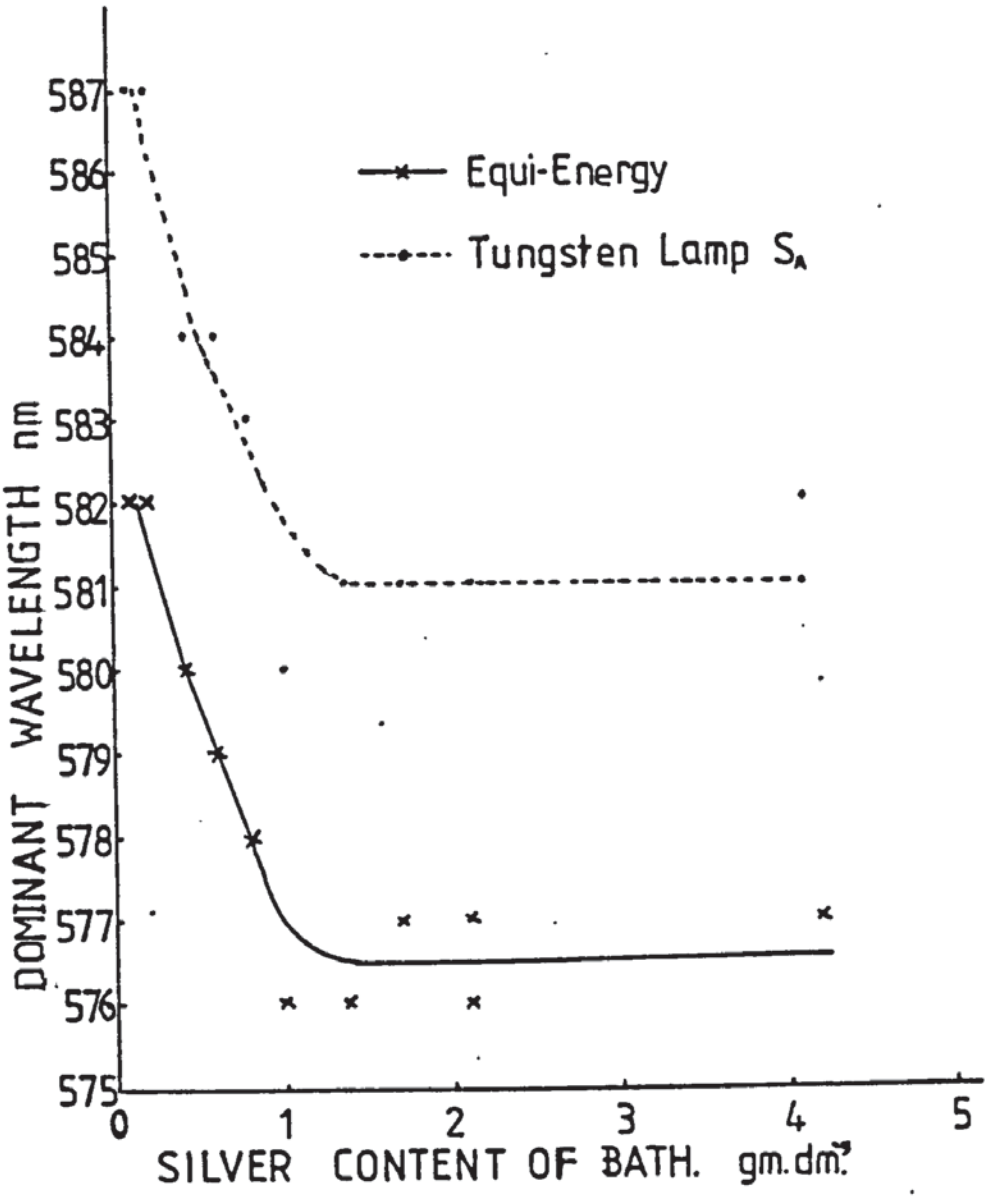

Fig. 7·6

The effect of bath silver content on dominant wavelength

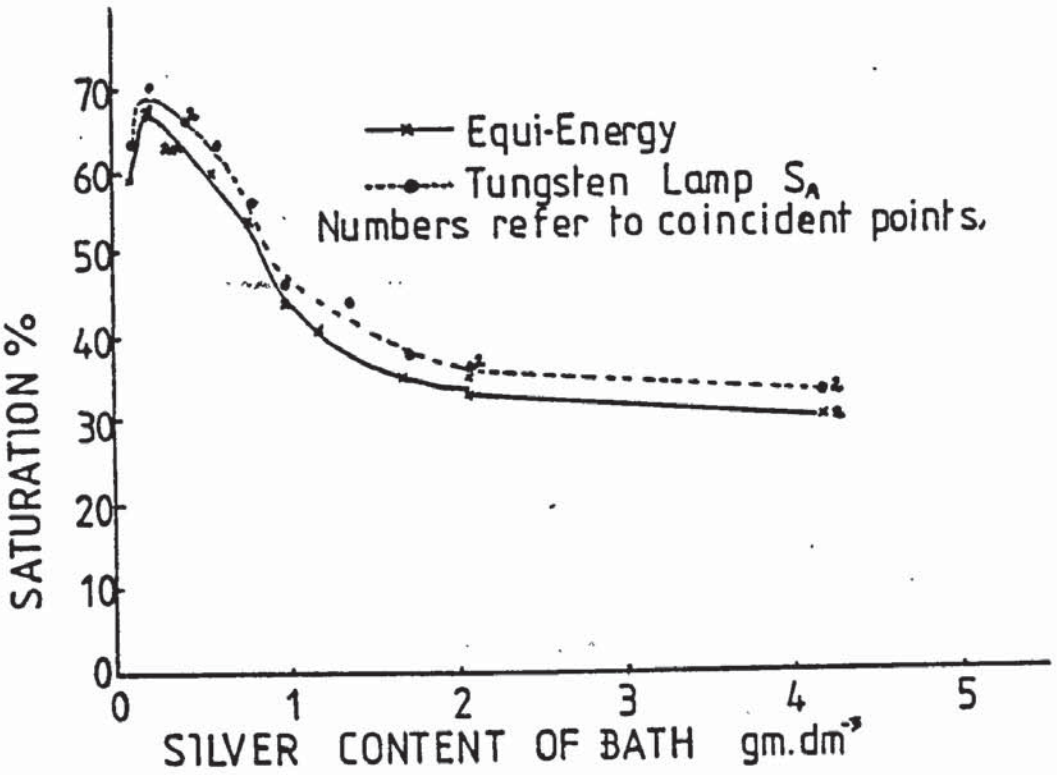

Fig. 7·7

The effect of bath silver content on % saturation

tungsten lamp conditions exhibited a curve of similar shape, but over a very much narrower range of values with the peak displaced to a higher silver content. Thus it is evident that under tungsten lamp conditions the colours would appear to contain more red and less blue. The appropriate diagrams show that saturation values were very similar under both illuminant conditions. The shape of the dominant wavelength curves were also similar except that the tungsten lamp values were about 5 nm higher. Luminosity values for both conditions were in the band 44-52% but they did not appear to follow any definable pattern.

7·4 THE SCANNING ELECTRON MICROSCOPE

7·4·1 The Silver Content of the Deposit

Selected samples were examined by the use of the Kevex attachment to the scanning electron microscope, and the results are given in Table 7·2 and Fig. 7·8. These results show that the silver content of the deposit varied linearly with silver content of the bath. The "nickel modified" values were slightly lower, but still maintained the linearity.

7·4·2 The Topography of the Electrodeposit

Figs. 7·9 to 7·13 show the texture of the deposit surfaces. These plates show that the deposit from gold baths containing silver consisted of "dimpled" nodules. The deposits were very similar for all silver contents tried, but they were different in character from silver-free gold deposits (Fig. 5·22) which although nodular were

(contd.p. 202.)

TABLE 7·2

THE KEVEX ANALYSIS RESULTS

KEY

Column 1 : Disc number

2 : Silver peak integral of standard

3 : Nickel peak integral of standard

4 : Silver peak integral of disc

5 : Nickel peak integral of disc

6 : Silver content of bath g/dm^3

7 : Apparent nickel content of deposit %

8 : Silver content of deposit %

9 : Modified silver content of deposit %

1	2	3	4	5	6	7	8	9
38	181871	87036	49937	8381	2·1	9·63	27·75	24·8
33	181871	87036	6811	2374	0·21	3·3	3·74	3·61
54	181871	87036	19541	7432	0·81	8·54	10·74	9·82
36	181871	87036	12380	1751	0·42	2·01	6·81	6·67
33 2nd run	187871	87036	7826	3093	0·21	3·55	4·30	4·14
36	187871	87036	12236	3749	0·42	4·31	6·73	6·43

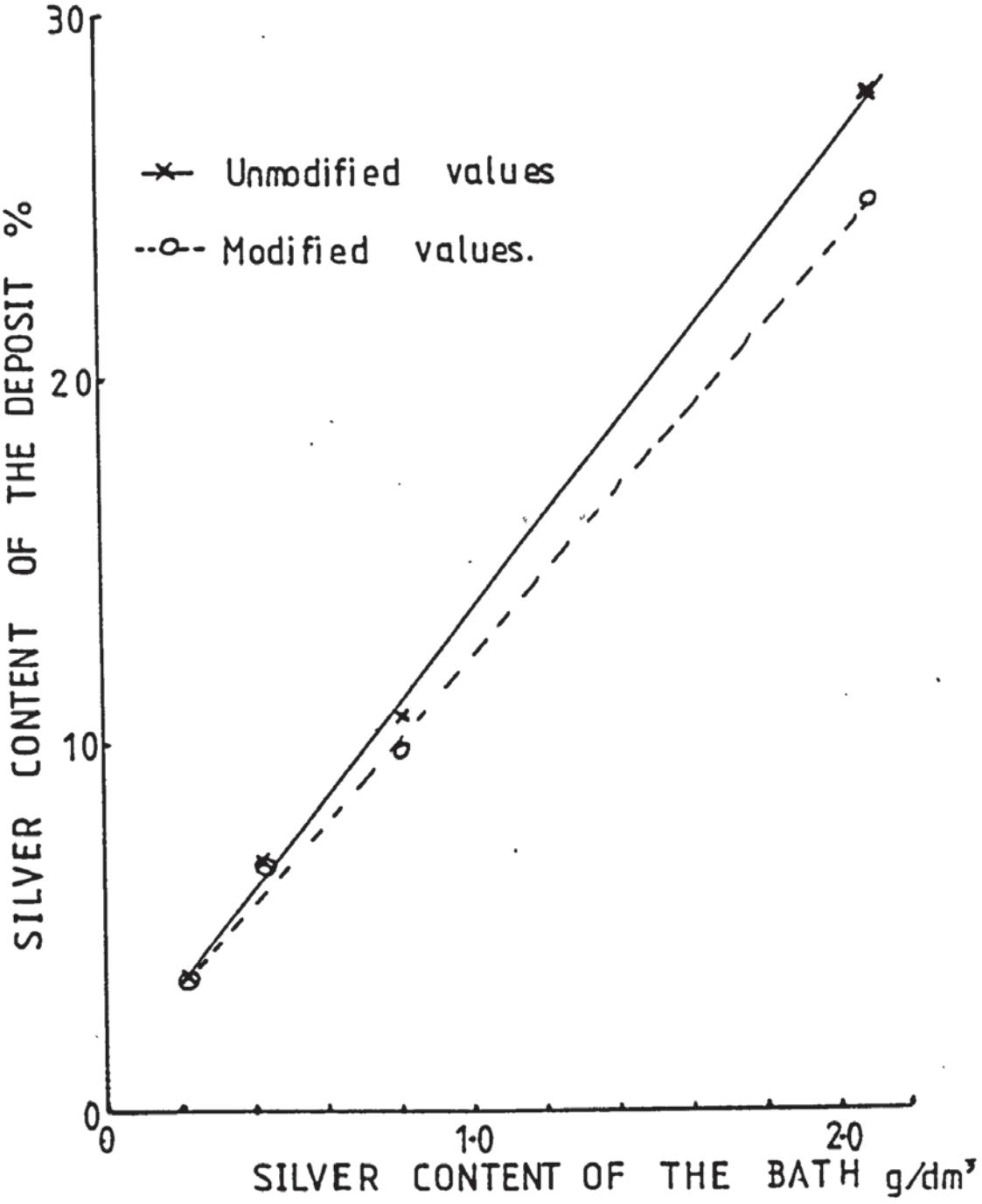

Fig. 7·8

The relationship between silver content of the bath and the deposit

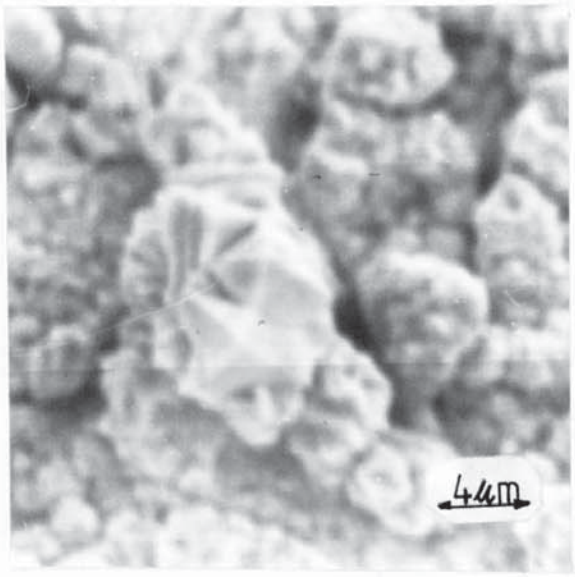

Fig. 7·9

Disc No. 34 (5K) 3·74% Silver

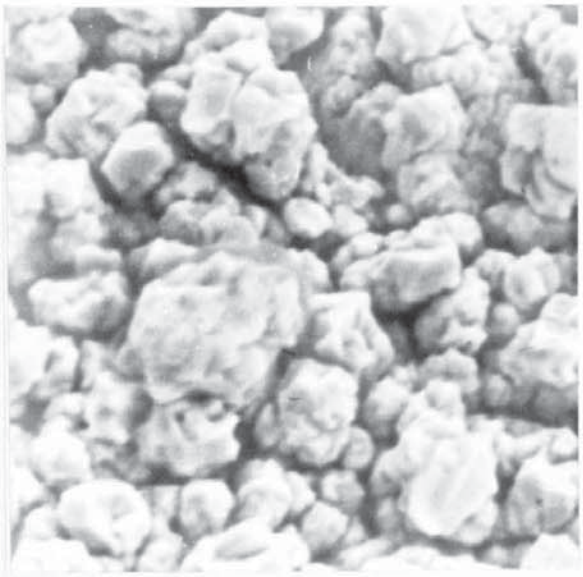

Fig. 7·10

Disc No. 36 (5K) 6·67% Silver

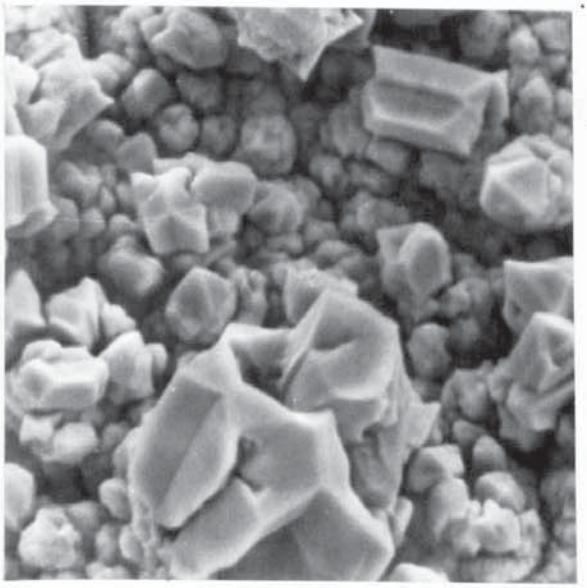

Fig. 7·11

Disc No. 54 (5K) 9·82% Silver

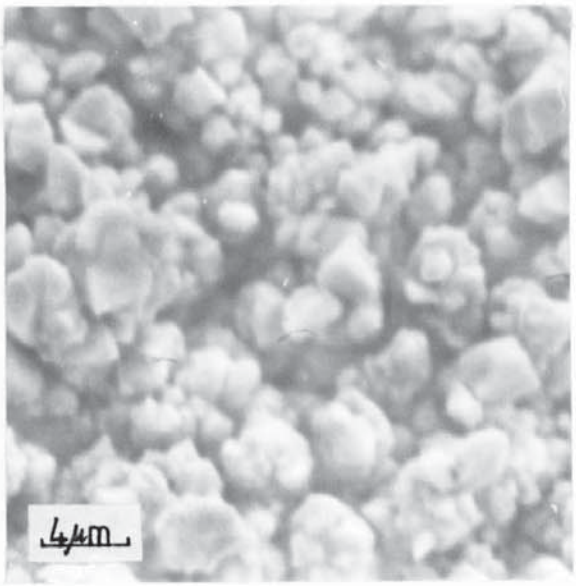

Fig. 7·12

Disc No. 38 24·8% Silver

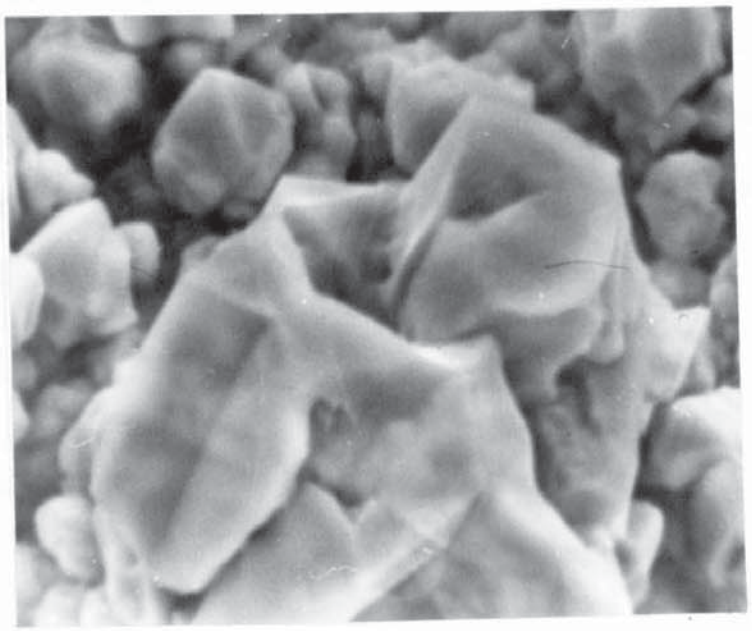

Fig. 7·13

Disc No. 54 (10K) 9·82% Silver

not dimpled. The dimpled nodules characteristic of the silver containing deposits varied in size from approximately 11 μm to 0·75 μm. The very large aggregates were the most unusual (Figs. 7·11 and 7·13), and did not appear to be associated with particular parts of the disc (edge for example). Closer examination of a particularly large nodule (10 K) revealed that it appeared to be multi-facetted which gave the so-called "dimpled" appearance. It had the aspect of a rather primitive dendrite, as if there had been a number of spines from which leaf-like, rather angular platelets had grown. The smaller nodules were also facetted. It must be emphasised that although the deposits appeared to consist of separate colonies the deposits although soft were quite coherent.

CHAPTER 8

THE HIDING POWER OF SELECTED COMMERCIAL ELECTROPLATING BATHS

8·1 INTRODUCTION

This series of experiments was designed to investigate the effect of deposit thickness on the development of a stable colour using two commercial gold electroplating baths designated P5 and 84C obtained from Precious Metals Distributers Ltd. Examples of the effect of plating time on the visual colour of the deposits are shown in Figs 8·1 and 8·2. The results of these experiments are given in Table 8·1A-C. Prior to electroplating the discs were polished to 6 μm diamond.

8·2 VISUAL APPEARANCE RELATED TO THE THICKNESS OF THE DEPOSIT

8·2·1 Solution P5

The thicknesses of the deposits produced in solution P5 were estimated by weighing, the weight being converted to a thickness by the use of a factor previously derived. In order to eliminate "freak" results these thicknesses were plotted against time (Fig. 8·3) and it was found that the relationship of deposit thickness with time estimated by this method was linear except for the last sample 900 secs). In order to determine if this was a trend or due to experimental error a plating test was conducted in which possible error introduced by stripping of Lacomit was eliminated. The test sample was cut from nickel foil with a thin integral current connector cut in one piece from the foil. The sample was electroplated in increments as indicated in Table 8·2. Weighing was carried out at each increment. The weight of the deposit was converted to a thickness by multiplying the weight by a conversion factor of 30·7, the derivation of this factor being given in Appendix 14. The graph

(contd. p. 213.)

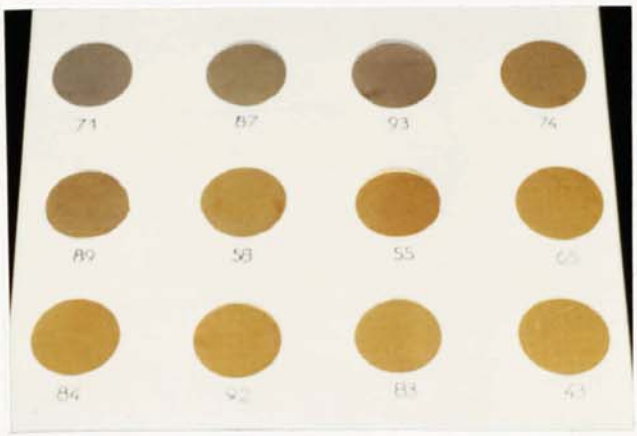

Disc No.	Plating Time (s)	Calculated Thickness (μm)
71	0	0
87	1	0·002
93	2	0·004
74	5	0·010
89	10	0·02
58	15	0·03
55	30	0·06
65	60	0·12
84	120	0·24
92	300	0·60
83	600	1·2
43	900	1·8

Fig. 8·1

Gold electroplated discs produced in Bath P5

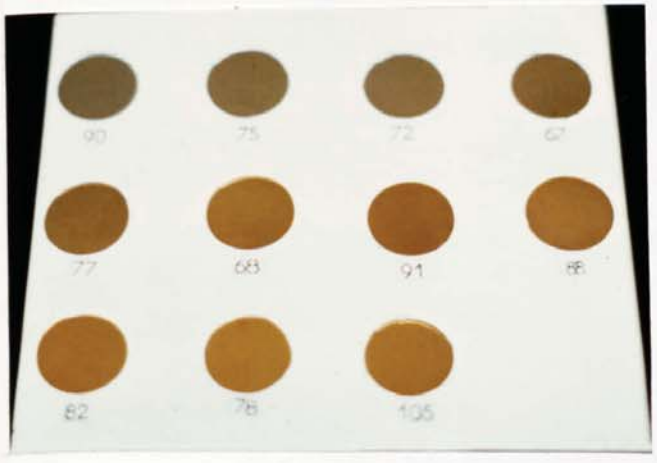

Disc No.	Plating Time (s)	Calculated Thickness (μm)
90	1	0·0011
75	2	0·0023
72	5	0·0056
67	10	0·0113
77	30	0·0338
68	60	0·0675
91	120	0·135
88	300	0·3375
82	600	0·675
78	900	1·0125
105	1200	1·35

Fig. 8·2

Gold electroplated discs produced in Bath 84C

Sample No.	Solution Used	Time (s)	Gain in Weight (g)	Calculated Thickness (μm)	Description
92	P5	300	0·0062	0·54	Bright yellow gold
84	P5	120	0·0026	0·23	Bright yellow gold
65	P5	60	0·0014	0·12	Bright yellow gold
55	P5	30	0·001	0·09	Bright yellow gold
58	P5	15	0·0001	0·01	Bright yellow gold
74	P5	5	0·0002	0·02	Pale gold bright
87	P5	1	-0·0001	-	No obvious gold
83	P5	600	0·0136	1·19	Bright gold
43	P5	900	0·0241	2·11	Bright yellow gold
93	P5	2	-0·0006	-	No obvious gold
89	P5	10	0·0005	0·04	Not full gold colour. Seems thin. Paler yellow gold.
90	84C	1	0	0	No obvious gold
75	84C	2	0·0001	0·01	Not gold coloured but very slight dulling
72	84C	5	0·0002	0·02	A very slight gold cast but not really gold coloured
67	84C	10	0·0013	0·11	A slight gold cast but not really gold coloured
77	84C	30	0·0002	0·02	Pale gold colour. Bright
68	84C	60	0·0001	0·01	Bright yellow gold
91	84C	120	0·0007	0·06	Bright orange gold
88	84C	300	0·0023	0·20	Bright orange gold
82	84C	600	0·0023	0·20	Bright orange gold
105	84C	1200	0·0141	1·23	Bright orange gold
78	84C	900	0·0091	0·80	Bright orange gold
92	none	0	-	-	Polished mirror bright nickel

Table 8·1A

The effect of electroplating time on bright baths

Sample No.	Chromaticity Coordinates					
	Equi-Energy			Tungsten Lamp S_A		
	x	y	z	x	y	z
92	0·390	0·383	0·227	0·493	0·421	0·086
84	0·392	0·381	0·227	0·496	0·419	0·85
65	0·388	0·380	0·232	0·493	0·419	0·088
55	0·388	0·380	0·232	0·493	0·419	0·088
58	0·378	0·371	0·251	0·486	0·416	0·098
74	0·351	0·351	0·298	0·465	0·412	0·122
87	0·332	0·327	0·341	0·451	0·402	0·147
83	0·395	0·385	0·220	0·498	0·420	0·082
43	0·401	0·387	0·212	0·503	0·419	0·078
93	0·327	0·331	0·342	0·445	0·406	0·149
89	0·369	0·365	0·266	0·479	0·416	0·105
90	0·320	0·317	0·363	0·441	0·399	0·160
75	0·338	0·335	0·327	0·456	0·406	0·138
72	0·324	0·324	0·352	0·445	0·402	0·153
67	0·339	0·336	0·325	0·456	0·406	0·138
77	0·345	0·345	0·310	0·460	0·410	0·130
68	0·374	0·373	0·253	0·482	0·419	0·099
91	0·374	0·375	0·251	0·482	0·421	0·097
88	0·373	0·370	0·257	0·482	0·419	0·099
82	0·385	0·376	0·239	0·491	0·418	0·095
105	0·381	0·371	0·248	0·488	0·417	0·095
78	0·385	0·373	0·242	0·492	0·416	0·092
92	0·329	0·328	0·343	0·448	0·403	0·149

Table 8·1B

Sample No.	Equi-Energy			Tungsten Lamp S_A		
	DM nm	S %	L %	DM nm	S %	L %
92	579	31	9	583	36	9
84	580	32	8	585	36	8
65	580	30	8	585	35	8
55	580	30	8	585	35	8
58	580	25	7	585	28	7
74	578	11	7	585	11	7
87	530	<1	7	564	2	7
83	580	34	9	585	38	9
43	580	35	9	586	42	9
93	487	2	8	469	2	8
89	579	19	9	584	24	9
90	472	5	8	457	3	8
75	570	2	9	500	2	9
72	477	3	7	453	2	7
67	576	3	7	595	2	7
77	577	7	9	587	7	9
68	578	24	8	583	28	8
91	577	25	10	582	28	
88	579	23	12	583	28	13
82	580	28	8	585	32	9
105	580	26	8	585	31	8
78	581	27	10	586	32	10
92	470	<1	7	420	1	7

Table 8•1C

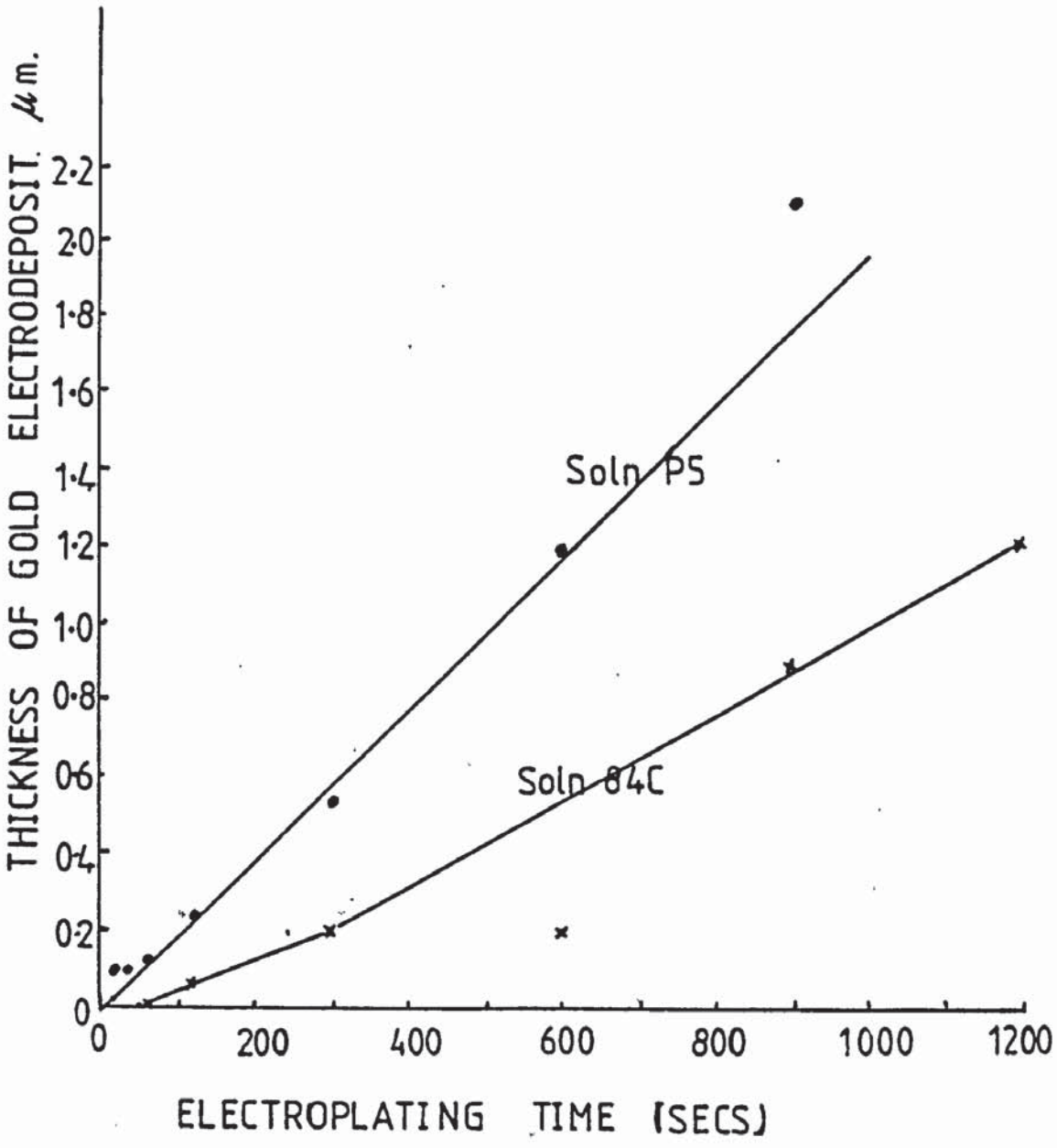

Fig. 8·3

The thickness time factors for baths P5 and 84C

TABLE 8·2

RESULTS OF TESTS FOR PLATING THICKNESS IN SOLUTIONS P5 AND 84C

KEY

Column 1 : Solution

2 : Time increment (seconds)

3 : Total time (seconds)

4 : Weight before increment (g)

5 : Weight after increment (g)

6 : Weight gain for increment (g)

7 : Total weight gain (g)

8 : Gold thickness (μm)

9 : Description

1	2	3	4	5	6	7	8	9
84C	5	5	1·8129	1·8129	0	0	0	No change
84C	10	15	1·8129	1·8133	0·0004	0·0004	0·0123	Very slight gold cast
84C	20	35	1·8133	1·8137	0·0004	0·0008	0·02463	Gold around edges
84C	40	75	1·8137	1·8140	0·0003	0·0011	0·0339	Gold creeping in but still nickel visible
84C	80	155	1·8140	1·8157	0·0017	0·0028	0·0862	Covered - bright gold
84C	160	315	1·8157	1·8208	0·0051	0·0079	0·2432	" " "
84C	320	635	1·8208	1·8316	0·0108	0·0187	0·5758	" " "
84C	640	1275	1·8316	1·8569	0·0253	0·044	1·3547	" " "
P5	5	5	1·6961	1·6964	0·0003	0·0003	0·0092	A gold cast
P5	10	15	1·6964	1·6973	0·0009	0·0012	0·0368	Fairly well covered
P5	20	35	1·6973	1·6985	0·0012	0·0024	0·0737	Covered - bright gold
P5	40	75	1·6985	1·7013	0·0028	0·0052	0·1596	" " "
P5	80	155	1·7013	1·7064	0·0051	0·0103	0·3162	" " "
P5	160	315	1·7064	1·7176	0·0112	0·0215	0·6599	" " "
P5	320	635	1·7176	1·7414	0·0238	0·0453	1·3905	" " "
P5	640	1275	1·7414	1·7860	0·0446	0·0899	2·7595	" " "

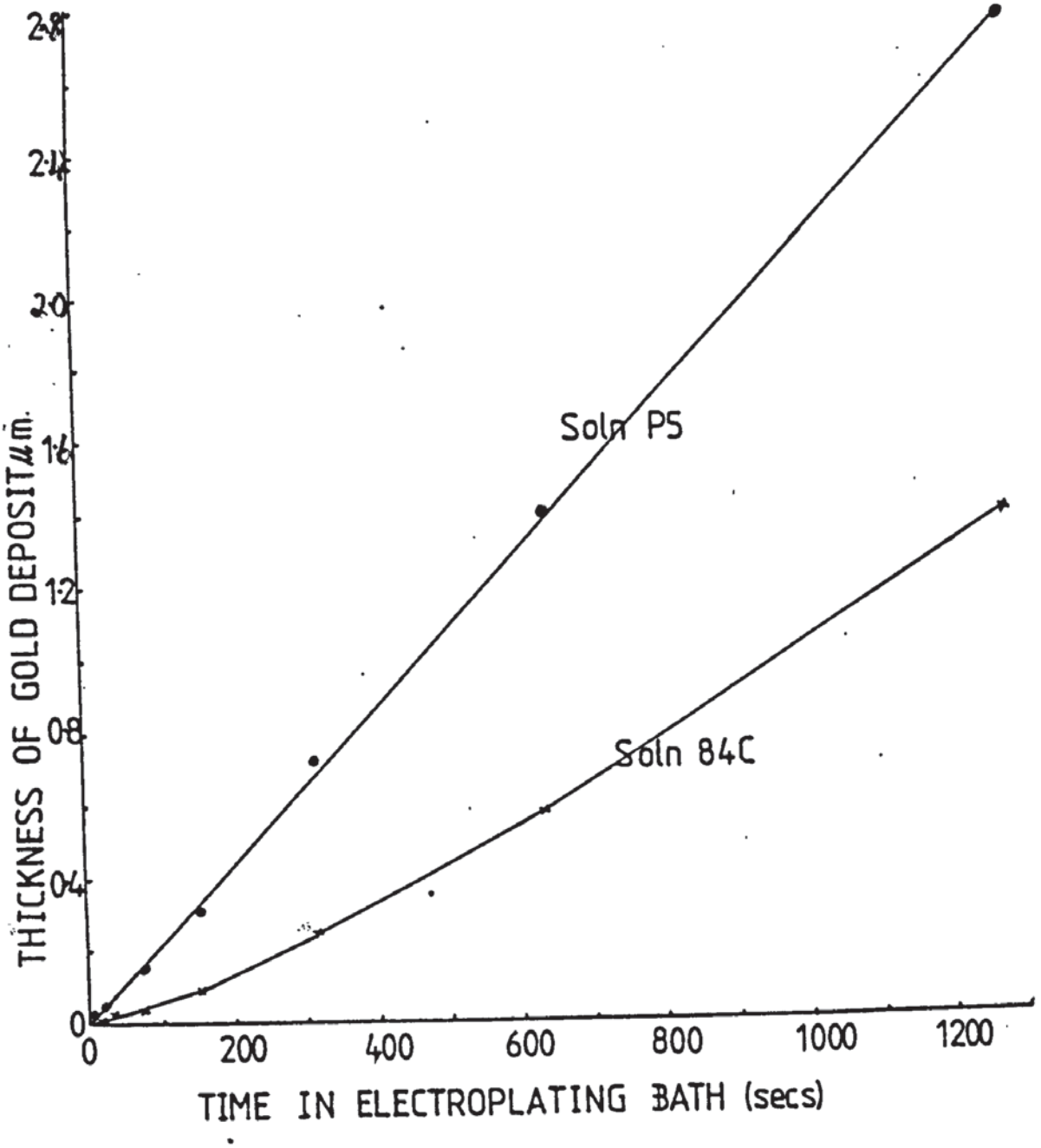

Fig. 8·4

The thickness-time plating test

drawn as a result of this experiment, given in Fig. 8·4, shows that the plating rate was very similar to that derived for the discs and that there was no sign of a departure from linearity in the region of 900 seconds. Thus the plating rate derived from the set of discs originally, namely 0·002 µm/s was held to be correct. As an additional check a cross-section of sample 83 was prepared and examined by means of the SEM. The calculation of thickness is given in Appendix 15 and it was found that the average thickness was 1·34 µm in 600 seconds, i.e. a plating rate of 0·0022 µm/s, and a vindication of the weight method. The photographs of the appropriate cross-sections are given in Fig. 8·5-8·6. The thickness values conformed well with the value of 0·0023 µm/s given in the appropriate instruction leaflet. Examination of the comments made at the time the experiments were conducted showed that the deposit was only described as bright yellow gold after a plating time of 15 seconds (calculated thickness 0·03 µm) and this designation was continued up to 900 seconds.

8·2·2 Solution 84C

The deposits produced in solution 84C did not rate the description "bright yellow gold" until 60 seconds had elapsed, and this changed to the description "bright orange" gold subsequently. It must be emphasised that these descriptions were subjective, and made when the discs were being dried and not made in comparison with any standard. In this solution 60 seconds was equivalent to 0·03 µm. It was found that for the low time periods the weight changes were erratic, which is quite understandable for such small increments. The graph as a whole (Fig. 8·3) did not appear to be linear, but was a

(contd. p. 215.)

Fig. 8·5

Disc No. 83 5K

Fig. 8·6

Disc No. 83 10K

curve with rate increasing slightly with time. A thickness test experiment was carried out similarly to that previously described for solution P5. The resulting graph (Fig. 8·4) conformed very closely to that derived for the discs and it was used for assessing probable gold thickness on the discs in the lower part of the curve which was unreliable for the discs. In order to provide a thickness check a cross-section of the deposit for a 1200 second sample was examined on the SEM (Figs. 8·7-8·9). Three magnifications were used and the results are given in Appendix 15. It was considered that if a number of measurements were taken on each photograph and averages taken then the greater accuracy of the higher magnifications would be reinforced by the larger scan area of the smaller magnification in contribution to overall accuracy. By this method the thickness of the gold deposit was found to be 1·4 μm for the 1200 second sample, which conformed well with 1·23 μm found by change in weight measurements.

8·3 THE OPTICAL PROPERTIES

8·3·1 The Reflectivity Curves

The plotted reflectivity curves were first examined to determine the time necessary (and by implication the thickness) for the onset of the reflectivity step associated with gold.

8·3·1·1 Solution P5

The shape of the curves (Fig. 8·10) after the establishment of the step was very much as expected for a gold electrodeposit, namely a sharp fall in reflectivity at a mid-point energy value of

(contd. p. 218.)

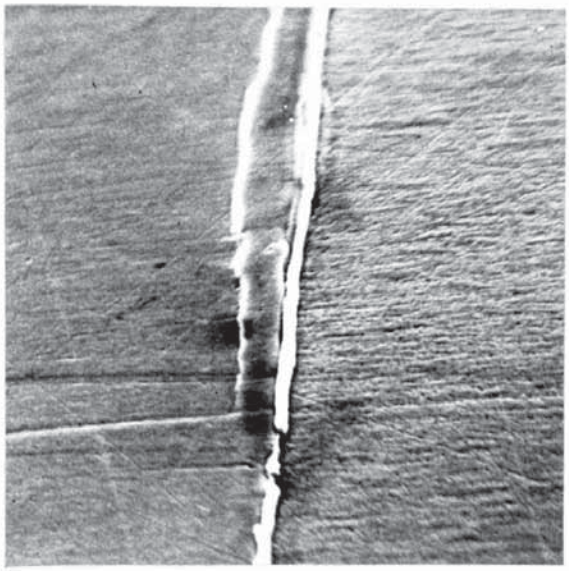

Fig. 8·7

Disc No. 105 1·4K

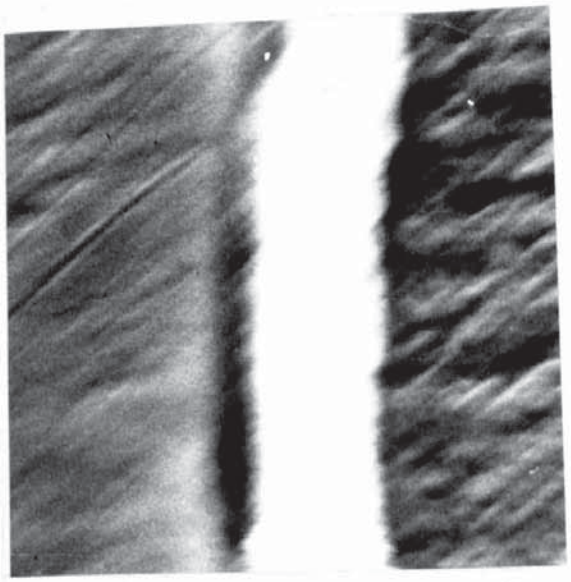

Fig. 8·8

Disc No. 105 13·9K

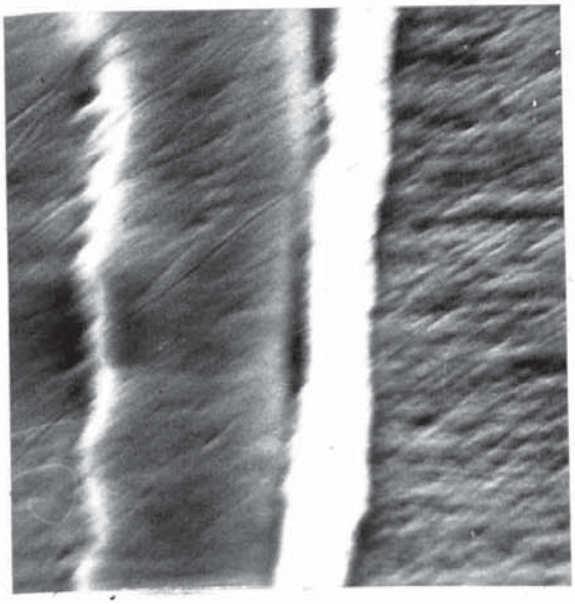

Fig. 8·9

Disc No. 105 6·9K

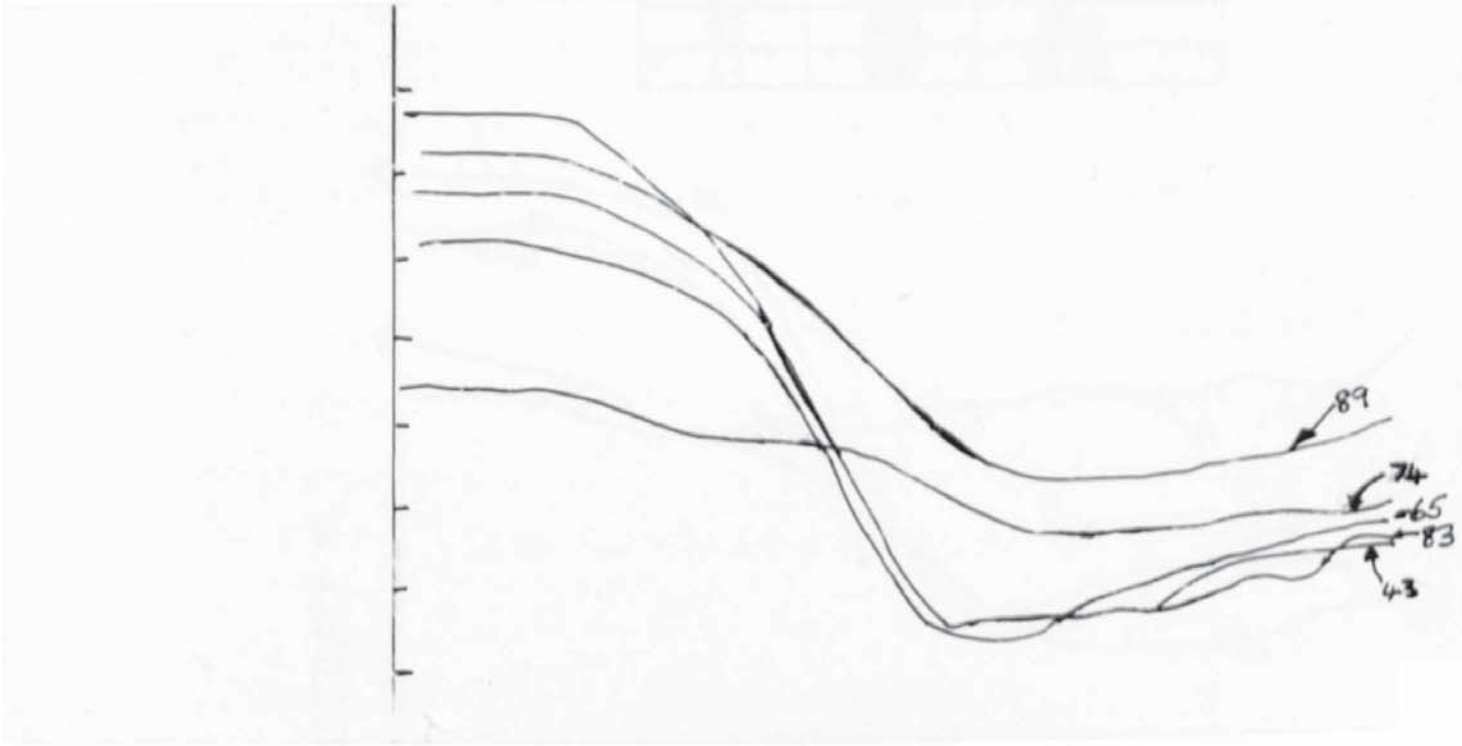
89
74
65
83
43

Disc No.	Time (secs)	Calculated Thickness μm
87	1	0·002
74	5	0·010
89	10	0·020
58	15	0·030
55	30	0·060
65	60	0·120
84	120	0·240
92	300	0·600
83	600	1·200
43	900	1·800

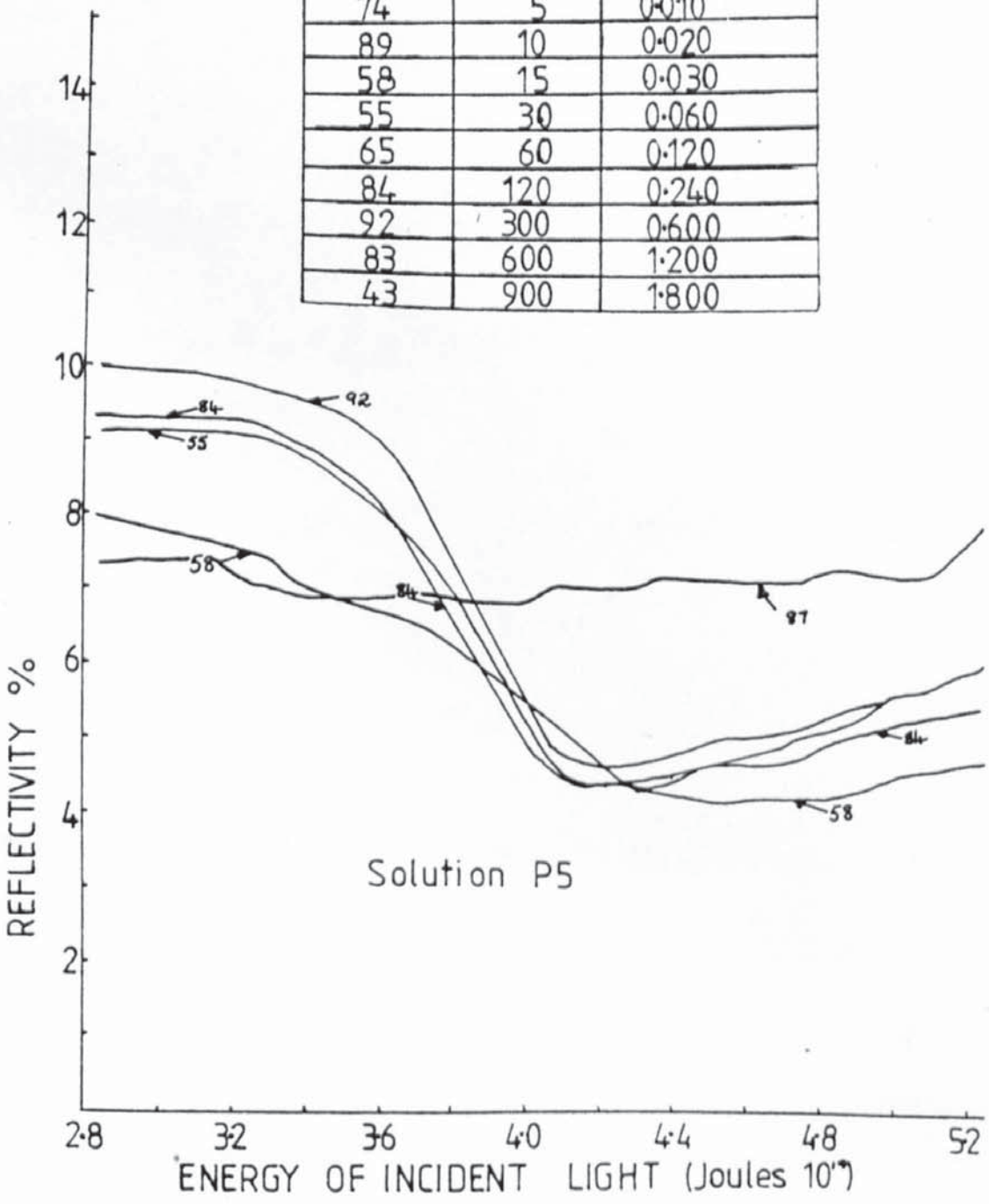

Fig. 8·10

Reflectivity curves for discs electroplated in solution P5

Disc No.	Time (secs)	Calculated Thickness μm
87	1	0·002
74	5	0·010
89	10	0·020
58	15	0·030
55	30	0·060
65	60	0·120
84	120	0·240
92	300	0·600
83	600	1·200
43	900	1·800

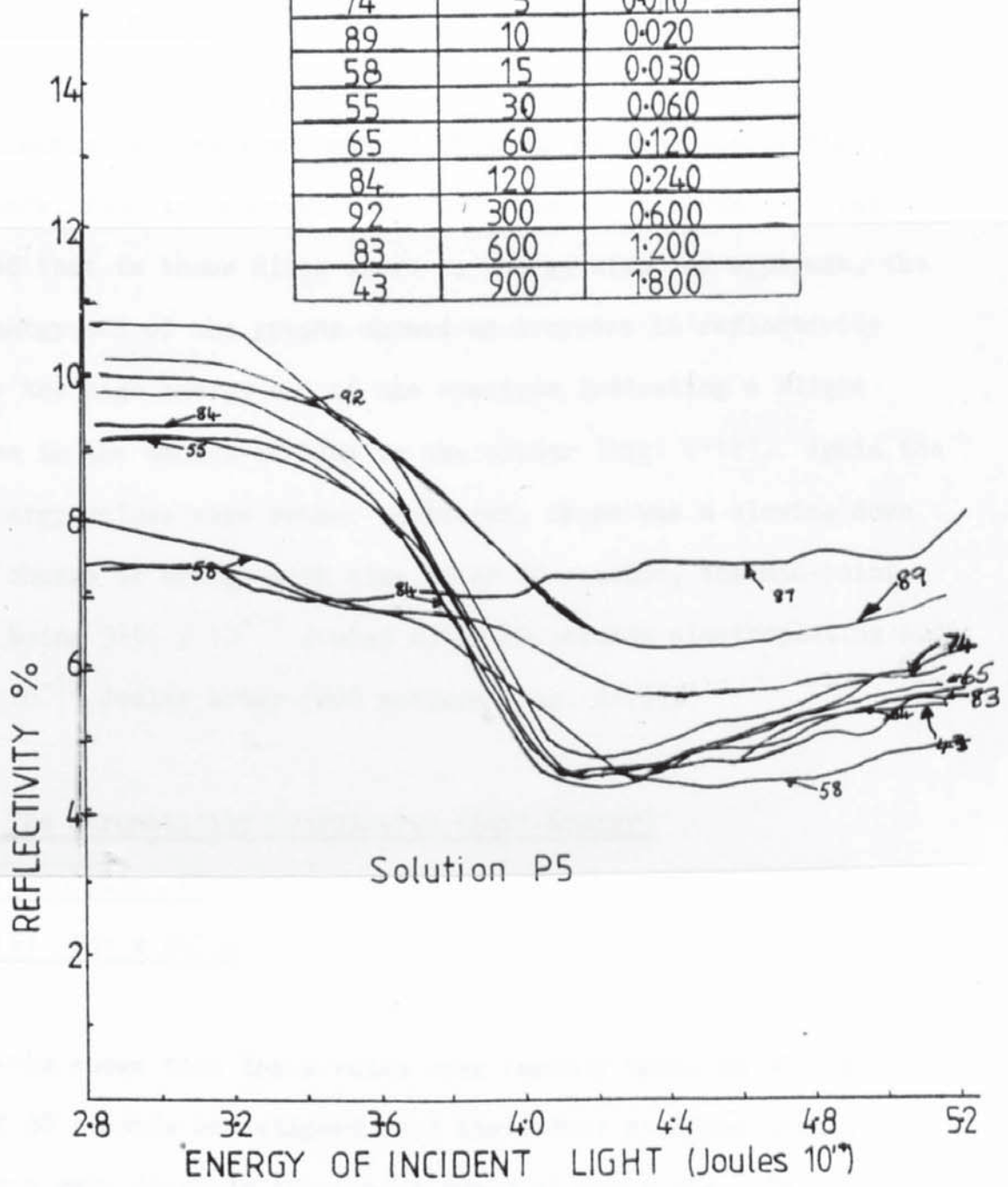

Fig. 8·10

Reflectivity curves for discs electroplated in solution P5

$3{\cdot}85 \times 10^{-19}$ Joules. Ten seconds electroplating time was required before a definite step was observed, although an embryo step was apparent after 5 seconds. Fig. 8·11 shows that although the values are rather scattered, the mid-point energy was fairly stable after 30 seconds, with perhaps an extremely slight downward trend.

8·3·1·2 Solution 84C

The reflectivity step was observed after an electroplating time of 60 seconds, with an indeterminate step after 30 seconds. It was observed that in those discs where an energy step was apparent, the high energy end of the graphs showed an increase in reflectivity towards the high energy end of the spectrum indicating a slight increase in the amount of blue in the colour (Fig. 8·12). Again the step energy values were rather scattered, there was a slowing down of the change of energy with time after 60 seconds, the mid-point energy being $3{\cdot}91 \times 10^{-19}$ Joules after 60 seconds electroplating and $3{\cdot}80 \times 10^{-19}$ Joules after 1200 seconds (Fig. 8·13).

8·3·2 The Chromaticity Coordinates (Equi-Energy)

8·3·2·1 Solution P5

8·3·2·1·1 The x Value

Fig. 8·14a shows that the x value rose rapidly until an electroplating time of 30 seconds had elapsed, and thereafter remained stable showing a very slightly increasing trend at the higher electroplating times.

(cont'd. p. 224.)

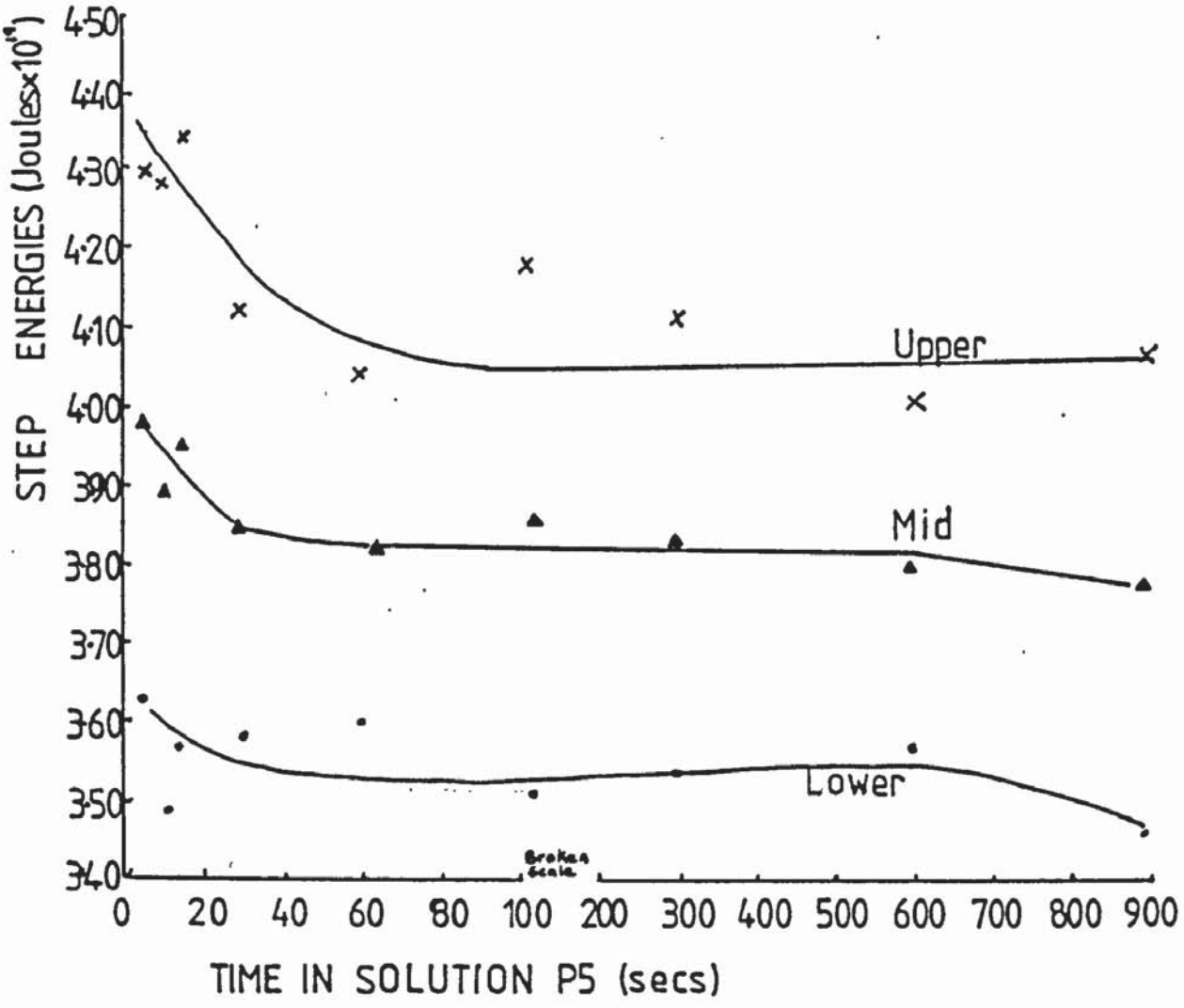

Fig. 8·11.

The mid-step energies calculated for discs in solution P5

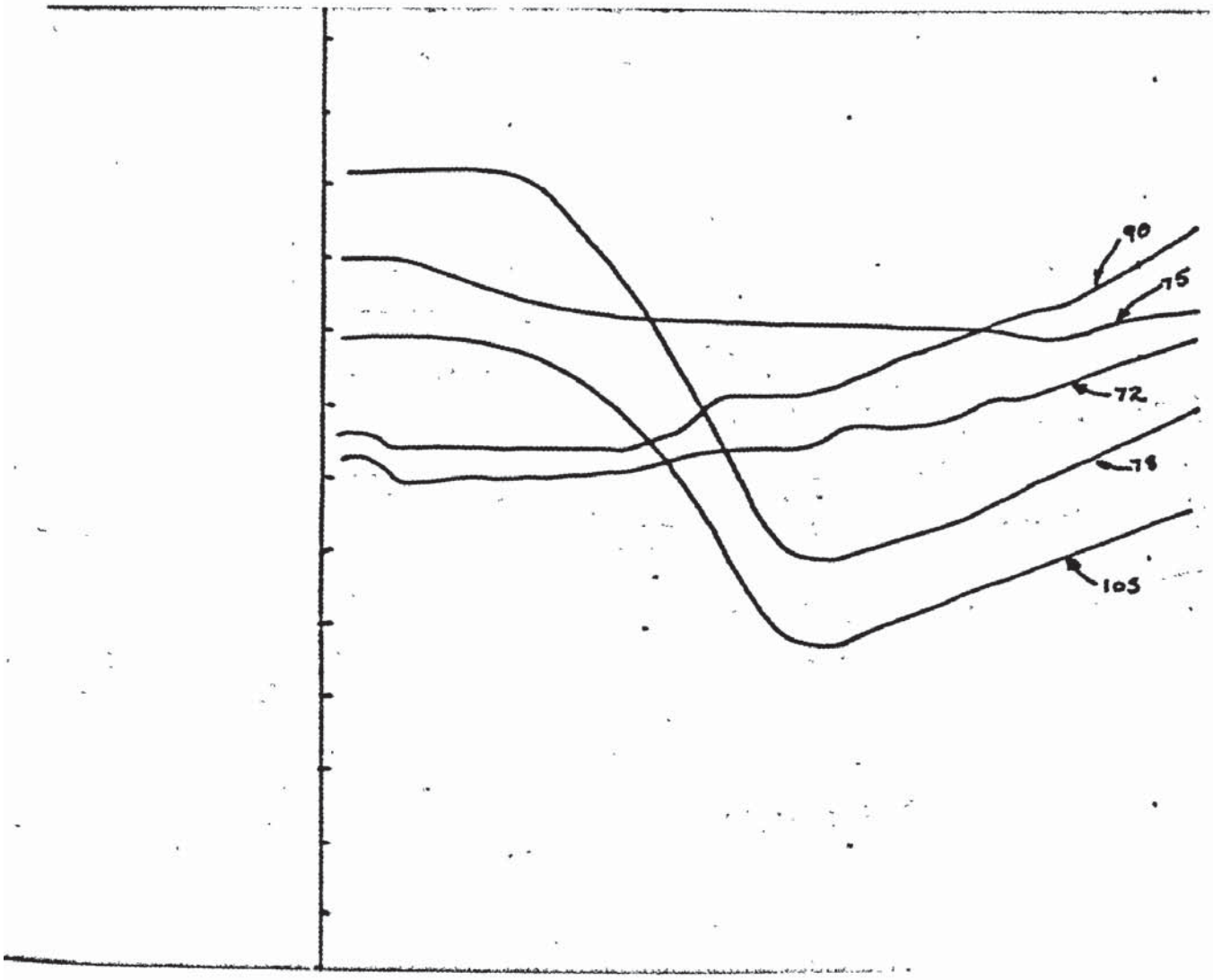
90
75
72
78
105

Disc No.	Time secs.	Calculated Thickness μm
90	1	0·0011
75	2	0·0023
72	5	0·0056
67	10	0·0113
77	30	0·0338
68	60	0·0675
91	120	0·1350
88	300	0·3375
82	600	0·6750
78	900	1·0125
105	1200	1·3500

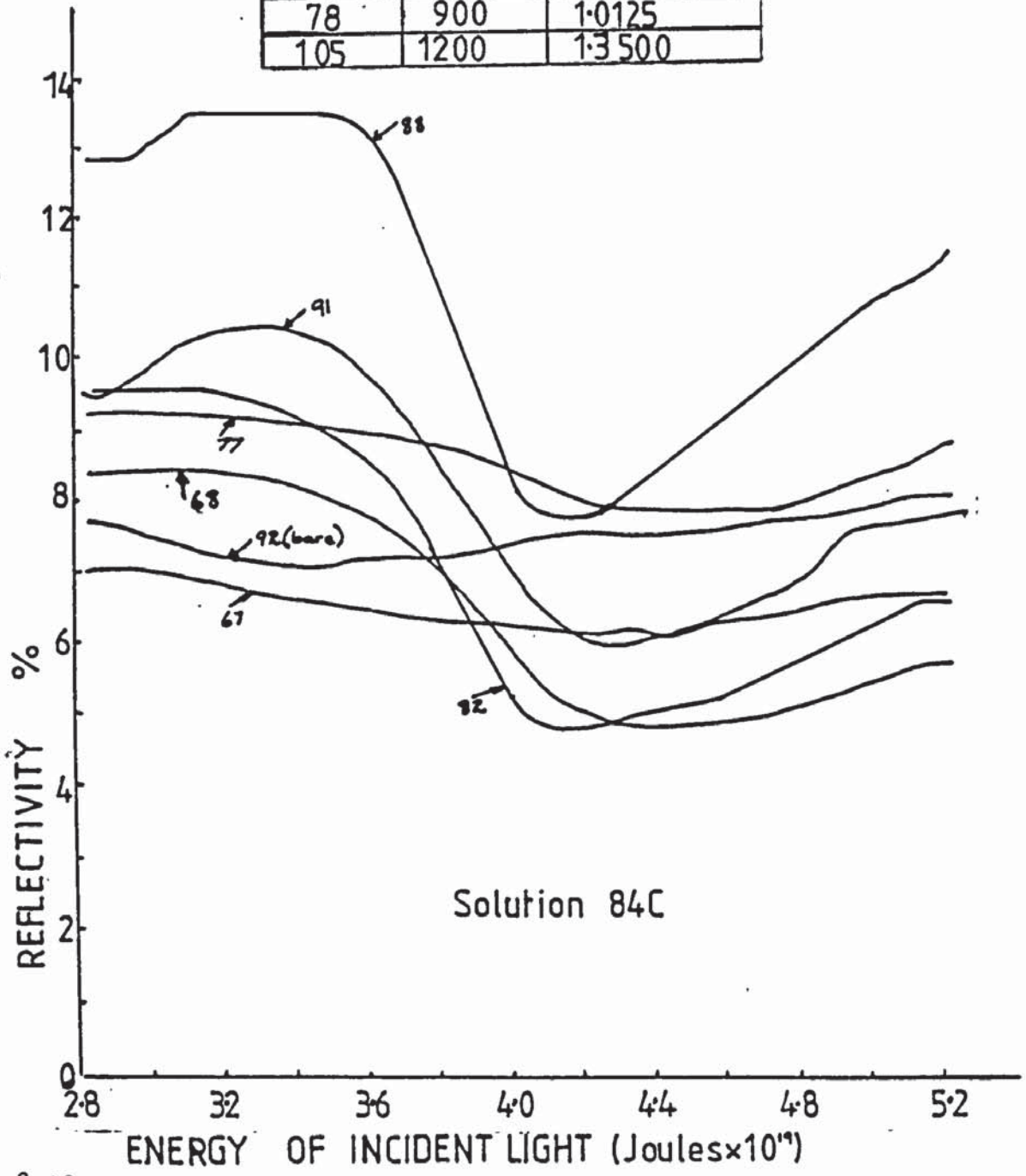

Fig. 8·12

Reflectivity curves for electroplated discs produced in bath 84C

Disc No.	Time secs.	Calculated Thickness μm
90	1	0·0011
75	2	0·0023
72	5	0·0056
67	10	0·0113
77	30	0·0338
68	60	0·0675
91	120	0·1350
88	300	0·3375
82	600	0·6750
78	900	1·0125
105	1200	1·3500

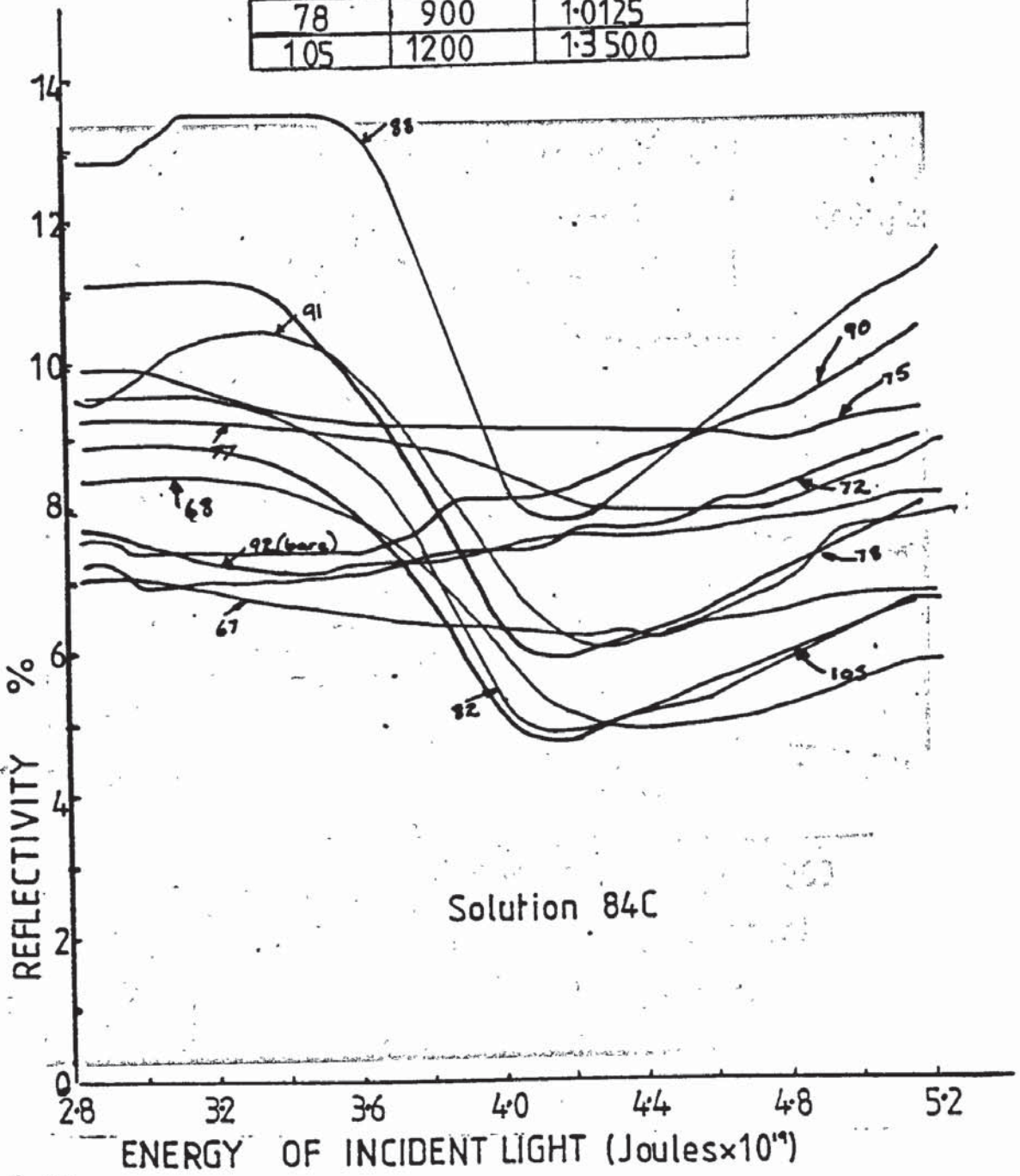

Fig. 8·12

Reflectivity curves for electroplated discs produced in bath 84C

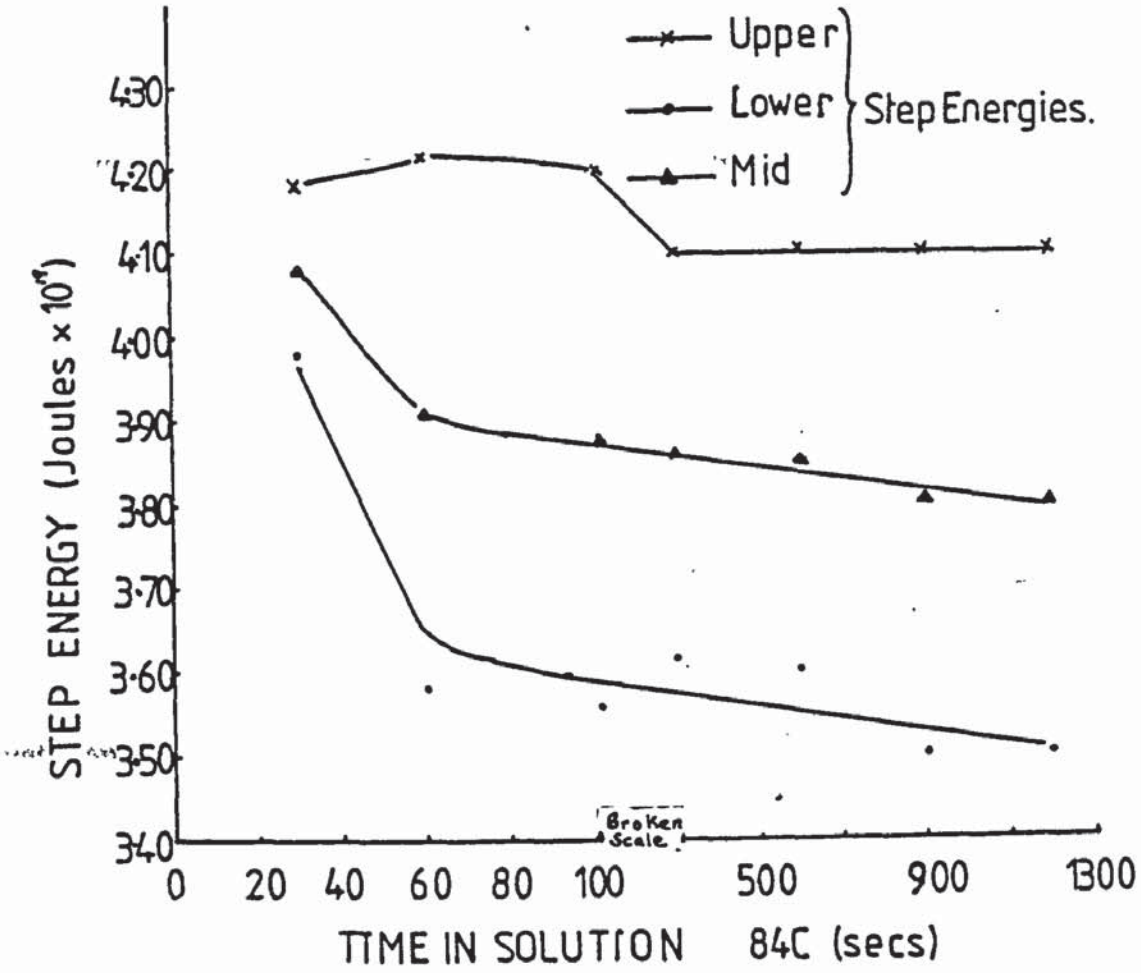

Fig. 8·13

The mid-step energies calculated for solution 84C

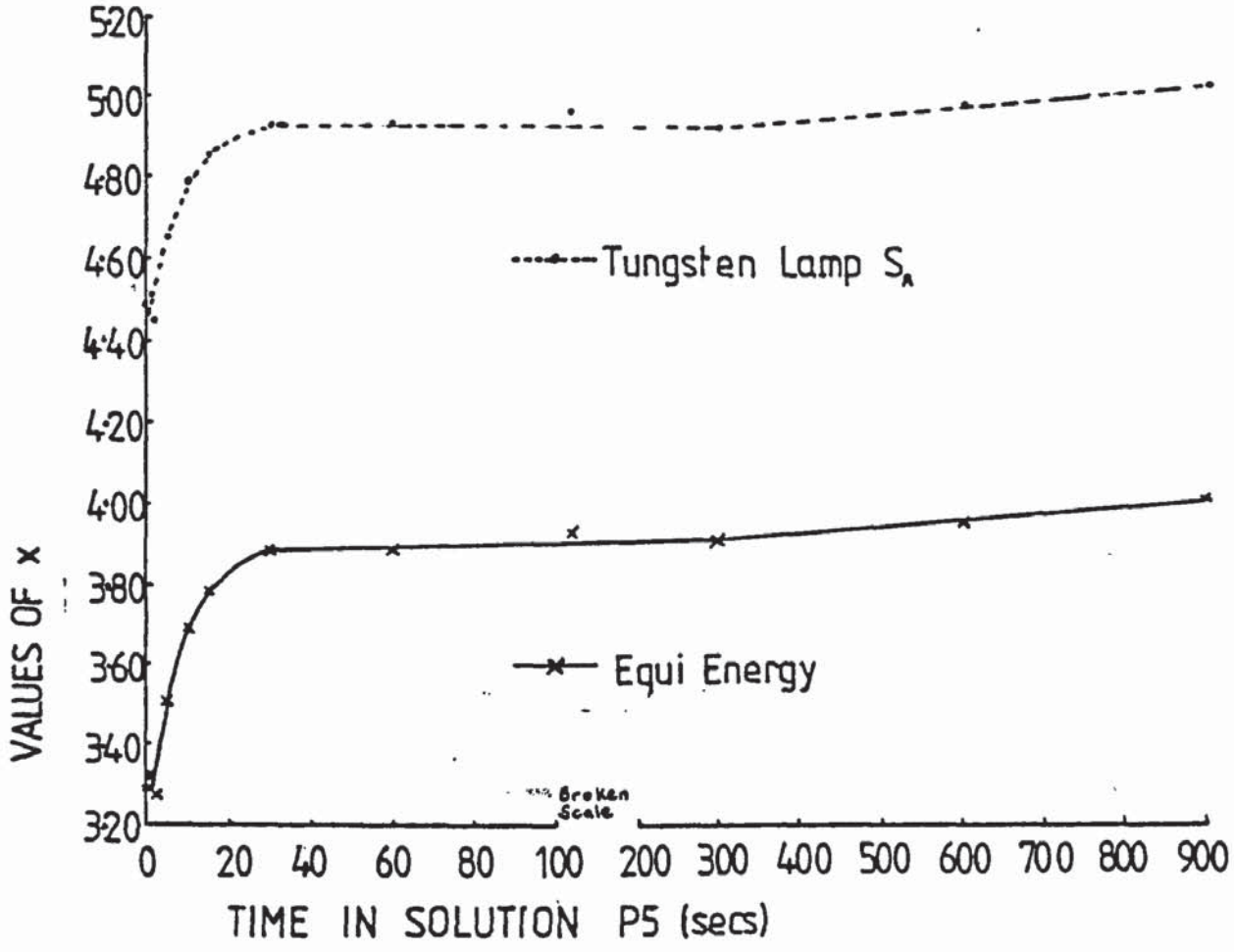

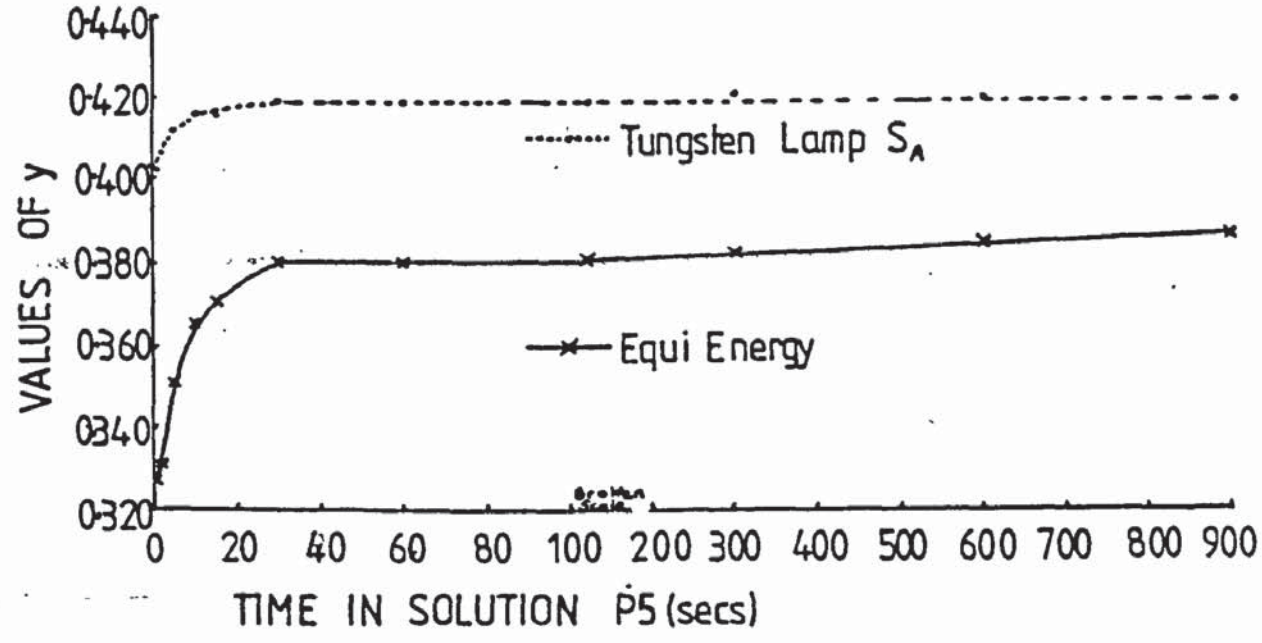

Fig. 8·14a and b

The x and y chromaticity coordinates for discs electroplated in solution P5 (6 µm diamond surface)

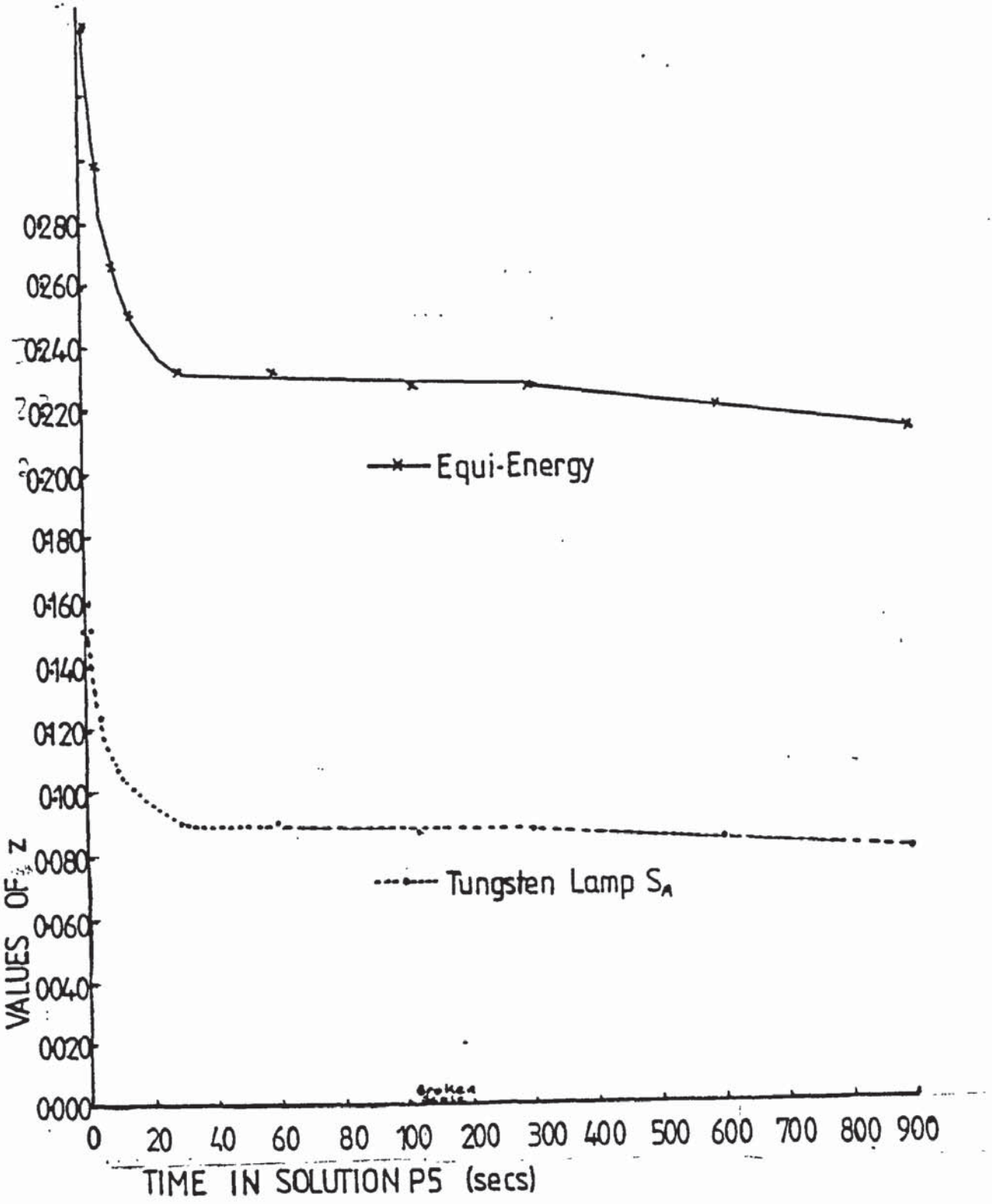

Fig. 8·14c

The z chromaticity coordinates for discs electroplated in solution P5 (6 µm diamond surface)

8·3·2·1·2 The y Value

Fig. 8·14b shows that stability was again attained after 30 seconds.

8·3·2·1·3 The z Value

Fig. 8·14c shows that stability was obtained as expected after 30 seconds.

8·3·2·2 Solution 84C

8·3·2·2·1 The x Value

The numerical value of x rose at a declerating rate up to 60 seconds, when stability was achieved; a step occurred after 300 seconds and thereafter a reversion to relative stability (Fig. 8·15a).

8·3·2·2·2 The y Value

A similar pattern was followed for the y value (Fig. 8·15b), stability being achieved after 60 seconds, no change being observed up to 1200 seconds (the final sample).

8·3·2·2·3 The z Value

The numerical value of z fell at a decelerating rate (Fig. 8·15c), relative stability being achieved after 30 seconds. A further fall in the value started at 300 seconds and continued on a very shallow slope.

(contd. p. 227.)

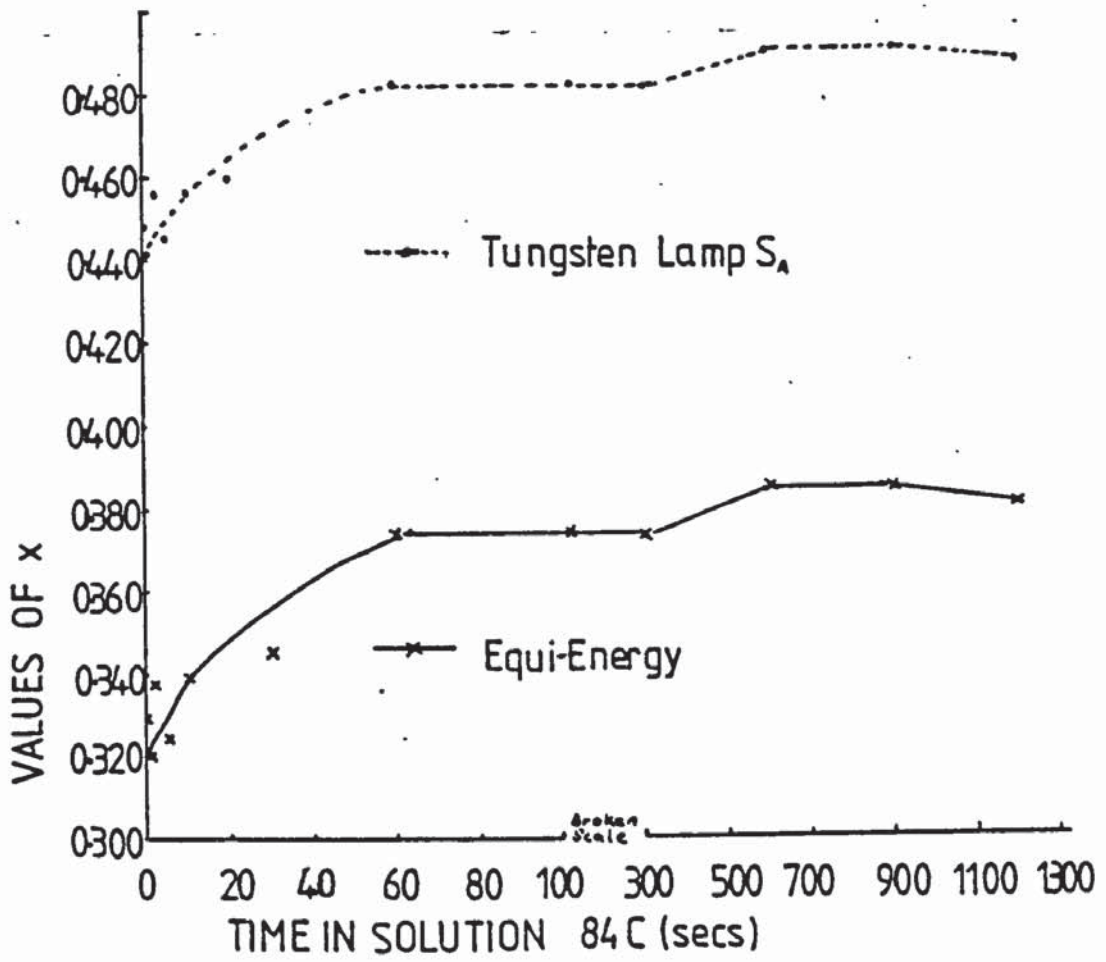

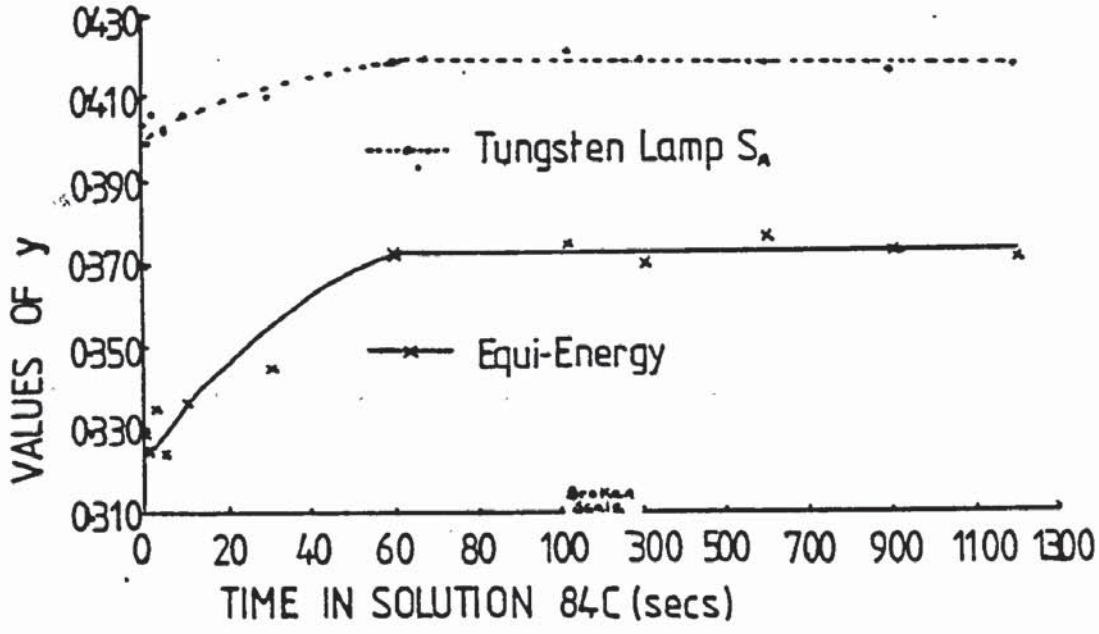

Fig. 8·15a and b

The x and y chromaticity coordinates for discs electroplated in solution 84C (6 μm diamond surface)

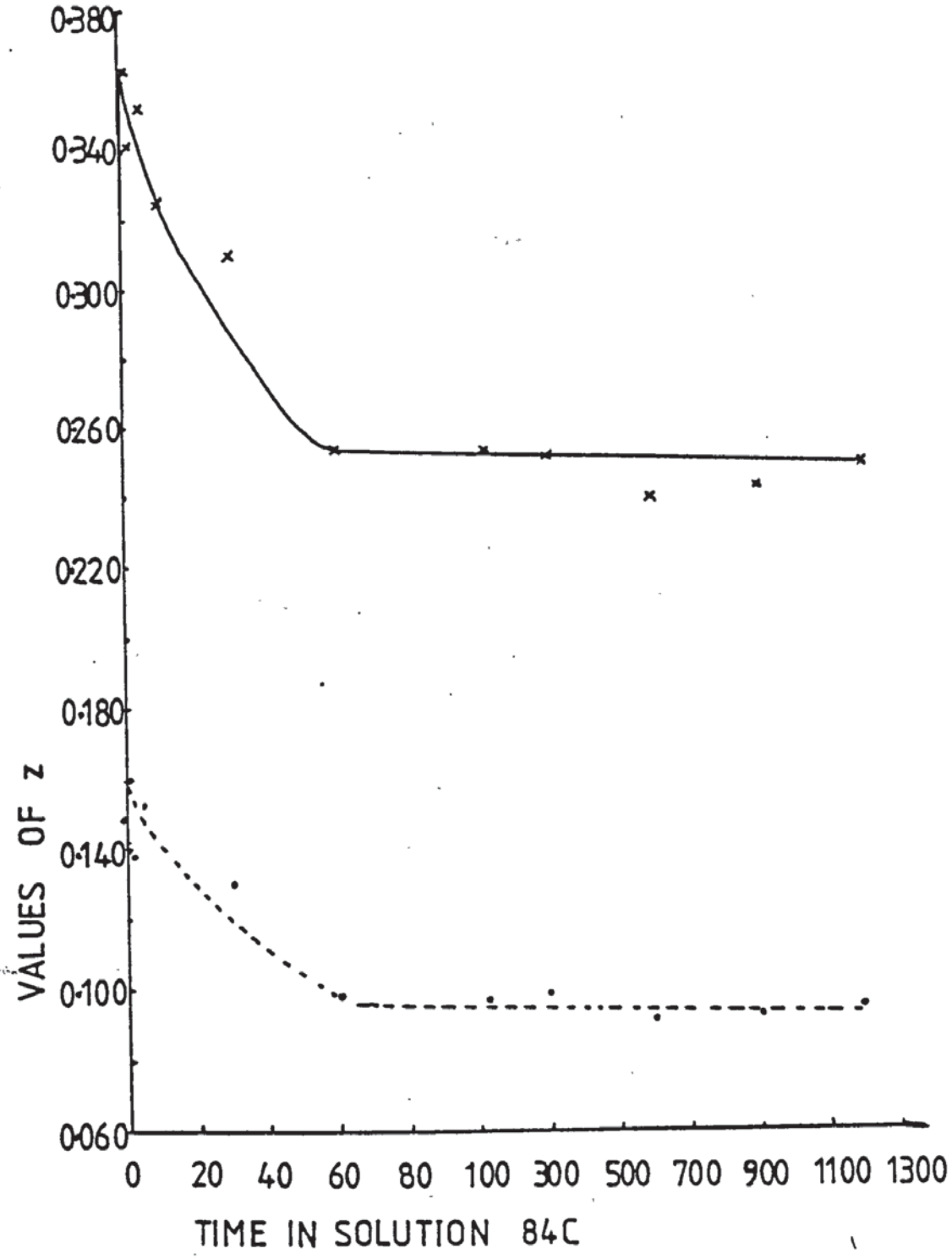

Fig. 8·15c

The z chromaticity coordinates for discs electroplated in solution 84C (6 μm diamond surface)

8·3·3 Dominant Wavelength, Saturation and Luminosity

8·3·3·1 Solution P5

Stable dominant wavelength values were very rapidly obtained (Fig. 8·16), i.e. after 5 seconds, even though the full gold colour had not developed. This rather surprising result is explained by reference to the saturation values given in Fig. 8·17 in which the percentage saturation of the colour rises very rapidly until 30 seconds of electroplating time, after which the saturation only increased very slightly with time, but even so the saturation was still not absolutely stable.

The luminosity values, given in Table 8·1C and plotted in Fig. 8·18 show that the values did not appear to be greatly affected by electroplating time, and the values were quite low (less than 10%). The only trend appeared to be one of slightly increased luminosity at the higher electroplating times, and scattered values (within a small range) at low time periods.

8·3·3·2 Solution 84C

Dominant wavelength stability was obtained after 10 seconds (Fig. 8·19), a very steep rise to this stable value being noted. Again saturation values were not stable (Fig. 8·20) until a greater electroplating time period had elapsed (60 seconds). Thereafter followed a period of stability and at 300 seconds a slight rise to a maximum at 600 seconds followed by a gradual fall to near the original stable value. The luminosity values were all quite low

(contd.p. 233.)

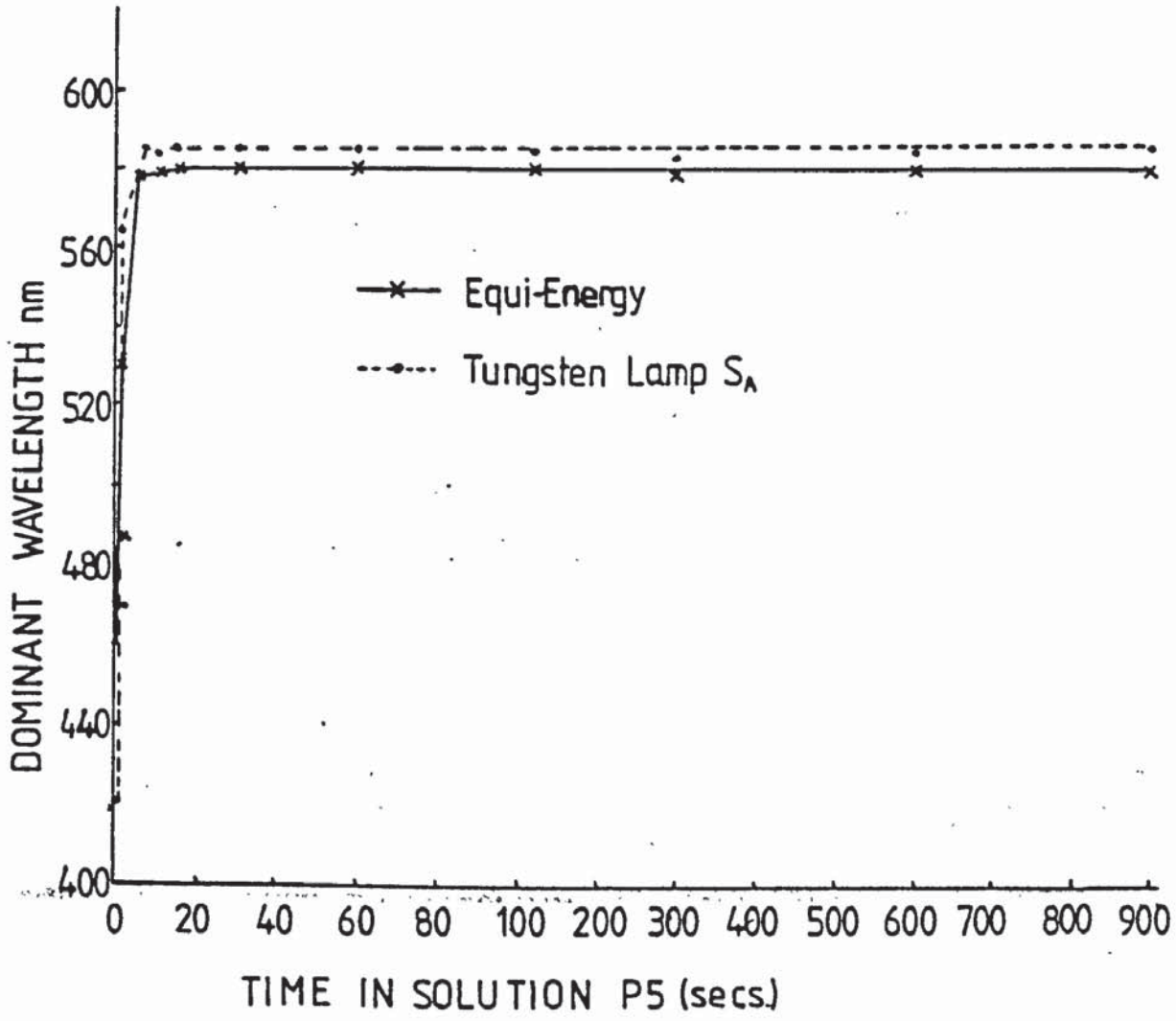

Fig. 8·16

Dominant wavelength v.alues for solution P5 (6 µm diamond surface)

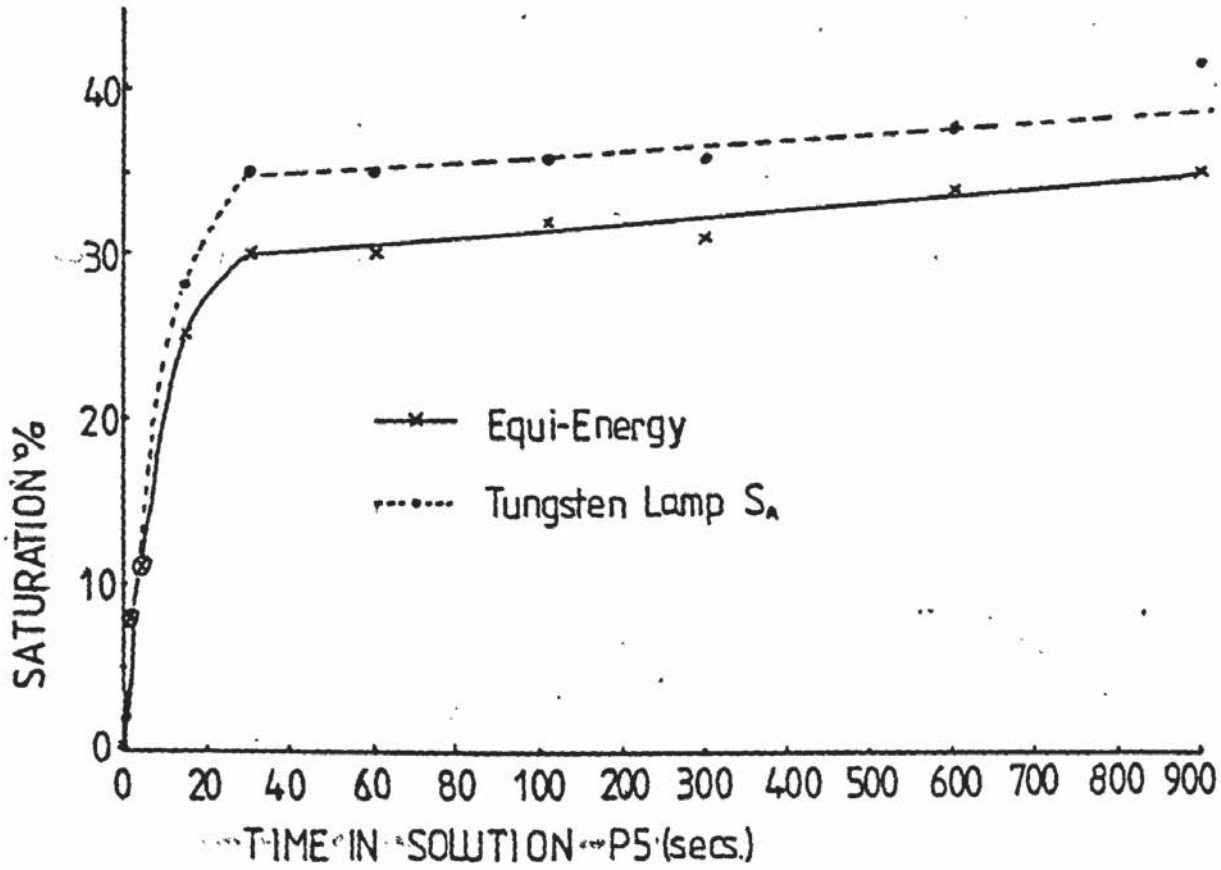

Fig. 8·17

Saturation values for solution P5 (6 μm diamond surface)

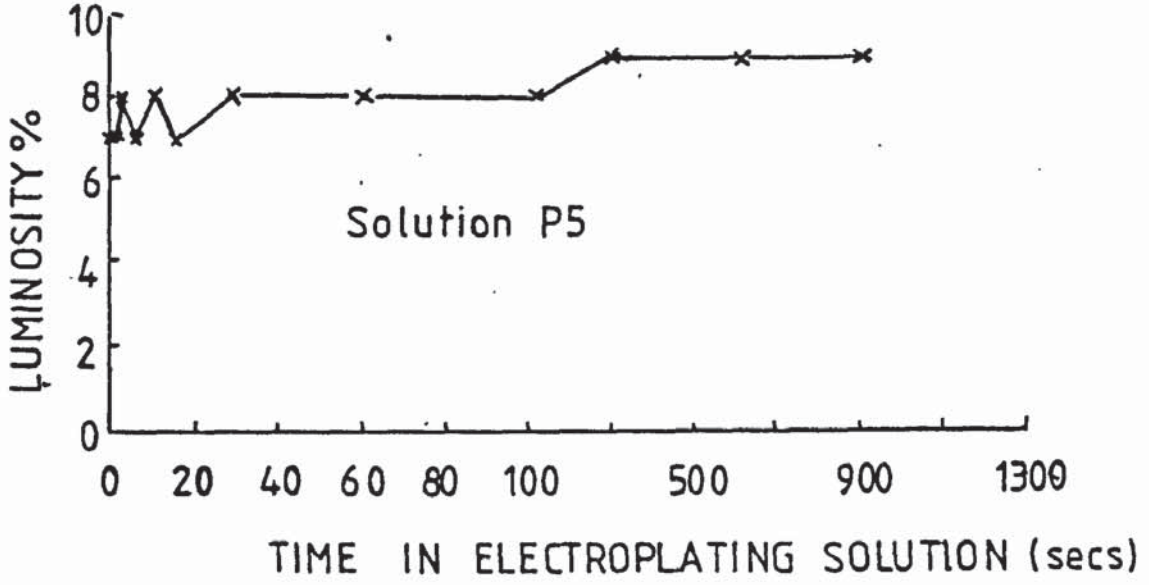

Fig. 8·18

Luminosity values for discs electroplated in solution P5 (6 μm diamond surface)

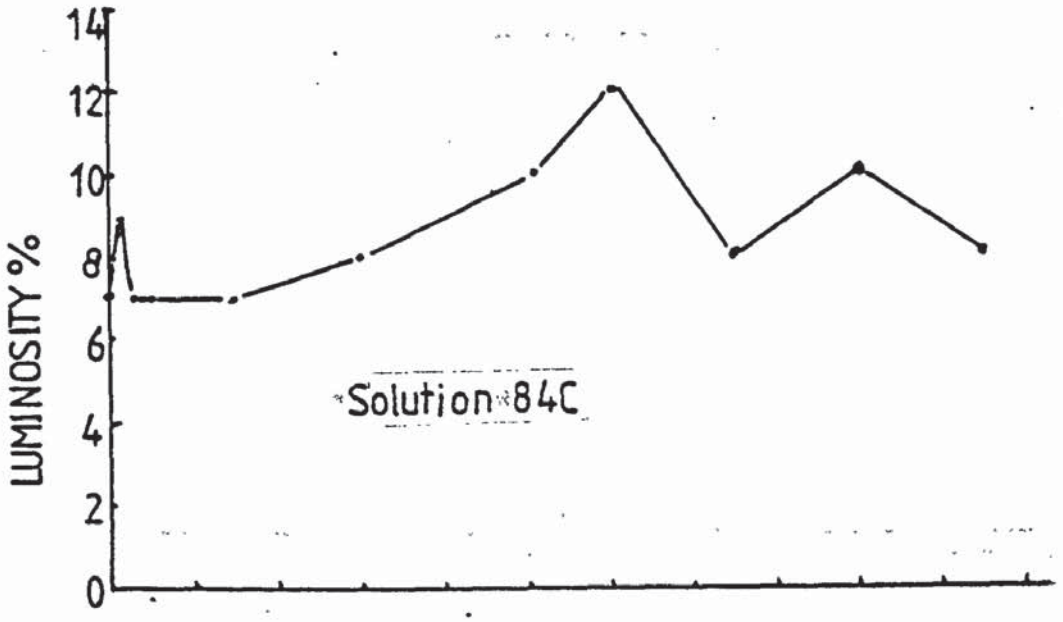

Fig. 8·21

Luminosity values for solution 84C (6 μm diamond surface)

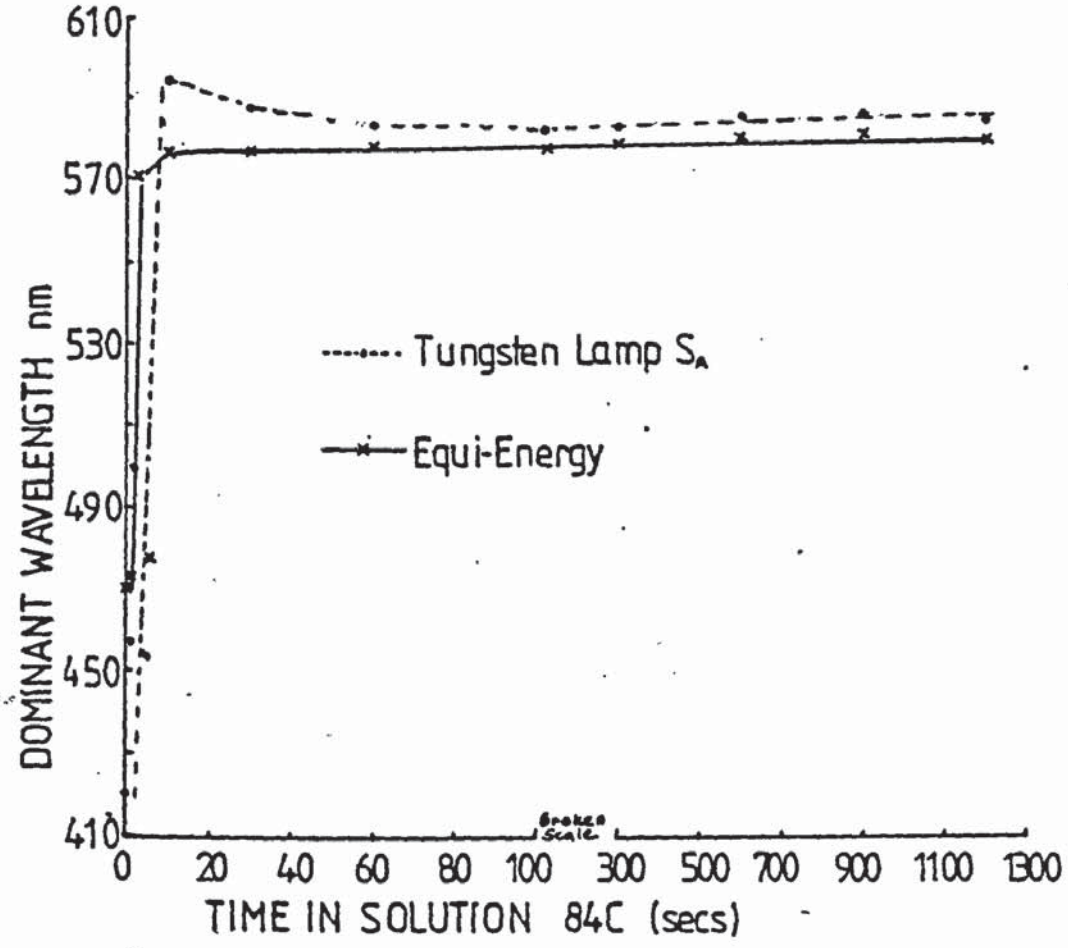

Fig. 8·19

Dominant wavelength values for solution 84C (6 μm diamond surface)

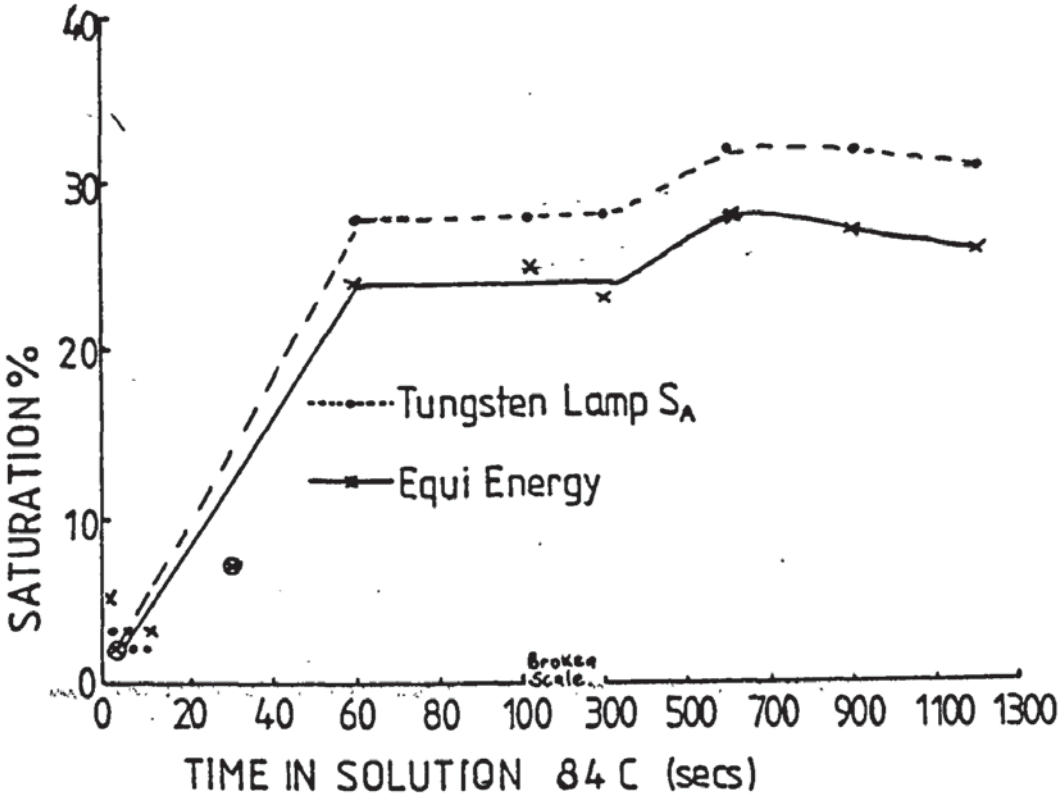

Fig. 8·20

Saturation values for solution 84C (6 μm diamond surface)

(Fig. 8·21) exhibiting an ascending trend from 7% to 13% over the time period 0-300 seconds. Thereafter the values were rather scattered but with a descending trend.

8·4 COMPARISON OF THE EQUI-ENERGY AND TUNGSTEN LAMP RESULTS

8·4·1 The Chromaticity Coordinates

The general shape of the x, y and z value graphs were very similar for both conditions, except that the x and y values were numerically higher for tungsten lamp conditions and the z value was lower.

8·4·2 Dominant Wavelength, Saturation and Luminosity Values

In both solutions it was found that the dominant wavelength graphs followed similar trends with the stable tungsten lamp values being approximately 6 nm higher than the equi-energy values, although in the 84C solution two values exhibited a slightly greater difference. In general then it can be said that the colours appeared to be slightly more orange under tungsten lamp illumination, and that both baths followed a similar pattern. The colours appeared to be approximately 4% more saturated under tungsten lamp, but luminosity values were almost identical under both conditions.

8·5 COMMENT

Assessment of stable colour is based upon stable values for the x, y and z coordinates and it was found this occurred at different time periods for the two solutions. If we examine the thickness factors

for the two solutions we find that the actual thicknesses at which stability was obtained were very similar, i.e. approximately 0·06 μm to 0·07 μm.

The stable chromaticity coordinates are somewhat different for the two baths, the average values being given in Table 8·3:

Solution	Average Stable Chromaticity Coordinates			Illuminant
	x	y	z	
P5	0·390	0·371	0·229	Equi-energy
84C	0·374	0·373	0·253	Equi-energy
P5	0·494	0·420	0·086	Tungsten lamp
84C	0·482	0·420	0·098	Tungsten lamp

Table 8·3 Average stable chromaticity coordinates

Under equi-energy conditions the colour obtained from solution P5 contained more red and less blue than the colour obtained from solution 84C. This was also borne out under tungsten lamp illumination but in a less marked fashion. Furthermore the colour appeared to contain more red and green and less blue in both solutions under tungsten lamp conditions. This confirms the indications from the reflectivity curves.

It was noticed that in both solutions slight changes occurred in the parameters in the thicker deposits and it is believed that this is because initially the colour changes due to the original nickel being covered as the gold continues to grow epitaxially, and as the

deposit grows thicker it will tend to become pseudomorphic, i.e. to be more influenced by its own crystal structure and by the solution. Even so the changes are only minor.

Taking all the parameters examined together it appears that solution 84C required twice the electroplating time of P5 but thickness measurements showed that this referred to approximately the same quantity of gold. The reflectivity values measured were surprisingly low (in the region of 10%) and these conformed as expected with the luminosity values.

8·6 THE EFFECT OF PRETREATMENT ON THE HIDING POWER OF P5

8·6·1 Introduction

The object of this series of experiments was to determine if the original surface quality had any effect on the hiding power of bath P5. Thus a series of discs machine lapped to 600 grit was prepared and each disc electroplated with a different quantity of gold. The results of these experiments are given in Table 8·4A-B and Figs. 8·22-8·23.

8·6·2 Appearance of the Discs

The first gold thickness (0·035 µm) was greyish-buff in colour and was not gold-like. At 0·0525 µm the deposit was definitely gold in appearance but it looked thin, shadows of nickel being visible. When a thickness of 0·1225 µm was present, the deposit was an attractive smooth yellow, and this description was given to the end

(contd.p.240.)

Disc No.	Solution	Time (s)	Calculated Thickness (μm)	Description
96	P5	15	0·035	Smooth greyish-buff
150	P5	30	0·0525	Smooth yellow, looks thin
99	P5	60	0·1225	Smooth yellow
151	P5	120	0·2888	Smooth yellow
124	P5	250	0·5075	Smooth yellow
98	P5	490	1·155	Smooth yellow

Table 8·4A

Disc No.	Chromaticity Coordinates Equi-Energy			Equi-Energy		
	x	y	z	DW	S%	L%
96	0·373	0·369	0·258	579	22	37
150	0·405	0·385	0·210	582	37	47
99	0·419	0·394	0·187	582	44	46
151	0·418	0·392	0·190	582	43	47
124	0·413	0·395	0·192	581	42	53
98	0·411	0·395	0·194	580	42	57

Table 8·4B

Optical Properties of Bright Gold Deposits on 600 Grit Finished Discs

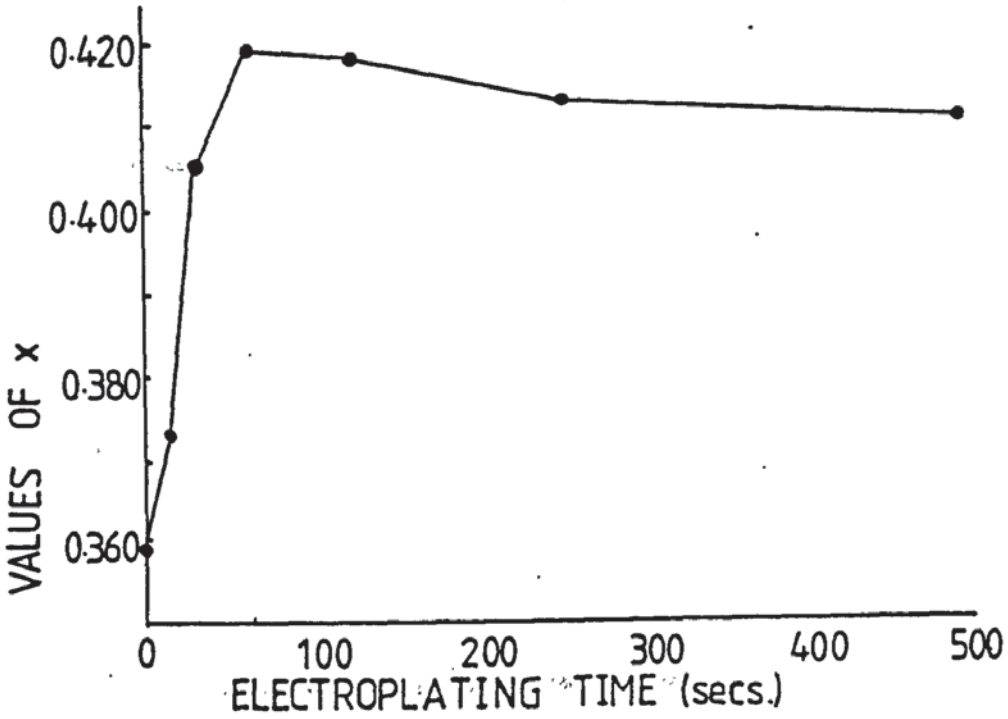

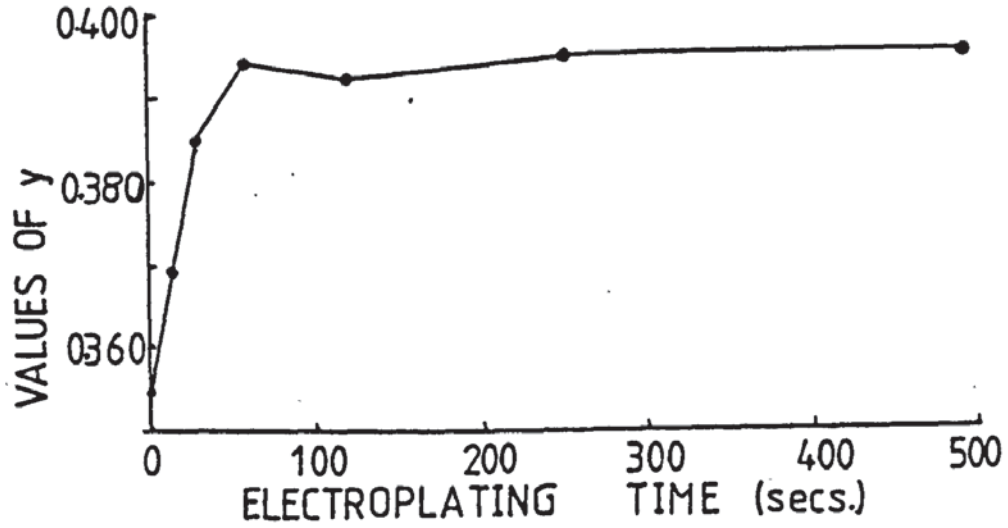

Fig. 8·22a and b

Equi-energy coordinates (x and y) for solution P5 (600 grit surface)

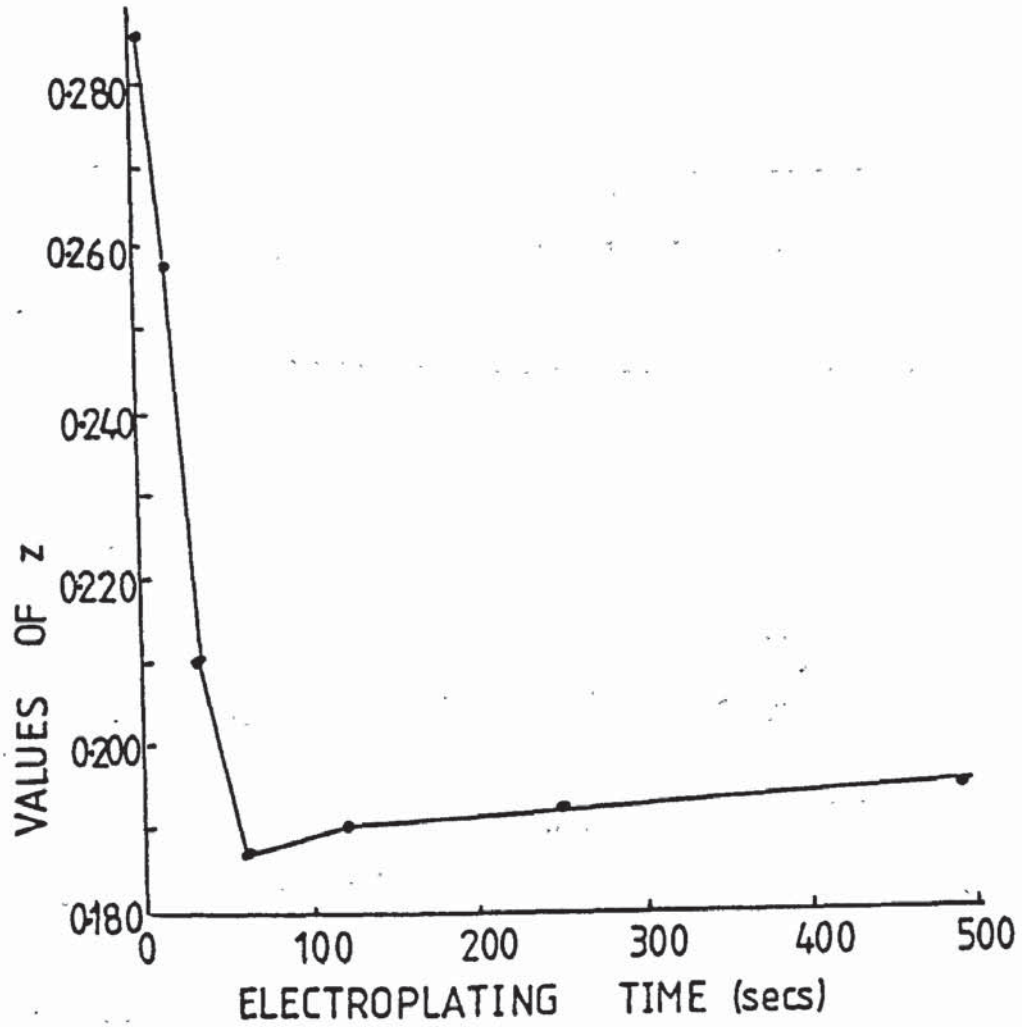

Fig. 8·22c

Equi-energy coordinates (z) for solution P5 (600 grit surface)

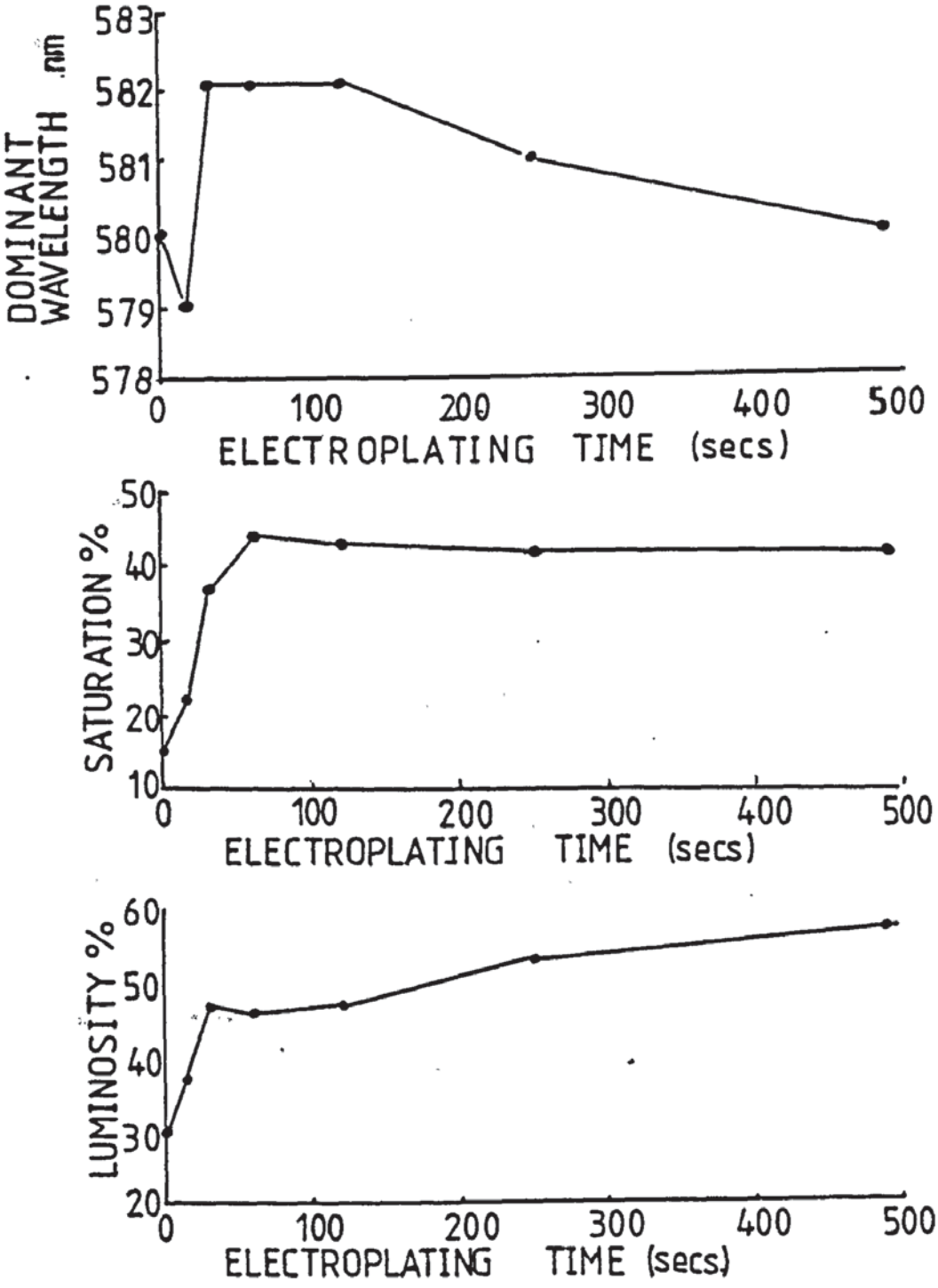

Fig. 8·23(a-c)

Optical properties for solution P5 (600 grit surface)

of the series (1·155 μm).

8·6·3 Optical Properties

8·6·3·1 The Chromaticity Coordinates

The equi-energy coordinates given in Fig. 8·22a-c 22a-c show that relative colour stability is achieved at a thickness of gold of 0·1225 μm, after which the x value decreased slightly with thickness while the z value increased slightly.

8·6·3·2 Dominant Wavelength, Saturation and Luminosity

Dominant wavelength stability was achieved at a thickness of 0·0525 μm and was maintained up to 0·29 μm after which it again fell, but it must be emphasised that the spread of dominant wavelength values was only 579-582 nm. Saturation stability was achieved at 0·1225 μm, and luminosity at 0·0525 μm, but this was only relative since luminosity continued to increase slightly with thickness (Figs. 8·23a-c).

8·6·4 Topography of Bright Deposits

Examination of the bright deposits on the SEM showed the surfaces to be featureless except for pre-existing defects (Figs. 8·24 and 8·25).

(contd. 242.)

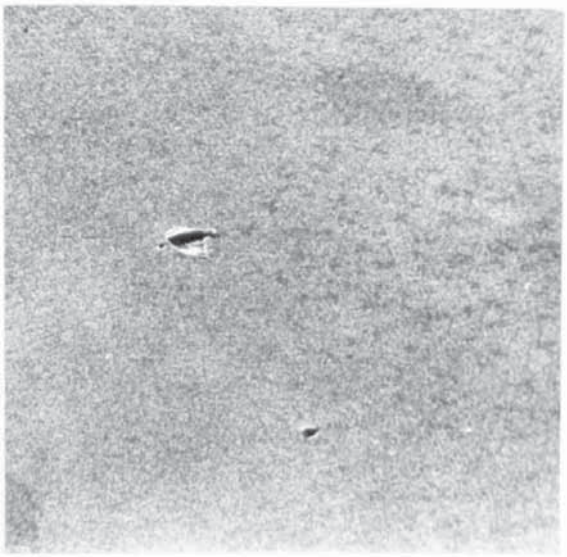

Fig. 8·24

No. 67 10 sec electroplate 500 X

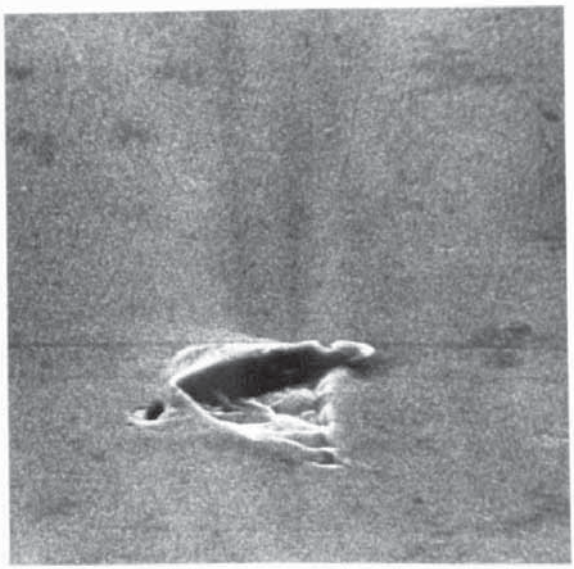

Fig. 8·25

No. 67 2K

CHAPTER 9

PRELIMINARY EXPERIMENTS ON THE GOLD-INDIUM SYSTEM

9·1 INTRODUCTION

In this series of experiments it was decided to investigate the gold-indium system to determine if it were possible to obtain a blue gold by electrodeposition. A blue inter-metallic compound, $AuIn_2$, is known to exist, and it was considered possible that this might be the basis of a blue colouration in the electrodeposit. It must be emphasised that these experiments were intended to indicate possibilities and not to investigate the system fully; this could well form the basis of future work. In the first part of the work indium was added to the basic gold solution and subsequently gold was added to a basic indium solution.

9·2 THE ADDITION OF INDIUM TO A GOLD ELECTROPLATING BATH

9·2·1 Electroplating of Discs

The experimental results, solutions used and electroplating conditions are given in Table 9·1.

Two sets of four discs were prepared, one set finished to 600 grit and the other to 6 μm diamond. After electroplating, those discs finished to 600 grit appeared to be lighter in colour than those finished to 6 μm diamond, and except for the final disc (4 g/dm^3 In) the 6 μm diamond discs were brighter and smoother than the 600 grit discs, which were matt. To the naked eye there appeared to be little difference in colour recorded when 0·1 g/dm^3 of indium was added to the bath, but when 1·0 g/dm^3 was added the immediate comment was that the discs exhibited the suspicion of a greenish tinge, and the final

(contd. p. 246.)

Sample No.	Solution Used	Description	Notes
104	Bath X	Clear yellow colour - bright	Disc polished to 6 µm diamond
109		Clear yellow colour - matt	Disc lapped to 600 grit
Strip 1		Clear yellow colour all over	
102	Bath X + 0·1 g/dm^3 indium as chloride	Clear yellow colour - bright	Disc polished to 6 µm diamond
41		Clear yellow colour - matt	Disc lapped to 600 grit
Strip 2		Clear yellow colour all over	
110	Bath X + 1 g/dm^3 indium as chloride	A suspicion of a greenish tinge	Disc polished to 6 µm diamond. Solution became opalescent
107		As above but matt, slight blue stains on reverse	Disc lapped to 600 grit
Strip 3		A paler yellow colour than S2. Constant colour all over	
101	Bath X + 4 g/dm^3 indium as chloride	Greenish khaki not bright. Blue stains on reverse	Disc polished to 6 µm diamond. Solution became cloudy
106		As above. Blue stains on reverse	Disc lapped to 600 grit
Strip 4		Green matt, blue stains on reverse	
S5		Brighter than S4. Greenish bronze colour	Solution as for S4 but 80 g/dm^3 dextrose added
S6		Pale greenish yellow	As S5 but current = 0·02 amps

Table 9·1A - Addition of indium to gold electroplating bath

Basic solution : Bath X ; Strip and Disc conditions : 65°C, 2·5 asd, for 5 minutes

Sample No.	Chromaticity Coordinates					
	Equi-Energy			Tungsten Lamp S_A		
	x	y	z	x	y	z
104	0·429	0·391	0·180	0·523	0·414	0·063
109	0·458	0·401	0·141	0·540	0·413	0·047
102	0·421	0·388	0·191	0·516	0·416	0·068
41	0·418	0·371	0·211	0·518	0·405	0·077
110	0·428	0·394	0·178	0·521	0·416	0·063
107	0·452	0·407	0·141	0·536	0·416	0·048
101	0·384	0·385	0·231	0·488	0·422	0·090
106	0·400	0·387	0·213	0·501	0·419	0·080

Table 9·1B

Sample No.	Equi-Energy			Tungsten Lamp S_A		
	DM nm	S%	L%	DM nm	S%	L%
104	584	45	31	589	51	33
109	585	57	48	590	63	51
102	583	43	21	588	49	22
41	587	36	35	594	43	37
110	583	46	35	589	52	37
107	584	58	40	589	62	43
101	578	31	27	582	34	27
106	580	35	16	587	39	17

Table 9·1C

DM : Dominant wavelength
S : Saturation
L : Luminosity

addition (4 g/dm^3 In) produced a khaki colouration. The electroplated discs are shown in Fig. 9·1. It was noticed that when the Lacomit stopping-off medium was removed, thin, patchy blue deposits were present on the back of some of the discs, where solution had obviously seeped under the lacquer. The discs affected in this way were those from the 1·0 and 4·0 g/dm^3 indium (both types of finish) with the higher indium content exhibiting the most definite blue colouration. Fig. 9·2 illustrates the type of blue colouration produced.

9·2·2 Bent Cathodes

In order to assess whether or not a blue colour was possible at extremes of current density not obtaining on the discs, bent cathodes, as previously described, were prepared, and these are illustrated in Fig. 9·3. Examination of the L-shaped cathodes did not show any area of blue, indeed the colours were very even over the whole range and were very similar to those obtained on the discs for the same bath compositions. Blue stains were obtained beneath the stopping-off medium on the highest indium content tried (4 g/dm^3). An un-stopped off disc electroplated in this final solution at a very low overall current density (0·17 rather than the normal 2·5 asd) gave a shiny greenish-bronze colour with a few dark marks. The dark marks were probably due to the thinness of the deposit. There was no sign of any blue colouration. Since during the course of these experiments it had been noticed that the solution became opalescent on the addition of 1·0 g/dm^3 of indium, and cloudy on the addition of 4·0 g/dm^3, it was decided to add 80 g/dm^3 of dextrose, such as is added to an indium

(contd. p. 249.)

Fig. 9·1

Discs electroplated in an indium containing gold solution

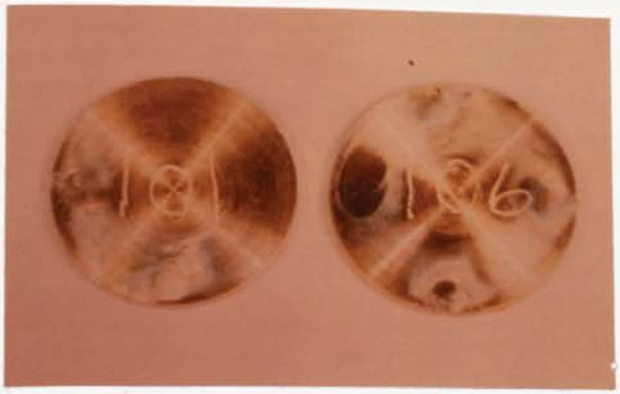

Fig. 9·2

The backs of selected discs

Fig. 9·3

The Bent Cathodes

Fig. 9·3b

Under the Lacomit of bent cathode S4

electroplating bath as a complexing agent. This cleared the cloudiness but there was no sign of any blue colouration, although the greenish-bronze deposit was smooth and semi-bright.

9·2·3 Optical Measurements on Discs

9·2·3·1 The Reflectivity Curves

Since reflectivity curves show some reflection at each wavelength it is not possible to judge changes in colour by examination of the curves, but nevertheless some observations may usefully be made. Up to 1·0 g/dm^3 of indium, all the curves are of the expected "gold shape", that is, a pronounced step was obtained in the reflectivity curve at a mid-point energy ranging from 3·66 x 10^{-19} J (In = 0), to 3·96 x 10^{-19} J (In = 4 g/dm^3) for the diamond finished samples and from 3·56 x 10^{-19} J to 3·76 x 10^{-19} J for the grit finished samples (Fig. 9·4). Fig. 9·5 indicates that for both types of surface the mid-step energy moved to progressively higher values with increase of indium content in the solution, and that the values for the diamond finished discs were somewhat higher than those for the grit finished samples. A slight anomoly was observed in the grit finished samples for the 0·1 g/dm^3 indium in that a fall in mid-point energy was noted. Fig. 9·4 shows that for the pure gold deposit and the 1·0 g/dm^3 indium deposit the grit finished samples exhibited greater reflectivity at the low energy end, and less reflectivity at the high energy end of the spectrum than the diamond finished samples. In the 0·1 g/dm^3 indium solution, the grit finished disc exhibited higher reflectivity over the whole spectrum, while the grit finished disc from the 4 g/dm^3 indium solution exhibited lower reflectivity over the whole of the

(contd. p. 251.)

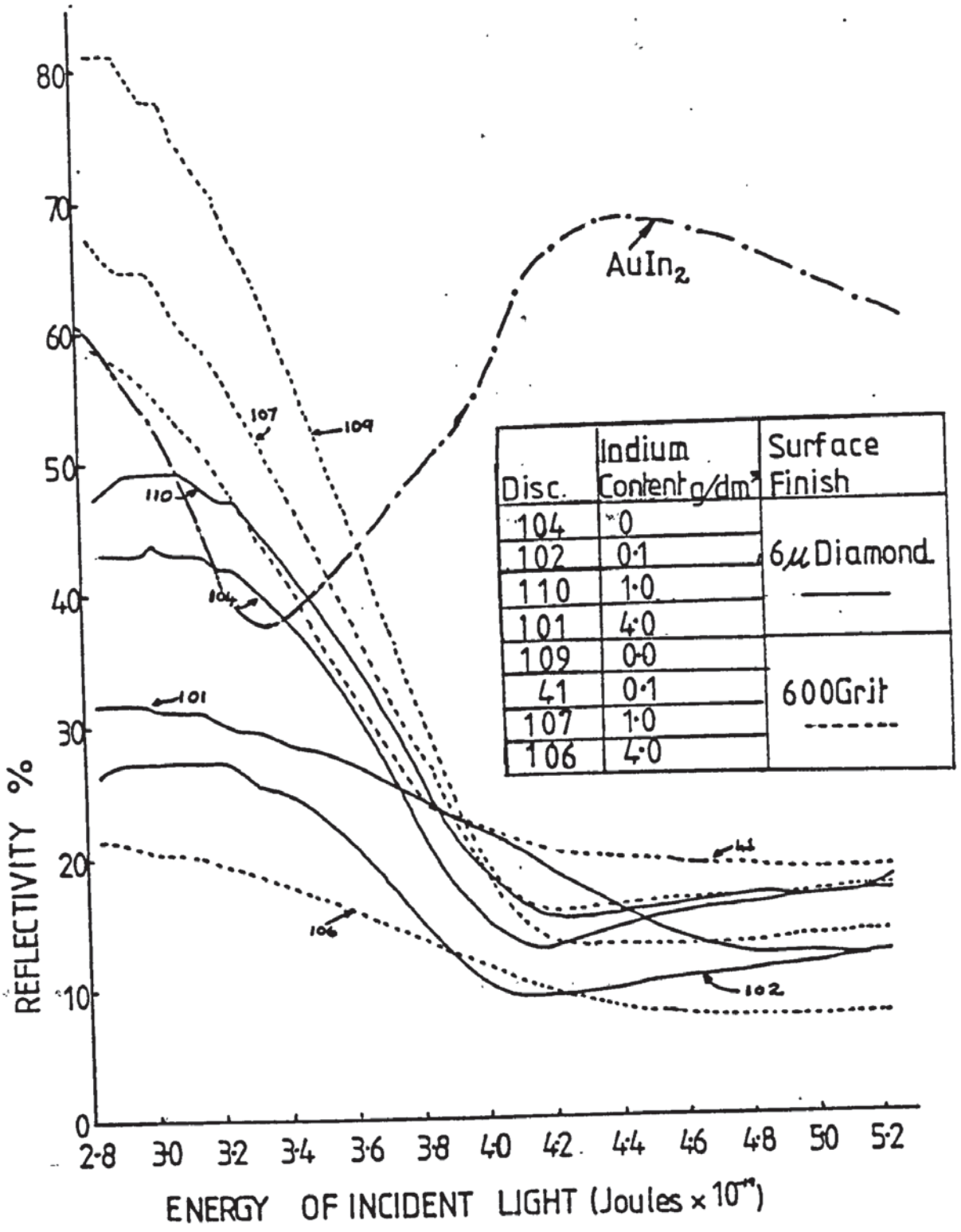

Fig. 9·4

Reflectivity curves for indium containing gold solutions

spectrum.

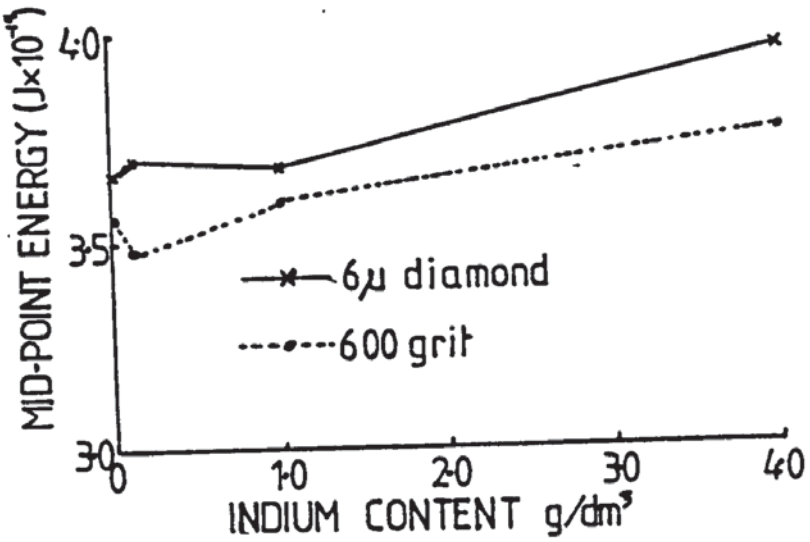

Fig. 9·5

Mid-step energy values for the indium containing gold solutions

None of the reflectivity curves resembled that obtained for $AuIn_2$, given by Saegar and Rodies[44] in which a minima is obtained and in which there is strong reflection for the high energy (blue) end of the spectrum (Fig. 9·4). Thus it would seem that there was no great quantity of $AuIn_2$ in the deposits obtained in this series of experiments.

9·2·3·2 The Chromaticity Coordinates

Since only three different indium contents were tested in this preliminary series of experiments it was not possible to plot the usual type of graph to indicate trends. Thus the x, y values have

been plotted on the relevant portions of the CIE chart (Figs. 9·6 and 9·7). Under equi-energy conditions the chromaticity coordinates listed in Table 9·1 indicate that in the absence of indium, the colour of the disc finished to 6 μm diamond contained less red and green but more blue than that finished to 600 grit. A similar effect was also noticed when the results were related to tungsten lamp conditions except that in this case there was a very small increase in greeness for the 600 grit finished disc. In order to illustrate the effect of the addition of indium + and - signs are included in the table of chromaticity coordinates (Table 9·2) to indicate either increase or decrease in the colour (red, green or blue), when compared to the appropriate indium-free deposit. If the increase or decrease is small, i.e.± 0·005, the sign is preceeded by δ, the absence of a ± sign indicates that there was no change. In all cases there was a decrease in redness and an increase in blueness when 0·1 g/dm of indium was added to the solution. The green parameter was somewhat equivocal, decreases, small in the case of 6 μm diamond being noted under equi-energy conditions, whilst under tungsten lamp conditions a small (δ) increase was noted for the diamond finished surface, with a decrease for the grit finished surface. Unexpectedly when the indium content of the solution was increased to 1·0 g/dm^3 the parameters reverted to being nearer to the original values. Under equi-energy conditions, small (δ) decreases in redness and blueness with a small increase (δ) in greeness for the diamond finished, while the grit finished was characterised by a decrease in redness (only just outside the δ qualifying limit), an increase in greeness and an unchanged blueness factor. Trends were similar for tungsten lamp conditions except that the diamond finished disc exhibited no

(contd p 256)

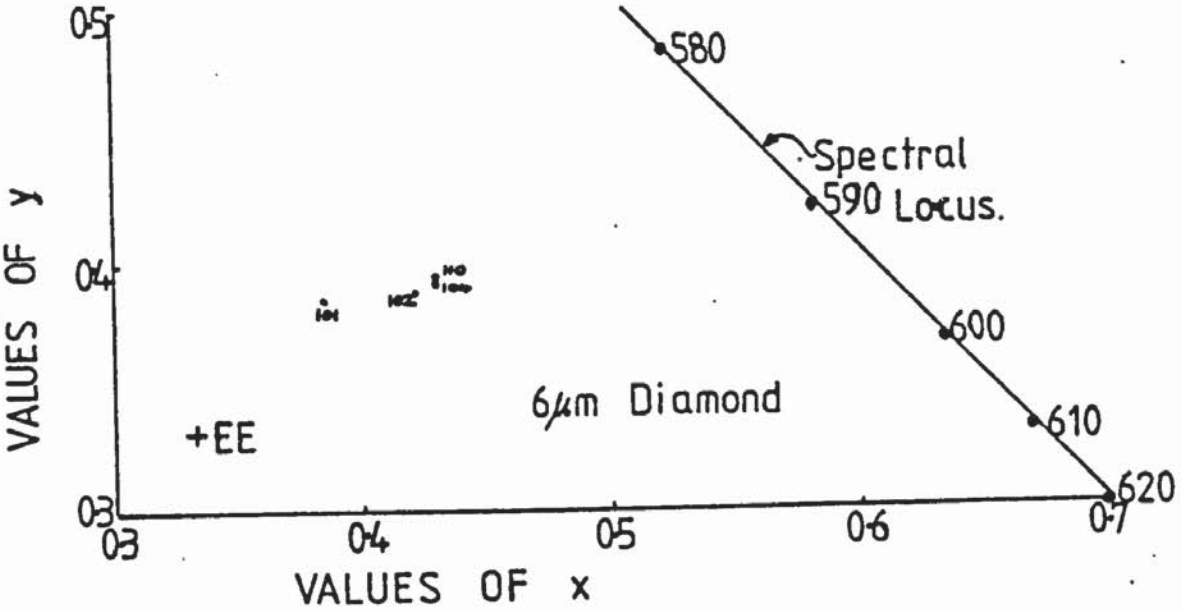

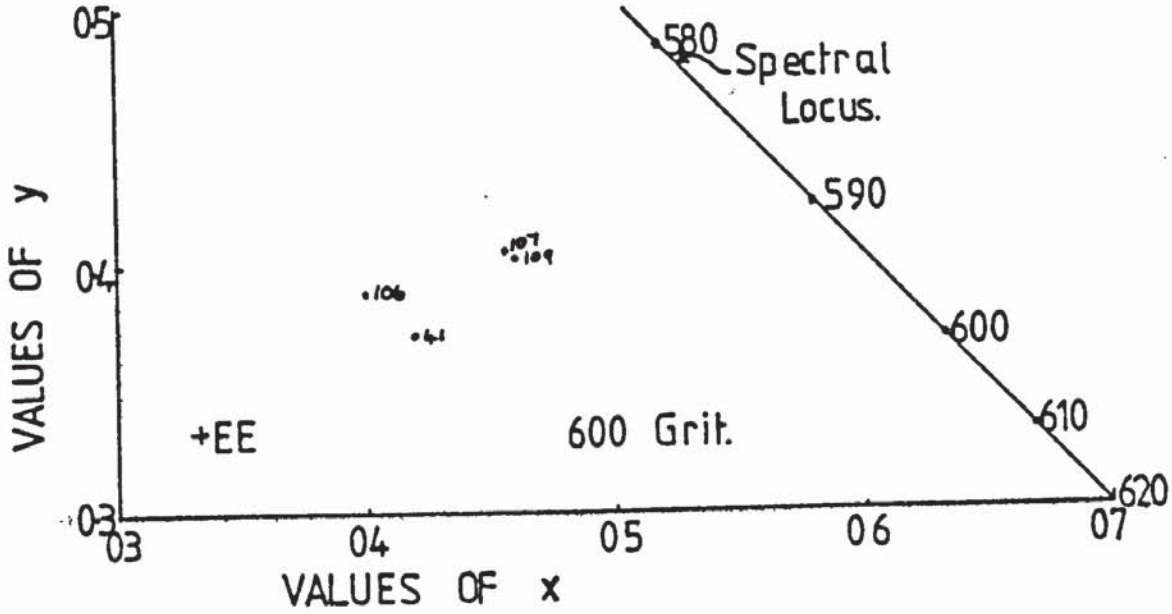

In Added g/dm³	6μm Diamond	600 grit
0	104	109
0·1	102	41
1·0	110	107
4·0	101	106

Fig. 9·6

Chromaticity coordinates (equi-energy) for indium containing gold solutions

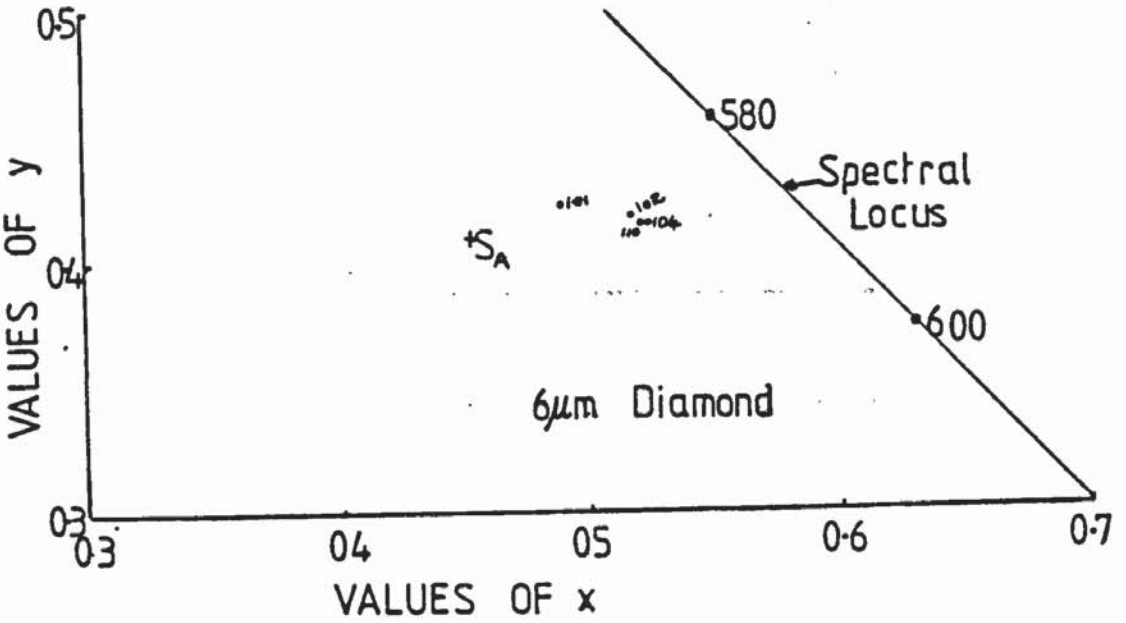

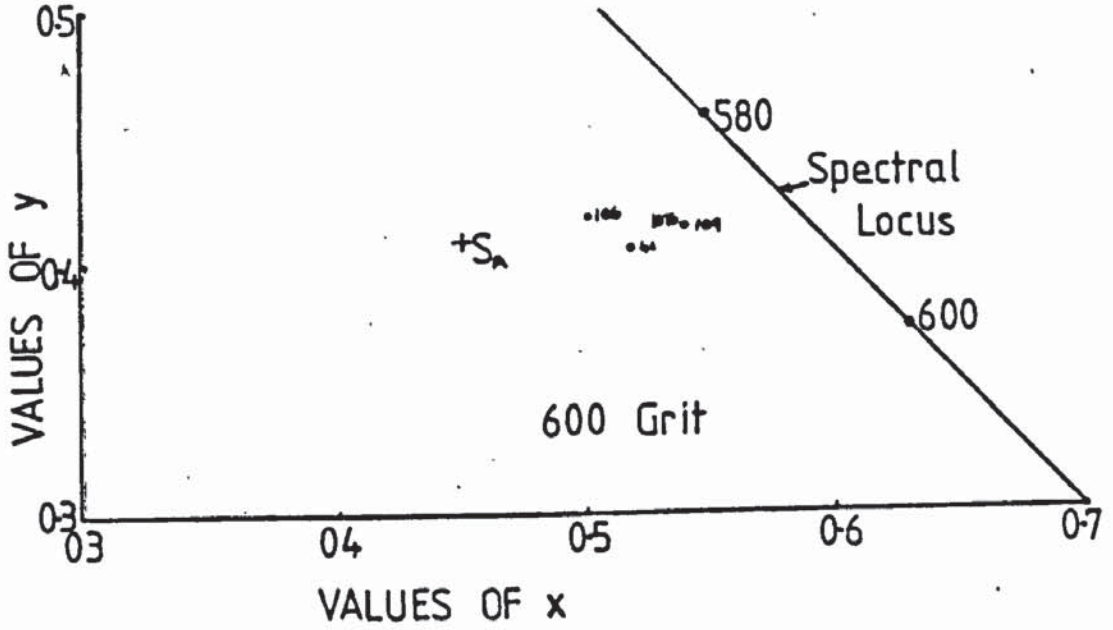

In Added g/dm³	6µm Diamond	600 Grit
0	104	109
01	102	41
10	110	107
40	101	106

Fig. 9·7

Chromaticity coordinates (tungsten lamp S_A) for indium containing gold solutions

Disc No.	Surface Finish	Reference Light Source	x	y	z	Indium Content g/dm^3
104	6 µm diamond	Equi-Energy	0·429	0·391	0·180	0
102	6 µm diamond	Equi-Energy	0·421 −	0·388 δ −	0·191 +	0·1
110	6 µm diamond	Equi-Energy	0·428 δ−	0·394 δ+	0·178 δ−	1·0
101	6 µm diamond	Equi-Energy	0·384 −	0·385 −	0·231 +	4·0
109	600 grit	Equi-Energy	0·458	0·401	0·141	0
41	600 grit	Equi-Energy	0·418 −	0·371 −	0·211 +	0·1
107	600 grit	Equi-Energy	0·452 −	0·407 +	0·141	1·0
106	600 grit	Equi-Energy	0·400 −	0·387 −	0·213 +	4·0
104	6 µm diamond	Tungsten Lamp	0·523	0·414	0·063	0
102	6 µm diamond	Tungsten Lamp	0·516 −	0·416 δ+	0·068 +	0·1
110	6 µm diamond	Tungsten Lamp	0·521 δ−	0·416 δ+	0·063	1·0
101	6 µm diamond	Tungsten Lamp	0·488 −	0·422 +	0·090 +	4·0
109	600 grit	Tungsten Lamp	0·540	0·413	0·047	0
41	600 grit	Tungsten Lamp	0·518 −	0·405 −	0·077 +	0·1
107	600 grit	Tungsten Lamp	0·521 −	0·416 δ +	0·063 +	1·0
106	600 grit	Tungsten Lamp	0·501 −	0·419 +	0·080 +	4·0

Table 9·2

Direction of Colour Change

change in its blueness value while the grit finished gave an increased blueness value albeit of smaller magnitude than that obtained in the 0·1 g/dm solution. It is interesting to note that this general increase in greeness, slight though it was in numerical terms, was detected immediately on removal from the bath, as the experimental record shows. When the indium content of the solution was increased to 4 g/dm^3 there was a very large decrease in redness and a large increase in blueness for both surfaces whether measured with respect to equi-energy or tungsten lamp. Moderate decreases in greeness were exhibited for both surfaces under equi-energy conditions, whilst moderate increases in greeness were obtained under tungsten lamp conditions.

9·2·3·3 Dominant Wavelength, Saturation and Luminosity

In general dominant wavelength values were slightly numerically higher for the grit finished discs, and higher for tungsten lamp than for equi-energy conditions. If we ignore the 0·1 g/dm^3 indium content, Fig. 9·8 shows there is generally a trend of fall in dominant wavelength values, as the indium content of the bath increases, indicating a movement away from the red end of the spectrum.

The colour parameters obtained with an indium content of 0·1 g/dm appeared at first glance to be anomalous, but if we examine them more carefully we see that for the grit finished discs there was a peak in the dominant wavelength values while for the diamond finished samples there was either a fall or a value similar to that obtained for the 1·0 g/dm indium content. Thus it appears that for

(contd. p. 258)

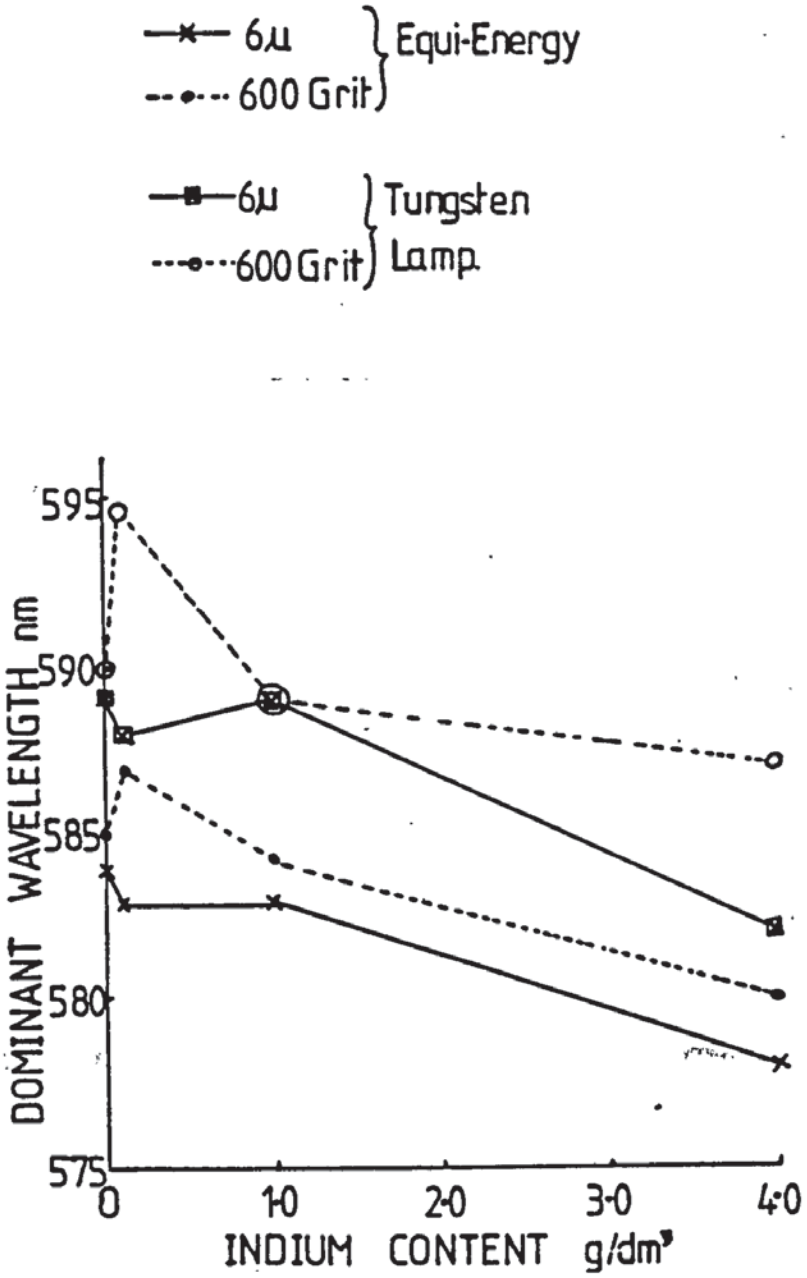

Fig. 9·8

Dominant wavelength values of discs electroplated in indium containing gold solutions

a small indium content the current density was probably the decisive factor. Indirectly surface finish would influence this, since a 600 grit surface would have a much greater surface than the diamond finished sample.

Assessment of saturation and luminosity values was again difficult due to the small number of results available. But Fig. 9·9 shows that ignoring the 0·1 g/dm^3 result there is little change in saturation up to 1·0 g/dm^3 indium but that saturation is considerably decreased at 4 g/dm^3 indium. This is confirmed for both surfaces tried and under both illuminant conditions. In general, the grit finished samples were slightly more saturated than the diamond finished ones, with the values related to the tungsten lamp conditions being slightly more saturated than those related to equi-energy conditions. In all cases a trough in saturation values was obtained at 0·1 g/dm^3 indium, slight in the case of diamond finished samples but more marked in the case of grit finished.

The luminosity values given in Fig. 9·10 show that in the case of diamond finished discs a decrease in luminosity was obtained in the disc from the 0·1 g/dm^3 indium solution followed by an increase for the 1·0 g/dm^3 disc to just above the indium-free value, then a substantial fall for the 4 g/dm^3 sample. The pattern was slightly different for the grit finished samples in that after the initial fall the value rose to near the original level for the 1·0 g/dm^3 disc and then a fall for the final disc (4 g/dm^3). The luminosity values calculated under tungsten lamp conditions followed the same pattern with the values being very slightly higher.

(cont'd.p.260.)

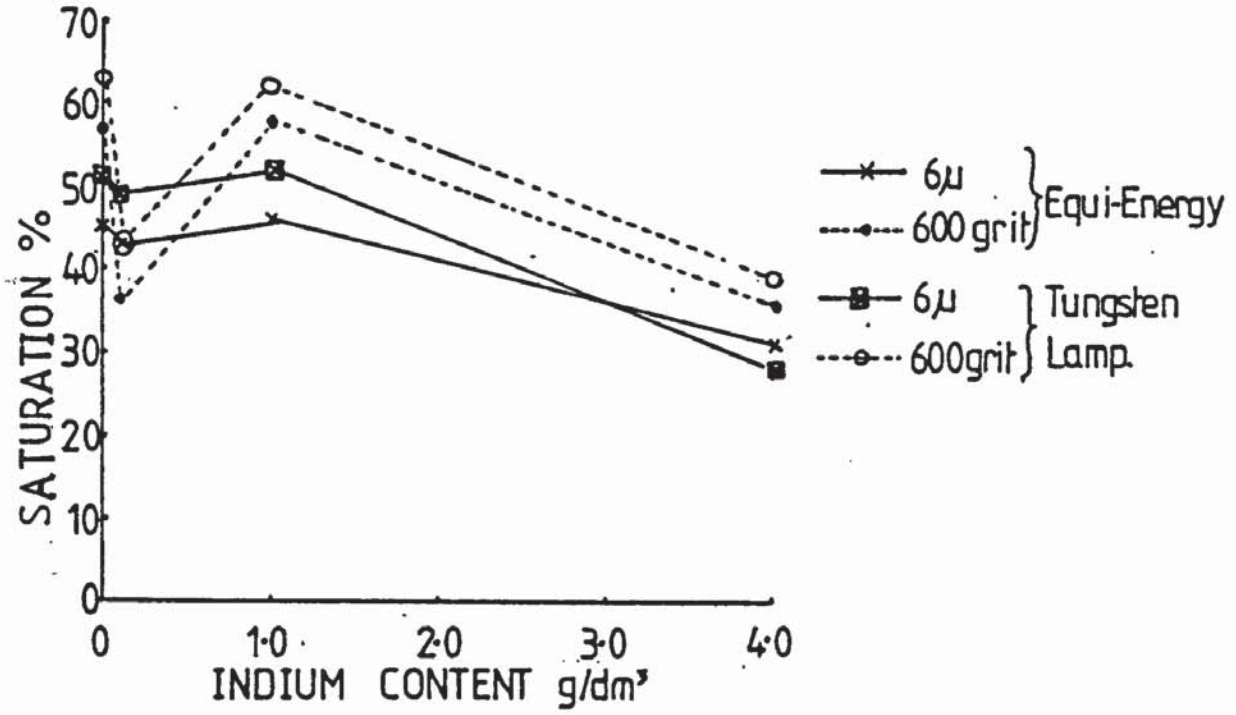

Fig. 9·9

Saturation values for discs electroplated in indium containing gold solutions

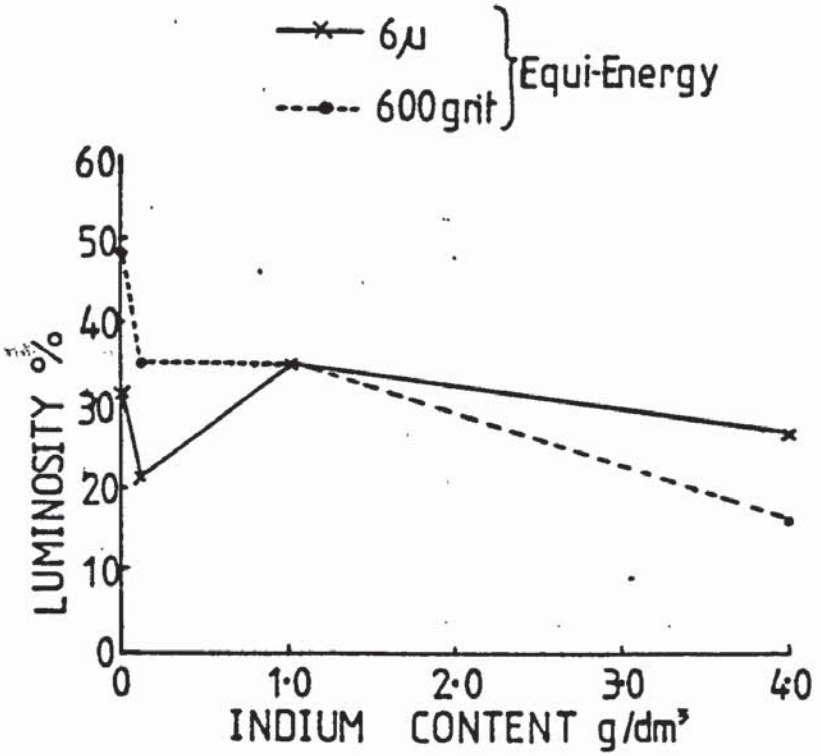

Fig. 9·10

Luminosity values for discs electroplated in indium containing gold solutions

9·3 COMMENT

Although the presence of indium in the solution appeared to move the colour of the gold away from red towards blue, no definite blue colouration was observed, except on the reverse of some of the discs. In view of the fact that this blue deposit was only found where the solution had seeped beneath the stopping off medium, it was considered likely that this deposit might be obtainable at extremely low current densities. Hence it was decided that any further work should be on Hull cell tests so that the effect of current density could be evaluated. In order to conserve solution a miniature Hull cell shown in Fig. 2·3a and described in Chapter 2 was developed.

9·4 HULL CELL TESTS

9·4·1 The First Series of Tests

In the first series of tests 4 g/dm^3 indium as chloride was added to the simple gold bath X, in order that the spectrum of current densities could be investigated in order to establish possible trends.

9·4·1·1 General Appearance of the Plates Produced in Indium-Containing Bath X

The experimental details and test results are given in Table 9·3A-B. Photographs of the plates are given in Fig. 9·11.

The first plate produced (M1) showed three things:

(i) Little change in colour or quality over the whole area of

(contd. p. 264.)

Plate No.	Solution Composition	Current mA	Time mins	Temp. °C	Description	Notes
M1	Bath X. Potassium gold cyanide = 3·75 g/dm^3. Potassium cyanide = 15 g/dm^3 + 4 g/dm^3 indium added as chloride	100	5	63	Colour buff to beige. Blue smudges on reverse side. Marking at low current density end due to stirring.	Solution magnetically stirred
M2	As above	10	5	64	Orange gold with marking on the low CD end. No blue on reverse.	As above but with a smaller follower
M3	As above	10	5	64	Very pale greyish yellow. No blue on reverse.	No stirring
M4	As above	10	10	64	Fawn. No blue on reverse.	No stirring
M5	As above	100	5	64	Greenish fawn.	No stirring
M6	Bath I. Indium as chloride = 15 g/l Potassium cyanide = 140 g/dm^3. Potassium hydroxide = 30 g/dm^3. Dextrose = 30 g/dm^3.	100	5	20	An even white deposit all over the plate and on the back.	No stirring
M7	Bath I. + 0·1 g/dm^3 of gold as cyanide.	100	5	20	An even white deposit A few slight blue stains on reverse.	No stirring
M8	Bath I. 0·29 g/dm^3 gold as cyanide	100	5	20	An even white deposit. A few blue stains on water-line on reverse	No stirring

Table 9·3A

Gold-indium Electroplating of Hull Cell Plates

Table 9·3A (continued)

Plate No.	Solution Composition	Current mA	Time mins	Temp. °C	Description	Notes
M9	Bath I. 0·35 g/dm^3 gold added as cyanide	100	5	20	Dark grey rough. Dark metallic when polished. A suspicion of blue stain on reverse	No stirring
M10	As above	100	5	20	As above	No stirring
M11	As above	100	5	20	Dark and rough but a little more blue	Stirred as M2
M12	As above	10	5	20	Dark blue streaks	No stirring

Table 9·3B

Sample No.	Chromaticity Coordinates						Equi-Energy			Tungsten Lamp S_A		
	Equi-Energy			Tungsten Lamps								
	x	y	z	x	y	z	DM nm	S %	L %	DM nm	S %	L %
M1	0·381	0·375	0·244	0·488	0·417	0·095	580	27	18	585	29	19
M2	0·430	0·386	0·184	0·525	0·410	0·065	585	44	23	592	49	24
M3	0;364	0·360	0·276	0·476	0·413	0·111	583	17	29	587	22	30
M4	0·378	0·366	0·256	0·468	0·414	0·100	582	23	16	587	26	17
M5	0·369	0·368	0·263	Front 0·478	0·417	0·105	582	21	16	583	24	17
	0·302	0·314	0·384	Back 0·421	0·402	0·177	483	10	15	483	8	14
M6	0·323	0·326	0·351	0·442	0·404	0·154	482	3	40	480	2	39
M7	0·317	0·324	0·359	0·435	0·405	0·160	483	5	41	482	4	40
M8	0·316	0·322	0·362	0·434	0·404	0·162	483	5	43	483	4	43
M9	0·319	0·322	0·359	0·438	0·403	0·159	480	5	8	477	3	8
M10	0·316	0·327	0·357	0·433	0·408	0·159	488	6	19	487	4	19
M11	0·314	0·321	0·365	0·432	0·404	0·164	488	7	8	483	4	8
M12	0·288	0·300	0·412	0·406	0·397	0·197	481	17	6	482	11	6

DM : Dominant Wavelength ; S : Saturation ; L : Luminosity

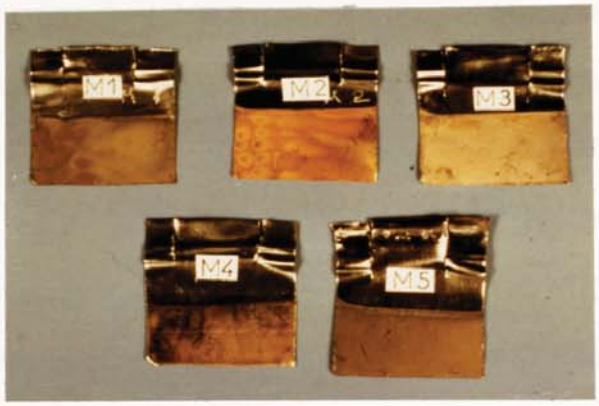

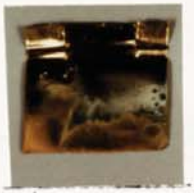

M1 Back

M5 Back

Fig. 9·11

Hull cell plates produced in indium containing gold solutions

the plate.

(ii) Circular markings were present on the low current density end of the plate, obviously associated with the holes in the cell and the flow of solution via these holes, induced by the magnetic stirrer.

(iii) Blue markings on the reverse of the plate.

Thus it was decided that the current density should be reduced for the second plate (M2), and that a smaller follower should be used for the magnetic stirrer. This change in conditions gave a warm gold colour over the whole plate, with flow marking still present on the low current density end of the plate. No blue marking was observed on the reverse of the plate. The third plate, which was a

repeat of M2 with stirring ommitted, gave a pale greyish yellow with no blue on the reverse. When the electroplating time was doubled to 10 minutes (M4) with other conditions remaining the same there was little change in result. The final plate in this series reverted to the original conditions except that there was no stirring. A greenish-fawn matt deposit was obtained, with a very definite blue deposit on the reverse.

9·4·1·2 The Reflectivity Curves

Since the Hull cell plates varied little in appearance over the whole range of current density, it was considered worthwhile to carry out colour measurements, selecting the centre of the plate as the test area. The reflectivity curves given in Fig. 9·12 show that the plate which had the most gold-like colour gave a reflectivity curve of the form associated with gold in previous tests, i.e. a step in the energy curve with a mid-point energy of $3{\cdot}5 \times 10^{-19}$ Joules. This was obtained with plate current of 10 mA with moderate stirring. A plate (M3) produced in the same way but without stirring gave an entirely different reflectivity curve, a very much shallower curve with a very poorly defined step being obtained. Rather similar shaped curves were obtained when the electroplating time was doubled (M5) except that in this case the actual reflectivity values were numerically lower. Again when the current was increased 10 times the shape of the curve was of similar form. These shallow curves all indicated colours described as fawn or greenish fawn. The back of plate M5 gave a reflectivity curve entirely different in character to any of the others, in that a shallow curve was evident

with the highest reflectivity at the high energy (blue) end of the spectrum.

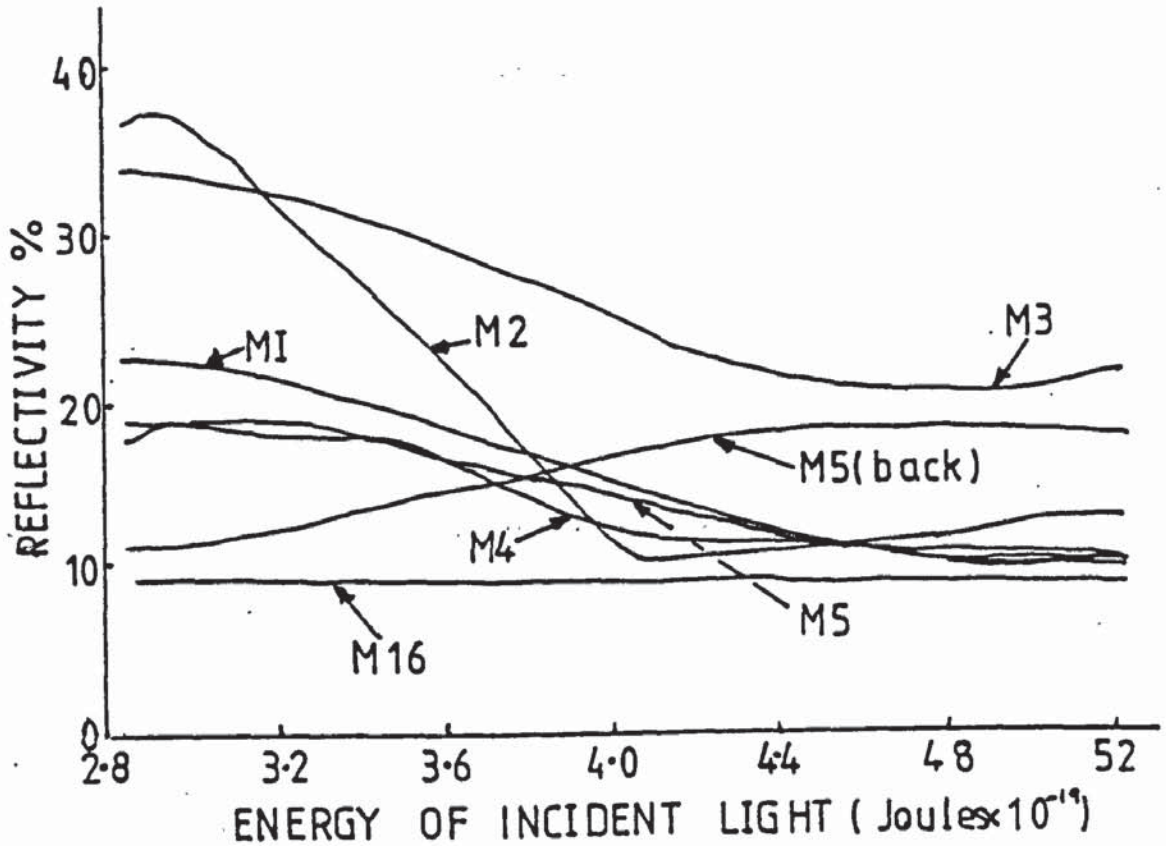

Fig. 9·12

Reflectivity curves for Hull cell plates produced in indium containing gold solutions

9·4·1·3 The Chromaticity Coordinates

When plotted on the chromaticity chart (Fig. 9·13) the obviously gold-coloured plate M2 was tending towards the yellow-orange part of the chart whilst those described as buff, beige, or greenish-fawn veered towards the green direction comparatively speaking. The

(contd. p. 268.)

Fig. 9·13

Chromaticity Coordinates for Hull cell plates (EE)

back of plate M5 on which a blue stain present was very definitely located in the blue direction of the chart. Similar trends were observed for coordinates calculated with respect to tungsten lamp conditions (Fig. 9·14).

9·4·1·4 Dominant Wavelength, Saturation and Luminosity

Dominant wavelength values supported the findings of the chromaticity coordinates, in that the value for M2 was nearer to the red end of the spectrum than the other samples and that the back of M5 (in the vicinity of the blue stain) was nearer to the blue end of the spectrum. Saturation values varied between 17 and 44%, with the gold-coloured plate exhibiting the highest value. Luminosity varied between 14 and 30% with the pale greyish yellow deposit of M3 having the highest value.

9·4·1·5 Comment

Previous results had shown the presence of a blue deposit and it was hoped to establish the current density range by the preliminary Hull cell tests. There was no sign of this on the plates but only on the reverse of some of them. It was considered possible that this was not necessarily a function of current density but perhaps of replenishment of the catholyte in the thin film of solution between the back of the plate and the cell, and that when the relative quantities of gold and indium were favourable then an intermediate intermetallic compound resulted. Thus it was decided to start with an indium electroplating solution and to add gold to this.

(cont'd. p.270.)

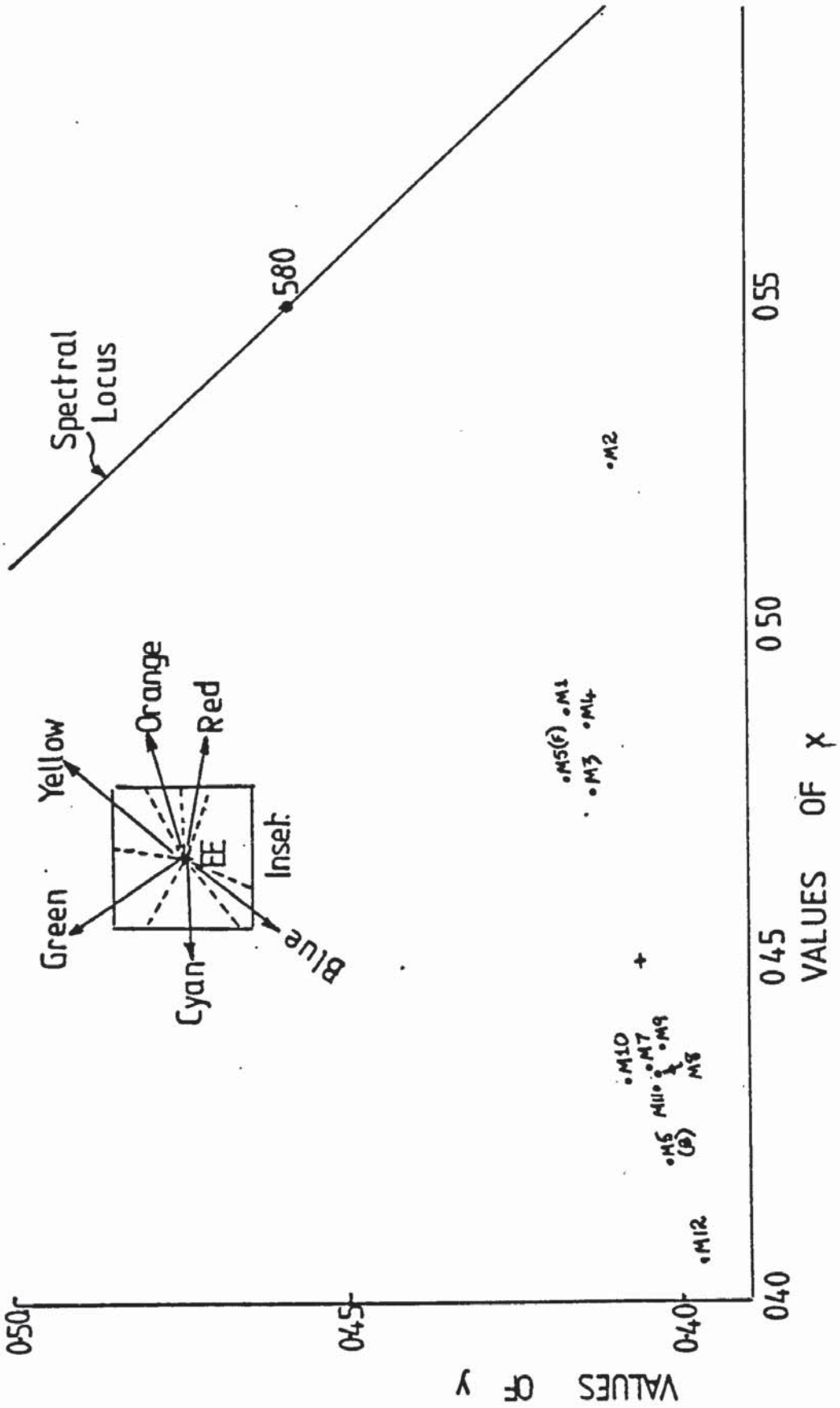

Fig. 9·14

Chromaticity coordinates for Hull cell plates (S_A)

9·4·2 The Second Series of Hull Cell Tests

In this series of tests gold was added to an indium electroplating solution, and the results of the experiments are given in Table 9·3A-B. Photographs of the plates are given in Fig. 9·15.

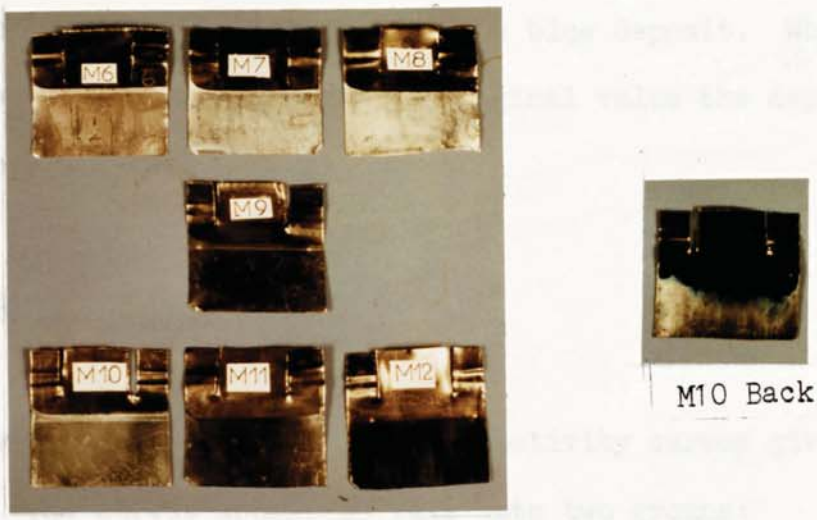

Fig. 9·15
Hull cell plates produced from a gold containing indium solution

9·4·2·1 The Appearance of the Hull Cell Plates

The gold-free indium solution produced a white, smooth deposit over the whole plate. The throwing power of the solution must have been excellent, since the back of the plate was also covered with a

similar deposit. There was no sign of any blue stains. The addition of 0·1 g/dm^3 of gold produced no visible change except that there were a few blue stains on the reverse associated with bubbles on the water-line. Increasing the gold content to 0·2 g/dm^3 gave a similar result. The deposit became dark grey and rough when 0·35 g/dm^3 of gold was added and this became dark and lustrous when polished. There were a few thin blue stains on the reverse plus a sizeable area of gold-coloured deposit. Stirring this solution gave a similar result with perhaps a very slightly more blue deposit. When the cell current was cut to one-tenth of its original value the deposit consisted of dark blue streaks.

9·4·2·2 The Reflectivity Curves

No energy steps are present in the reflectivity curves given in Fig. 9·16. The curves appear to fall into two groups:

(i) Plates with low reflectivity over the whole spectrum with slightly higher reflectivity at the high energy (blue) end. These plates comprised those from the highest gold content tested (0·35 g/dm). Those electroplated at 100 mA were designated dark and rough and exhibited very similar curves. The plate which was designated "blue-streaked" (10 mA) showed comparitively less reflectivity at the low energy (red) end of the spectrum.

(ii) Plates with moderate reflectivity over the whole spectrum. Only one of the plates tested fell into this category and this was a plate from group (i) which was polished to a dark lustrous metallic colour.

(contd p 273)

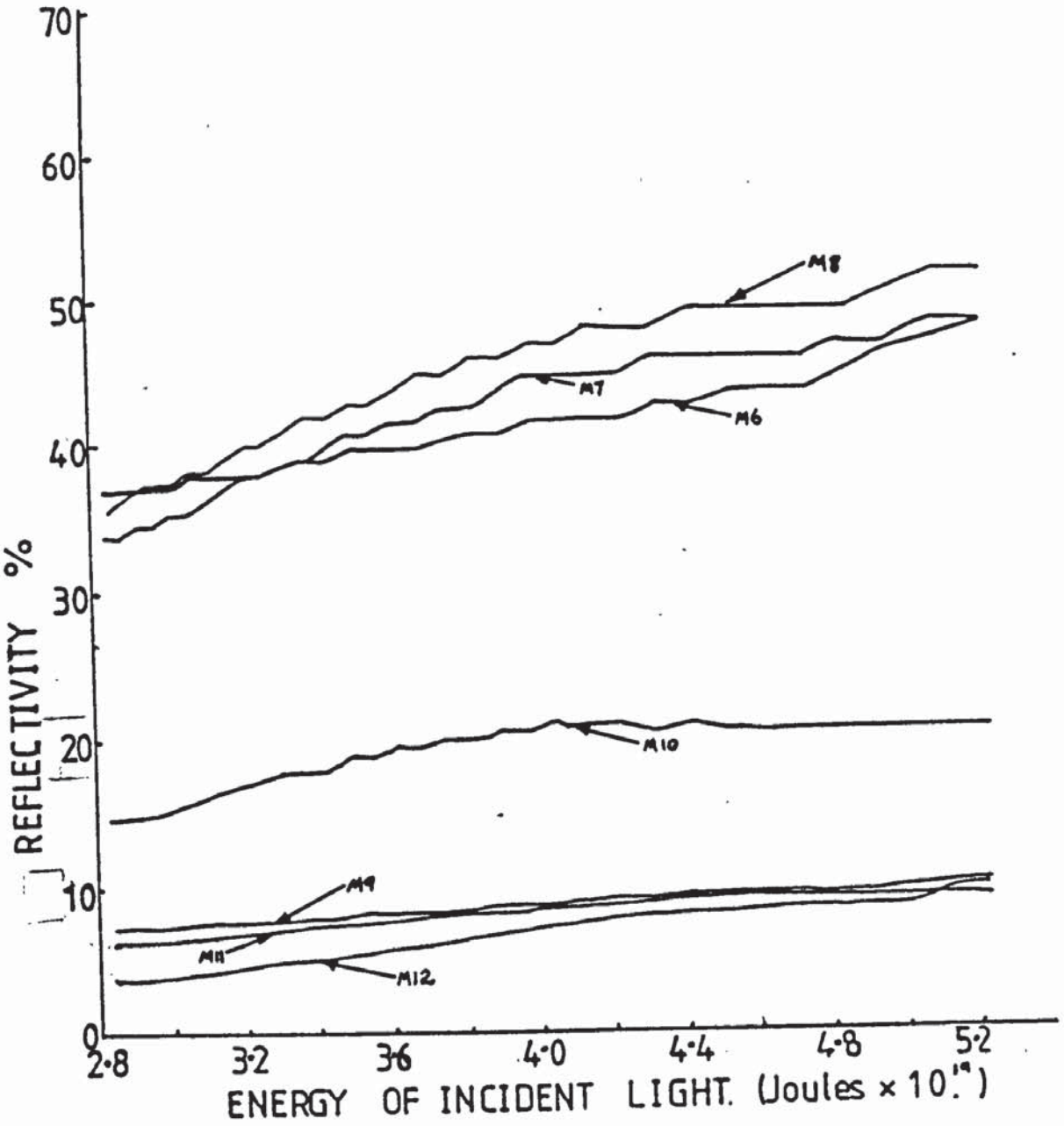

Fig. 9-16

"Reflectivity curves for Hull cell plates in a gold containing indium solution

(iii) Plates with fairly high reflectivity over the whole of the spectrum, with greater reflectivity at the high energy (blue) end. These plates comprised the lower gold contents (0, 0·1 and 0·2 g/dm^3). It was noted that the first addition of gold increased the reflectivity of the middle part of the spectrum but lowered it at the red end. Similar comparitive results were obtained when 0·2 g/dm of gold was added except that reflectivity values were slightly higher at each energy value.

9·4·2·3 The Chromaticity Coordinates

The chromaticity coordinates given in Fig. 9·13 shows that when considered with respect to equi-energy conditions all the plates (except M12) are quite near to the white point, the addition of gold appearing to move the deposit very slightly in the direction of the cyan-blue compartment of the diagram. The blue-streaked, low current density plate showed a very definite movement in the blue direction. Similar trends were exhibited for the tungsten lamp conditions. (Fig. 9·14).

9·4·2·4 Dominant Wavelength, Saturation and Luminosity

Since the most of the colours measured were near to the white point, saturation values were very low. The dominant wavelength values were all in the blue part of the spectrum when measured with respect to both illuminants, but with the addition of gold moved towards cyan. Although all saturation values calculated were low it is interesting

to observe that gold containing solutions gave slightly higher values (3→5→6). The low current density plate gave a much more saturated colour (17%) at a wavelength moving towards a more intense blue.

Fairly high luminosity values (in the region of 40%) were obtained up to a gold content of 0·2 g/dm, but when the dark deposits emerged much lower luminosities were recorded (6-8% with the exception of the stirred sample which was 19%).

CHAPTER 10

DISCUSSION OF RESULTS

10·1 INTRODUCTION

In this chapter the various parts of the work are discussed in an attempt to point out the salient features of each part. The discussion is carried out in the following order:

(i) The colour measuring process.

(ii) The covering power of gold deposits.

(iii) The colour of alloy electrodeposits.

(iv) Suggestions for further work.

Where necessary for clarity some discussion has been included in the previous relevant chapters.

10·2 THE COLOUR MEASURING PROCESS

10·2·1 The White Standard

Although it might be expected that a freshly condensed magnesium oxide film would give the best white standard, in fact it was found that there was very little difference between that and a pressed magnesium oxide standard. Since the preparation of the condensed film was very time consuming it was decided that the pressed analar magnesium oxide would be suitable. In order to obviate deterioration a fresh standard was prepared for each batch of discs measured, and since they were measured in small batches the standard was only used for quite a short time (<30 minutes) before renewal. The standard zero curve was measured and recorded on the graph, prior to the spectrophotometric measurement on each disc in order to give the most accurate measurement of absorbance over the spectrum covered.

10·2·2 Reproducibility of the Colour Measuring Process

The colour measuring process itself was found to be very reproducible since the absorbance measurements were repeated on the discs by two methods:

(i) By repeating the graphical measurement, and when this was done the second graph was found to be coincident with the first.

(ii) By measuring the absorbance at randomly selected wavelengths, and when this was done the values were found to be identical to the original graphs. This method was used the most frequently.

10·2·3 Reproducibility of the Measurements on the Discs

This was judged in three ways, namely:

(i) Discs were produced under ostensibly the same conditions and the results compared.

(ii) In some cases the discs were electroplated in pairs, colour measurements made and the results compared.

(iii) The results for some sets of discs were plotted and it was observed whether or not the results fitted on to a defined curve.

With respect to colour measurements on bare nickel discs several different pre-treatments were tried and within each group reproducibility was quite good, although occasionally one sample would give an atypical result. Where samples were electroplated

together the results were very close, and this was considered to be very encouraging, since we can expect slight differences due to positioning in the bath with respect to electrodes, etc. The most telling fact with respect to reproducibility was considered to be the fact that in nearly all cases where various values were plotted definite trends were shown. There were always assignable reasons for the presence of "rogue values".

Thus it was considered that the colour measuring system chosen was very suitable to fulfil the objects of the research.

10·3 THE TREATMENT OF THE RESULTS

10·3·1 Introduction

Much information can be derived from the graphs of spectrophotometric measurements. Since it was hoped that this work would lead to practical recommendations to aid in the control of coloured gold solutions it was decided to assess the work with respect to such practical considerations as chromaticity coordinates, saturation, dominant wavelength, luminosity and reflectivity curves. Although it is not possible to know what colour is under consideration merely by observation of the reflectivity curves they are valuable because they indicate at which energy value of incident light maximum absorption occurs. It is usual for any reflectivity step to be distributed over a range of energy, and in order for comparisons to be made the mid-step energy was computed. The method is described in Appendix 16. It was found useful to represent changes in such parameters as chromaticity coordinates, dominant wavelength,

saturation, luminosity and mid-step energy graphically with respect to electroplating time (thickness), or addition of alloying element.

10·3·2 The Standard Illuminants

Although no real light source gives an equal distribution of energy throughout its spectrum it is considered quite proper to calculate coordinates with respect to a theoretical equi-energy source, since providing the light source is stated comparisons may usefully be made. In this present work most of the colours were also calculated with respect to a tungsten light source S_A. It was found that when calculated with respect to tungsten lamp conditions the x coordinates were somewhat numerically higher while the z coordinates were slightly lower, which would tend to indicate slightly more red and less blue under tungsten lamp conditions. It is important to note that whichever standard was taken the same inferences were drawn. although in some cases the equi-energy curves were slightly easier to interpret.

10·4 PRELIMINARY EXPERIMENTS

The preliminary experiments were very heartening since those which could be compared to the solid alloy measurements by Saegar and Rodies[44] (gold and copper) conformed very well.

10·5 EFFECT OF PRETREATMENT

It is postulated that the reason that the reflectivity decreases with grit size on the hand ground samples is that the diffuse

reflectance optical system collects light reflected from the surface over the range 35° to 55° and the scratch pattern of the surface might be expected to influence the angle at which the reflected rays leave the surface. Increasing fineness of the surface as exemplified by the 600 grit samples might be expected to continue this downward trend, and the fact that this did not happen probably resides in the fact that the character of the surface was entirely different for the machine lapped (see chapter 4) enabling a greater collection of reflected rays. The subsequent fall in reflectivity for the diamond finished samples is probably due to the fact that the reflection is more nearly specular.

These differences in reflectivity which we might term "geometric" should not affect the chromaticity coordinates, since incident rays of different wavelength should respond similarly to the geometry of the surface. But it was found that although the chromaticity coordinates were found to be very similar for similar treatments there was quite a difference if we compare one treatment with another.

From Table 10·1, the results appear to fall into three groups:

(a) hand ground on 180 and 320 grit, and original machined followed by a nickel strike.

(b) 320 grit followed by a nickel strike and diamond polished followed by a nickel strike.

(c) Machine lapped followed by a nickel strike.

There does not seem to be any definable pattern that might be ascribed to structural differences, and it is suggested that the reason for the dominant wavelengths of the grit finished samples

(contd.p. 282.)

Treatment	Average Chromaticity Coordinates		
	x	y	z
Hand ground on 180 grit silicon carbide paper	0·346	0·345	0·309
As above but silicon carbide paper 320 grit	0·344	0·342	0·314
As above but followed by a nickel strike	0·330	0·329	0·341
As above but original machined surface	0·346	0·345	0·309
As above but lapped to 600 grit	0·359	0·335	0·286
Diamond polished nickel struck	0·329	0·328	0·343

Table 10·1

Effect of pre-treatment on average chromaticity coordinates

suggesting an orange colouration is due to very slight tarnishing of these samples, their larger true surface area subtending a larger solid angle to the atmosphere than the diamond polished samples. Since quite reproducible results were obtained for the same type of pretreatment, it was decided to adopt a particular pretreatment for each set of experiments. For the matt finished samples a 600 grit machine lapped finish was adopted and for the bright gold baths a 6 μm diamond finish was used, both being given a nickel strike. It was also the practice to measure the absorbance curves before electroplating so that any atypical curves could be detected and rejected.

10·6 THE COVERING POWER OF GOLD ELECTRODEPOSITS

10·6·1 Introduction

If asked to predict the outcome of gradually increasing the gold thickness of a gold deposit on a base metal substrate, we would probably expect that the colour would gradually change with thickness, as the deposit covered the substrate, and that when covering was complete a stable colour would be obtained. The experimental results appeared to substantiate this but the results appeared to be affected by surface pretreatment and the type of gold electroplating solution.

10·6·2 The Reflectivity Curves

Reflectivity curves exhibiting an absorption edge were obtained for gold electroplated discs, and the mid-step energies calculated by the

method given in Appendix 16. The onset of the energy step was preceeded by an embryo energy step indicated by a slight change in slope of the reflectivity curve, but the step proper only appeared when a very definite gold appearance was exhibited by the disc. For example in bath P5 an embryo step appeared after 5 seconds electroplating (calculated thickness 0·010 μm) described as "pale gold bright" and a full step after 10 seconds electroplating (calculated thickness 0·02 μm) when the deposit was described as "not full colour, seems thin, pale gold bright". Thus it is obvious that a definite energy step appears long before the substrate is completely covered. Stable mid-point energies conformed quite well to those found by Saeger and Rodies, which were Saeger and Rodies thermal alloy $3{\cdot}78 \times 10^{-19}$ J, bath X $3{\cdot}58 \times 10^{-19}$ J and bath 84C $3{\cdot}85 \times 10^{-19}$ J (average). The Saeger and Rodies curves were of similar shape to those obtained in the present work but in general of much higher reflectivity.

10·6·3 The Thickness of the Electrodeposit

In all except the initial preliminary experiments the measured parameters were plotted against time in the electroplating bath and then the time at which any particular change occurred was converted to a thickness by the use of the appropriate factor, derived from average values as described in Appendix 14. The factor for bath X was found to be 0·008 μm/s, and for bath P5 0·002 μm/s. The factor for bath 84C was found to vary with electroplating time as a result of a plating thickness test and thus the thickness was related to time by means of interpolation of the values given in Table 8·2.

10·6·4 Stability of Measured Parameters

The stability of the colour of the deposits was judged by reference to the chromaticity coordinates, dominant wavelength, saturation and luminosity. The judgements were made on the basis of the thickness of the deposit or the electroplating time. Ideally a parameter would be adjudged stable when the graph for this parameter started to become horizontal with thickness, but in some cases it was necessary to accept stability when the graph changed to an extremely shallow slope from a steep one, indicating only slight change in parameter with thickness. Table 10·2 shows the thickness values at which various parameters were judged stable.

The average chromaticity coordinate values (the average of those values on the stable part of the curve) show that if we compare the coarser finishes (320 grit and original machined) with the finer finish (600 grit) then bath X gave slightly different coordinates. The coarser finishes exhibited slightly more redness and slightly less blue than the more finely finished samples. This could well be a current density effect, if we examine the Talysurf measurements in Appendix 11 we see that the cla for the original machined samples (on which the averages were calculated) is 1·7 μm, whereas that for the 600 grit samples is 0·12 μm. Thus although the geometric surface area of the discs will be the same the true surface area is likely to be different. It must be emphasised that the series of experiments in which 320 grit and original machined surfaces were considered together was only a preliminary excursion designed to establish trends and that the 600 grit samples were done on the basis

(contd. p. 287.)

Solution and Pretreatment	Average Chromaticity Coordinates at Stability			Thickness for Stability µm	Description at Stability
	x	y	z		
X, 320 grit and original machined	0·472	0·406	0·122	0·6	-
X, 600 grit	0·451	0·402	0·147	0·23	Golden yellow
P5, 6 µm diamond	0·392	0·383	0·225	0·06	Bright yellow gold
84C, 6 µm diamond	0·379	0·373	0·248	0·064	Bright yellow gold
P5, 600 grit	0·419	0·394	0·187	0·1225	Smooth yellow
	Dominant Wavelength at Stability				
X, 320 grit and original machined	584			0·38	-
X, 600 grit	584			0·16	Clear yellow gold
P5, 6 µm diamond	580			0·01	Pale gold bright
84C 6 µm diamond	576			0·0082	A slight gold cast but not really gold coloured
P5, 600 grit	582			0·0525	Smooth yellow looks thin

Table 10·2

The thickness at which colour stability occurs assessed by various parameters

Table 10·2 continued

Solution and Pretreatment	Saturation at Stability	Thickness for Stability m	Description at Stability
X, 320 grit and original machined	59	0·8	-
X, 600 grit	51	0·23	Golden yellow
P5 6 µm diamond	30	0·06	Bright yellow gold
84C 6µm diamond	24	0·064	Bright yellow gold
P5, 600 grit	44	0·1225	Smooth yellow

of these. Nevertheless it has been considered proper to consider the first series even though something of a hybrid. An experiment discussed in section 5·2·5 appeared to suggest that as the deposits thicken the effect of original surface decreases. The bright deposits produced gave chromaticity coordinates indicating rather more blue with less red and green in the colour, 84C being even more so than P5. Fig. 10·1 shows that this was borne out when these average chromaticity coordinates were plotted onto the chromaticity chart. All the colours were yellow but the bright samples were slightly less orange than the matt samples and much less saturated. Stable dominant wavelength values also indicated the greater "orangeness" of the matt samples. Discs electroplated in bath P5 with a 600 grit pretreatment exhibited chromaticity coordinates, and thus CIE chart positions, intermediate between the other two conditions.

10·6·5 The Thickness at which Stability occurs

Assuming that complete covering is achieved with chromaticity coordinate

Type of Solution	Surface	Stability obtained at thickness	Number of atomic layers
Bath X, matt deposit	Original machined or 320 grit	0·6 μm	2948
Bath X, matt deposit	600 grit machmachine lapped	0·234 μm	1150
Solution P5, bright deposit	6 μm diamond	0·06 μm	295
Solution 84C, bright deposit	6 μm diamond	0·064 μm	314
P5, bright deposit	600 grit	0·1225 μm	601

Table 10·3 - Thickness for stability

(contd. p. 289.)

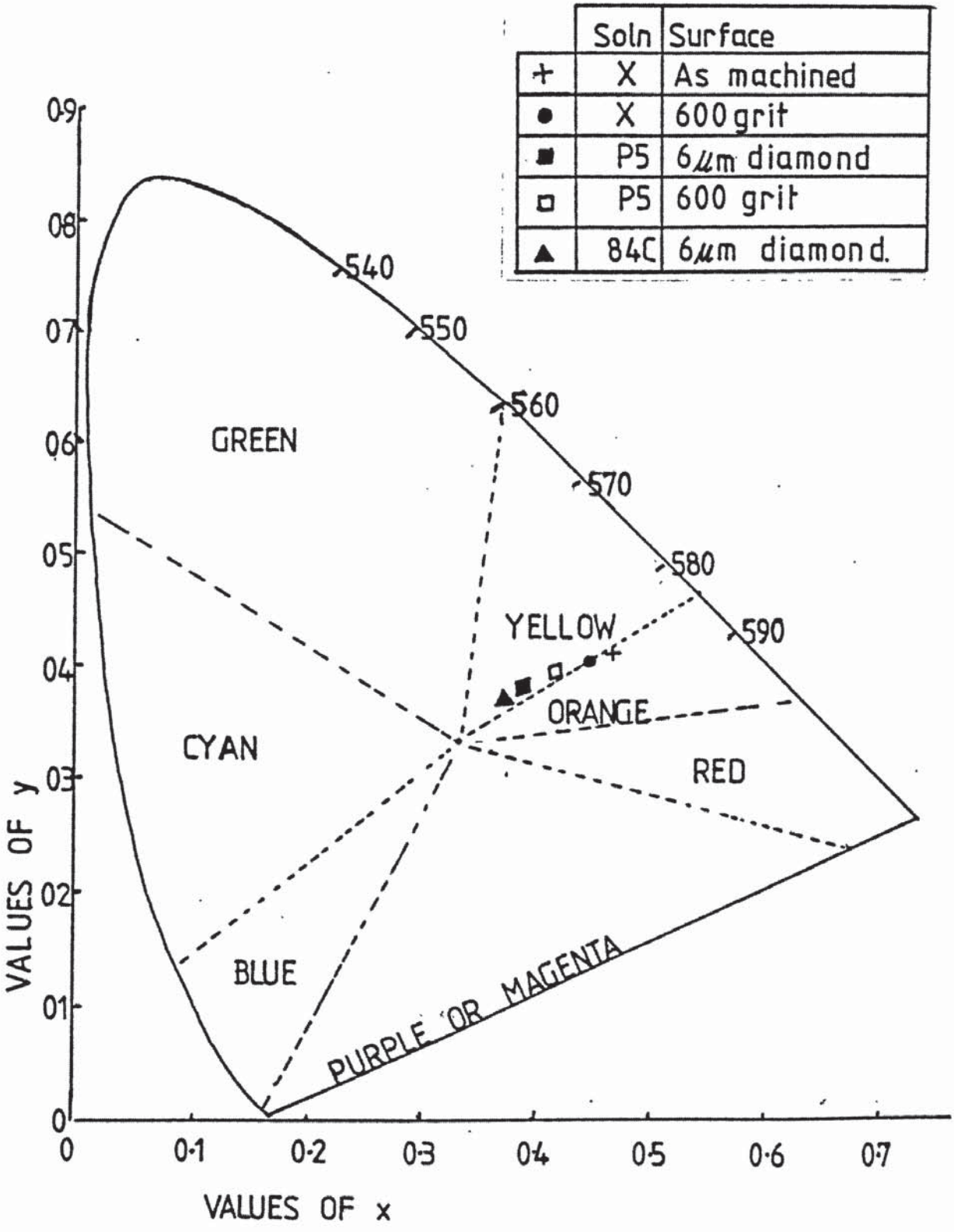

Fig. 10·1

Effect of surface treatment on CIE position

stability, Table 10·3 shows that the covering power is dependent on both the original surface finish and the type of electroplating, the matt electroplating bath requiring approximately twice the thickness on the original machined surface as on the 600 grit finished, and the bright bath (P5) requiring only about half the thickness of the matt bath on a comparable original finish (600 grit). The bright bath on a diamond finish requires the least gold for complete coverage.

It is perhaps true to say that actual thickness on a rough surface may be much less than weight increments suggest, since the deposit must follow the contours of the larger true surface area, but it must be remembered that in any commercial electroplating venture the amount of gold will be calculated with reference to the original geometric surface area.

It is postulated that deposits grow by a similar mode to that for the vacuum deposits discussed in section 1·5·3. That is by projection of arms into the liquid with only slow lateral growth. It is believed that it is only when the lateral growth finally obscures the original surface that covering is complete. In the bright baths the presence of addition agents means that perpendicular growth is inhibited, and thus lateral growth is facilitated. Thus covering is accomplished at much lower thicknesses. This is important in gold electroplating practice, since it means that not only is it preferable to use bright baths to cut out buffing costs but also from the point of view of efficient covering.

It is interesting to note that in the case of both the bright gold

baths tested the plating times which gave chromaticity coordinate stability coincided with the first description of bright yellow gold, such descriptions as thin and blotchy being applied to lower time periods. Similarly to the descriptions for the matt deposits.

10·7 THE ADDITION OF COPPER TO A GOLD ELECTROPLATING BATH

10·7·1 Discussion of the Results obtained

On the addition of an alloying element to a parent metal we might expect to see a gradual graduation of colour of the parent metal to that of the alloying metal. The results obtained in the present work for the addition of copper to a gold electroplating bath do not seem to conform to this proposition, except for the low bath copper contents. As we increase the bath copper content the gold darkens and then becomes reddish in character, but further increases lead to a decolourisation of the gold, exemplified by the emergence of a fawn or putty coloured deposit, which on further increase of bath copper content gives way to a re-emergence of redness. The chromaticity coordinates, saturation, dominant wavelength, luminosity, and mid-step energy all show an undulatory character consistent with these changes. Fig. 10·2 shows the x and y coordinates plotted on the relevant portion of the CIE chart, and from this we see that as we increase the bath copper content the coordinates which are situated in the yellow-orange part of the chart move towards the red-orange direction. By eye these discs (up to 0·9 g/dm^3) had all been assessed as yellow, but it must be remembered that this assessment was carried out on an individual basis and was not comparative. It is interesting to note that the measuring process was picking up nuances of colour long before

(cont'd. p. 292)

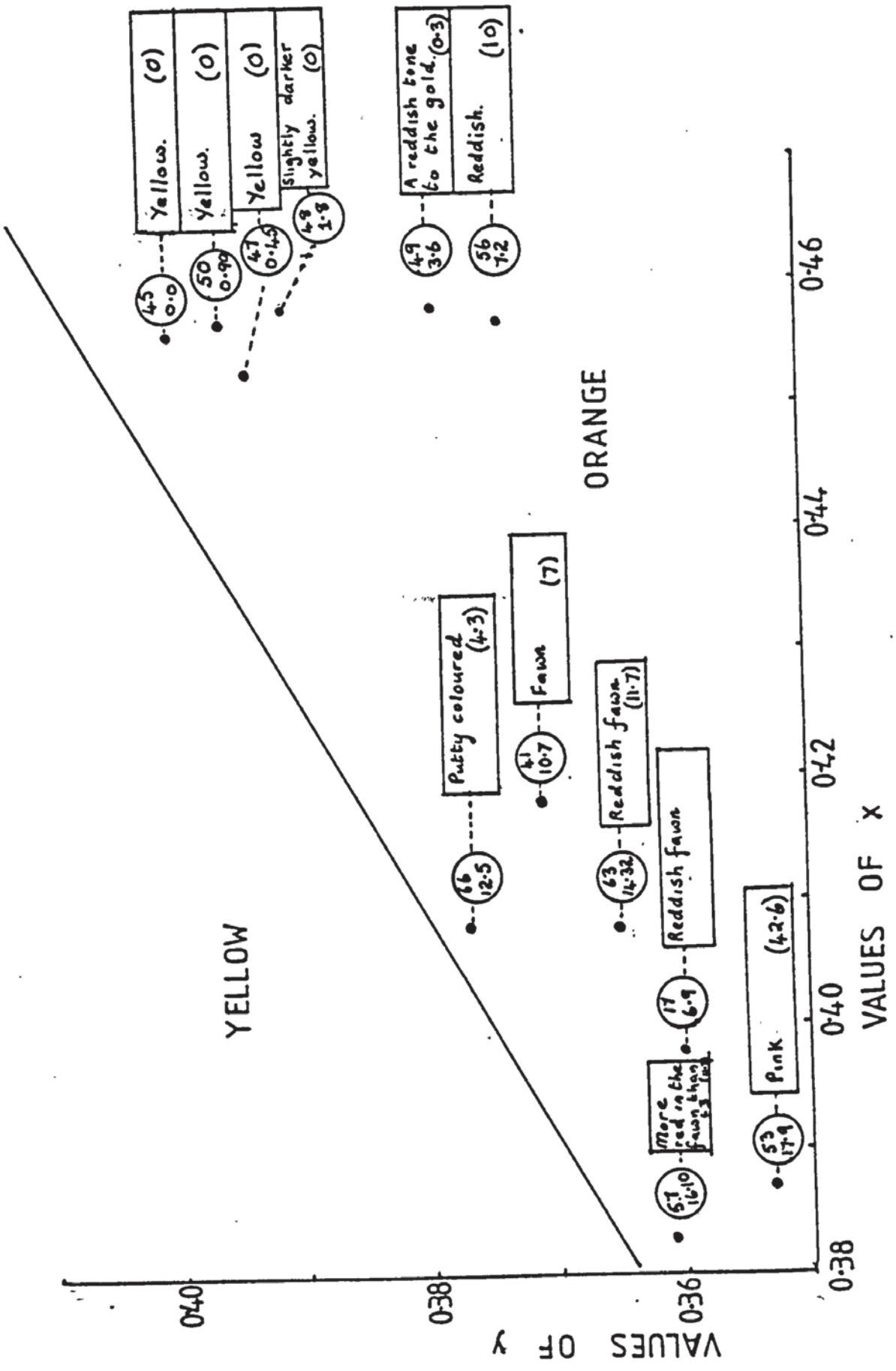

Fig. 10·2

Effect of bath copper content on CIE position

they were obvious to the eye. The first change detected by eye was a darkening of the deposit (1·8 g/dm^3) but it is interesting to note that up to this point no copper was detected in the deposit. On the other hand it is patently obvious that there must have been traces of copper in the deposit because of the movement of the parameter and it is believed that these traces were insufficient to be detected. Further increases of copper in the bath resulted in increasing redness of the deposit until at 3·6 g/dm^3 of copper in the bath 0·3% of copper was detected in the deposit, and at 7·2 g/dm^3 bath copper content, 10% of copper was detected in the deposit. Up to this point the change in colour with bath copper content was as expected. But at a bath composition of 10·7 g/dm^3 there was a sudden movement across the chart, meaning a drop in saturation and a movement back towards the yellow area, i.e. a drop in redness, exemplified by the deposit becoming decolourised and described as fawn. At this point the copper content of the deposit had fallen to 7%. A further increase in bath copper content resulted in a further drop in deposit copper content and further decolourisation (12·5 g/dm^3). Further increases in bath copper content re-established the redness and at the same time the copper content of the deposit increased.

Thus it seems that some factor affecting the colour occurs in the region 7-14% copper in the bath. It is believed that consideration of the relevant structures might provide a clue as to the controlling factors.

The work of Saeger and Rodies inter alia postulates that the existence of a step in the reflectivity curve for gold is due to the conditions of energy band transitions and selection rules being favourable for an intense absorption process at 2·3 electron volts ($3{\cdot}68 \times 10^{-19}$ J). A step is also present in the visible spectrum for copper at somewhat lower energies. The present results confirm this, the value for copper foil giving a stepped curve at lower energies than the Saeger-Rodies curve for fine gold. Electrodeposited gold and copper gave stepped curves but at energies lower than those for the solid metals. This may well be due to the crystal structure of the electrodeposits, banded or columnar structures being commonly obtained in electrodeposits. The gold-copper equilibrium diagram given in Fig. 6·18 indicates that gold and copper form a continuous series of solid solutions exhibiting a congruent point. Thus we would expect that as the copper content of the solution increases (and thus the deposit) there would be a gradual movement of the reflectivity step from higher to lower energies. Examination of the mid-step and top-step energies show that this is borne out for the lower copper contents, but then a change occurs, apparently coincident with the decolourisation of the deposit (fawn, putty coloured). The emergence of this decolourisation process appears to be related to an increase in step energy. Decolourising is unlikely to be due to widening of band gaps since both gold and copper exhibit a step, and a step is still exhibited here. Nickel and palladium also decolourise gold for a different reason, namely the occurrence of virtually bound states. Again this is unlikely to be the case

here, since the deposition of the reflectivity curves does not resemble that given by Saeger and Rodies for gold-nickel in which the energy for the transitions due to the virtually bound state remains practically unaffected by the quantity of the alloying addition, only the intensity of the adsorption process being changed. Thus the remaining possibility appears to be the formation of intermetallic compounds, since in this case an entirely new band structure is formed. The gold-copper equilibrium diagram given in Fig. 1·14 indicates an area of superlattice at low temperatures. Two intermediate compounds occur in the gold-copper system CuAu containing 24% copper and Cu_3Au containing 49% copper. Thus a hypothesis may be advanced that as the bath copper content increases copper goes into solid colution with consequent increase in redness, between 7 and 14% copper content the ratios of the complex ions present in the catholyte are such that the formation of intermetallic compounds, probably based on CuAu, are favoured. It is not suggested that the entire deposit consists of CuAu, the analysis results do not support this, but Brenner and others have postulated that gold-copper deposits consist of mixtures of solid solutions, gold and copper crystals, and gold-copper intermetallic compounds, and it is believed in the present instance that the intermetallic compound formation predominates. In the higher copper content ranges when redness is re-established it is believed that solid solution formation again becomes dominant. It must be emphasised that the above is circumstantial only and to confirm it should be the basis of further work involving exhaustive studies of this system by X-ray diffraction methods.

It is believed that the actual copper cyanide complex present controls the copper content of the deposit since the discs electroplated in the solution in which copper was added as copper carbonate did not fit on to the curves for the other majority of the discs (in which copper was added as copper cyanide). This is understandable since the different possible complexes will have different instability constants which will result in different E values for the Cu^{+}/Cu electrode.

The scanning electron microscope results showed that the copper content of the deposit influenced the character of the deposit nodules formed, negligible copper contents giving dimpled nodules while higher contents (approximately 10%) gave smoother rounded nodules. The electron microscope pictures also appeared to support the contention that the non-conforming discs (copper added as carbonate) were actually of much higher deposit content than was to be expected from the bath content.

No mention of this decolourisation is mentioned in the work of Roberts and Clarke but this is probably because their alloys were thermal alloys quenched from 600°C.

10·8 THE ADDITION OF SILVER

10·8·1 Introduction

The results of silver additions to the gold solutions appeared to be much more straightforward than the additions of copper. This is believed to be due to structure of the alloys formed as exemplified

by the appropriate thermal equilibrium diagram.

10·8·2 The Reflectivity Curves

The movement of the reflectivity curves progressively to the high energy end of the spectrum with increasing silver content of the bath confirmed the findings of Saeger and Rodies for solid alloys. As the decolourisation of the deposit proceeded it was noted that not only did the energy step move towards the ultra-violet end of the spectrum but that the step became less definite, the slope of the step becoming less steep. Thus we see the influence of silver, moving the energy step progressively but also becoming more horizontal so that it would be expected ultimately to conform to the near horizontal graph for pure silver.

10·8·3 The Measured Parameters

It was found that all the parameters were easy to relate to the change in bath silver content. It is believed that this is due to the fact that bath silver content relates linearly to deposit silver content and that this in turn is due to the configuration of the appropriate thermal equilibrium diagram, given in Fig. 1·15. The liquidus and solidus are very close together with only a very narrow melting range, a continuous range of solid solutions being exhibited. There is no sign of compound formation or superlattice in the α region. Thus we might logically expect a smooth change in the parameters as the silver content of the solid solution increases. This in fact was substantiated by the experimental results, a smooth change in all

parameters (except luminosity which showed no definable trend) being obtained until the deposit was described as cream, and when it contained approximately 25% of silver. At this point the rate of change of the parameters decreased greatly.

10·8·4 Comment

The results obtained seem to bear out those of Saeger and Rodies for thermal alloys in which the reflectivity step moved to higher energies with increasing silver contents, which is thought to be due to the continuous widening of the energy gaps between the d-bands and the Fermi level. The shifting of the reflectivity step to the higher energies means that as the silver content of the bath (and thus of the deposit) increases, the deposit becomes increasingly more green and as the edge continues to move a greater selection of the available wavelengths in the visible spectrum are reflected and the deposit becomes cream or off-white. Saeger and Rodies aver that the height of the step and the slope remain roughly the same for thermal alloys but it was found for electrodeposits that in fact the slope changed quite considerably. On the other hand the work done by Saeger and Rodies seemed to be directed towards the higher silver contents while this present work has been more concerned with lower silver contents. It was also observed that the shape of the reflectivity curve for a gold deposit was as shown in Fig. 10·3a, i.e. a straight line portion A-C indicating the reflectivity step, but as silver is added to the solution a change in direction occurs as shown in Fig. 10·3b at B. So that as well as changing and moving to higher energies the step changes in character. If we plot the

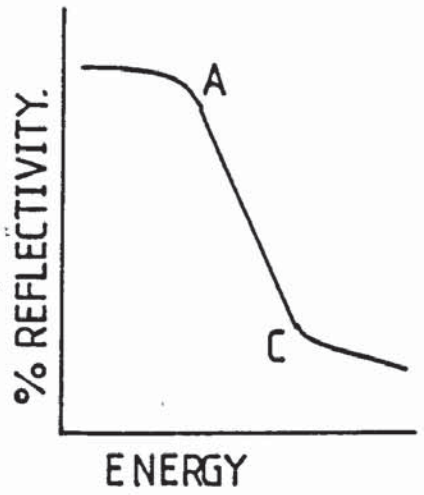

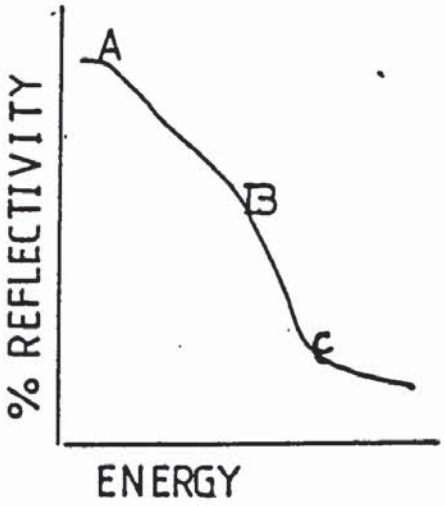

Fig. 10·3a

Fig. 10·3b

Shape of reflectivity curves

energy position at break we find that a graph of the form shown in Fig. 10·4 is obtained showing that for low silver contents (up to 0·6 g/dm^3 in the bath) the break occurred at low and similar values but at 0·8 g/dm^3 there was a sudden increase in break energy, and this corresponded to the first mention of a greenish tinge in the deposit.

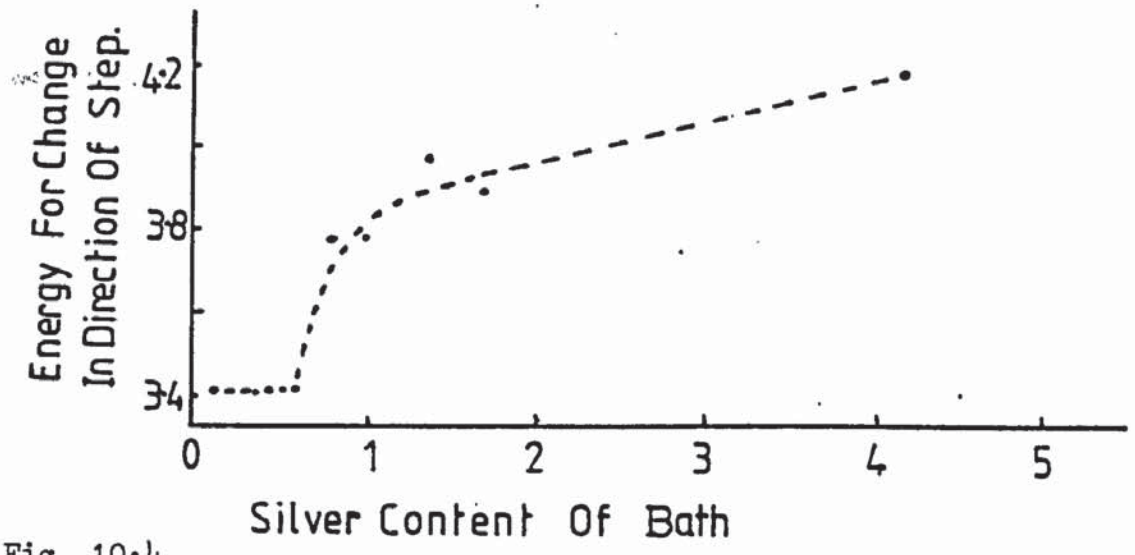

Fig. 10·4

Step direction change

As the silver content increases the break point moves to higher energies and the deposit becomes decolourised. Obviously as the break point moves to the left the portion A-B occupies more of the spectrum and eventually would be expected to occupy the whole of the visible spectrum.

10·9 THE ADDITION OF INDIUM

10·9·1 The Use of the Miniature Hull Cell

Providing that stirring was not too intense, the miniature dip type Hull cell was satisfactory. It is considered that this type of cell would be very satisfactory for investigations such as the present one where expensive ingredients are involved.

10·9·2 Addition of Indium to a Gold Electroplating Solution

There was no sign of the minimum-maximum curve obtained by Saeger and Rodies for $AuIn_2$ intermetallic compounds, but intense blue colourations were found beneath the Lacomit stopping off medium. This could have meant that the compound was deposited at extremely low current densities, or that due to the restrictions imposed on diffusion, replacement of ions was made more difficult and at some stage the proportion of gold ions to indium was just that required to enable the intermetallic compound to be deposited. Bent cathodes did not indicate any area of obvious blue colouration except again below the stopping-off medium. Miniature Hull cell tests on the highest indium content tried (4 g/dm^3) showed no sign of any blue colouration even on the extreme low current density, and even though the current

on the plate was very low (10 mA). It was interesting to note that the Hull cell plates done at a higher total current (100 mA) exhibited blue stains on the reverse. The reflectivity curve for the reverse of plate M5 gave a reflectivity edge opposite to that obtained for gold, i.e. low reflectivity in the low energy part of the spectrum, and higher reflectivity in the high energy (blue) part of the spectrum, with a reflectivity step between them. From these results then it seemed that it was possible to obtain a blue gold deposit probably consisting largely of $AuIn_2$, but it did not seem to be possible to define a current desnity range, since in all cases where a blue colouration was present it was in positions of restricted solution access.

10·9·3 Addition of Gold to an Indium Electroplating Solution

Since there seemed to be a possibility that the prerequisite for the production of a blue gold deposit was the correct ratio of gold to indium ions, it was considered worthwhile to investigate the addition of gold to an indium solution. It was found that the pure indium solution, unadulturated with gold, gave a white deposit with excellent throwing power as indicated by the very good covering of the back of the plate. There was absolutely no sign of any blue colouration on the back of the plate. This is important since it shows that the blue stains were due to the presence of both gold and indium. As the gold content of the solution built up clear blue stains were again observed on the reverse of the Hull cell plates, while the fronts of the plates became progressively dull, grey and rough — the only sign of blueness being a few dark metallic streaks

obtained on a low current plate on the highest gold content tried. But this blueness was of the dark metallic variety and not the sky blue obtained on the reverse of the plates.

10·10 THE SCANNING ELECTRON MICROSCOPE STUDIES OF THE TOPOGRAPHY OF SURFACES

As discussed elsewhere the type of mechanical treatment applied to a surface influences not only the fineness or coarseness of the surface but also the shape and character of any protruberances or indentations produced, ploughed, unoriented furrows for 600 grit machine lapped, oriented scratches for hand ground, and glassy featureless for the diamond polished. These conditions were very efficiently differentiated by the SEM techniques employed.

It was interesting to observe the different character of the deposits obtained in the matt electroplating baths all were nodular in character but the nodules themselves were different in character, rounded composite nodules for pure gold deposits, dimpled nodules for the lower copper contents which changed to very smooth rounded nodules in the higher copper contents, dimpled nodules of more complicated character for the silver containing deposits, featureless glassy deposits for the bright golds. Although different in colour, the texture of all the matt deposits appeared very similar to the naked eye, but as stated differences were revealed by the SEM.

10·11 SUGGESTIONS FOR FURTHER WORK

The present work has continually revealed further work that needs to be carried out. This is not a matter for gloom but rather one for anticipation. The author hopes to engage in further work on one of the following topics:

(i) An investigation of the covering power of various solutions by the methods used in this present work to determine if a specification based on the methods used here could be derived for a general statement of covering power.

(ii) The investigation of the gold-copper system by X-ray diffraction methods to determine the precise nature of the structural changes which occur in gold-copper deposits.

(iii) The investigation of the gold-indium system in an attempt to obtain a blue gold deposit, under practical conditions. It is possible that recourse to different complexing agents might allow the requisite ratio of gold to indium to be present in the catholyte.

(iv) The production of an atlas of chromaticity coordinates for the whole gamut of gold electroplating baths, embracing different plating parameters such as current density, temperature, surface treatment. This could then be consulted by commercial electroplaters in the way that standards are at present compared.

CONCLUSIONS

It is concluded that:

1. The method of measuring colour by means of spectrophotometric methods using a diffuse reflectance attachment provides an excellent method of measuring the colour of gold and gold alloy electrodeposits, and it is considered that commercial electroplaters could efficiently control their process by this means.

2. The surface treatment of the substrate affected the chromaticity coordinates of the substrate.

3. The thickness of gold required to cover the underlying nickel substrate varied according to the type of gold bath (bright or matt) and according to the type of surface finish.

4. A bright bath on a diamond polished surface requires approximately 0·06 μm but it requires 0·12 μm on a 600 grit finished surface whilst a matt bath requires a thickness of 0·234 μm on a 600 grit finished surface.

5. The experiments indicated that as the electrodeposit thickened the effect of the condition of the substrate on the final colour became less marked.

6. From the point of view of economy of gold, which is becoming ever more pressing, commercial electroplaters should secure

the finest surface finish possible prior to the electrodeposited gold layer.

7. The effect of addition of copper to a gold electroplating bath was satisfactorily monitored, and the results inferred that the structural characteristics of the gold-copper system greatly influenced the colour measurements.

8. The effect of addition of silver to the gold electroplating bath was satisfactorily monitored, and the results inferred that the structural homogeneity of the system ensured a smooth transition of the various parameters measured.

9. The topography of the electrodeposits as revealed by electron microscope studies is affected by the type of electroplating solution used.

10. The characteristics of the reflectivity curves obtained for electrodeposits are quite similar to those obtained by Saeger and Rodies for thermal alloys.

11. The production of a blue gold electrodeposit appears to be a possibility.

APPENDICES

APPENDIX 1

Colour Changes in Gold Deposits

Alloying Element	Colour
Copper	Yellow to pale red to red
Nickel	Yellow via pale yellow to white
Cobalt	Yellow via orange to green
Cadmium	Yellow to green
Bismuth	Yellow to violet
Palladium	Yellow to pale yellow
Indium and silver	Sky blue

APPENDIX 2

The Spectrum of White Light

Wavelength nm	Colour
400-450	Violet
450-500	Blue
500-570	Green
570-590	Yellow
590-620	Orange
620-700	Red

APPENDIX 3

Definition of Terms Used in Colour Technology

Hue	This denotes the kind of colour, that is, whether it appears green or blue. It is the attribute which allows the eye to distinguish different parts of the spectrum.
Saturation	Indicates the extent to which the hue is diluted with white. Colours appear whiter or greyer as the saturation is reduced.
Lightness	Denotes brightness, brilliance or intensity that is the extent to which a material appears to reflect or transmit light.
Luminosity	This is the corresponding term to lightness, usually used when referring to light sources, but it may be used for reflected light, and it has been in the present work.
Luminance Factor	This corresponds to lightness being the proportion of incident light reflected or transmitted by an object.
% Luminosity	By convention the luminosity is represented by the y product total and is calculated

as follows:

$$\frac{\text{"y" product total}}{\text{"y" product total if reflectivity 100\%}} \times 100 = \% \text{ Luminosity}$$

Colour Temperature

Theoretically colour temperature is the temperature at which a perfect black body emits light of the same colour as the source in question. Since most light sources only approximate to black bodies the values quoted are in fact correlated colour temperatures.

APPENDIX 4

Standard Illuminants

Illuminant	Description
S_A	A gas-filled tungsten filament lamp operated at a colour temperature of 2854 K, typical of average artificial tungsten lamp illumination
S_B	Typical of a sunlight with a colour temperature of 4900 K
S_C	Typical of an overcast sky (average daylight) with a colour temperature of 6700 K
D_{6500}	Typical of average daylight with a colour temperature of 6500 K
D_{5500}	Represents a yellower daylight, colour temperature of 5500 K
D_{7500}	A bluer daylight (north skylight), colour temperature of 7500 K

Notes: (i) For the mathematical purposes of the CIE system the energy distributions over the spectrum are specified in the form of tables giving their energy values at each wavelength.

(ii) Although S_B and S_C represent sunlight and daylight fairly well they are seriously deficient at wavelengths below 400 nm. Thus the "D" series has been defined to represent daylight over the wavelength range 300 to 830 nm.

APPENDIX 5

Method of Conversion of Measured Chromaticity to CIE Values

Suppose the equivalents in CIE XYZ units for equal quantities of instrumental R G and B stimuli are as follows:

1·0R = 0·7479X + 0·2481Y + 0·0000Z

1·0G = 0·1501X + 0·7218Y + 0·0751Z

1·0B = 0·1470X + 0·0491Y + 0·8349Z

This means that 1·0 unit each of the instrumental stimuli match white, and thus that the proportions of each of the CIE stimuli given match each of the instrumental stimuli.

Supposing a certain colour is matched by 20% of R, 50% of G and 30% of B, then conversion to X, Y and Z values is as follows:

For X : (0·2 x 0·7479) + (0·5 x 0·1501) + (0·3 x 0·1470) = 0·2678X

For Y : (0·2 x 0·2841) + (0·5 x 0·7218) + (0·3 x 0·0491) = 0·4325Y

For Z : (0·2 x 0·0000) + (0·5 x 0·0751) + (0·3 x 0·8249) = 0·2850Z

Total = 0·9862

The chromaticity coordinates are calculated by dividing each tristimulus value by the sum of the three. The chromaticity coordinates are designated by the lower case x, y and z.

$$x = \frac{0{\cdot}2687}{0{\cdot}9862} = 0{\cdot}2725 \; ; \; y = \frac{0{\cdot}4325}{0{\cdot}9862} = 0{\cdot}4385 \; ; \; z = \frac{0{\cdot}2850}{0{\cdot}9862} = 0{\cdot}2890$$

The chromaticity coordinates may be stated as above to define the colour. By convention the Y value is taken to represent the

luminosity of the colour. The ratio of the Y value for the colour to the sum of the Y values of the transformation equations taken as a percentage gives the luminosity value.

$$\text{Luminosity} = \frac{0{\cdot}4325}{1{\cdot}0550} \times 100 = 41\%$$

APPENDIX 6

Calculations from Spectrophotometric Measurements

In an actual determination absorbance measurements are taken from a spectrometer graph at 10 nanometer intervals but for the purposes of illustration values will be taken at 50 nanometer intervals. Absorbance values are converted to reflectivity values by the relationship $\%R = 10^{2-A}$.

Disc No. 107

Wavelength nm	EE Distribution coefficients				Tristimulus Values		
	x	y	z	%R	x	y	z
400	0·0143	0·0004	0·0679	13·49	0·1929	0·0054	0·9160
450	0·3362	0·0380	1·7721	12·88	4·33026	0·4894	22·8246
500	0·0049	0·3230	0·2720	19·5	0·0956	6·2985	5·304
550	0·4334	0·9950	0·0087	37·15	16·1008	36·9643	0·3232
600	1·0622	0·6310	0·0008	53·48	56·8065	33·7459	0·0428
650	0·2835	0·1070	0·0000	63·10	17·8889	6·7517	0·0000
700	0·0114	0·0041	0·0000	67·61	0·7649	0·2751	0·0000
			Total		96·1799	84·5303	29·4106

Total X + Y + Z = 96·1799 + 84·5303 + 29·4106

= 210·1209

$$x = \frac{96·1799}{210·1209} = 0·458 \; ; \; y = \frac{84·5303}{210·1209} = 0·403 \; ; \; z = \frac{29·4106}{210·1209} = 0·139$$

$$\text{Luminosity} = \frac{Y \times 100}{\Sigma \bar{y} \times 100} = \frac{84·5303 \times 100}{2·0985 \times 100} = 40·3\%$$

Note: If calculated with respect to other standard illuminants the

distribution coefficient must be weighted with respect to the energy distribution of the particular illuminant used..

For example, suppose we consider illuminant S_A:
At 400 nm, wavelength energy distribution = 14·71%, therefore weighted distribution coefficient E = 14·71 x 0·0143 = 0·2104.

This can be done for x, y and z over the spectrum at wavelength interval desired. A factor may be selected to ensure that the sum of the y coefficients = 100 in order to simplify luminosity calculations.

The Dominant Wavelength

If the coordinates of x and y are plotted on the CIE chart the colour is exactly defined. Consider a colour M (Fig. A7)
If we project a line through the white point W to the spectral locus, the point where this line cuts the spectral locus P is the dominant wavelength. For a colour N in the magenta segment the dominant wavelength is defined by its complementary wavelength by drawing a line from N through W to the spectral locus (Q).

Saturation

The saturation or purity of a colour is related to the amount of white contained in the colour. If it is situated on the spectral locus it is fully saturated (100%) whilst at the white point the saturation is zero.
% Saturation of M = WM/WP x 100 ; % Saturation of N = WN x 100/WR.

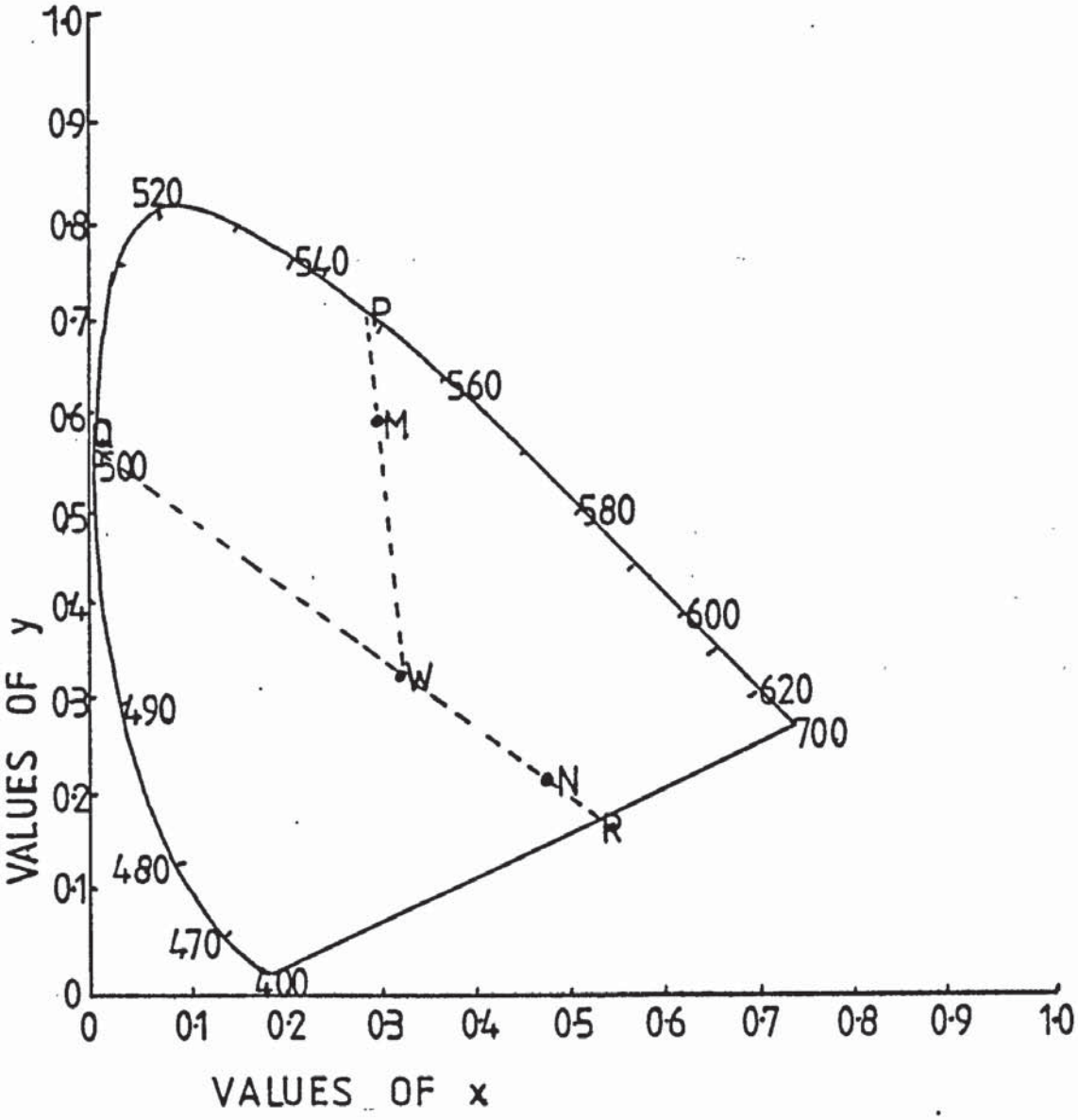

Fig. A1

Definition of dominant wavelength and saturation

APPENDIX 7

Element	Electron Arrangement														
	K	L		M			N				O				P
	1s	2s	2p	3s	3p	3d	4s	4p	4d	4f	5s	5p	5d	5f	6s
Gold	2	2	6	2	6	10	2	6	10	14	2	6	10		1
Silver	2	2	6	2	6	10	2	6	10		1				
Copper	2	2	6	2	6	10	1								

APPENDIX 8

The Wavelength of X-Rays Given Out when an Electron Fills the Vacant Electron Site in one of the Orbitals of an Excited Atom

$$\lambda = \frac{hc}{\Delta E}$$

Consider that an electron has been knocked out of the K shell of a molybdenum atom. If an electron from the L shell jumps in to fill the vacancy then ΔE would be:

Energy of K shell - Energy of L shell

$3{\cdot}2042 \times 10^{-15}$ J $- 4{\cdot}1655 \times 10^{-16}$ J $= 2{\cdot}78 \times 10^{-15}$ J

$$\lambda = \frac{6{\cdot}62 \times 10^{-34} \times 2{\cdot}998 \times 10^{8}}{2{\cdot}7877 \times 10^{-15}}$$

$= 0{\cdot}071$ nm

APPENDIX 9

Sample Calculation for Kevex Analysis

Peak integral for copper standard = 221103

Peak integral for standard under the same conditions = 26886

$$\text{Copper content of sample} = \frac{26886}{221103} \times 100$$

$$= 12 \cdot 16\%$$

APPENDIX 10

Solutions used and the Conditions of Operation

Cathodic Alkali Degreaser

Sodium carbonate $NaCO_3 10H_2O$ = 165 g/dm^3

Sodium hydroxide NaOH = 15 g/dm^3

Temperature : 80°C ; Current density : 10 asd ; Time : 5 minutes

Hydrochloric Acid Dip

10% AR Hydrochloric Acid in distilled water

Temperature : Room

Wood's Nickel Strike Bath

Nickel chloride $NiCl_2 6H_2O$ = 240 g/dm^3

Hydrochloric acid (conc) = 123 cc/dm^3

Temperature : Room ; Current density : 3·0 asd ; Time : 5 minutes

Gold Electroplating Bath X

Potassium gold cyanide $KAu(CN)_2$ = 3·75 g/dm^3

Potassium cyanide KCN = 15 g/dm^3

Temperature : 65°C ; Current density : 2·5 asd ; Time : as required for thickness

This bath was used wherever a pure gold matt deposit was required. It was also used to investigate the addition of indium to a gold electroplating bath.

Gold Electroplating Bath Y

Potassium gold cyanide $KAu(CN)_2$ = 2·7 g/dm^3

Potassium cyanide KCN = 27 g/dm^3

Temperature : 25°C ; Current density : 0·5 asd ; Time : 20 minutes

This bath was used in the experiments on the addition of copper. Except otherwise stated the copper was added as CuCN together with sufficient potassium cyanide to complex.

Gold Electroplating Bath Z

Potassium gold cyanide $KAu(CN)_2$ = 2·9 g/dm^3

Potassium cyanide KCN = 40 g/dm^3

Temperature : 50°C ; Current density : 1·0 asd ; Time : 10 minutes

This bath was used in experiments where silver was added in the form of AgCN complexed with the requisite amount of KCN.

Copper Cyanide Bath

This bath was used to prepare the copper standard, and disc 62.

Copper cyanide CuCN = 15 g/dm^3

Sodium cyanide NaCN = 28 g/dm^3

Sodium hydroxide NaOH = 3 g/dm^3

Temperature : 60°C ; Current density : 2 ASD

Watt's Nickel Electroplating Bath

This bath was used to prepare the nickel standard, and to electroplate the cross section samples prior to metallography.

Nickel sulphate $NiSO_4 6H_2O$ = 450 g/dm^3

Nickel chloride $NiCl_2 6H_2O$ = 60 g/dm^3

Baric acid H_3BO_3 = 30 g/dm^3

Temperature : 60°C ; Current density : 4 asd

Silver Electroplating Bath

Silver cyanide AgCN = 36 g/dm^3

Sodium carbonate $NaCO_3$ = 45 g/dm^3

Potassium cyanide KCN = 60 g/dm^3

Temperature : Room ; Current density : 0·5 asd ; Time : 7 minutes

This bath was used to prepare the silver standard.

Indium Plating Bath

Indium chloride $InCl_3$ = 15 g/dm^3

Potassium cyanide KCN = 140 g/dm^3

Potassium hydroxide KOH = 30 g/dm^3

Dextrose = 30 g/dm^3

This bath was used for Hull cell tests in some cases with the addition of gold cyanide under the conditions given in the appropriate table.

Bright Gold Electroplating Solutions P5 and 84C

These are commercial electroplating baths supplied by PMD Chemicals and copies of their appropriate data sheets follow.

APPENDIX 11

Results of Talysurf Measurements on Nickel Discs

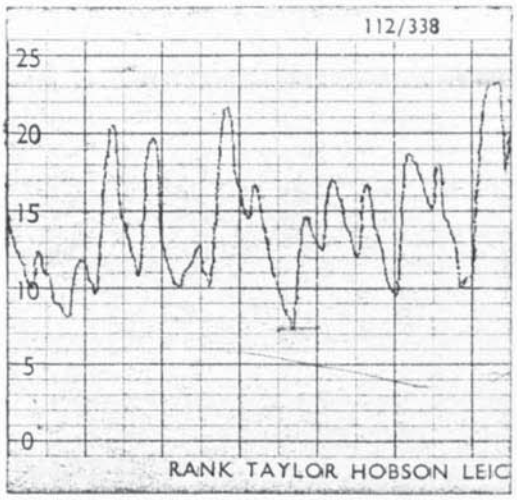

Surface: Original machined

Magnification: x 2000

CLA: 1·7 µm

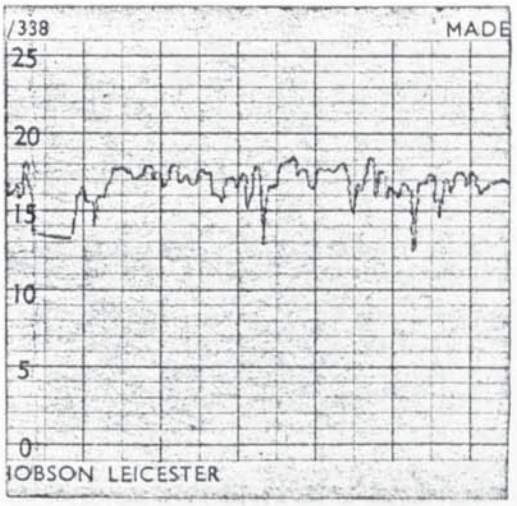

Surface: 320 grit hand ground

Magnification: x 10 000

CLA: 0·14 µm

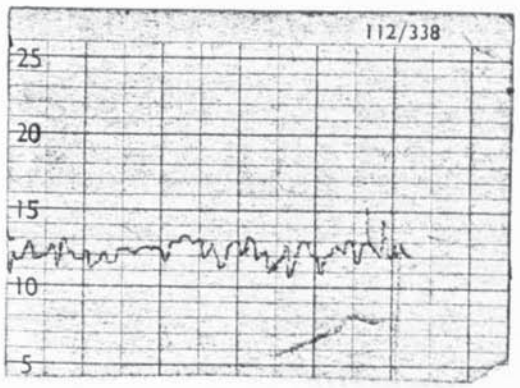

Surface: 600 grit machine lapped

Magnification: x 10 000

CLA: 0·12 µm

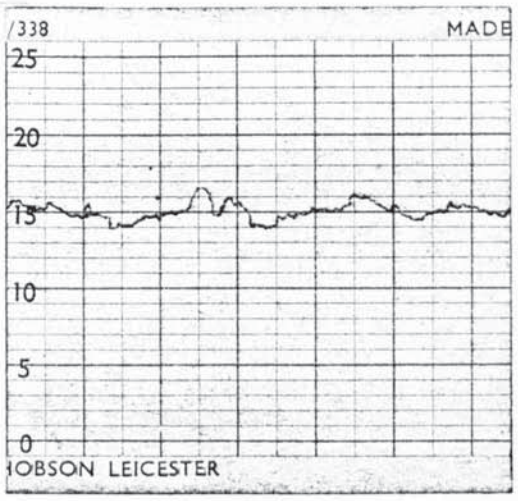

Surface: 6 µm diamond

Magnification: x 50 000

CLA: 0·023 µm

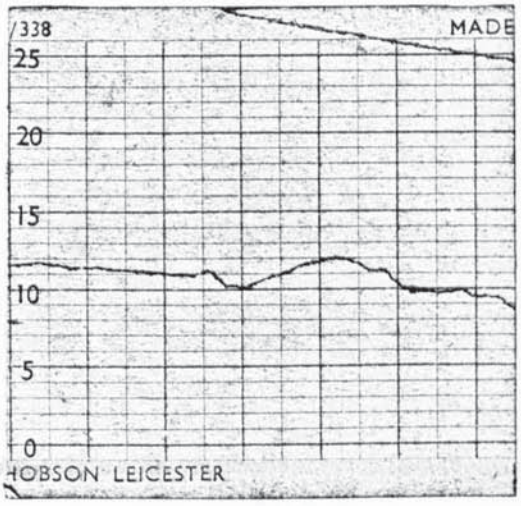

Surface: 1 µm diamond

Magnification: x 10 000 then
x 50 000

CLA: 0·04 µm

APPENDIX 12

Computer Programmes

(a) The Product Totals

```
000  76 LBL
001  38 SIN
002  03  3
003  03  3
004  32 X:T
005  43 RCL
006  02  02
007  67  EQ
008  39 COS
009  99 PRT
010  91 R/S
011  76 LBL
012  11  A
013  99 PRT
014  42 STO
015  00  00
016  02  2
017  75  -
018  43 RCL
019  00  00
020  95  =
021  22 INV
022  28 LOG
023  42 STO
024  00  00
025  71 SBR
026  35 1/X
027  01  1
028  44 SUM
029  01  01
030  71 SBR
031  35 1/X
032  01  1
033  44 SUM
034  01  01
035  71 SBR
036  35 1/X
037  98 ADV
038  01  1
039  44 SUM
040  01  01
041  44 SUM
042  02  02
043  61 GTO
044  38 SIN
045  76 LBL
046  39 COS
047  04  4
048  42 STO
049  01  01
050  71 SBR
051  34 FX
052  05  5
053  42 STO
054  01  01
055  71 SBR
056  34 FX
057  06  6
058  42 STO
059  01  01
060  71 SBR
061  34 FX
062  91 R/S
063  76 LBL
064  35 1/X
065  43 RCL
066  00  00
067  65  ×
068  73 RC*
069  01  01
070  54  )
071  99 PRT
072  72 ST*
073  01  01
074  92 RTN
075  76 LBL
076  34 FX
077  03  3
078  02  2
079  42 STO
080  03  03
081  00  0
082  42 STO
083  00  00
084  76 LBL
085  50 I×I
086  73 RC*
087  01  01
088  44 SUM
089  00  00
090  03  3
091  44 SUM
092  01  01
093  97 DSZ
094  03  03
095  50 I×I
096  43 RCL
097  00  00
098  99 PRT
099  92 RTN
```

(b) The Chromaticity Coordinates

```
000  43 RCL
001  01  01
002  75  -
003  43 RCL
004  02  02
005  95  =
006  99 PRT
007  22 INV
008  28 LOG
009  95  =
010  99 PRT
011  76 LBL
012  32 X↕T
013  42 STO
014  10  10
015  43 RCL
016  10  10
017  65  ×
018  43 RCL
019  03  03
020  95  =
021  99 PRT
022  76 LBL
023  38 SIN
024  42 STO
025  11  11
026  43 RCL
027  11  11
028  85  +
029  43 RCL
030  04  04
031  95  =
032  99 PRT
033  76 LBL
034  39 COS
035  42 STO
036  12  12
037  43 RCL
038  10  10
039  65  ×
040  43 RCL
041  05  05
042  95  =
043  99 PRT
044  76 LBL
045  30 TAN
046  42 STO
047  13  13
048  43 RCL
049  13  13
050  85  +
051  43 RCL
052  06  06
053  95  =
054  99 PRT
055  76 LBL
056  57 ENG
057  42 STO
058  14  14
059  43 RCL
060  12  12
061  85  +
062  43 RCL
063  14  14
064  85  +
065  43 RCL
066  07  07
067  95  =
068  99 PRT
069  76 LBL
070  58 FIX
071  42 STO
072  15  15
073  43 RCL
074  12  12
075  55  ÷
076  43 RCL
077  15  15
078  95  =
079  99 PRT
080  43 RCL
081  14  14
082  55  ÷
083  43 RCL
084  15  15
085  95  =
086  99 PRT
087  43 RCL
088  07  07
089  55  ÷
090  43 RCL
091  15  15
092  95  =
093  99 PRT
094  91 R/S
```

APPENDIX 13

Nickel Modification Technique

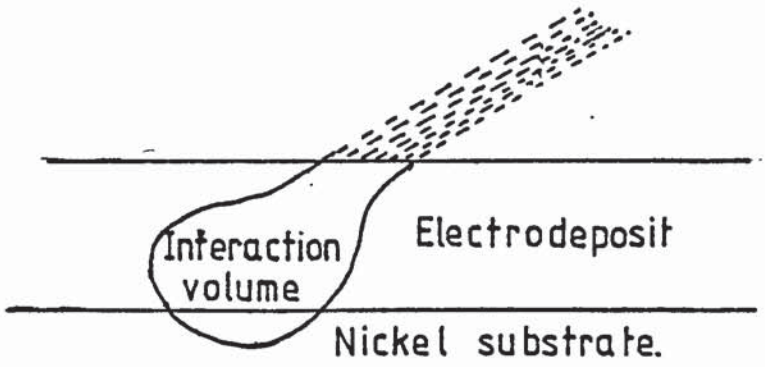

Fig. A2

Effect of interaction volume

Since deposits being tested were so thin it is possible that the interaction volume was picking up some of the nickel substrate. Thus it was considered that if 3% nickel was measured it inferred that only 97% of the interaction volume was being used to measure the alloying element in the deposit.

Example

Suppose the results were:

Copper 10%

Nickel 3%

Modified copper = $\frac{10}{97} \times 100 = 10{\cdot}3\%$

APPENDIX 14

Calculation of Thickness from Weight Increases

$$\text{Density} = \frac{\text{mass}}{\text{thickness x area}}$$

$$\text{Thickness} = \frac{\text{mass}}{\text{density x area}}$$

$$= \frac{\text{mass}}{19{\cdot}3 \text{ x area}}$$

Example for Thickness Test Pieces

Area (both sides) = 16·9 sq cm

$$\text{Thickness in cm} = \frac{\text{mass}}{19{\cdot}3 \text{ x } 16{\cdot}9} = \frac{\text{mass}}{326}$$

$$\text{Thickness in } \mu\text{m} = \frac{\text{mass x } 10^4}{326} = \text{mass x } 30{\cdot}7$$

APPENDIX 15

Calculation of Thickness of Disc 83

A. Magnification 10K

2 μm bar on negative = 0·525 cm

Deposit on negative

(i) 0·345 cm

(ii) 0·330 cm

(iii) 0·344 cm Average = 0·345 cm

(iv) 0·350 cm

(v) 0·355 cm

Average thickness of deposit = $\frac{0·345 \times 2}{0·525}$ = 1·314 μm

B. Magnification 5K

4 μm bar on negative = 0·52 cm

Deposit on negative

(i) 0·180 cm

(ii) 0·175 cm

(iii) 0·176 cm Average = 0·177 cm

(iv) 0·180 cm

(v) 0·176 cm

Average thickness of deposit = $\frac{0·177}{0·52} \times 4$ = 1·362 μm.

Average of A and B measurements = 1·34 μm

Calculation of Thickness of Disc 105

Measurement No.	Deposit Measurement mm
1	2
2	2
3	2
4	1·5
5	1·3
6	1·9
7	1·7
8	1·5
9	2
10	2

Average = 1·79 mm

Magnification on photograph

$1400 \times \frac{9}{10 \cdot 6} = 1189$

Thickness of deposit = $\frac{1 \cdot 79 \times 10^{-3}}{1189}$ m = 1·5 μm

Measurement No.	Deposit Measurement mm
1	8
2	8
3	9
4	9
5	9
6	8
7	7·5
8	7·5
9	7
10	8

Average = 8·1 mm

Magnification on photograph

$$\frac{6900 \times 9}{10{\cdot}6} = 5858$$

Thickness of deposit = $\frac{8{\cdot}1 \times 10^{-3}}{5858}$ m = 1·38 μm

Measurement No.	Deposit Measurement mm
1	17·5
2	15
3	14·5
4	15
5	15
6	16
7	17
8	15·5
9	15
10	15

Average = 15·6 mm

Magnification on photograph

$$\frac{13\ 900 \times 9}{10{\cdot}6} = 11\ 802$$

Thickness of deposit = $\frac{15{\cdot}6 \times 10^{-3}}{11\ 802}$ = 1·32 μm

Average thickness for all magnifications = 1·4 μm

APPENDIX 16

Calculation of Mid-Step Energy

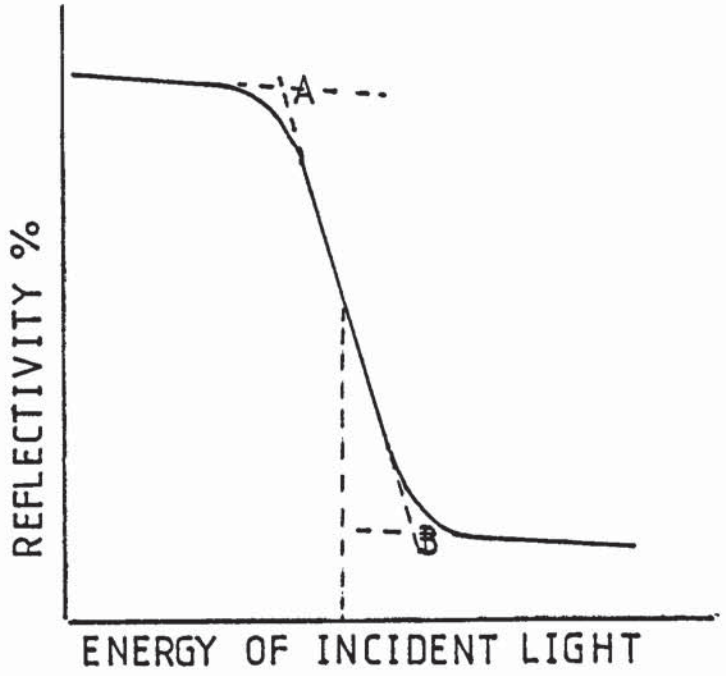

Fig. A3

Mid step energy

The mid-step energy is taken by dropping a perpendicular from the mid point of the line AB.

REFERENCES

1. Gilchrist J. D. — Extraction Metallurgy. p. 1 Pergamon Press 1969

2. Potter E. C. — Electrochemistry. p. 88 Cleaver Hume Press Ltd

3. Hambly A. & Winters R. — Engineering Materials. p. 2 O.U.P.

4. Fischer J. & Weimer E. — Precious Metals Plating. p.149

5. Fischer J. & Weimer E. — Precious Metals Plating. p.116 Robert Draper Ltd 1964

6. Oldham A. — Metal Industry (N.Y.) 1939 37 p. 72

7. Parker E. A. — Plating. 1951 38 p. 1134-40, 1156, 1256-9

8. Parker E. A. — Plating. 1952 39 p. 43-6, 50

9. Fishlock D. J. — Metal Colouring. p. Robert Draper Ltd 1962

10. Metal Finishing December 1967

11. Blum & Hogaboom — Electroplating and Electroforming p. 89-94. McGraw Hill Book Co 1949

12. Clulow F. W. — Colour - Its Principles and Applications Fountain Press 1972

13. British Standards Institution (BS 1611:1953)

14. Commission Internationale de L'Eclairage (CIE)

15. Societe Francaise des Chrysanthemistes. Repertoire des Couleurs (1905)

16. Ridgeway R. — Colour Standards and Colour Nomenclature (1912)

17. Wilson R. F. — Wilson Horticultural Colour Chart

18. Baumann P. — Baumanns neue Farbentonkarte

19. Seguy E. — Code Universal des Couleurs (1936)

20. Maez A., Paul M, Rea — Dictionary of Colour (1930)

21. Hesselgren S. — Colour Manual 1953

22. Granville W. C. & Jacobson E. J. — J. Opt. Soc. Am. 1944 34 p. 382

23. Wright W. D. — The Measurement of Colour Adam Hilger Ltd 1968

24. Nickerson D. J. — J. Opt. SocAm. 1940 30 p. 575

25. Grassman H. — Poggendorfs' Ann. 1853 89 p. 69

26. Blottiau — Rev. d'Opt. 1947 26 p. 193

27. Trezona P. W. — Proc. Phys. Soc. B. 1953 66 p. 548

28. Trezona P. W. — Proc. Phys. Soc. B. 1954 67 p. 513

29. Stiles W. S. — Optica. Acta. 1955 2 p. 168

30. Stiles W. S. — Optica. Acta. 1963 10 p. 229

31. Guild J. — Trans. Opt. Soc. 1925 27 p. 106

32. Donaldson R. — Proc. Phys. Soc. 1935 47 p. 1068

33. Donaldson R. — Proc. Phys. Soc. 1947 59 p. 554

34. Fawcett G. S. — Proc. Phys. Soc. 1944 56 p. 8

35. Judd D. B., Haupt G. W. & Chamberlain C. J. — J. Opt. Soc. 1962 52 p. 813

36. Schofield R. K. — J. Sci. Instru. 1939 16 p. 74

37. Morris M. — Paint Technology 1960 24 (No. 270) p. 26

38. Optica. Acta. 1970 17 p. 10

39. Guild J. — Phil. Trans. Roy. Soc. A. 1931 230 p. 149

40. Wright W. D. — Trans. Opt. Soc. 1928-29 30 p. 141

41. Stiles W. S. — Physical Soc. Year Book 1955 p. 44

42. Judd D. B. — J. Opt. Soc. Am. 1963 53 p. 1012

43. Speranska Optics and Spectroscopy (Trans. Opt. Soc. Am.) 1959 7 p. 424

44. Saeger K. E. & Rodies J. — Gold Bulletin 10 No. 1 1977 p. 10-14

45. Osborne C. F., Fletcher G. C. & Miller R. — J.Phys.F. 4 March 1974

46. Fong. C. Y. — Physical Rev. B 11 No. 8 April 1975

47. Koster W. & Stahl — Z. Metallkunde 1967 58 p. 768

48. Fukutani H. & Sueoka — Optical Properties and Electronic Structure of Metals and Alloys. Edited by Abeles F. North Holland Publishing Corp. Amsterdam 1966 p. 565

49. Abeles F. — J.Phys.Radium 1962 23 p. 677

50. Abeles F. — Optical Properties and Electronic Structure of Metals and Alloys. Edited by Abeles F. North Holland Publishing Corp. Amsterdam 1966 p. 553

51. Lowenheim F. A. — Electroplating p 58-59 McGraw Hill

52. Bockris J. O. — Electrochemical Science p. 200-1 Taylor and Francis 1972

53. Vook J. — Journal of Crystal Growth Netherlands 31975 Pt. 1 p. 353

54. Bockris J. O. — Electrochemical Science Taylor and Francis Ltd 1972 p 202-4

55. Potter E. C. — Electrochemistry Cleaver Hume Press Ltd p. 298-303

56. Grube G. — Heraeus Festchr. z 70 Geburtst Wilhelm Heraeus p. 34-44 (1930)

57. Zvolner — Thesis for M.Sc. degree Evanston Illinois 1941

58. Raub E. — Z.Electrochem 95 1951 p. 146-151

59. Krasikov B. S. — Zhur Prikland Khim 32 (Eng. Lang.) p. 855

60. Metals Handbook. Rev. Ed. Am. Soc. for Metals. Cleveland Ohio 1948 p. 1170

61. Raub — Metalloberflache 7A 1953 p. 17-27

62. Raub E. & Sauter F. — Metalloberflache 10 No. 3 1956 p. 65-72

63. Page R. T. — Metal Finishing Journal October 1973 to May 1974

64. Leeds J. M. & Clarke M. — Trans. Inst. Met. Fin. 46 1968 p. 1

65. Financial Times, Monday 1st October 1979

66. Brenner A. — Electrodeposition of Alloys Vols. I and II. Academic Press 1963

67. Dole M. — Trans. Electrochem. Soc. 82 1942 p. 241-255

68. Krasikov — Zhur Prikland Khim 1959 (Eng. Trans) p. 843-845

69. Parker E. A. — Plating 38 1951 p. 1134-1140 and p. 1256-1259 and 39 1952 p. 43-46

70. Fedot'Ev N. P., Kluglova E. G. & Vyacheslavov — Zhur Prikland Khim (Eng. Trans.) 32 1959 p. 2063-2070

71. Field S. — Trans. Faraday Soc. 16 (1920-21) p. 502-511

72. Raub E. & Bihlmaier — Galvanishe Weissgoldniederschlage Mitt. Forschungsinst Probieramts. Edelmetallestaatlhoheren Fachschule. Schwab Gmund 11 1937 p. 59-65

73. Fedot'Ev N. F., Ostroumova N. M. & Vyacheslavov — Zhur Prikland Khim 27 No. 1 1954 p. 43-51 and 29 1956 p. 489-492

74. Fedot'Ev N. P., Ostroumova N. M. Vyacheslavov P. M. & Grilikles S. — Legkaya Prom. 17 No. 3 1957 p 43-44

75. Atanasyants A. G., Kudryavtsev & Karataev V. M. — Zhur Prikland Khim 30 1958 (Eng. Trans) p. 926-930

76. Gardam G. E. — Trans. of the Institute of Metal Finishing 44 1966 p. 186-188

77. Gardam G. E. — Trans. Inst. Met. Fin. 44 1964 p. 190

78. Roberts & Clarke — Gold Bulletin 12 No. 1 January 1979

79. Leuser J. — Metall. 3 1949 p. 105-110 and 128

80. Wise E. M. (Ed.) — Gold Recovery Properties and Applications. D Van Nostrand & Co Inc Princeton N.J. 1964 p. 62

81. Richards B. P. — Metal Finishing Journal August/September 1971 p. 208-213

82. Loebich O. Gold Bulletin 1972 5 p. 2-10

83. Dickson P. F. & Jones M. C. NBS. Tech. Note 348 1966

84. Otter Z. Phys. 1961 161 p. 163-539

85. Pfestorf G. Ann Physik 4 Folge 1926 81 906

86. Schultz L. G. J. Opt. Soc. Am. 1954 44 p. 357-362

87. Knosp Z. Metallkunde 1969 60 p. 526

88. Philip Compte Rend. 1958 247 p. 1104

89. Robin S. Ibid 1953 236 p. 674

90. Stabe Feinwerklechnik 1953 57 p. 199